SUSTAINABLE REINFORCING FILLER FOR ECO-FRIENDLY TIRES

A STEP TOWARDS UNDERSTANDING THE REINFORCING POTENTIAL OF HYDROTHERMALLY TREATED LIGNIN

Priyanka Sekar

SUSTAINABLE REINFORCING FILLER FOR ECO-FRIENDLY TIRES

A STEP TOWARDS UNDERSTANDING THE REINFORCING POTENTIAL OF HYDROTHERMALLY TREATED LIGNIN

DISSERTATION

to obtain
the degree of doctor at the University of Twente,
on the authority of the rector magnificus,
prof. dr. ir. A. Veldkamp,
on account of the decision of the Doctorate Board
to be publicly defended
on Friday 28 June 2024 at 16.45 hours

by

Priyanka Sekar

This dissertation has been approved by:

Promotor
prof.dr. A. Blume

Co-promotor
dr. A.G. Talma

UNIVERSITY OF TWENTE.

SUNCOAL | UPM A UPM company

Graduation Committee:

Chair / secretary: prof.dr.ir. H.F.J.M. Koopman

Promotor: prof.dr. A. Blume
                            University of Twente,
                            ET, Elastomer Technology and Engineering

Co-promotor: dr. A.G. Talma
                            University of Twente,
                            ET, Elastomer Technology and Engineering

Committee Members: prof.dr.ir. C.G.P.H. Schroën
                            University of Twente,
                            TNW, Soft matter, Fluidics and Interfaces

                            dr. M.P. Ruiz Ramiro
                            University of Twente,
                            TNW, Sustainable Process Technology

                            prof.dr.ir. I.M. Gitman
                            University of Twente,
                            ET, Computational Design of Structural Materials

                            prof.dr. K.S. Mikkonen
                            University of Helsinki,
                            Department of Food and Nutrition

                            dr. E. Sarlin
                            Tampere University,
                            Faculty of Engineering and Natural Sciences

                            dr. J. Podschun
                            SunCoal Industries GmbH

To my beloved mother

"மகள்தாய்க்கு ஆற்றும் உதவி இவள்தாய்

என்நோற்றாள் கொல் எனும் சொல்."

-Adapted from "Thirukkural" (kural 70)

Summary

Brown is the pathway to Green!

The environmental impact of tires, such as the greenhouse gas emissions and strong dependency on fossil-based raw materials, raises sustainability-related concerns. To address ongoing challenges, the tire industry is shifting towards a circular economy by adopting sustainable measures and developing ecological tires to mitigate their carbon footprint. This includes the use of sustainable alternatives, such as bio-based and recycled materials, to supersede the current raw materials employed in the formulation of the rubber compound, as well as implementing more efficient production processes that reduce waste and emissions. In recent years, the development of sustainable rubber compounds has gained more attention in the tire industry. A typical rubber compound for tire formulation primarily comprises non-polar rubber (natural/synthetic), reinforcing filler, processing oil, curatives, antioxidants, and antidegradants in different proportions. Rubber and reinforcing filler occupy a major proportion of the rubber compound. To achieve a high degree of sustainability in a compound, one of the promising solutions would be to replace non-renewable rubber and/or reinforcing filler with a sustainable alternative. Since the addition of filler also impacts the compound hysteresis behavior, it might affect the tire's rolling resistance and durability in a negative way, leading to environmental concerns about an increase in CO_2 emission as well as in microplastic pollution. Hence, identifying an alternative bio-based or recycled reinforcing filler that offers an optimal balance between tire performance and environmental sustainability is a promising approach to the development of ecological tires. In recent decades, lignin, a side-stream of paper pulping and bio-refinery industries, has gained considerable attention as a potential alternative to conventional reinforcing fillers such as carbon black and silica, primarily due to its renewable nature, non-edible plant origin, and widespread availability. Besides, it possesses unique characteristics, such as high carbon content, good antioxidant properties, lightweight, biodegradability, and thermal stability. However, past investigations with lignin (Kraft, Lignosulfonates, etc.) in non-polar rubber compounds classified it as a non-reinforcing filler due to its lower stress-strain properties than conventional reinforcing fillers, carbon black, and silica. This was attributed to its hydrophilic nature due to polar functional groups and its relatively large particle size (in the micrometer range), affecting its compatibility and dispersion in the non-polar rubber. Consequently, alternate strategies, such as chemical modification of lignin, use of different mixing methods (like latex mixing technique, high-temperature dynamic heat treatment, etc.), and hybrid filler techniques, have been considered for the practical application of lignin in rubber. Nevertheless, only a limited improvement in reinforcing

effects was observed. The use of a hydrothermal process can overcome the existing challenges in the application of lignin. This process generates tailor-made lignin with specific morphologies, particle size, and controlled surface functionalities. This improved filler characteristic of lignin can lead to a better reinforcing effect in rubber. This thesis focuses on the viability of softwood Kraft lignin subjected to hydrothermal treatment (HTT) as a filler for rubber. This lignin is termed hydrothermally treated lignin.

This thesis aims to understand the reinforcing effect of hydrothermally treated (HTT) Kraft lignin in a non-polar rubber, compared to reinforcing carbon black and silica. In this thesis, a conventional mechanical mixing technique (mixing all the ingredients directly in an internal mixer) is used to mix and produce rubber compounds, whether unfilled, filled with HTT lignin, or filled with any other filler. The reinforcing potential of the HTT lignin-filled rubber compounds was evaluated in terms of cure, filler-filler interaction, and mechanical properties. To understand the filler dispersion behavior in the rubber matrix, morphological studies by atomic force microscopy (AFM) were carried out for the selected samples.

The initial study carried out in this thesis aimed to differentiate the structural and morphological characteristics of softwood Kraft lignin before and after the hydrothermal process, followed by evaluating the reinforcing properties of hydrothermally treated Kraft lignin in a blend of solution styrene butadiene/butadiene rubber (SSBR/BR) compared to the Kraft lignin-filled (initial feedstock), the reinforcing carbon black-filled and silica/silane-filled rubber compounds. The analytical studies conducted between HTT lignin and Kraft lignin indicated that the hydrothermal treatment process reduces the oxygen content, decreases the particle size, and alters the particle morphology of Kraft lignin by generating micro-pores. As a result, the achieved cure and reinforcing properties of the HTT lignin-filled SSBR/BR compound are better than those of the Kraft lignin-filled one. Furthermore, an improved filler dispersion in the rubber matrix was observed for the HTT lignin-filled vulcanizate compared to Kraft lignin, indicating better compatibility of HTT lignin with the used rubber matrix. However, the reinforcing power of HTT lignin is relatively low in the investigated rubber system compared to the reinforcing carbon black (N330) and silica (Ultrasil® 7000)/silane (bis(triethoxysilylpropyl)tetrasulfide). This can be attributed to the relatively low specific surface area (SSA) of HTT lignin and the presence of a high amount of still available polar functional groups. This makes it less compatible with the used non-polar rubber matrix and affects its micro-dispersion in the rubber matrix. Besides, the HTT lignin-filled compound shows an extended scorch time and a slower cure rate than the carbon black-filled or silica/silane-filled compounds, indicating that curing ingredients could be adsorbed at the lignin surface. This study reveals that chemical or physical shielding of polar functional groups of HTT lignin is still required to improve further the in-rubber properties of the HTT lignin-filled rubber compound.

Therefore, the next phase of the study dealt with altering the surface chemistry of the HTT lignin by using silane- and non-silane-based surface modifiers that can potentially promote the compatibility of HTT lignin with the rubber and, thereby, enhance its reinforcing performance. This study primarily aimed to understand the impact of modification on the reinforcing effects of HTT lignin but was also extended to discern the functional groups of HTT lignin involved in the coupling reaction with the selected surface modifier. Surface modification of filler can be done by two methods: (i) in-situ, where modification is performed in the internal mixer with rubber and other rubber ingredients, and (ii) ex-situ, where modification is performed outside the mixer without a rubber and other rubber ingredients. In the case of silane-based modifiers, the modification reactions were performed in-situ during the mixing of rubber compounds based on the outcomes of the prior art. For non-silane-based modifiers, modification of HTT lignin was always carried out ex-situ before the rubber mixing procedure. This was done (i) to ensure conversion and (ii) to avoid any side reactions of selected modifiers with other rubber ingredients. Modification conditions for ex-situ were determined and selected based on the model study using HTT lignin model substance, vanillyl alcohol, and the selected modifier.

The first part of the modification study investigated the use of the following silane-based agents for modifying HTT lignin based on their established effectiveness in modifying silica fillers:

(i)   sulfur-containing silane, bis(triethoxysilylpropyl)tetrasulfide(Si69®/TESPT),
(ii)   unblocked or shielded thiol silane, (3-mercaptopropyl) mono ethoxy polyether silane (Si363®/MPMEPS),
(iii)   blocked thiol silane, octanoylthio-1 propyltriethoxysilane (NXT®/OTPTES),
(iv)   octyltriethoxysilane (OCTEO)

TESPT, MPMEPS, and OTPTES are bifunctional silanes possessing two reactive functionalities that can interact with filler and rubber and, thus, can act as coupling agents. In contrast, OCTEO is a monofunctional silane with only a filler reactive group, which can serve as a shielding agent. It was found that the in-situ modification of HTT lignin using coupling agents enhances the in-rubber properties of the HTT lignin-filled compound compared to the shielding silane, OCTEO. Furthermore, the results of this study indicate that the impact of silane coupling agents in rubber compounds filled with HTT lignin depends on the specific type of silane employed. Especially the shielded thiol coupling silane, Si363®/MPMEPS, and sulfur-containing coupling silane, Si69®/TESPT, show improved mechanical properties compared to the blocked thiol coupling silane, NXT®/OTPTES. A modification of HTT lignin using TESPT and MPMEPS silanes has been found to create sponge-like HTT lignin clusters in the rubber matrix, which affects the micro-dispersion of HTT lignin. However, this phenomenon was not observed when using OTPTES. This unexpected behavior of silanes led to further investigations of the coupling mechanism of HTT lignin and silane using model lignin substances, vanillyl alcohol, and

guaiacol. It was revealed that the (un)hydrolyzed ethoxy functionalities of the silane are less or not reactive to HTT lignin; in contrast, the coupling between the silane and HTT lignin occurs via the thiol group. Furthermore, the (un)hydrolyzed ethoxy functionality is prone to oligomerization, which leads to the formation of HTT lignin clusters. When such a coupling reaction occurs between HTT lignin and silane in a rubber matrix, the overall reaction leads to the generation of a sponge-like HTT lignin cluster, i.e., rubber is trapped within the filler cluster as a result of self-condensation of (un)hydrolyzed ethoxy functionality present on the thiol-coupled HTT lignin surface. The investigations suggest that the aliphatic hydroxy groups of HTT lignin in the α-position on the aromatic ring, combined with the para-hydroxy group of HTT lignin, are involved in the coupling reaction with the thiol groups of silane. Consequently, the reaction between HTT lignin and silane results in a thioether interfacial bond (-C-S-Si) rather than the expected -C-O-Si interfacial bond. The outcome of this study suggests that the coupling mechanism for HTT lignin and silane is distinct from the conventional silica/silane coupling mechanism, where the ethoxy functional group of silane, reacts with the silanols of silica, and the second functionality of silane, the sulfur, reacts to the rubber leading to silica-silane-rubber coupling. Thus, a new coupling mechanism for silane-modified HTT lignin has been proposed based on these findings.

Since this study demonstrates that thiol reacts with the surface functional group of HTT lignin and the clustering of HTT lignin occurs in the presence of triethoxysilyl groups, a follow-up study was carried out to examine a thiol-based non-silane coupling agent for HTT lignin surface modification. The choice for non-silane-based thiol agents was to avoid clustering of filler particles; thereby, an improved micro-dispersion of HTT lignin should be achieved, leading to improved mechanical properties.

The second part of the modification study thus evaluated the non-silane-based thiol modifiers, such as 1,2-bis(2-mercaptoethoxy)ethane (MEE) and liquid polysulfide polymer with thiol end groups (LPST) for HTT lignin. As the thiol functionality is also reactive to rubber, it is unclear to which extent the thiol moieties participate in the coupling reaction with the filler and/or with the rubber. Therefore, the ex-situ modification was performed to modify HTT lignin first, followed by mixing the thiol-modified HTT lignin in a pure SSBR system. The filler characterization study shows that the grafting efficiency of MEE (69 %) is higher than that of LPST (41 %). Regardless of grafting efficiency, both the thiol-modified HTT lignin-filled SSBRs have similar cure and tensile properties but they are better than the unmodified HTT lignin-filled ones. In contrast, the achieved in-rubber properties of both thiol-modified HTT lignin-filled vulcanizates were lower than that of the reinforcing carbon black (N330) filled compound. This was ascribed again to the lower degree of filler-polymer interactions and the lower specific surface area of the thiol-modified HTT lignin. Furthermore, the findings of the study suggest that using thiol functionalities as both rubber and filler reactive groups is challenging due to the preference for the HTT lignin-thiol reaction over the rubber-thiol one. To address this, a non-silane-based as well as non-thiol-based surface modifier, i.e., a modifier without a

sulfur or thiol moiety, was investigated to enhance the mechanical properties of HTT lignin compared to carbon black. For this reason, the third part of this modification study thus is focused on the epoxide coupling agent, allyl glycidyl ether (AGE), which is a non-silane-based and non-thiol-based surface modifier. It is assumed that the epoxide functionality of AGE reacts with HTT lignin, and the allyl functionality participates in the sulfur vulcanization of rubber, thereby chemically coupling HTT lignin with the rubber. The coupling reaction between HTT lignin and the epoxide of AGE was initially confirmed using a model study with vanillyl alcohol. This study shows that the phenolic -OH groups of HTT lignin participate in the coupling reaction with AGE. Two different concentrations (low and high) were used for ex-situ modification of HTT lignin, and the resulting modified HTT lignins were used as fillers for pure SSBR. The in-rubber studies show that low AGE-modified HTT lignin-filled SSBR compounds have better in-rubber properties than unmodified- and high-AGE-modified-HTT lignin-filled compounds. This was attributed to the enhanced chemical polymer-filler interaction via the allyl functionality and shielding of the polar functional groups of HTT lignin. The high AGE-modified HTT lignin-filled SSBR compound has inferior mechanical properties and lower apparent crosslink density than the unmodified HTT lignin-filled one. The observed phenomenon could be explained by the side reaction of the allyl group, wherein the self-crosslinking of AGE via allyl moieties in the presence of free sulfur takes place. This is likely due to the substantial grafting of allyl groups in high AGE-modified HTT lignin, allowing the self-crosslinking reaction via the available free sulfur in the compound to prevail over the polymer-filler interaction. As a result, the self-crosslinking reaction of AGE consumes the sulfur, adversely affecting the polymer-filler and polymer-polymer interaction. Thus, it seems that the probability of coupling or side reactions is influenced by the concentration or degree of grafting of the AGE.

The modification studies carried out by using different surface modifiers, such as silanes, thiols, and epoxide, indicate that the application of surface modifiers can efficiently enhance the reinforcing properties of HTT lignin-filled rubber compounds to a certain level, resulting in a semi-reinforcing filler compared to the highly reinforcing carbon black. The result indicates that considering the specific surface area of the filler, the reinforcing effect of HTT lignin can be improved further by achieving strong interfacial interactions between HTT lignin and the rubber. Among the investigated modifiers, regardless of filler clustering or poor micro-dispersion, the silane-based coupling agent, TESPT, shows the best reinforcing effect in the HTT lignin-filled SSBR/BR compound. This can be attributed to the high filler-polymer interactions resulting from the coupling between unreacted thiol or sulfur functionality of silane and the double bonds of rubber, as well as the condensation between ethoxy groups of the silane and ethoxy of the functionalized rubber compared to the other modifiers.

Overall, it can be concluded from the present study conducted with one particular grade of lignin, softwood Kraft lignin, that a post-treatment process like hydrothermal

treatment enhances the reinforcing effects of lignin in a non-polar rubber. Further development in the HTT process to reduce the particle size and/or alter the surface chemistry is essential to utilize lignin as a reinforcing filler in a non-polar rubber. The surface modification studies with HTT lignin reveal that it is reactive towards the rubber reactive functionalities, particularly thiol (-SH). This characteristic of HTT lignin poses a challenge in identifying an appropriate coupling agent for surface modification, as in the case of a silica/silane system. Besides, it was demonstrated that the ethoxy functional group is not reactive to HTT lignin. This finding emphasizes the existing knowledge gap in the modification of HTT lignin. The use of ethoxy functionality in combination with the thiol group can facilitate coupling between HTT lignin and an end-chain triethoxysilyl functionalized rubber via the condensation of the ethoxy groups. Therefore, it is crucial to clearly understand the coupling between HTT lignin, modifier, and functionalized or non-functionalized rubber to fully envisage the potential of HTT lignin as a reinforcing filler. Thus, the two key challenges associated with rubber reinforcement by HTT lignin have been identified in this thesis and need to be addressed in future works.

Samenvatting

Bruin is de weg naar groen!

De milieu-impact van banden zoals uitstoot van broeikasgassen en de sterke afhankelijkheid van fossiele grondstoffen geeft aanleiding tot bezorgdheid over duurzaamheid. Om de aanhoudende uitdagingen het hoofd te bieden, werkt de bandenindustrie aan een circulaire economie door duurzame maatregelen te nemen en banden te ontwikkelen met een kleinere ecologische voetafdruk. Dit omvat het gebruik van duurzame alternatieven zoals natuurlijke en gerecyclede materialen ter vervanging van de huidige grondstoffen die worden gebruikt bij het compounderen van rubber, evenals het implementeren van efficiëntere productieprocessen die afval en emissies verminderen. De laatste jaren heeft de ontwikkeling van duurzame rubbersamenstellingen meer aandacht gekregen in de bandenindustrie. Een typische rubbersamenstelling voor banden bestaat voornamelijk uit apolair rubber (natuurlijk/synthetisch), versterkende vulstof, olie, vulkanisatiemiddelen, antioxidanten en antidegradanten in verschillende verhoudingen. Rubber en versterkende vulstof zijn de voornaamste componenten in deze. Om een hoge mate van duurzaamheid qua materiaalsamenstelling te bereiken, zou een van de meest belovende oplossingen zijn om niet-hernieuwbaar rubber en/of versterkende vulstof te vervangen door een duurzaam alternatief. Aangezien de toevoeging van een vulstof ook van invloed is op het hysteresegedrag van de rubber, kan dit de rolweerstand en daarmee de duurzaamheid van een band op een negatieve manier beïnvloeden, wat wederom leidt tot bezorgdheid over het milieu over een toename van CO_2 uitstoot en vervuiling door microplastics. Daarom is het ontwikkelen van alternatieve biologische of gerecyclede versterkende vulstoffen, die voor een optimale balans zorgen tussen bandenprestaties en duurzaamheid, een veelbelovende weg voor de ontwikkeling van ecologische banden. In de afgelopen decennia heeft lignine, een zijstroom van de papierpulp- en bioraffinage-industrie, veel aandacht gekregen als een potentieel alternatief voor conventionele versterkende vulstoffen zoals roet en silica, voornamelijk vanwege het hernieuwbare karakter, de plantaardige oorsprong zonder competitie met de voedselproductie, en de goede beschikbaarheid. Bovendien bezit het unieke eigenschappen zoals een hoog koolstofgehalte, goede bescherming tegen oxidatie, lichtgewicht, biologische afbreekbaarheid en thermische stabiliteit. Eerdere onderzoeken met lignine (Kraft, lignosulfonaten, enz.) in apolaire rubberverbindingen hebben echter aangetoond dat het als niet-versterkende vulstof werkt vanwege de lagere trek-rekeigenschappen vergeleken met conventionele versterkende vulstoffen zoals roet en silica. Dit werd toegeschreven

aan de hydrofiele eigenschappen van lignine als gevolg van polaire functionele groepen en de relatief grote deeltjes (micrometers), waardoor de compatibiliteit met en dispersie in het apolaire rubber werd gehinderd. Daarom zijn alternatieve strategieën zoals chemische modificatie van lignine, het gebruik van aangepaste mengmethoden (zoals latex-mengtechniek, dynamische warmtebehandeling bij hoge temperatuur, enz.) en hybride vulstofsystemen overwogen voor de praktische toepassing van lignine in rubber. Niettemin werd slechts een beperkte verbetering van de versterkende effecten waargenomen. Modificatie via een hydrothermaal proces kan de bestaande uitdagingen bij de toepassing van lignine overwinnen. Dit proces genereert lignine met een specifieke morfologie, deeltjesgrootte en oppervlaktefunctionaliteiten. Deze verbeterde eigenschappen van lignine kan vervolgens leiden tot een hoger versterkend effect in rubber. Dit proefschrift richt zich op de haalbaarheid van zachthout Kraft lignine onderworpen aan hydrothermale behandeling (HTT) als vulstof voor rubber, het zogenaamde 'hydrothermisch behandeld lignine'.

Dit proefschrift heeft tot doel het versterkende effect van hydrothermisch behandelde (HTT) Kraft lignine in een apolair rubber te onderzoeken, in vergelijking met het versterkend effect van roet en silica. In deze studie wordt een conventioneel mengproces (het direct mengen van alle ingrediënten in een interne menger) gebruikt om rubbermengsels te maken, zonder of met HTT lignine of een andere vulstof. Het versterkend effect van de met lignine versterkte rubbermengsels werd geëvalueerd qua vulkanisatiegedrag, vulstof-vulstofinteractie en mechanische eigenschappen. Om het dispersiegedrag van de vulstof in de rubbermatrix te studeren, werden morfologische studies door middel van 'atomic force microscopy' (AFM) uitgevoerd van geselecteerde monsters.

De eerste studie die in dit proefschrift werd uitgevoerd, had tot doel de structurele en morfologische kenmerken van zachthout Kraft-lignine voor en na het hydrothermale proces te vergelijken. De volgende stap was het evalueren van de versterkende eigenschappen van hydrothermisch behandeld Kraft-lignine in een mengsel van solutie styreen-butadieen en butadieenrubber (SSBR/BR), in vergelijking met onbehandeld Kraft lignine, en met roet en silica/silaan versterkte rubber. De vergelijkende studies, die zijn uitgevoerd met HTT lignine en Kraft-lignine gaven aan, dat het hydrothermale behandelingsproces het zuurstofgehalte verlaagt, de deeltjesgrootte verkleint en de deeltjesmorfologie van Kraft-lignine verandert door microporiën te genereren. Als gevolg hiervan zijn de vulkanisatie- en versterkende eigenschappen van het met HTT lignine versterkte SSBR/BR-rubber verbeterd vergeleken met die van het met Kraft lignine versterkte materiaal. Bovendien werd de vulstofdispersie in de rubbermatrix verbeterd door HTT lignine in vergelijking met Kraft-lignine, wat wijst op een betere compatibiliteit van HTT lignine met de rubbermatrix. De versterkende kracht van HTT lignine is echter relatief laag in het onderzochte rubbersysteem in vergelijking met het versterkende effect van carbon black (N330) en silica (Ultrasil® 7000)/silaan (bis(triethoxysilylpropyl)tetrasulfide)). Dit kan worden toegeschreven aan het relatief lage

specifieke oppervlak (SSA) van HTT lignine en de aanwezigheid van een groot aantal nog beschikbare polaire functionele groepen. Dit maakt het minder compatibel met de apolaire rubbermatrix en beïnvloedt de microdispersie. Bovendien vertoont het met HTT lignine versterkte rubber een langere scorchtijd en een vertraagde vulkanisatiesnelheid dan een met roet of met silica/silaan versterkt mengsel. Dit geeft aan dat de vulkanisatiemiddelen aan het lignineoppervlak kunnen worden geadsorbeerd. Deze studie toont aan dat chemische of fysische afscherming van polaire functionele groepen van HTT lignine nog steeds nodig is om de rubbereigenschappen van het materiaal met deze vulstof verder te verbeteren.

Daarom focusseerde de volgende fase van het onderzoek op het veranderen van de oppervlaktechemie van HTT lignine door gebruik te maken van silaan- en niet-silaan-gebaseerde oppervlaktemodificatie, die mogelijk de compatibiliteit van HTT lignine met rubber kan bevorderen en daardoor de versterking kan verbeteren. Deze studie was in de eerste plaats gericht op het ophelderen van het effect van modificatie op de versterking door HTT lignine, en werd uitgebreid naar de functionele groepen van HTT lignine, die betrokken zijn bij de koppelingsreactie met de geselecteerde oppervlaktemodificatie agentia. Dit onderzoek kan op twee manieren worden uitgevoerd: (i) in-situ, waarbij de modificatie wordt uitgevoerd in de interne menger in aanwezigheid van rubber en andere ingrediënten, en (ii) ex-situ, waarbij modificatie buiten de menger wordt uitgevoerd bij afwezigheid van rubber en ingrediënten. In het geval van modificatie op basis van silaan werden de reacties in-situ uitgevoerd tijdens het mengen gebruik makend van de stand der techniek. Voor niet-silaan modificatie werd de reactie van HTT lignine altijd ex-situ uitgevoerd voorafgaande aan het mengproces. Dit werd gedaan (i) om een voldoend hoge mate van reactie te garanderen en (ii) om eventuele nevenreacties van de modificatiemiddelen met andere rubberingrediënten te voorkomen. De modificatiecondities voor ex-situ reactie werden bepaald en geselecteerd op basis van een modelstudie met behulp van een HTT lignine model: vanillylalcohol, en het gekozen modificatie agens.

In het eerste deel van de modificatiestudie werd het gebruik van de volgende op silaan gebaseerde middelen voor het modificeren van HTT lignine onderzocht, gekozen op basis van hun effectiviteit voor het modificeren van silica:

(v)   zwavelhoudend silaan, bis(triethoxysilylpropyl)tetrasulfide (Si69®/TESPT),
(vi)   niet-geblokkeerd of afgeschermd thiolsilaan, (3-mercaptopropyl)mono-ethoxypolyethersilaan (Si363®/MPMEPS),
(vii)   geblokkeerd thiolsilaan, octanoylthio-1-propyltriethoxysilaan (NXT®/OTPTES),
(viii) octyltriethoxysilaan (OCTEO)

TESPT, MPMEPS en OTPTES zijn bifunctionele silanen met twee reactieve functionaliteiten die kunnen interageren met de vulstof en met het rubber, en zo kunnen fungeren als koppelingsagentia. OCTEO daarentegen is een monofunctioneel silaan met

maar een reactieve groep, en kan alleen als afschermingsmiddel dienen. Het bleek dat de in-situ modificatie van HTT lignine met behulp van koppelingsmiddelen de eigenschappen van het rubber verbetert in vergelijking met de afschermende silaan, OCTEO. Bovendien geven de resultaten van deze studie aan, dat het effect van silaan-koppelingsmiddelen afhankelijk is van het specifieke type silaan dat wordt gebruikt. Vooral het afgeschermde thiolsilaan, Si363®/MPMEPS, en het zwavelhoudende silaan, Si69®/TESPT, vertonen verbeterde mechanische eigenschappen in vergelijking met het geblokkeerde thiolsilaan, NXT®/OTPTES. Een modificatie van HTT lignine met behulp van TESPT- en MPMEPS-silaan blijkt sponsachtige HTT lignineclusters in de rubbermatrix te veroorzaken, wat de microdispersie van HTT lignine beïnvloedt. Dit fenomeen werd echter niet gezin bij gebruik van OTPTES. Dit onverwachte gedrag van silanen leidde tot verder onderzoek naar het koppelingsmechanisme van HTT lignine en silaan met behulp van een modelstof voor lignine, vanillylalcohol, en guaiacol. Er werd aangetoond dat de (on)gehydrolyseerde ethoxy-functionaliteiten van het silaan minder of niet reactief zijn met HTT lignine; de koppeling tussen silaan en HTT lignine vindt plaats via de thiolgroep. Bovendien is de (on)gehydrolyseerde ethoxyfunctionaliteit gevoelig voor oligomerisatie, wat leidt tot vorming van HTT lignineclusters. Wanneer een dergelijke koppelingsreactie optreedt tussen HTT lignine en silaan in een rubbermatrix, leidt deze reactie tot vorming van een sponsachtige HTT ligninecluster, d.w.z. rubber wordt opgesloten in de vulstofcluster als gevolg van zelfcondensatie van (on)gehydrolyseerde ethoxygroepen, die aanwezig zijn op het thiol-gekoppelde HTT lignine oppervlak. Dit onderzoek suggereert dat de alifatische hydroxygroepen van HTT lignine in de α-positie van de aromatische ring gecombineerd met de para-hydroxylgroep betrokken zijn bij de koppelingsreactie met de thiolgroepen van het silaan. Bijgevolg resulteert de reactie van HTT lignine met silaan in een thioether-binding (-C-S-Si) in plaats van de verwachte -C-O-Si-binding. De uitkomst van deze studie suggereert dat het koppelingsmechanisme voor HTT lignine en silaan verschilt van het conventionele silica/silaan koppelingsmechanisme, waarbij de ethoxy-groep van het silaan reageert met de silanol-groep van silica, en de tweede functionele groep van het silaan, de zwavel-groep, reageert met de rubber, wat leidt tot een silica-silaan-rubberkoppeling. Daarom is op basis van deze bevindingen een nieuw koppelingsmechanisme voor silaan-gemodificeerde HTT lignine voorgesteld.

Aangezien deze studie aantoont, dat een thiol-groep reageert met een functionele groep van HTT lignine, en clustering van HTT lignine optreedt in aanwezigheid van triethoxysilylgroepen, werd een vervolgstudie uitgevoerd: een thiol zonder silaan functionaliteit werd onderzocht voor HTT lignine oppervlaktemodificatie. De keuze voor thiolen, die niet op een silaan zijn gebaseerd, was gemaakt om clustering van vulstofdeeltjes te voorkomen. Hierdoor zou een verbeterde microdispersie van HTT lignine moeten worden bereikt, wat weer zou moeten leiden tot verbeterde mechanische eigenschappen.

Het tweede deel van de modificatiestudie evalueerde de thiolen zonder silaan functionaliteit zoals 1,2-bis(2-mercaptoethoxy)ethaan (MEE) en een vloeibaar polysulfidepolymeer met thiol-eindgroepen (LPST). Ook is de thiolfunctionaliteit reactief met rubber, het is onduidelijk in welke mate de thiolgroepen deelnemen aan de koppelingsreactie met het rubber en/of met de vulstof. Daarom werd ex-situ modificatie uitgevoerd om eerst HTT lignine te modificeren, gevolgd door het mengen van de thiol-gemodificeerde vulstof in een SSBR-systeem als zodanig. Uit de karakterisering van de vulstof blijkt dat MEE (69 %) efficiënter is dan LPST (41 %). Ongeacht de efficiëntie, hebben beide met thiol gemodificeerde HTT lignine versterkte SSBR's vergelijkbare vulkanisatie- en trek-rek eigenschappen, en zijn ze beter dan het rubber met niet-gemodificeerde HTT lignine. Daarentegen waren de bereikte rubbereigenschappen van beide met thiol gemodificeerde HTT lignine versterkte vulkanisaten lager dan die van met roet (N330) versterkte rubber. Dit werd opnieuw toegeschreven aan de lagere mate van vulstof-polymeerinteracties en het lagere specifieke oppervlak van de thiol-gemodificeerde HTT lignine. Bovendien suggereren de bevindingen van de studie dat het gebruik van thiolfunctionaliteiten als reactieve groepen voor zowel rubber als vulstof een uitdaging is vanwege de voorkeur voor de HTT lignine-thiolreactie boven de rubber-thiolreactie. Om dit aan te pakken werd een oppervlaktemodificatie met een agens welk óf geen silaan óf geen thiol groep bevat, onderzocht om de mechanische eigenschappen van HTT lignine te verbeteren in vergelijking met roet. Om deze reden is het derde deel van deze modificatiestudie gericht op een epoxide koppelingsmiddel, allylglycidylether (AGE), voor een oppervlaktemodificatie die niet op silaan en niet op thiol is gebaseerd. Er wordt verondersteld dat de epoxide-functionaliteit van AGE reageert met HTT lignine, en de allyl-functionaliteit draagt bij aan de zwavelvulkanisatie van rubber, waardoor HTT lignine chemisch wordt gekoppeld aan het rubber. De koppelingsreactie tussen HTT lignine en de epoxide groep van AGE werd bevestigd met behulp van een modelstudie met vanillylalcohol. Deze studie toont aan dat de fenol-OH groepen van HTT lignine onderdeel zijn van de koppelingsreactie met AGE. Twee verschillende concentraties (laag en hoog) werden gebruikt voor ex-situ modificatie van HTT lignine, en de resulterende gemodificeerde HTT lignines werden gebruikt als vulstoffen voor SSBR als zodanig. De in-rubber studies tonen aan dat de met een lage concentratie AGE gemodificeerde HTT lignine versterkte SSBR betere rubbereigenschappen heeft dan het met niet-gemodificeerde en met een hoge AGE-concentratie gemodificeerde HTT lignine versterkte rubber. Dit werd toegeschreven aan de verbeterde interactie tussen polymeer en vulstof via de allylfunctionaliteit en afscherming van de polaire functionele groepen van HTT lignine. Het met een hoge concentratie AGE gemodificeerde HTT lignine versterkte SSBR rubber heeft inferieure mechanische eigenschappen en een lagere crosslink-dichtheid dan bij gebruik van niet-gemodificeerde HTT lignine. Dit kan worden verklaard door de nevenreactie van de allylgroep, waarbij een zelf-vernetting van AGE via allylgroepen in aanwezigheid van vrije zwavel plaatsvindt. Dit is waarschijnlijk te wijten aan de reactie van allylgroepen van een HTT lignine gemodificeerd met een hoge concentratie AGE, waardoor de zelf-vernetting via beschikbare vrije zwavel kan

domineren boven de interactie tussen polymeer en vulstof. Als gevolg hiervan verbruikt de zelf-vernetting van AGE zwavel, wat een negatieve invloed heeft op de interactie tussen polymeer en vulstof en tussen de polymeren onder elkaar. Het lijkt er dus op dat de waarschijnlijkheid van koppeling of nevenreacties wordt beïnvloed door de concentratie of mate van reactie van AGE.

De modificatiestudies die zijn uitgevoerd met behulp van verschillende oppervlaktemodificaties met silanen, thiolen en epoxide, geven aan dat de toepassing van oppervlaktemodificatie agentia de versterkende eigenschappen van HTT lignine efficiënt kan verbeteren tot een bepaald niveau, wat resulteert in een semi-versterkende vulstof in vergelijking met het hoog versterkende roet. Het resultaat geeft aan dat, rekening houdend met het specifieke oppervlak van de vulstof, het versterkende effect van HTT lignine verder kan worden verbeterd door sterkere grensvlakinteracties tussen HTT lignine en rubber. Van de onderzochte modificatie agentia, ongeacht de clustering van vulstoffen of slechte microdispersie, vertoont het op silaan gebaseerde koppelingsagens, TESPT, het grootste effect in het met HTT lignine versterkte SSBR/BR-mengsel. Dit kan worden toegeschreven aan de hoge graad van interactie tussen vulstof en polymeer als gevolg van de koppeling tussen niet-gereageerde thiol- of zwavelfunctionaliteiten van het silaan en de dubbele bindingen van rubber, evenals de condensatiereactie tussen ethoxygroepen van het silaan en van het gefunctionaliseerde rubber in vergelijking met de andere modificatie agentia.

Over het algemeen kan uit de huidige studie, die is uitgevoerd met één bepaalde graad lignine: zachthout Kraft-lignine, worden geconcludeerd dat een nabehandelingsproces zoals hydrothermale behandeling de versterkende effecten van lignine in een apolair rubber versterkt. Verdere ontwikkeling van het HTT-proces om de deeltjesgrootte te verkleinen en/of de oppervlaktechemie te veranderen, is essentieel om lignine te kunnen gebruiken als versterkende vulstof in een apolair rubber. De oppervlaktemodificatiestudies met HTT lignine tonen aan dat het reactief is ten opzichte van de rubber-reactieve functionaliteiten, met name thiol (-SH). Deze eigenschap van HTT lignine vormt een uitdaging bij het identificeren van een geschikt koppelingsagens voor oppervlaktemodificatie zoals in het geval van een silica/silaansysteem. Bovendien werd aangetoond dat de ethoxy-functionele groep niet reactief is voor HTT lignine. Deze bevinding benadrukt de bestaande kennislacune in de modificatie van HTT lignine. De aanwezigheid van ethoxy-groepen in combinatie met een thiolgroep kan de koppeling tussen HTT lignine en een in de eindketen triethoxysilyl-gefunctionaliseerd rubber vergemakkelijken via condensatie van de ethoxygroepen. Daarom is het van cruciaal belang om de koppeling tussen HTT lignine, modificatieagens en gefunctionaliseerd of niet-gefunctionaliseerd rubber beter te begrijpen, om het potentieel van HTT lignine als versterkende vulstof volledig te kunnen zien. De twee belangrijkste uitdagingen die verband houden met rubberversterking door HTT lignine zijn uiteindelijk in dit proefschrift geïdentificeerd en moeten in toekomstige studies verder worden uitgewerkt.

TABLE OF CONTENTS

8. Conclusions and Recommendations 193

Research deliverables 201

Acknowledgements 203

1. Introduction

This chapter provides a brief background to the need for sustainability in tires. It also outlines the main objective and structure of this thesis.

1.1 Motivation

In the last two decades, environmental concerns related to the massive exploitation of non-renewable fossil resources and a drastic increase in carbon dioxide (CO_2) emission led to an ever-growing interest in the transition from a linear "take-make-dispose" economy towards a circular economy (CE) for a sustainable society.[1] It is estimated that by 2050, the population growth will expand to 9 billion, whereas the generated waste will surge to 3.40 billion tons worldwide.[2,3] Without critical thinking towards a CE, such a boom worsens the ecological imbalance by over-exploiting the available geological resources and results in one-time disposal of the used products on a large scale.[2,3] The rubber industry, particularly the tire industry, is one of the huge manufacturing sectors that follows a linear route of production.[4] With the rising population, it is expected that global tire consumption will increase to about 2.5 billion tons by 2025, and around 1200 million tires are anticipated to be disposed of as waste annually by 2030.[5,6] This enormous growth is dependent on petroleum resources, which affects the ecological balance of the environment. This raises sustainability-related concerns in the tire industry. Therefore, the ultimate mission of key tire companies such as Bridgestone, Continental, Goodyear, Michelin, Pirelli, etc., is to develop 100 % sustainable tires by 2050 and to reduce significantly the tire's carbon footprint.[7–11] To achieve this, the tire industry is steering away from using non-renewable fossil resources to renewable alternatives derived from different sources such as bio-, packaging- and plastic-wastes, even materials that are recycled from worn-out tires. This includes: (i) rubbers from another natural resource, like, guayule or dandelion; (ii) the ISCC PLUS (International Sustainability and Carbon Certification) mass balance approach for certified materials, for example, styrene-butadiene rubber produced from styrene and butadiene obtained from packaging materials and bio-ethanol, respectively; (iii) fillers such as recovered carbon black and silica produced from tire waste and rice husk, respectively; (iv) plasticizers from soybean oil; (v) polymer fibers from recycled PET bottles; (vi) recycled steel fiber from the waste tire.[12] An overview of different raw materials that are gaining attention in the production of sustainable tires is illustrated in **Figure 1.1**. The current target achieved by Bridgestone is around 75 %, followed by Goodyear, Continental, Michelin, and Pirelli in the range of 70 %, 65 %, 58 %, and 30 %, respectively, by using a combination of renewable and recycled materials.[7–11] For example, in 2023, Continental launched the UltraContact NXT tire consisting of 32 % of renewable materials, 5 % of recycled materials, and 28 % of ISCC PLUS (International Sustainability and Carbon Certification) mass balance approach certified materials from bio, bio-circular, and/or circular feedstock.[13]
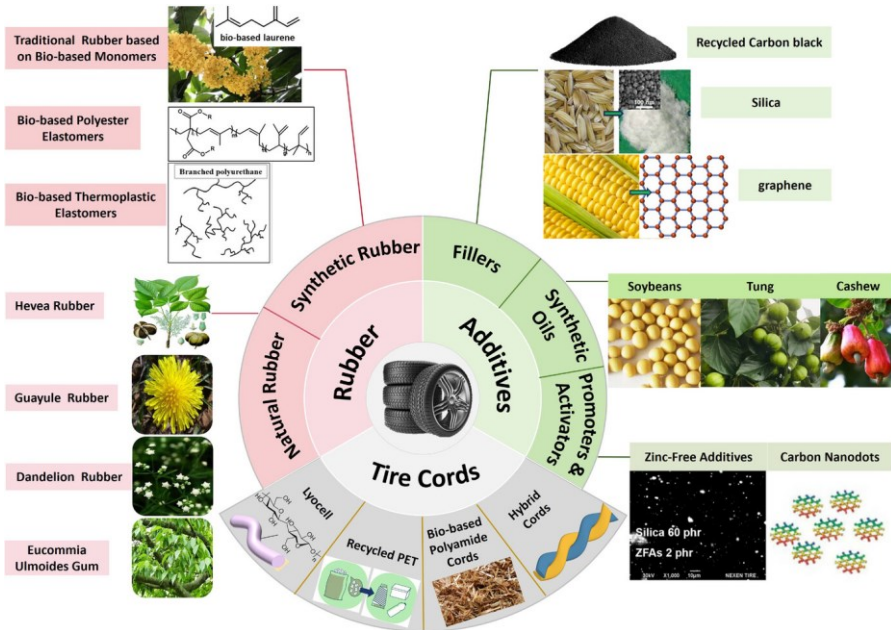
Figure 1.1 Currently used sustainable raw materials in tires [Reproduced from the published article of S. Deng et al.[4]]

Another objective of the tire producers is to minimize the vehicle's fuel consumption caused by tire rolling resistance and the resulting CO_2 emission. The tire's rolling resistance accounts for 20 - 30 % of a vehicle's fuel consumption and CO_2 emission of 24 %.[14] It is estimated that a 30 % reduction in the rolling resistance of a passenger car tire results in a 3 - 6 % improvement in fuel savings depending on the vehicle type, road and driving conditions.[15] Besides the fuel economy, the energy loss due to rolling also affects the tire performance, such as handling, traction, treadwear, etc., and durability of the tire as the increase in the temperature during the cyclic deformation changes the viscoelastic properties of the rubber compound.[15] Thus, fine-tuning the total hysteresis loss of the rubber compound by proper selection of ingredients can have a significant impact on the rolling resistance of a tire.[15] Among the ingredients, reinforcing particulate fillers used for the reinforcement of rubber substantially contribute to the increase in compound hysteresis. It can also be observed from **Figure 1.2** that filler accounts for 24 - 26 wt.% in the tire composition, next to polymers.[1] In the past, a huge reduction in rolling resistance (20 %) was carried out by replacing conventional carbon black with silica as a filler.[16] As the production of carbon black and silica involves the usage of non-renewable (fossil-based mineral oil) and finite resources (sodium silicate and sulfuric acid), respectively, a transition towards the use of fully bio-based fillers as an alternative to conventional silica and carbon black can enable the accomplishment of sustainability and fuel economy goals. In this context, the use of lignin derived from lignocellulosic biomass has attracted the scientific community owing to its wide-scale availability and renewable nature.[17] The advent of biorefineries will also generate more quantities of lignin than demanded by the

1

current market. It is estimated that by 2030, lignin generation will increase by 225 million tons per year.[18] Thus, in terms of volume, it has the potential to replace the current fillers in the future.
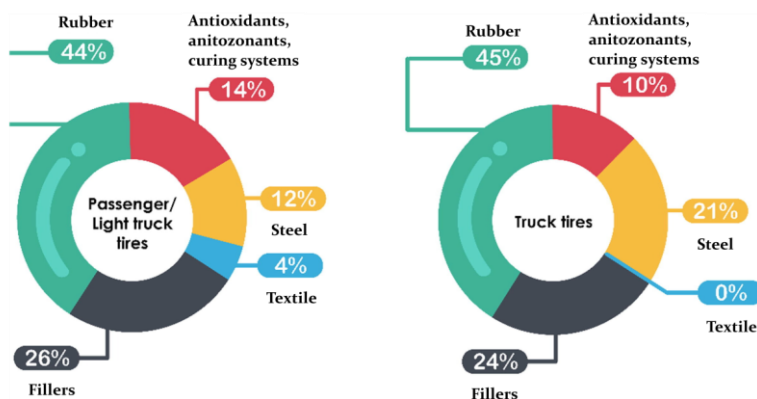

Figure 1.2 Raw material composition of a passenger car (left) and truck tires [Reproduced from the published article of J. Araujo-Morera et al.[1]]

Numerous studies were carried out in the past to effectively utilize different kinds of technical lignin, such as Kraft, lignosulphonate, and organosolv, in rubber with the aim to enhance the reinforcement characteristics like morphological, physiochemical, thermal, and mechanical properties.[19–29] These studies concluded that the interfacial adhesion between lignin and rubber is weak due to the self-aggregation of lignin, thereby resulting in a low reinforcing effect.[19–29] This is related to the high polarity of lignin due to the presence of different functionalities, such as hydroxy, carboxyl, and carbonyl. To overcome the dispersion and compatibility issues of lignin in rubber, some authors intensively used surface modifiers to hydrophobize lignin.[24,30,31] In spite of the improved properties, the level of reinforcement achieved is still lower in comparison to the conventionally used fillers. This is presumed to be due to the large particle size (or low specific surface area) and high polarity of lignin compared to the reinforcing carbon black filler. One of the promising strategies for enhancing the characteristics of lignin for filler application is to utilize the hydrothermal treatment (HTT) process.[32] This technique can reduce the functional groups of the lignin and can produce a relatively non-reactive and thermally stable material with a higher surface area compared to unprocessed lignin.[33–36] Thus, it can be hypothesized that the reinforcing effects of HTT lignin in a non-polar rubber are better than those of the unprocessed lignin. Besides, the presence of still available polar functional groups offers a hydrophilic nature to the HTT lignin but, at the same time, makes it versatile for hydrophobation by surface modification. This, in theory, can promote the compatibility of HTT lignin with the rubber and enhance its reinforcing performance. In addition to the above-mentioned technical advantage, the recent environmental cradle-to-gate assessment of lignin-based HTT filler conducted using life

cycle assessment (LCA) highlights that substitution of the conventional fillers carbon black and silica by HTT lignin can offer significant reduction in greenhouse gas emissions (approximately 5 kg of CO_2 equivalent/kg of filler can be saved), air pollutant emissions (80 - 93 % lower sulfur dioxide (SO_2) emissions), and 88 - 98 % lower polycyclic aromatic hydrocarbon (PAH) emissions during the production process.[33]

1.2 Objective of the Research

The ultimate objective is to use a lignin-based filler as an alternative to non-sustainable carbon black and silica and therewith, develop a partially sustainable compound for rubber applications. In this direction, hydrothermally treated (HTT) Kraft lignin produced by SunCoal Industries GmbH is exploited as a filler for a non-polar rubber compound. Thus, the thesis is focused on:

(i) investigating and understanding the reinforcing potential of hydrothermally treated Kraft lignin in non-polar rubber in comparison to the conventional reinforcing fillers;

(ii) discerning the potential of silane and non-silane-based modifiers for HTT lignin and analyzing their impact on the in-rubber reinforcement of HTT lignin-filled composites;

(iii) elucidating the mechanism of coupling between HTT lignin and modifiers, which can potentially broaden the scope of HTT lignin filler for rubber applications.

1.3 Outline of the Thesis

The thesis is structured into eight chapters:

Chapter 2 gives a brief overview of the structure and applications of lignocellulosic (LC) biomass derivatives. Lignin is extensively reviewed with emphasis on its extraction techniques, the obtained material properties and its application in rubber. A brief introduction to the hydrothermal process is presented.

Chapter 3 presents preliminary studies carried out to understand the existing difference in the material properties of commercially available Kraft lignin and hydrothermally treated (HTT) Kraft lignin. Furthermore, the reinforcing potential of hydrothermally treated lignin in comparison to the untreated lignin and highly reinforcing carbon black and silica is investigated in a tire tread formulation.

Chapter 4 covers the exploitation of silane-type modifiers to enhance the compatibility between HTT lignin and rubber. Four different silanes are employed, and their in-rubber properties are evaluated.

1

Chapter 5 explores in depth the underlying mechanism of coupling between silane and HTT lignin to improve rubber performance. Model studies with substituted phenols of similar chemical structures like lignin are carried out to elucidate the possible reactions. Based on these results, a coupling mechanism is proposed.

Chapter 6 focuses on the possible use of dithiols as a lignin coupling agent based on the results of Chapter 5. It investigates the impact of thiol modification on the properties of HTT lignin and on the in-rubber properties of HTT lignin-filled rubber compounds.

Chapter 7 investigates the reactivity of different non-silane-based surface modifiers with HTT lignin. It explores the use of an epoxide-based coupling agent for HTT lignin and investigates its influence on the in-rubber properties.

Chapter 8 summarizes the main findings of this work and provides recommendations for future endeavors on this topic.

References

(1) Araujo-Morera, J.; Verdejo, R.; López-Manchado, M. A.; Hernández Santana, M. Sustainable Mobility: The Route of Tires through the Circular Economy Model. Waste Management 2021, 126, 309–322.

(2) Arruda, E. H.; Melatto, R. A. P. B.; Levy, W.; Conti, D. de M. Circular Economy: A Brief Literature Review (2015–2020). Sustainable Operations and Computers 2021, 2, 79–86.

(3) Suchek, N.; Fernandes, C. I.; Kraus, S.; Filser, M.; Sjögrén, H. Innovation and the Circular Economy: A Systematic Literature Review. Business Strategy and the Environment 2021, 30 (8), 3686–3702.

(4) Deng, S.; Chen, R.; Duan, S.; Jia, Q.; Hao, X.; Zhang, L. Research Progress on Sustainability of Key Tire Materials. SusMat 2023, 3 (5), 581–608.

(5) Shoul, B.; Marfavi, Y.; Sadeghi, B.; Kowsari, E.; Sadeghi, P.; Ramakrishna, S. Investigating the Potential of Sustainable Use of Green Silica in the Green Tire Industry: A Review. Environ Sci Pollut Res Int 2022, 29 (34), 51298–51317.

(6) Ul Islam, M. M.; Li, J.; Roychand, R.; Saberian, M.; Chen, F. A Comprehensive Review on the Application of Renewable Waste Tire Rubbers and Fibers in Sustainable Concrete. Journal of Cleaner Production 2022, 374, 133998.

(7) https://www.bridgestone.com/responsibilities/environment/resources/ (accessed 2023-11-23).

(8) https://www.continental-tires.com/products/b2c/car/sustainable-tires/ (accessed 2023-11-23).

(9) https://corporate.goodyear.com/us/en/responsibility/sustainable-sourcing/sustainable-materials (accessed 2023-11-23).

(10) https://www.michelin.com/en/innovation/vision-concept/sustainable/ (accessed 2023-11-23).

(11) https://corporate.pirelli.com/corporate/en-ww/sustainability/sustainability (accessed 2023-11-23).

(12) Thomas, J.; Patil, R. The Road to Sustainable Tire Materials: Current State-of-the-Art and Future Prospectives. Environ. Sci. Technol. 2023, 57 (6), 2209–2216.

(13) https://www.continental.com/en/press/press-releases/20230614-ultracontact-nxt/ (accessed 2023-11-23).

(14) Tires and Fuel Economy. https://www.energy.gov/energysaver/tires-and-fuel-economy (accessed 2023-11-23).

(15) Zhang, P.; Morris, M.; Doshi, D. Materials Development for Lowering Rolling Resistance of Tires. Rubber Chemistry and Technology 2016, 89.

(16) Jacobsson, M. Improving Hysteresis through Filler Modifications and Smart Compounding. Rubber World 2013, 247, 22–26.

(17) Roy, K.; Debnath, S. C.; Potiyaraj, P. A Review on Recent Trends and Future Prospects of Lignin Based Green Rubber Composites. J Polym Environ 2020, 28 (2), 367–387.

(18) Bajwa, D. S.; Pourhashem, G.; Ullah, A. H.; Bajwa, S. G. A Concise Review of Current Lignin Production, Applications, Products and Their Environmental Impact. Industrial Crops and Products 2019, 139, 111526.

1

1

(19) Keilen, J. J.; Pollak, A. Lignin for Reinforcing Rubber. Rubber Chemistry and Technology 1947, 20 (4), 1099–1108.

(20) Kumaran, M. G.; De, S. K. Utilization of Lignins in Rubber Compounding. Journal of Applied Polymer Science 1978, 22 (7), 1885–1893.

(21) Setua, D. K.; Shukla, M. K.; Nigam, V.; Singh, H.; Mathur, G. N. Lignin Reinforced Rubber Composites. Polymer Composites 2000, 21 (6), 988–995.

(22) Košíková, B.; Gregorová, A. Sulfur-Free Lignin as Reinforcing Component of Styrene–Butadiene Rubber. Journal of Applied Polymer Science 2005, 97 (3), 924–929.

(23) Frigerio, P.; Zoia, L.; Orlandi, M.; Hanel, T.; Castellani, L. Application of Sulphur-Free Lignins as a Filler for Elastomers: Effect of Hexamethylenetetramine Treatment. BioResources 2014, 9.

(24) Bahl, K.; Swanson, N.; Pugh, C.; Jana, S. C. Polybutadiene-g-Polypentafluorostyrene as a Coupling Agent for Lignin-Filled Rubber Compounds. Polymer 2014, 55 (26), 6754–6763.

(25) Buono, P.; Duval, A.; Verge, P.; Averous, L.; Habibi, Y. New Insights on the Chemical Modification of Lignin: Acetylation versus Silylation. ACS Sustainable Chem. Eng. 2016, 4 (10), 5212–5222.

(26) Barana, D.; Ali, S. D.; Salanti, A.; Orlandi, M.; Castellani, L.; Hanel, T.; Zoia, L. Influence of Lignin Features on Thermal Stability and Mechanical Properties of Natural Rubber Compounds. ACS Sustainable Chem. Eng. 2016, 4 (10), 5258–5267.

(27) Mohamad Aini, N. A.; Othman, N.; Hussin, M. H.; Sahakaro, K.; Hayeemasae, N. Lignin as Alternative Reinforcing Filler in the Rubber Industry: A Review. Frontiers in Materials 2020, 6, 329–347.

(28) Hait, S.; De, D.; Ghosh, P.; Chanda, J.; Mukhopadhyay, R.; Dasgupta, S.; Sallat, A.; Al Aiti, M.; Stöckelhuber, K. W.; Wießner, S.; Heinrich, G.; Das, A. Understanding the Coupling Effect between Lignin and Polybutadiene Elastomer. Journal of Composites Science 2021, 5 (6), 154–169.

(29) Shorey, R.; Gupta, A.; Mekonnen, T. H. Hydrophobic Modification of Lignin for Rubber Composites. Industrial Crops and Products 2021, 174, 114189.

(30) Chen, C.; Zhu, M.; Li, M.; Fan, Y.; Sun, R.-C. Epoxidation and Etherification of Alkaline Lignin to Prepare Water-Soluble Derivatives and Its Performance in Improvement of Enzymatic Hydrolysis Efficiency. Biotechnology for Biofuels 2016, 9 (1), 87.

(31) Jiang, C.; He, H.; Yao, X.; Yu, P.; Zhou, L.; Jia, D. The Aggregation Structure Regulation of Lignin by Chemical Modification and Its Effect on the Property of Lignin/Styrene–Butadiene Rubber Composites. Journal of Applied Polymer Science 2018, 135 (5), 45759.

(32) Sekar, P.; Martinho, R. P.; Talma, A. G.; Gojzewski, H.; Stücker, A.; Schwaiger, B.; Podschun, J.; Blume, A. Horizons in Coupling of Sulfur-Bearing Silanes to Hydrothermally Treated Lignin toward Sustainable Development. ACS Sustainable Chem. Eng. 2023.

(33) Meisel, K.; Röver, L.; Majer, S.; Herklotz, B.; Thrän, D. A Comparison of Functional Fillers-Greenhouse Gas Emissions and Air Pollutants from Lignin-Based Filler, Carbon Black and Silica. Sustainability 2022, 14 (9), 5393.

(34) Wittmann, T. Method for Obtaining Stabilized Lignin Having a Defined Particle-Size Distribution from a Lignin-Containing Liquid. US20170247255A1, 2017.

(35) Wikberg, H.; Ohra-Aho, T.; Pileidis, F.; Titirici, M. M. Structural and Morphological Changes in Kraft Lignin during Hydrothermal Carbonization. ACS Sustainable Chem. Eng. 2015, 3 (11), 2737–2745.

(36) Titirici, M. M.; Antonietti, M. Chemistry and Materials Options of Sustainable Carbon Materials Made by Hydrothermal Carbonization. Chemical Society Reviews 2010, 39 (1), 103–116.

1

1

Chapter **2**

2. Potential of Lignin in Material Applications

A review on the exploration of lignin for high-value applications and the existing challenges

The present review discusses one of the essential feedstocks for sustainable material development, lignocellulosic biomass. The chemical compositions of lignocellulosic biomass are briefly discussed, with more emphasis on lignin's chemical structure, extraction techniques, and the available technical lignins and their current and future applications. A particular focus is given to the application of lignin in rubber, including the practical implementation challenges and current approaches to overcome them.

2.1 Lignocellulose Biomass, a Sustainable Carbon Source

Lignocellulosic (LC) biomass is considered to be one of the most abundant, cheap, carbon-neutral renewable feedstocks for the transition from a linear to a circular economy, thereby addressing the growing demands of society and environment-related issues.[1,2] An estimate of around 181.5 billion tons of LC biomass is produced globally every year via photosynthesis.[3,4] Of which, 8.2 billion tons of LC are currently used as fodder and for energetic and material purposes like construction, paper production, etc.[5] The sources of these LC biomasses largely depend on non-edible plant resources such as agricultural wastes, forestry residues, grasses, and woods, which do not compete with the food and animal feed supplies.[5] Further, these biomasses can easily grow on non-arable lands and most often do not serve ecological functions such as retaining soil humus content or replacing nutrient withdrawal by harvested wood. Such features make it a potential candidate for replacement of petroleum-based raw materials over other bio-based feedstocks (crops containing starch, sugar, and vegetable oil) in the production of low molecular-weight chemicals, monomers, fillers, and bio-fuels.[4,6]

LC biomass is a renewable carbon-rich material found abundantly in the macro and microfibrils of the rigid walls of plant cells. It is constituted by approximately 95 wt.% of three main biopolymer components: cellulose, hemicellulose, and lignin.[7] The remaining 5 wt.% is composed of minor components such as inorganic ashes and organic extractives such as small aromatic molecules, fats, and waxes.[8] In the plant cell wall, the cellulosic polymer chains are tightly bound together by hydrogen bonds as bundled fibrils that are embedded in an amorphous matrix of hemicellulose and lignin, as shown in **Figure 2.1**. This kind of arrangement results in complex, non-uniform, three-dimensional network structures within the cell walls, depending on the type of LC. The developed stiff structure contributes to the inherent physicochemical barrier properties of LCs.[2,9,10]
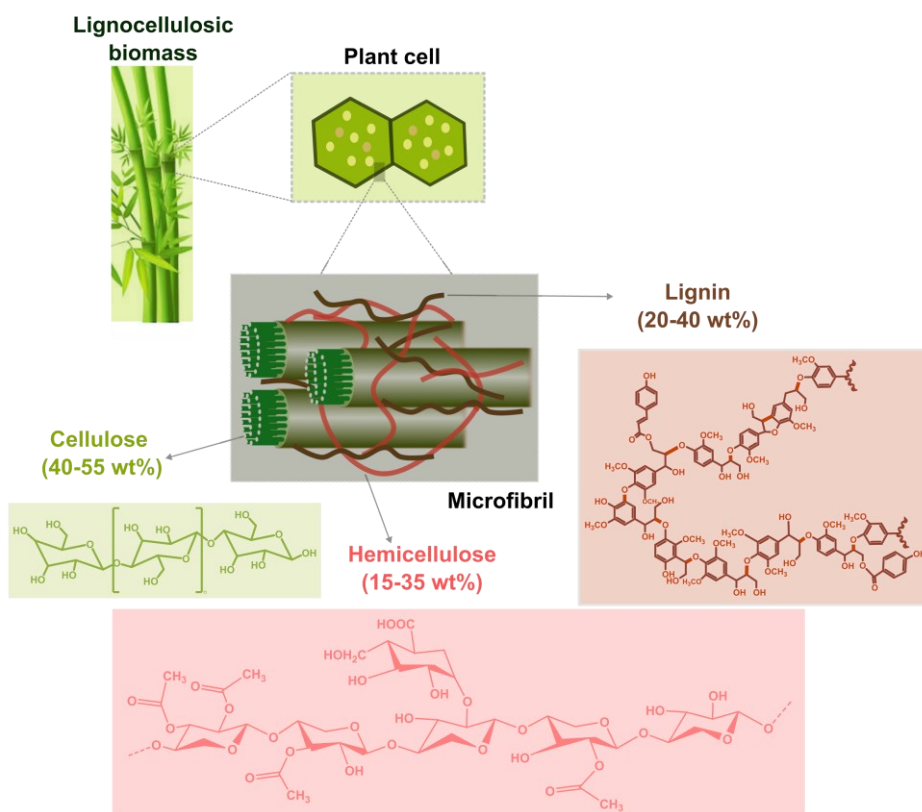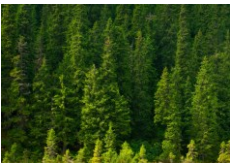
Figure 2.1. Structural overview of the major components of lignocellulosic biomass in the plant cell wall: Cellulose, linear C6 sugar glucose chains (green); hemicelluloses, branched sugar chains (red); and lignin, aromatic three-dimensional branched polymer of phenylpropanoid units (brown)[2,8]

The quality and relative composition of the LC components vary according to species, plant types (softwood, hardwood, or grasses), tissues, and maturity of the plant cell wall.[2,9,10] **Table 2.1** summarizes the variation in composition of major LC components depending on the plant species and types.

Table 2.1. Composition of lignocellulosic biomass components in various lignocellulosic materials (Data reproduced from Isikgor et al.[2], Menon et al.[11], Danso-Boateng et al.[12])

Lignocellulosic biomass		Cellulose (%)	Hemicellulose (%)	Lignin (%)
Hardwood	Poplar	45 - 51	25 - 28	10 - 21
	Oak	38 - 46	19 - 30	22 - 29
	Eucalyptus	39 - 46	24 - 28	29 - 32
Softwood	Pine	42 - 49	15 - 23	23 - 29
	Douglas fir	35 - 48	20 - 22	15 - 21
Agricultural waste	Wheat straw	35 - 39	22 - 30	12 - 16
	Barley straw	36 - 43	24 - 33	6 - 10
	Rice straw	29 - 35	23 - 26	17 - 19
	Sugarcane bagasse	25 - 45	28 - 32	15 - 25
	Corn cobs	34 - 41	32 - 35	6 - 16
Grasses	Sorghum Straw	32 - 35	24 - 27	15 - 21
	Switchgrass	35 - 40	25 - 30	15 - 20

Cellulose is the most abundant linear homopolysaccharide, comprising β-glucopyranose units linked by β-1,4-glucosidic bonds[13] with a degree of polymerization (DP) ranging from 500 to 15000 glucose units.[14] It accounts for about 40 - 50 wt.% of the total weight of LC biomass.[15] The linear configuration of the cellulose chains is the result of extensive intrachain hydrogen bonding between hydroxy groups and oxygens of the adjoining ring molecules. This leads to the formation of elementary cellulose fibrils, which further aggregate into larger microfibrils by Van der Waals and intermolecular hydrogen bonding.[16–18] Within the microfibrils, there are regions where the cellulose chains are arranged in highly ordered (crystalline) and disordered (amorphous) structures.[16–18] The fibrous structure and strong hydrogen bonding make cellulose strongly resistant to hydrolysis and enhance the mechanical strength of LCs.[7] Cellulose has been dominantly utilized for the production of paper for ages.[19] It is also widely used in the textile industry and pharmaceuticals. Recently, nanofibers of cellulose have been explored in other applications such as nonwoven tissues, membranes, coatings, and absorbent materials.[18,20,21]

Hemicelluloses are an amorphous heteropolymer composed of different 5- and 6-carbon monosaccharide units such as pentoses (xylose, arabinose), hexoses (mannose, galactose, glucose), and lesser amounts of rhamnose, glucuronic acid, methyl glucuronic acid, and galacturonic acid.[22] It accounts for about 15 - 35 wt.% of the dry mass of annual and perennial plants.[23] The DP of hemicellulose is lower than cellulose, and it ranges between 80 - 200.[24] Unlike cellulose, hemicelluloses are less crystalline due to different monomeric compositions and, hence, can be readily hydrolyzed by acids to their monomer components. Depending on the biomass feedstock, the structure, the length and type of the main chain, and the distribution and type of side chain vary.[25] For example, hemicelluloses of hardwood-type biomass are composed of glucuronoxylan polysaccharides with some acetyl groups, whereas softwood contains glucomannans ones.[25,26] Hemicelluloses are used to produce alcohol by fermentation and sorbitol by reduction, which has primary applications in food, toothpaste, cosmetics, explosive manufacturing, etc.[27]

Lignin is the second most abundant natural polymer and accounts for approximately 15 - 30 % of the weight basis of all-natural, non-fossil organic carbon on the Earth.[28] Lignin is a complex, aromatic polymer constituted of phenylpropanoid subunits (C_9, **Figure 2.2(a)**) such as p-hydroxyphenyl (H-unit), guaiacyl (G-unit), syringyl (S-unit), and formed by polymerization of hydroxycinnamyl alcohols such as p-coumaroyl, coniferyl, and sinapyl alcohols as shown in **Figure 2.2 (b) and (c)**.
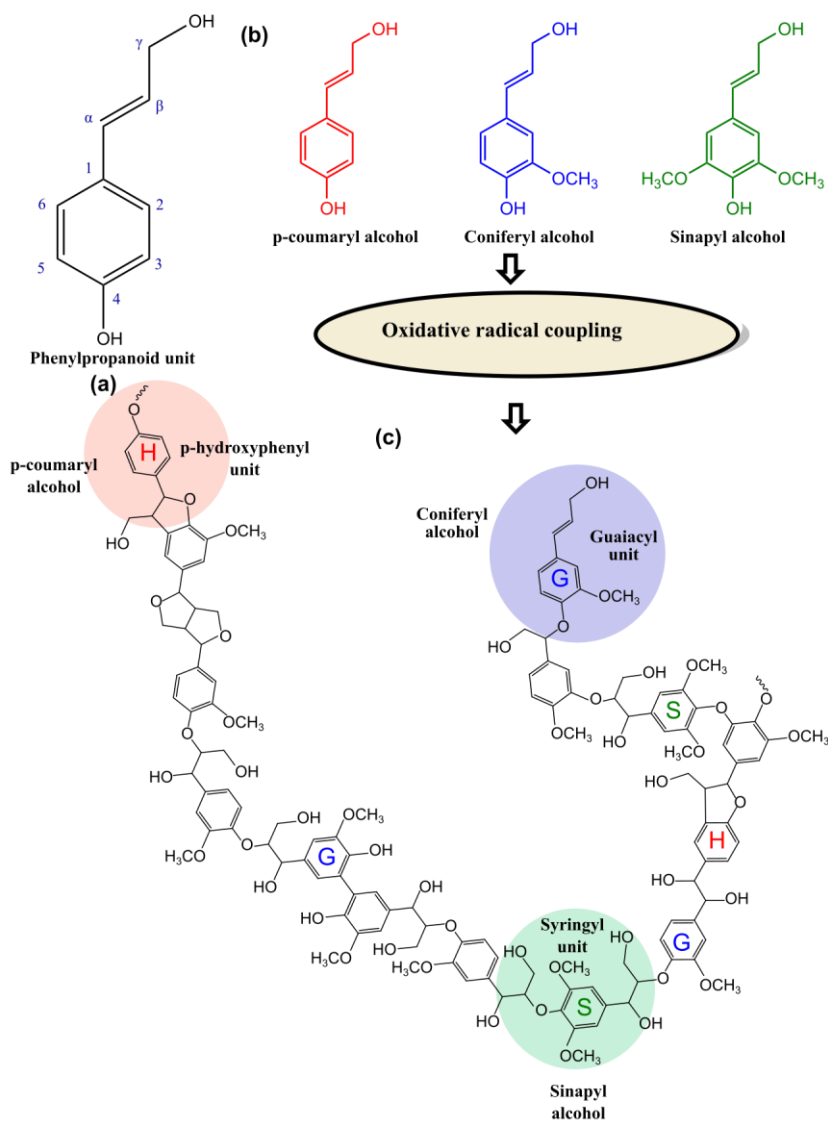
2

2

Figure 2.2. (a) General structure of monomer or monolignol; (b) Type of major monomers or monolignols of lignin, differing in the degree of methoxylation; and (c) their corresponding polymeric units

The content of monolignols (key building blocks, H/G/S) and the resulting lignin structure vary depending on the plant type, as represented in **Table 2.2**, and it is common to address lignin in terms of its source.[29] For instance, softwood lignin is made up of more than 90 % of coniferyl alcohol (G-unit), and the remaining consists of p-coumaryl alcohol units (H-unit). In contrast, hardwood lignin is made of varying ratios of coniferyl (G-unit) and sinapyl alcohol (S-unit) type. In addition to the different proportional compositions of the monolignols, the total lignin content also varies depending on the plant type. In

general, the lignin content of softwood (25 - 31 wt.%) is higher than that of hardwood (16 - 24 wt.%) and grasses (16 - 21 wt.%).[30,31]

Table 2.2. Proportions of monolignols and total bond linkages in different plant types (Data from Notley et al. [29] and Liu et al.[30])

		Hardwood (%)	Softwood (%)	Herbaceous (%)
Monolignols	H -unit	0 - 8	0 - 5	5 - 33
	G-unit	25 - 50	95 - 100	33 - 80
	S- unit	46 - 75	0	20 - 54
Inter-unit linkages between monolignols	β-O-4	50 - 65	43 - 50	74 - 84
	α-O-4	<1	5 - 7	n.d.*
	4-O-5	6 - 7	4	n.d.
	5-5	<1	5 - 7	n.d.
	β-β	3 - 12	2 - 6	1 - 7
	β-5	3 - 11	9 - 12	5 - 11
	β-1	<2	<2	<2

*n.d.- unknown

These different monolignols are connected in a random fashion either by alkyl-aryl ether units, i.e., C-O-C (α-O-4, β-O-4, 4-O-5), or by carbon-carbon, C-C linkages (β-β, β-5, β-1, 5-5) to form complex, three-dimensional molecular architectures, as shown in **Figure 2.3**.

Again, the distribution of chemical linkages between the monomers varies significantly depending on the species (refer to **Table 2.2**).[29] Among the aforementioned interunit linkages, β-O-4 covalent bonds formed through the coupling of the phenolic radicals of β carbon with the hydroxy group at the 4 position of the phenylpropane structure are the predominantly existing connections in both hardwood and softwood lignin.[29,32] This bond plays a decisive role in the yield of phenolic hydroxy groups and is susceptible to different isolation and degradation processes. The C-C linkages are less likely to degrade.[28] Having defined the basic units of lignin and the possible interconnections between monomers, the understanding of functional groups of lignin is also of paramount importance. The oxygen in the lignin belongs to a variety of functional groups. It is known from the monolignols that the attached oxygen is either in the form of methoxy groups or in

aliphatic and phenolic hydroxy groups, as represented in **Figure 2.2**.[29] In monolignols and lignin polymer biosynthesis, several other functional groups can be found, such as primary and secondary aliphatic hydroxy, carbonyl groups such as ketone and aldehyde as well as carboxylic acid groups, as illustrated in **Figure 2.3**.[33] These functional groups confer unique functional properties to lignin depending upon their amount, nature, and isolation process. The presence of different monolignols and variation in their composition (H/G/S), wide distribution of interunit linkages, and the resulting functionalities impart remarkable differences in the structure and composition of lignin.
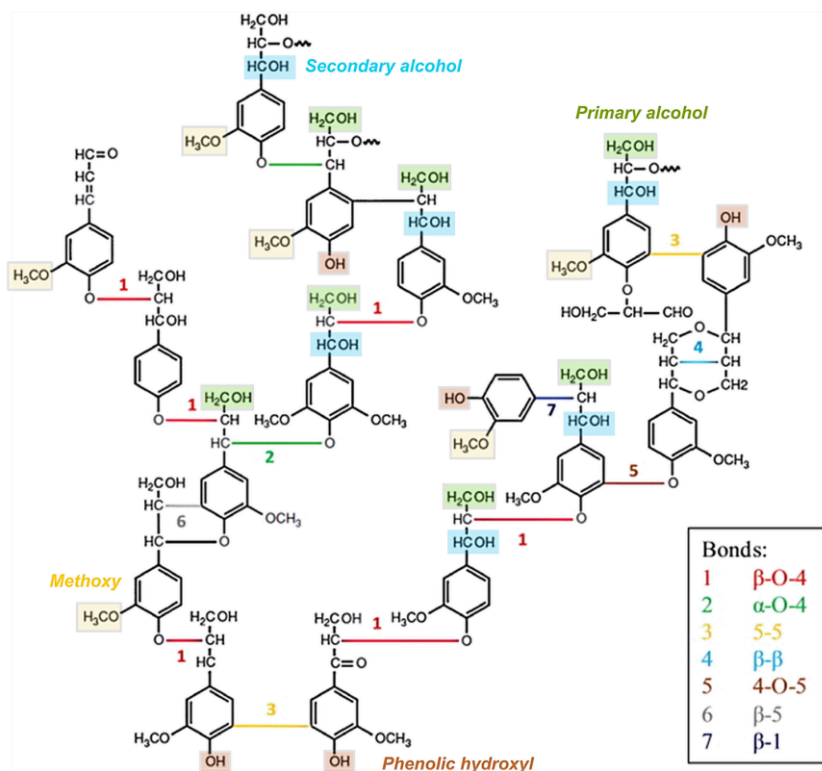

Figure 2.3. Representative structure of lignin showing different interunit linkages between monolignols and functional groups [Reproduced from the published article of E. Windeisen et al. with permission from Elsevier[34]]

2.2 Extraction of Lignin from Lignocellulosic Biomass

Numerous cutting-edge pretreatment techniques have been developed to date to isolate different components of LC biomass and allow for the efficient valorization of the isolated components. The pretreatment processes primarily focus on separating lignin either as an insoluble solid residue or as a soluble matter from biomass and are only interested in the carbohydrate fractions (i.e., cellulose and hemicellulose). This is named in the literature as delignification.[35,36] In paper and pulp industries, lignin is isolated from LC by fractionation, and in biorefineries, lignin is separated by enzymatic hydrolysis of

polysaccharides in order to utilize the carbohydrate portion, for example, paper and cellulosic ethanol production, respectively, as presented in **Figure 2.4**. Pulping methods result in structurally heavily modified lignins, while lignins obtained from biorefineries contain minor structural modifications.[35]
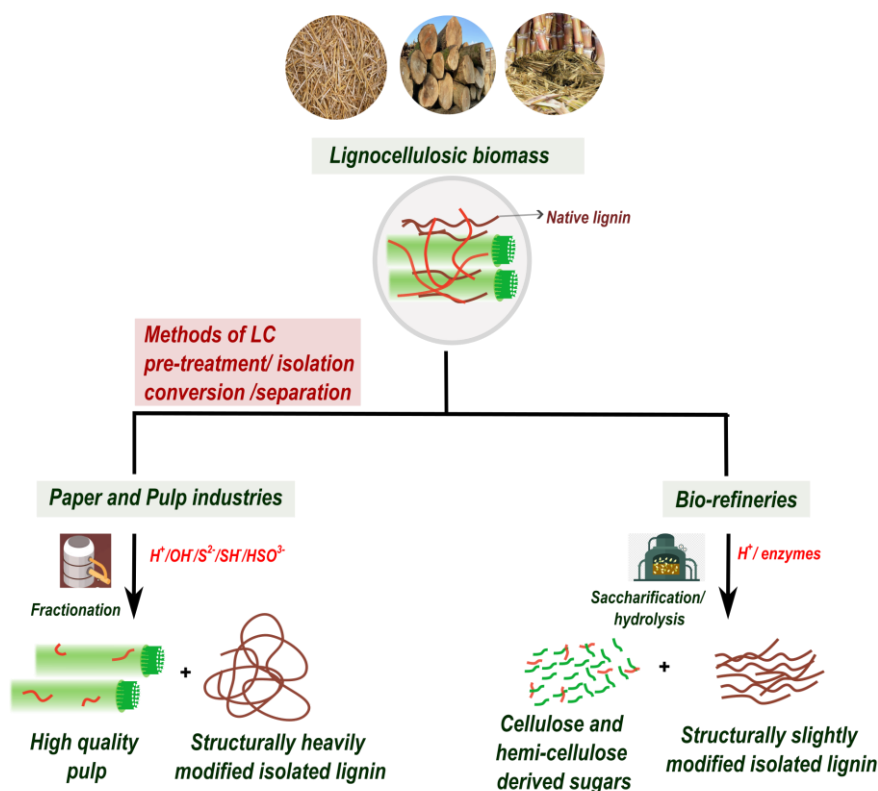
Figure 2.4. Valorization of lignocellulosic biomass[35]

It is estimated that the production of lignin on earth is around ~500 - 3600 million tons annually.[37] Currently, 50 million tons of lignin in the form of black liquor (by-product from Kraft lignin process containing 90 - 95 % soluble lignin fragments and other extractives) is produced alone each year by paper and pulp industries.[37] Furthermore, the bioethanol industry in the USA alone generates around 0.15 million tons of residual lignin annually.[37–39] Of these generated quantities, only 1 - 2 % of lignin is being utilized (which will be discussed later in **Section 2.3**), and the rest is discarded. Due to the high carbon content in lignin, it is a potential resource for many applications. This section will discuss concisely the extraction techniques followed in paper and biorefinery industries to give an insight into structural changes of native lignin.

2

2.2.1 Paper and Pulp Industries

Traditionally, lignin is extracted in huge volumes by commercial pulping industries, which use various delignification technologies to separate lignin from plant polysaccharides in order to produce commodity cellulose. The resulting lignins, in general, are addressed as industrial or technical lignins. The widely used chemical pulping processes to extract lignin from LC are sulfate (Kraft), sulfite (Lignosulfonate), soda, and organosolv (named after the usage of organic solvent in the process).[28,40] All the employed methods have the same working principle, chemical degradation or depolymerization of the polymeric lignin structure caused by scission of β-O-4 and other linkages. This makes lignin fragments and other components of LC, such as hemicellulose, rosin, soaps, and inorganic compounds, soluble in the pulping media, which is named black/brown liquor depending on the extraction process or, in general, pulping liquor.[28] However, the extraction methods are defined by different processing parameters such as temperature, pH, concentration, the type of solvent, and pressure, which influence the final lignin quality and other properties such as extraction yield, lignin functionality, molar mass, and solubility. This is mainly because, depending on the process and its parameters, new lignin structures (condensed structures with stable C-C bonds) can be formed by repolymerization reactions, and new types of end groups can also be generated. It is reported that the differences between lignin from various plant sources are minor in relation to the differences that can originate from the pulping processes.[41] Thus, it is important to select the best valorization path for converting lignin to value-added products. **Table 2.3** summarizes different isolation protocols for the extraction of lignin.

In the Kraft or sulfate process, a white liquor, which is a mixture of sodium hydroxide (NaOH) and sodium sulfide (Na_2S), taken typically in a ratio of 1:0.25-0.70 mol/l respectively, is used to generate Kraft/sulfated lignin at temperatures between 150 - 180 °C.[31] Under these conditions, the α- aryl and β-aryl ether bonds of lignin break, followed by the formation of quinone methide (QM). The formed QMs can react with the hydrogen sulfide anions, resulting in the introduction of reactive thiol functionalities in the lignin structures. These groups, at high pH values, react further to form different functionalities such as double bonds, aldehyde, ketone, etc. This allows lignin depolymerization and generation of soluble lignin fragments at pH values above 12.

Recovery of lignin fractions from black liquor can be achieved through LignoBoost technology.[42] In this technique, lignin is precipitated by CO_2 injection, reducing the pH to 9 - 10.5, and subsequently, filtered and washed by redispersing it in dilute H_2SO_4 (pH 3) to maximize the quantity and purity of lignin recovered from the black liquor.[28] The composition of precipitated Kraft lignin depends on the conditions of precipitation. For instance, lignin precipitated at lower pH values (about 3 or 4) can result in lower methoxyl and a higher carboxyl content of lignin.[43,44] The number average molecular weight (M_n) of lignin from this process varies between 1000 and 3000 g/mol.[45]

In the sulfite process, lignin is isolated by using a heated aqueous solution of a sulfite or bisulfite salt with counter-cations such as sodium, ammonium, magnesium, or calcium. Generally, calcium sulfite ($CaSO_3$) or magnesium sulfite ($MgSO_3$) is used in pulping liquor, and the presence of sulfonic groups makes the process acidic in nature. Depending on the type of the used cation and its solubility in aqueous solutions, the pH of the reaction mixture can be varied between 1 and 13.5.[28,31] This broad variation in pH of the pulping solution, thus, allows the sulfonation of the lignin aliphatic chain at distinct locations by attacking β-O-4 and C_α linkages. This process enriches the carboxylic and phenolic hydroxy functionalities in the lignin structure. The presence of these polar functionalities enhances the water-solubility of the resulting lignin. This facilitates the lignin to be soluble in the aqueous pulping liquor along with hemicellulose. The lignins produced by the sulfite process are known as lignosulphonates. Unlike Kraft lignins, it is not possible to precipitate lignosulfonates by changing the pH as the lignin is soluble throughout the entire pH range.[46] Thus, recovery of lignosulfonate lignin from the aqueous mixture can only be achieved by techniques such as precipitation by a cationic substance, e.g., a long-chain aliphatic amine to form a water-insoluble salts or ultrafiltration.[28,31,43] The obtained lignosulfonates have high molecular weight compared to other delignification processes, for instance, the number average molecular weight (M_n) ranges from 15,000 - 50,000 g/mol.[45]

The soda process was the first used chemical pulping method and is typically utilized to extract lignin from LC other than woods, for example, sugarcane bagasse or flax.[47,48] During this process, the LC is added to an aqueous solution of sodium hydroxide (NaOH, 13 - 16 %), and the mixture is heated up to 140 - 170 °C. This results in lignin depolymerization, where cleavage of α-aryl ether and β ether bonds occur, resulting in the generation of free phenolic groups.[31] The resulting lignin fragments can easily be isolated from the pulping liquor via centrifugation or filtration process once the solution is acidified.[28] The obtained lignin has higher purity and lower molecular weight (M_n- 800 – 3000 g/mol) than that obtained by the sulfite process.[28,45]

The organosolv process involves an aqueous–organic solvent mixtures, such as ethanol, acetone, methanol, and organic acids (acetic or formic acid), to isolate LC components. This process targets the breakage of β-O-4 bonds, thus creating an enormous amount of phenolic hydroxy functionalities in the resulting lignin.[40] Depending on the solvent employed, the polarity, structure, and properties of organosolv lignin vary. The lignins from this process can be recovered from the pulping liquor by acid precipitation. This acidic method has several advantages over the other discussed processes: (i) it allows the isolation of all three components found in the LC biomass simultaneously; (ii) it is environmentally a more friendly method as it lacks sulfur, elevated temperatures, and high pressures depending on the organosolv medium; and (iii) it results in lignin of relatively high purity with a lower number average molecular weight around 500 - 5500 g/mol.[40,45,47,50]

2

Table 2.3. Summary of commercial extraction techniques and the obtained technical lignins (Data obtained from Lobato-Peralta et al.,[31] Kun et al., [47] Luo et al.[49])

Lignin type	Method of Separation	Extraction agent and conditions	Sulfur content (%)	Purity
Kraft or Sulfate	Precipitation or ultrafiltration	Alkaline (NaOH, Na$_2$S) 150 - 170 °C pH=13 1 - 3 hr Vapor pressure	Moderate (1 - 3)	Moderate
Lignosulfonate or Sulfite	Ultrafiltration	Acid /Alkaline (H$^+$, HSO$_3^-$) 125 - 150 °C pH=1 - 2 1 - 7 hr Vapor pressure	High (3 - 8)	Low - moderate
Soda	Precipitation or ultrafiltration	Alkaline (NaOH) 140 - 170 °C pH=11 - 13 2 - 5 hr Vapor pressure	Free	Moderate - high
Organosolv	Dissolved air flotation, Precipitation	Acid (Acetic acid/formic acid/water) Ethanol 130 - 200 °C pH=4 - 13* 2 - 3.5 MPa* *process dependent	Free	High

2.2.2 Cellulosic Ethanol Biorefineries

A versatile platform for the transformation of LC biomass into a wide range of biochemicals and biofuels/bioenergy is offered by biorefineries. Like the paper industry, biorefineries are also primarily interested in polysaccharides (i.e., cellulose and hemicellulose). Due to lignin's strong binding with cellulose and hemicellulose, it often poses challenges to separate it from the polysaccharides. This typically involves a hydrolytic pretreatment technology for the production of ethanol.[41] The pretreatment is

either catalyzed by the addition of mineral acid (acid hydrolysis technique) or autocatalyzed by biomass-derived organic acids to separate the carbohydrate fraction of biomass and lignin.[4,41] Due to the non-volatile nature of the LC biomass, most of the involved separation techniques are solvent-based in contrast to the distillation operation which is predominant in petroleum refineries.[51] Nevertheless, the conversion process to intermediates and derived monomers is energy-intensive and strongly affected by factors such as the crystallinity of cellulose, its surface area and pore volume, composition and content of lignin, degree of polymerization, structure of hemicellulose, etc.[9,10] And most importantly, lignin obtained from biorefineries is used as low-grade boiler fuel to provide heat and power to the process and is often underutilized. Other advanced technologies for conversion are enzyme-based biomass-to-ethanol process that includes subsequent enzymatic hydrolysis and fermentation.[52] This technique produces high-quality lignin that can be used in the preparation of polymeric materials, unlike lignosulphonates and Kraft lignins.[52–54]

2.3 Current and Prospective Applications of Lignin

The current existing markets of lignin are limited to low-value products or to those where lignin is used as an energy resource. A vast portion of lignin is being utilized in the paper and pulp industry to generate heat and electricity. As quoted before, it is estimated that the pulp and paper industry alone extracts around 50 million tons of lignin per year, and it is considered the major industrial source of lignin.[55] Of these, less than 2 % is being treated and utilized as a chemical product like adhesives, binders, cement, and dispersants. Only 1 % of annually produced lignin is being commercialized for its application in the preparation of bio-chemicals.[55] The remaining 98 - 99 % of lignin is burnt for energy generation to recover and recycle the pulping chemicals. Especially, the black liquors from the Kraft process, after drying, are usually burnt in the recovery boiler to isolate these chemicals, while the thermal energy liberated from the combustion of lignin is used as a power source for pulping mills.[55] Until now, this way of lignin utilization has been identified as the easiest and simplest one. Nevertheless, this way of lignin utilization is considered to be a waste of resources. Lignosulphonate/sulfite lignin is used in many applications, in the formulation of pesticides, phenol, and urea formaldehyde thermosets, as dispersants, dyes, in the preparation of activated carbon for wastewater treatment, etc.[56] It is also used as an additive in concrete admixtures to retain moisture and as a soil stabilizer to increase the stiffness of the soil. Due to its high sulfur content (approx. 5 %), it is also used as fuel for the pulp mill. Soda lignin is used as a plasticizer in the cement industry.[48] The pulp liquors from the soda pulping mill can be employed directly in mortar application and in concrete mixtures.[48] And due to its high purity, it is also used as a precursor for raw materials and for synthesis.[54]

The under-utilization of lignin in high-value applications is primarily due to its non-uniform structure, chemical reactivity, and presence of various organic and inorganic impurities obtained as a result of different isolation processes and the lignin sources.[54] As

a consequence, a wide variety of physical and chemical properties of lignin are possible. Despite this, several efforts were made to understand the structure, composition, and features of the final lignin and utilize them in high-end and high-volume applications such as (i) a polymer component, for instance, as a comonomer in reactions with urea-formaldehyde, phenolics, epoxides, urethanes, etc.;[57–60] (ii) a raw material/precursor to produce chemicals (such as vanillin, phenol) or carbon fiber.[61,62] And as stated before, the differences introduced by isolation methods and plant species play a decisive role in the final properties of the polymers and composites.

To circumvent this issue, two approaches are extensively being explored by academic and industrial communities. A simple overview of the approaches is schematized in **Figure 2.5.**

(i) Chemical modifications of technical lignin: This allows to fine-tune the physiochemical properties of different extracted lignin types. It enhances the chemical reactivity of the lignin with the used polymer types, reduces the brittleness of lignin-derived polymer, and facilitates processability. The transformation of lignin by chemical modification involves the addition of chemically active sites or conversion of hydroxy groups. This is facilitated by several functional groups present in the lignin, especially the aliphatic and phenolic hydroxy groups. Different functionalization strategies such as hydroxyalkylation,[63] amination,[64,65] nitration,[66] demethylation,[67] phenolation,[68] alkylation,[69] urethanization,[70,71] etherification,[72] silylation,[73] esterification,[73,74] methoxy group substitution,[75] etc., are being vastly studied for the preparation of a wide range of value-added chemicals, building blocks, and polymers. For instance, hydroxymethylation of phenolic units of lignin using formaldehyde results in the formation of lignin-phenol formaldehyde. This allows the replacement of toxic non-renewable phenol by lignin, which is commercially used to produce phenol-formaldehyde resin, which is widely utilized as an adhesive for plywood.[76] Similarly, esterification using acetic anhydride improves the processability of lignin during dry spinning, leading to the production of high-strength carbon fiber.[77]

(ii) Lignin-first method or reductive catalytic fractionation (RCF) is primarily focused on retaining the original structure and properties of the native lignin, i.e., fractionation of lignin from LC prior to carbohydrate conversion.[35] Techniques such as base-catalyzed depolymerization (e.g., steam explosion) or other fragmentation processes (hydrogenation, oxidation), biochemical (e.g., enzymes or fungi), or thermal degradation (e.g., hydrothermal or pyrolysis) are employed to isolate lignin from other lignocellulosic components.[45] Using this approach, fragmented lignin can serve as a carbon source and for the production of chemicals like hydroxylated aromatics, aldehydes, aliphatic acids, and vanillin.[35]
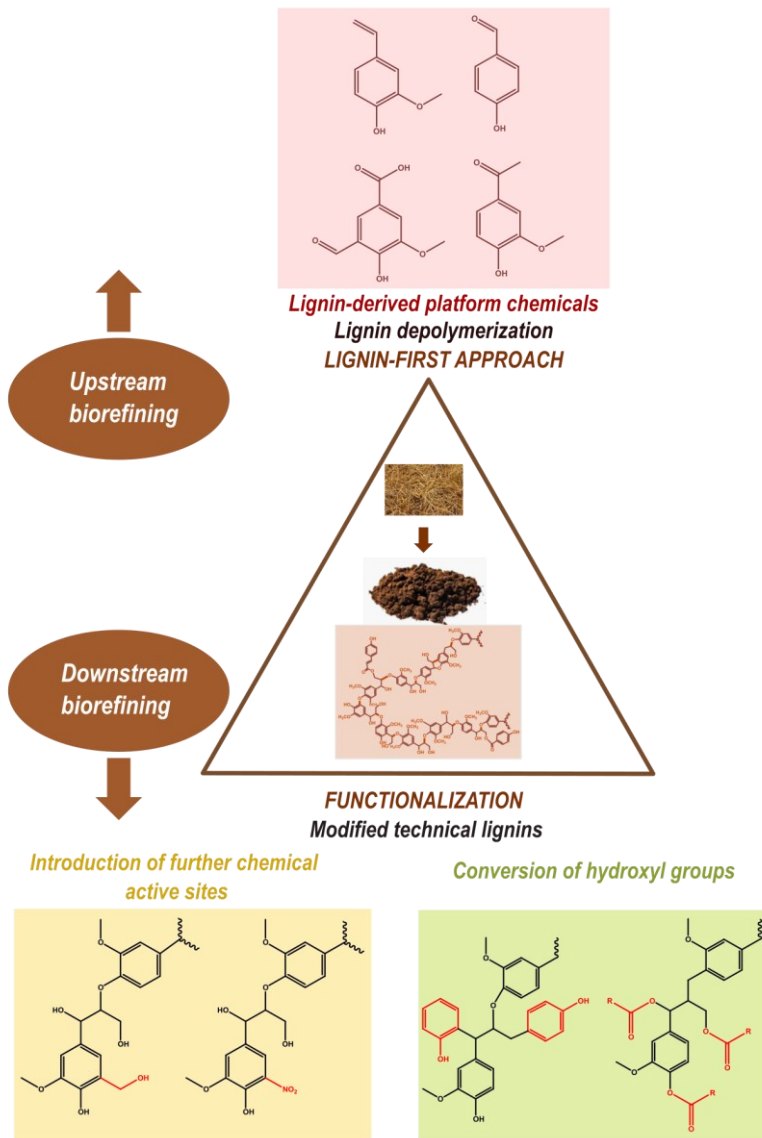
Figure 2.5. Different approaches to move towards high-end applications of lignin

The other potential applications of different lignin types after using different optimization strategies are summarized in **Table 2.4.**

2

Table 2.4. Potential applications of different technical lignin types after efficient valorization (Reproduced from the published article of D.S. Bajwa et al. with permission from Elsevier[78])

Material category	Lignin Type	Products	Potential applications
Aromatic macromolecules and fine chemicals	Kraft, Organosolv	Monomers, dimers, aromatic phenols, alkyl phenols, aromatic aldehydes and alcohols, acids, aryl ketones, anti-oxidants, dispersants, polyurethanes, phenolic resins, vanillin	Industrial chemicals, biobased adhesives, multifunctional materials, building blocks for biobased products
Carbon materials, Biofuels	Kraft, Sulfite, Soda, Organosolv	Biochar, bio-oil, syngas, activated carbon, carbon fibers, carbon black	Light-weight polymer composites, adsorbents, electrochemical devices, automotive
Polymer and nanomaterials	Kraft, Organosolv	3D Printing resin, scaffolds, lignin nanotubes, hydrogels	Biomedical applications, tissue engineering, drug delivery
Energy storage	Kraft	Li-ion, Na-Ion batteries (electrodes), supercapacitors, solar cells	Energy devices, batteries, fuel cells
Building materials	Soda, Sulfite, Kraft	bitumen, cement additive, dispersant, reinforcement	Construction pavements, cement panels
Other specialized applications	Kraft, Sulfite, Soda, Organosolv	Soil conditioner, controlled release agent in fertilizers and pesticides, sequestering agent, contaminant absorbent, fire retardant	agriculture, textiles, soil reclamation, water purification, fire suppression

2.4 Lignin-based Reinforcing Fillers for Rubber

Being a renewable material, lignin possesses several special characteristics, such as high carbon content, good physico-chemical, biodegradability, thermal stability, and antioxidant properties, which make it a suitable material for rubber application.[79,80] Several attempts were made already in the past to use lignin as a compounding ingredient in rubber serving as an antioxidant,[81] a coupling agent[82], plasticizer[83] or a filler[84]. Like the principal reinforcing fillers carbon black and silica, it is anticipated that the addition of lignin will provide certain reinforcement to rubber, i.e., improve strength (tensile, tear)

or further in-rubber properties (abrasion, fatigue, etc.) to meet the demands of specified rubber applications like tires, hoses, seals, belts, etc. Different types of technical lignin (unmodified and modified) were investigated as reinforcing fillers in various rubber types (non-polar and polar) by researchers.[85–89] The most frequently employed lignin source for these studies has been from chemical pulping operations.[90] This section will briefly discuss the challenges faced by lignin as a reinforcing filler and some strategies carried out by researchers to address these issues.

The development of lignin-based rubber compounds requires processing technologies to efficiently incorporate lignin into rubber, which aids in the desired physical properties. Past studies used two different methods for lignin incorporation: (i) latex mixing or co-precipitation and (ii) mechanical mixing or dry milling. The latex co-precipitation method is identified as the most efficient mixing technique to improve the incorporation of lignin into the non-polar rubber matrix, such as natural rubber (NR) and styrene butadiene rubber (SBR).[84,88,89,91,92] This method involves the mixing of a solution of lignin and rubber latex, which facilitates a homogeneous dispersion of the lignin particles. This is done by preparing first an aqueous suspension of lignin in water or caustic alkali. After that, it is mixed with rubber latex under intensive stirring, followed by coagulation using dilute acid. Finally, the coagulated rubber/lignin crumb or a coherent sheet is washed and dried. The dried rubber/lignin is mixed with other rubber ingredients in a two-roll mill. The first research work using lignin as a reinforcing filler, dating back to 1947, used this method to incorporate Kraft lignin into natural or synthetic rubber. It was found that a higher degree of filler dispersion was obtained, and the achieved tensile strength was comparable to that of channel black at low loadings (38.5 phr volume loading).[84] While, with increased lignin content (77 phr volume loading), the obtained tensile strength and tear strength were superior.[84] Using this co-precipitation technique, Kumaran et al. could successfully incorporate different loadings of sodium lignosulphonate into NR, which was unachievable using the mechanical mixing method.[85] The prepared composites showed improved tear, abrasion, flex crack, and crack growth resistance, whereas other physical properties such as modulus, tensile strength, and compression set properties were negatively affected by increasing lignin content.[85] Alkali lignin, when coagulated with NR latex using the co-precipitation method, showed improvements in oil resistance and enhanced strength at a loading between 10 and 12 %.[93] Similarly, sulfate lignin (50 parts) coagulated with SBR latex (100 parts) also showed good reinforcement properties and improved the thermal stability of the vulcanizate.[94] Albeit the excellent reinforcing properties achieved by the latex mixing method and the feasibility of this technique for mixing commonly used rubbers, the process is tedious and time-consuming. The processing time largely depends on the flocculation and filtration rate of the precipitation, for instance, if the ratio of lignin to rubber is high or if the coagulated mixture is difficult to filter and wash.[95] Also, the co-precipitation method utilizes acid flocculants, which, depending on the pH, can result in irreversible aggregation of lignin particles, further negatively affecting the processability and in-rubber properties.[96,97] Other factors such as

2

temperature, concentration of lignin and surfactant, and type of lignin also play a decisive role in the precipitation process and the in-rubber properties.

The use of the mechanical mixing method, involving the mixing of lignin with rubber and other rubber ingredients in either a laboratory roll mill or internal mixer, surpassed the drawbacks of latex mixing. This way of incorporating lignin into a rubber matrix is considered to be the simplest and most straightforward way, as it involves less processing time. However, works carried out by different researchers highlighted that achieving a sufficient dispersion of lignin within the rubber matrix using this method is not possible due to the agglomeration of lignin particles.[85] This tendency of lignin agglomeration arises from the intermolecular hydrogen bonding between the available hydroxy groups of lignin, affecting its compatibility with hydrocarbon rubber and, subsequently, undermining the reinforcing properties of lignin-reinforced rubber.[85,86,88] Earlier studies carried out in the 1970s by Kumaran et al. affirm that when different loadings of sodium lignosulphonate (0, 10, 20 phr) were mixed with NR using a two-roll mill, lignin could not be dispersed well into the matrix. This is mainly observed due to the aforementioned issue, i.e., lignin aggregation by intermolecular forces, which cannot be readily broken by the generated mechanical forces.[85] Similar conclusions about the conventional mixing process were also drawn from a recent investigation carried out by Barana et al.[88] In this study, the quality of dispersion of soda grass lignin in NR matrix was achieved by two different mixing methods: conventional and latex mixing methods were compared. It was reported that the conventional mixing method develops large lignin particles, while latex mixing resulted in finer aggregates of lignin particles homogeneously dispersed in the rubber matrix, as presented in **Figure 2.6 (a), (b), (c)**.[88] And depending on the dispersion quality, the achieved in-rubber properties also varied significantly.
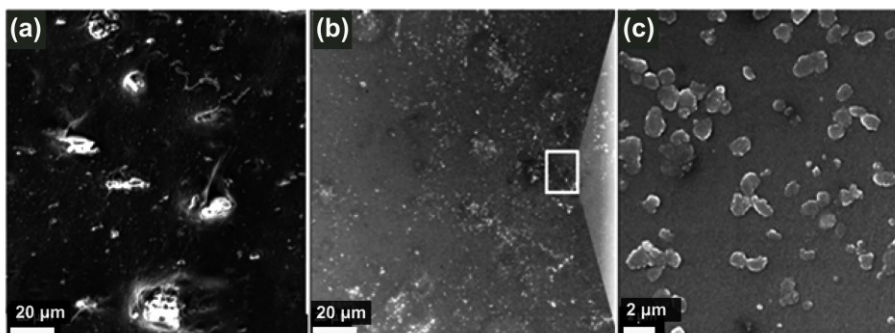

Figure 2.6. Microscopic images of Soda grass lignin incorporated in the NR matrix by (a) mechanical mixing and (b) latex mixing. (c) Magnified view of lignin particles dispersed in NR matrix by latex mixing [Reprinted (adapted) with permission from the published article of D. Barana et al.[88] Copyright © 2016 American Chemical Society]

Some studies feature that lignin loadings only up to a certain level can be easily dispersed into a rubber matrix by conventional mixing methods without affecting the physico-mechanical properties of lignin-reinforced composites. For instance, Košíková et al. found that the addition of sulfur-free lignin up to 30 phr positively improved the mechanical, thermo-oxidative, and other physical properties of NR. For a filler loading above 30 phr, a deteriorating behavior was observed due to the development of large particle sizes and lack of interfacial interaction with the elastomer.[87]

Thus, both the latex and conventional processing methods limit the wide-scale application of lignin as a filler in the rubber industry.

Jiang et al. proposed a different mixing technique, high-temperature dynamic heat treatment (HTDHT), to tackle the problems related to lignin mixing. The technique was applied to well-disperse sulfate lignin (40 phr) with epoxidized natural rubber (ENR) (25 mol % epoxy groups) at different temperatures.[96] The morphological studies performed by Field Emission Scanning Electron Microscope (FESEM) for ENR/lignin composites prepared at different mixing temperatures imply that an increasing mixing temperature promotes a better dispersion of lignin in the ENR matrix. This results in a better filler-polymer interaction (see **Figure 2.7**).
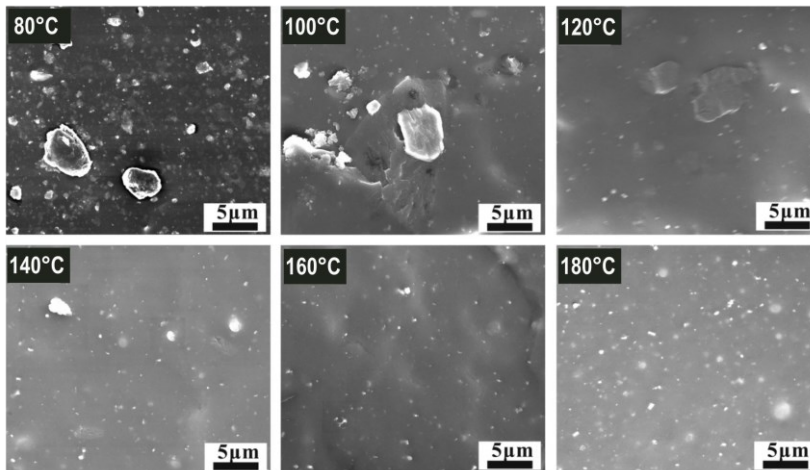

Figure 2.7. Field Emission Scanning Electron Microscopic (FESEM) images of fractured surfaces of sulfate lignin/ epoxidized natural rubber (ENR) prepared by high-temperature dynamic heat treatment mixing method at different heat treatment temperatures for 30 minutes [Reprinted from the published article of C. Jiang et al. with permission from John Wiley and Sons[96]]

This study was further extended to elucidate the advantages of the HTDTH technique on the mixing of ENR/lignin composites over the conventional mixing technique. It was observed that the achieved mechanical properties of heat treated rubber composites were significantly higher than that of conventionally mixed rubber compounds. The tensile strength and tear strength of the heat-treated ENR composites filled with 40 phr lignin

were increased by 114 % and 23 %, respectively, compared to the conventionally mixed compound with a similar loading.[96] The differences in the obtained reinforcing properties between the two mixing methods (HTDHT and conventional mixing) were found to be due to the improved compatibility of lignin and ENR during the HTDHT method, as demonstrated by morphological studies (**see Figure 2.8**). Albeit the improvement in overall in-rubber properties, using such a high mixing temperature is less attractive for other elastomers, especially unsaturated rubbers like NR, which can readily undergo thermo-oxidative degradation.[98]
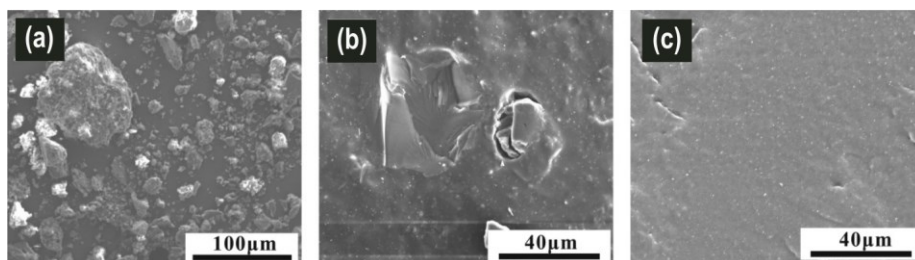

Figure 2.8. Field Emission Scanning Electron Microscopic (FESEM) images of (a) lignin powder and (b) and (c) fractured surfaces of sulfate lignin/ epoxidized natural rubber (ENR) composite containing 40 phr of lignin prepared by conventional and high-temperature dynamic heat treatment mixing method, respectively [Reprinted from the published article of C. Jiang et al. with permission from John Wiley and Sons[96]]

Alternate strategies, such as surface modification of lignin prior to addition into the rubber matrix and use of a hybrid filler system, i.e., partial replacement of conventional fillers carbon black (CB), silica, and other inorganic fillers with lignin, were proposed and investigated to widen the application of lignin as a filler for rubber compounds. Surface modification technology assists in improving the processability and dispersion of lignin in the rubber matrix by utilizing the available functionalities and interfering in the hydrogen bonding interactions between lignin. In a study performed with Nitrile rubber (NBR) and between different filler systems such as CB (N765), phenolic resin- and benzoyl peroxide-modified lignin, the latter showed better thermal stability, compression properties, and superior elongation at break and hardness.[99] In addition, it was easier to disperse the modified lignin in the rubber matrix by the conventional mixing method compared to the unmodified one. Similarly, other lignin types, sulfur-free lignin modified with hexamethylenetetramine[100] and lignosulfonates modified with cyclohexylamine[101] using mechanical mixing, showed in an SBR compound higher reinforcing ability and better dispersion compared to the unmodified one. Barana et al. used esterification reactions to modify softwood Kraft lignin in order to improve its compatibility with NR.[102] As a result of the modification, an increase in the 100 % and 300 % modulus was observed in comparison to the unmodified one.[102] Jiang et al. modified sulfate lignin with different surface modifiers such as formaldehyde (F), glyoxal (G), and glutaraldehyde (GD) prior to co-precipitation with SBR latex and found that the dispersion and filler-polymer interaction varied largely with the used modifier type.[97] Formaldehyde-modified lignin

(LF) filled SBR composite showed higher modulus compared to the compounds containing glyoxal- (LG) and glutaraldehyde-modified lignins (LGD). It is reported that this effect is observed due to the uniform dispersion of LF in the composite maintaining an oblate shape with a mean particle size of about 100 nm compared to the LG- and LGD, which agglomerated in the matrix.[97] Bahl et al. used Polybutadiene-g-polypentafluorostyrene (PB-g-PPFS) coupling agent to improve the compatibility of Kraft lignin in SBR matrix where a non-covalent coupling (π-π interaction) is assumed to be formed between the aromatic hydrocarbons in lignin and aromatic fluorocarbons in PPFS via arene-perfluoroarene and a subsequent covalent bond is assumed to be formed between PB-g-PPFS-lignin and rubber. It is expected that this coupling is responsible for improving the mechanical properties of the Kraft lignin-filled SBR vulcanizates.[103] Mohamad Aini et al. used oligomeric compatibilizers like epoxidized natural rubber (ENR) and liquid polybutadiene rubber (LBR) as coupling agents to improve the dispersion and interfacial adhesion of lignin with the non-polar rubber.[104] Shorey et al. performed silylation of Kraft lignin using 3-(triethoxysilyl) propyl isocyanate to improve the dispersion and compatibility of lignin in the natural rubber matrix.[105] Silane coupling agent like bis(3-triethoxysilyl propyl)tetrasulfide (TESPT) was also used as a lignin surface modifier to improve the interfacial adhesion between lignin and polybutadiene rubber.[106] It was reported that the use of a unique reactive mixing technique (high temperature-driven, four-stage mixing process) for lignin enabled the development of strongly reinforced BR composites. The four-stage mixing process includes: (i) stage 1: mixing of lignin, rubber, ZnO, and stearic acid in the two-roll mill at room temperature for 10 minutes; (ii) stage 2: mixing of the obtained components at 155 °C for 10 minutes with a rotor speed of 50 rpm in an internal mixer; (iii) stage 3: mixing of the obtained mix from stage 2 with TESPT at 120 °C for 10 minutes with a rotor speed of 50 rpm; (iv) stage 4: mixing the masterbatch from stage 3 with accelerators and curatives in a two-roll mill at room temperature for 10 min. This type of mixing results in the mechanical performance of 50 phr lignin/TESPT-containing composite superior to CB (N330) filled BR ones.[106]

Hybrid filler technology is another approach to introducing lignin into rubber compounds, i.e., mixing lignin along with conventional reinforcing fillers like carbon black (CB) and silica. The idea behind introducing dual filler systems into a rubber matrix is to potentially exhibit improved vulcanizate characteristics with regard to single-filler reinforced compounds through a combination of the benefits of each type of filler. In the studies carried out so far, the role of lignin in the chosen hybrid filler system is to promote the dispersion of the other used fillers by suppressing their network formation in the rubber matrix. For example, Cao et al. observed that an increasing amount of lignin aided together with montmorillonite clay (MMT) into an NBR matrix improves the dispersibility and reinforcing properties.[107] In a similar approach, Xiao et al. used lignin to improve the dispersion of layered double hydroxide (LDH) clay in the SBR matrix. Also, it was observed that with increasing lignin content (3 - 15 phr) in LDH, the tensile strength, elongation at

break, and hardness enhanced further.[108] Bahl et al. used the hybrid fillers N330 (CB) /lignosulphonate lignin (LS) in the ratio of 90:10 and 80:20 in SBR to improve the viscoelastic properties. The addition of LS along with CB strongly improved the dispersion of N330 in the SBR matrix, as illustrated in **Figure 2.9**. This behavior is caused by the formation of non-covalent π-π stacking interaction between CB and LS, as observed by Raman spectroscopy. As a result, the filler-filler interactions of CB are reduced, leading to a lower viscoelastic loss. However, an increased lignin content deteriorated the tensile strength and hardness of the final compound.[109]
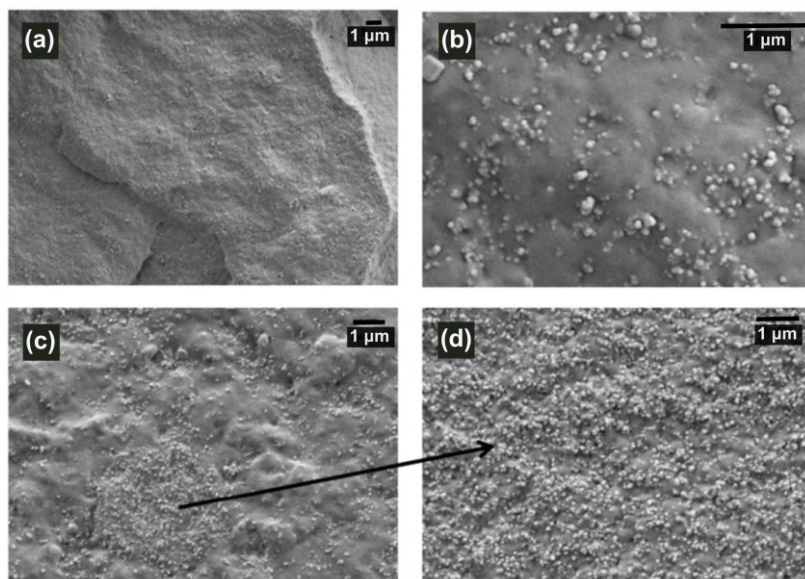

Figure 2.9. Scanning Electron Microscopic (SEM) images of fractured surfaces of SBR vulcanizates containing (a,b) 30 phr N330 carbon black and (c,d) hybrid filler with 90:10 carbon black: Lignosulfonate [Reprinted from the published article of K. Bahl et al. with permission from Elsevier[109]]

Yu et al. investigated the synergistic effects (i.e., improvement in overall mechanical properties) of silica/lignin in NR. The study was carried out using different amounts of alkali lignin (10, 20, 30, 40, 50 phr) obtained from bagasse, which were co-precipitated with NR latex. After that, the dried NR/lignin was mixed with other ingredients and silica filler (type FINE-siL518) with varying proportions by a two-roll mill. The findings concluded that only partial replacement of silica by lignin (20 phr max.) improves the processability, anti-aging resistance, and anti-flex cracking properties as well as mechanical properties of NR vulcanizates.[91] In a recent study, Liu et al. observed a notable synergistic effect in silica (Zeosil 1165MP)/lignin-filled NR vulcanizates. In this study, the lignin content (10, 20, 30, 40, 50 phr) had only a minor effect on the achieved properties.[110] This investigation was further extended to the lignin/N330 CB blend.[110] Unlike the silica/ lignin system, good tensile strength and elongation at break were obtained only when less

than 30 phr of lignin loading was used. However, moduli at 100 % and 300 % of lignin/N330 CB-filled NR vulcanizate were negatively affected by increasing the lignin content from 10 to 50 phr.[110]

Besides the observed dispersion difficulties and the resulting inferior physical properties, some studies reported that the addition of lignin negatively affects the cure characteristics of the rubber compound. This is explained by lignin's acidic nature.[87,94,96,99] For example, Griffith et al. reported that a co-precipitation of oxidized alkali lignin with NR latex delayed the cure rate.[111] It was assumed that this behavior was observed due to the excessive generation of hydrogen sulfide (H_2S) by the reaction between lignin and sulfur, which acts as a chain terminator delaying the vulcanization process. To tackle this, heavy metal oxides such as lead, copper, and bismuth oxides were introduced to improve the curing behavior.[111] These metal oxides, in combination with a dithiocarbamate accelerator, are found to activate the vulcanization of lignin-natural rubber co-precipitates faster than the compound containing only zinc oxide activator. Further, it was observed that the lead oxide-containing lignin compound showed superior tensile strength compared to the other metal oxide compounds.[111] All these negative effects (i.e., inferior cure and physical characteristics, poor interfacial adhesion of lignin with rubber) arise due to the presence of different polar functional groups of lignin.[87,94,96,99] Especially, the hydroxy groups on the lignin's surface tend to agglomerate via hydrogen bonding and also have the capability to adsorb basic accelerators, resulting in incompatibility issues and curing problems, respectively.[100] A recent approach, dual crosslinking network (covalent and non-covalent networks), was used to enhance the cure properties, dispersion, and compatibility of lignin in the rubber matrix.[112] Wang et al. explored the advantages of using the dual crosslinking network in the N660 CB/ alkali lignin-filled NBR system. Zinc chloride ($ZnCl_2$) was used in this study to introduce a second sacrificial non-covalent network (zinc-based coordination bonds) between lignin and Zn^{2+} ions, in addition to the covalent network between rubber and sulfur.[112] The developed network in CB/lignin/NBR provided outstanding mechanical properties compared to the CB/NBR compound. This is because of the involvement of polar functionalities of lignin in the formation of a secondary network, which reduces the filler-filler interactions. Li et al. extended the dual-networking approach to NR along with other discussed approaches, such as chemical modification as well as the use of a hybrid filler system.[113] The use of a chemically modified lignin with (2-dodecen-1-yl)succinic anhydride in a blend with CB seems to result in the formation of an integrated network layer at the NR/lignin interface upon an extra addition of zinc dimethacrylate (ZDMA) which improves the dispersion (**Figure 2.10**). Due to the formation of this network, comparable mechanical properties were observed when 30 wt.% of carbon black (N330) was replaced with modified lignin.[113]
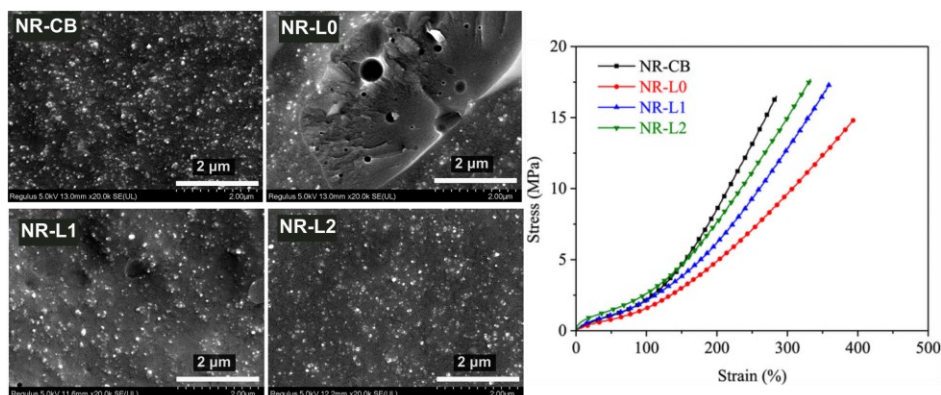
Figure 2.10. Scanning Electron Microscopic (SEM) images (Left side) and mechanical properties of N330 carbon black filled (NR-CB), CB/unmodified lignin filled (NR-L0), and CB/modified lignin filled (NR-L1 and NR-L2) natural rubber vulcanizates, where L1 and L2 are lignin samples modified with two different amount of 0.12 and 0.24 mol (2-dodecen-1-yl) succinic anhydride modifier. The amount of N330 CB used was 50 phr, and the hybrid system consisted of 35 phr N330 and 15 phr (un)modified lignin [Reprinted (adapted) with permission from the published article of M. Li et al.[113]]

From the above-discussed literature, a conclusion can be drawn that an optimal improvement in the in-rubber properties is achieved only with a lower amount of lignin in either fully- or partially-filled compounds. Beyond certain levels of lignin loading, it is found that the properties of lignin-filled compounds with and without surface modification deteriorate due to a lack of interfacial interaction between lignin and the used rubber system. As a result, combined reinforcing effects, i.e., strength (resistance to fracture) and stiffness properties, are only moderately pronounced in lignin-reinforced compounds compared to the reinforcing CB- and silica-filled compounds. Similar effects are also observed for the lignin composites prepared by hybrid technologies and surface modification. This, thus, makes it a challenging filler for rubber reinforcement. The functional groups of lignin and the particle size primarily play a dominant role in its dispersion within the rubber matrix, especially in non-polar elastomers.

One of the emerging technologies to overcome the above-described challenges of technical lignin is to use treatment methods like thermochemical processes to transform lignin chemically and physically.[114,115] Hydrothermal technology (HTT) is one of the thermochemical processes that can reduce the high degree of heterogeneity in the composition imparted by the pulping process and decrease the amount of functionalities on the surface of lignin.[116]

2.5 Hydrothermal Treatment of Lignin for High-value Applications

Hydrothermal treatment technology (thermochemical process) is one of the valorization processes that offer the potential for producing value-added compounds and functional carbon from lignin. It is considered to be a sustainable, cost-effective, and environmentally benign process compared to conversion technologies like catalyst-based depolymerization.[117] In the hydrothermal process, the feedstock from the pulping process (e.g., black liquor) or any other biorefineries is mixed with water at temperatures in the range of 160 - 370 °C in a pressurized reactor vessel.[114,116,118,119] The pressure maintained inside the reactor is the saturation pressure of the water at a given temperature. The typically studied residence time for hydrothermal treatment varied between 1 and 72 h.[118] The main reaction product is solid hydrochar and byproducts that are aqueous water-soluble and insoluble liquids (HTT liquor). Gaseous streams are produced as well as a result of hydrolysis and cleavage of the ether bond and the C–C bonds, dehydration, demethoxylation, and alkylation of lignin.[120,121] The resulting solid product possesses rough and porous surfaces with highly ordered crystalline structures with increased carbon content and improved hydrophobicity depending on the process conditions.[122] Overall, improved material properties with easier handling and storage characteristics are observed with the HTT process.[116] **Figure 2.11** illustrates that with increasing hydrothermal temperature, different particle morphologies can be obtained. An irregular polygonal shape of the lignin before hydrothermal treatment is changed to the rough and irregular fluffy product after the process.[122] By increasing the temperature to 365 °C, the size of the particles become smaller with disappearing pores that are initially generated due to the release of volatiles.[122] In addition, most of the functional groups are eliminated during the process, with the exception of hydroxy groups, which can subsequently be used for further functionalization.[122] Hydrochar can be produced using a range of wide variety of available biomass, including agricultural waste, sewage sludge, or algae, via the HTT process, ensuring sustainability in raw material sourcing.[123] Extensive researches on the application of hydrochars were conducted in diverse areas, e.g., solid fuel, hydrogen energy storage, asphalt modifier, supercapacitor electrode materials, CO_2 capture in catalysis, pollutant adsorbents, etc.[124] Still, the potential application of hydrochar as a functional filler for rubber has not been fully investigated, leading to a significant research gap in determining the dominating factors of HTT lignin that contribute its reinforcing performance, such as particle size, morphology or surface chemistry. This part of the research will be covered in this thesis.
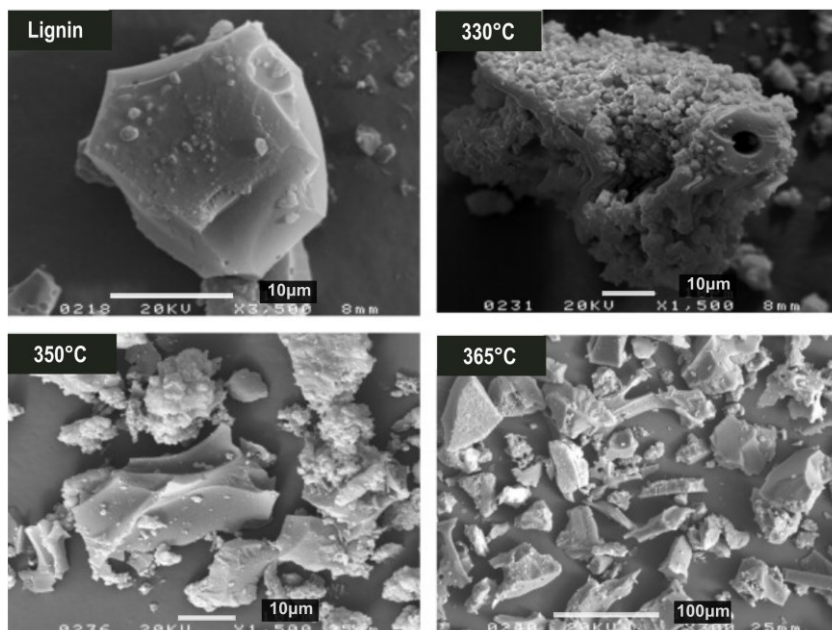
Figure 2.11. Scanning Electron Microscopic (SEM) images of lignin and different hydrothermal chars produced by varying hydrothermal temperatures [Reprinted from the published article of J. Hu et al. with permission from Elsevier[122]]

2.6 Concluding Remarks

To summarize, lignin, one of the components of lignocellulosic biomass, is considered a promising alternative renewable feedstock because of its aromatic structure, high carbon content, antioxidant properties, reinforcing capability, and biodegradability for applications in the place of petroleum-derived materials. The application of lignin as a filler for rubber has attracted researchers over other bio-fillers like starch, etc., due to its chemical rigidity and abundance. Considerable research efforts in chemical modifications, hybrid technologies, and mixing methods have been taken for the practical application of lignin in rubber. Still, issues such as compatibility and dispersion are discernible due to lignin's heterogeneity and structural complexities stemming from plant sources and industrial pulping treatment, as presented in **Figure 2.12**.
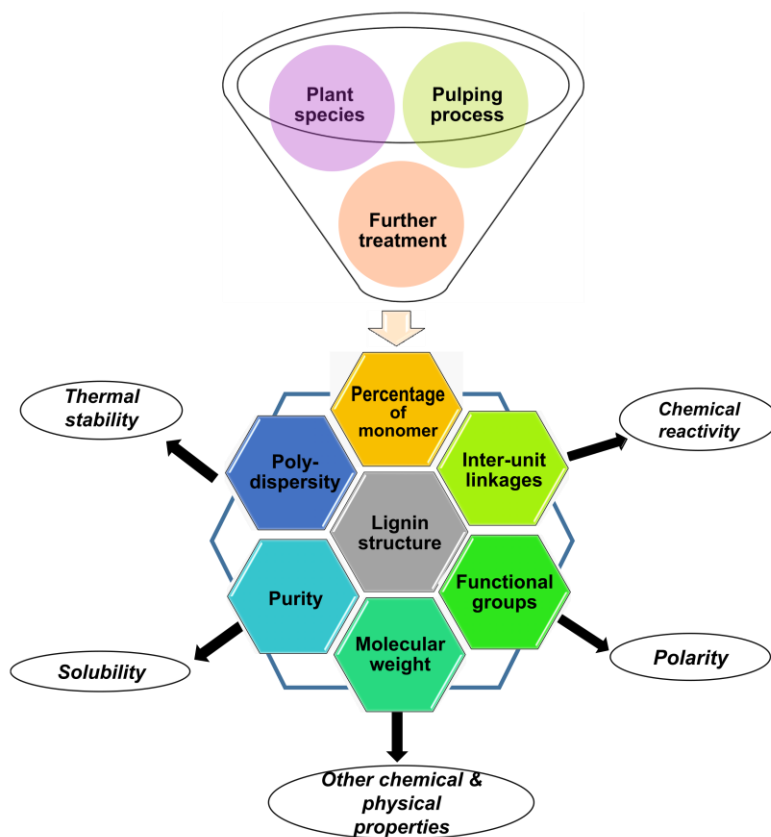
Figure 2.12. Challenges in Lignin valorization[125]

Given the complex material, the introduction of new process strategies that can reduce structural diversity arising due to the isolation techniques and can minimize reactive functionalities might foster a way for a wide-scale utilization of lignin in rubber. In recent years, the development of a hydrothermal process to transform lignin into a homogeneous material having specific morphologies, pore structures (nano, meso, and macropores), and controlled surface functionalities has been recognized and intensively studied. Regardless of the enormous studies carried out on hydrothermal lignin in different applications, its utilization for rubber applications has received limited attention and requires more detailed research.

References

(1)   Sun, Y.; Cheng, J. Hydrolysis of Lignocellulosic Materials for Ethanol Production: A Review. *Bioresource Technology* **2002**, *83* (1), 1–11.

(2)   H. Isikgor, F.; Remzi Becer, C. Lignocellulosic Biomass: A Sustainable Platform for the Production of Bio-Based Chemicals and Polymers. *Polymer Chemistry* **2015**, *6* (25), 4497–4559.

(3)   Paul, S.; Dutta, A. Challenges and Opportunities of Lignocellulosic Biomass for Anaerobic Digestion. *Resources, Conservation and Recycling* **2018**, *130*, 164–174.

(4)   Dahmen, N.; Lewandowski, I.; Zibek, S.; Weidtmann, A. Integrated Lignocellulosic Value Chains in a Growing Bioeconomy: Status Quo and Perspectives. *GCB Bioenergy* **2019**, *11* (1), 107–117.

(5)   Cherubini, F. The Biorefinery Concept: Using Biomass Instead of Oil for Producing Energy and Chemicals. *Energy Conversion and Management* **2010**, *51* (7), 1412–1421.

(6)   Lewandowski, I. Securing a Sustainable Biomass Supply in a Growing Bioeconomy. *Global Food Security* **2015**, *6*, 34–42.

(7)   Khan, M. U.; Usman, M.; Ashraf, M. A.; Dutta, N.; Luo, G.; Zhang, S. A Review of Recent Advancements in Pretreatment Techniques of Lignocellulosic Materials for Biogas Production: Opportunities and Limitations. *Chemical Engineering Journal Advances* **2022**, *10*, 100263.

(8)   Bertella, S.; Luterbacher, J. S. Lignin Functionalization for the Production of Novel Materials. *Trends in Chemistry* **2020**, *2* (5), 440–453.

(9)   Taherzadeh, M. J.; Karimi, K. Pretreatment of Lignocellulosic Wastes to Improve Ethanol and Biogas Production: A Review. *International Journal of Molecular Sciences* **2008**, *9* (9), 1621–1651.

(10)   Millán, D.; González-Turen, F.; Perez-Recabarren, J.; Gonzalez-Ponce, C.; Rezende, M. C.; Da Costa Lopes, A. M. Solvent Effects on the Wood Delignification with Sustainable Solvents. *International Journal of Biological Macromolecules* **2022**, *211*, 490–498.

(11)   Menon, V.; Rao, M. Trends in Bioconversion of Lignocellulose: Biofuels, Platform Chemicals & Biorefinery Concept. *Progress in Energy and Combustion Science* **2012**, *38* (4), 522–550.

(12)   Danso-Boateng, E.; Fitzsimmons, M.; Ross, A. B.; Mariner, T. Response Surface Modelling of Methylene Blue Adsorption onto Seaweed, Coconut Shell and Oak Wood Hydrochars. *Water* **2023**, *15* (5), 977.

(13)   Etale, A.; Onyianta, A. J.; Turner, S. R.; Eichhorn, S. J. Cellulose: A Review of Water Interactions, Applications in Composites, and Water Treatment. *Chem. Rev.* **2023**, *123* (5), 2016–2048.

(14)   Ummartyotin, S.; Manuspiya, H. A Critical Review on Cellulose: From Fundamental to an Approach on Sensor Technology. *Renewable and Sustainable Energy Reviews* **2015**, *41*, 402–412.

(15)   Aziz, T.; Farid, A.; Haq, F.; Kiran, M.; Ullah, A.; Zhang, K.; Li, C.; Ghazanfar, S.; Sun, H.; Ullah, R.; Ali, A.; Muzammal, M.; Shah, M.; Akhtar, N.; Selim, S.; Hagagy, N.; Samy, M.; Al Jaouni, S. K. A Review on the Modification of Cellulose and Its Applications. *Polymers* **2022**, *14* (15), 3206.

(16)   Moon, R. J.; Martini, A.; Nairn, J.; Simonsen, J.; Youngblood, J. Cellulose Nanomaterials Review: Structure, Properties and Nanocomposites. *Chem. Soc. Rev.* **2011**, *40* (7), 3941–3994.

(17)   Ling, Z.; Chen, S.; Zhang, X.; Takabe, K.; Xu, F. Unraveling Variations of Crystalline Cellulose Induced by Ionic Liquid and Their Effects on Enzymatic Hydrolysis. *Sci Rep* **2017**, *7* (1), 10230.

(18) Li, T.; Chen, C.; Brozena, A. H.; Zhu, J. Y.; Xu, L.; Driemeier, C.; Dai, J.; Rojas, O. J.; Isogai, A.; Wågberg, L.; Hu, L. Developing Fibrillated Cellulose as a Sustainable Technological Material. *Nature* **2021**, *590* (7844), 47–56.

(19) Hubbe, M. On Paper – A Celebration of Two Millennia of the Work and Craft of Papermakers. *BioRes* **2013**, *8* (4), 4791–4792.

(20) Bae, J.; Kwon, H.; Kim, J. Safety Evaluation of Absorbent Hygiene Pads: A Review on Assessment Framework and Test Methods. *Sustainability* **2018**, *10* (11), 4146.

(21) Thillaipandian, H.; Dev, V. R. G. Wet Laying Nonwoven Using Natural Cellulosic Fibers and Their Blends: Process and Technical Applications. A Review. *Journal of Natural Fibers* **2019**, *18*, 1–11.

(22) Scheller, H. V.; Ulvskov, P. Hemicelluloses. *Annual Review of Plant Biology* **2010**, *61* (1), 263–289.

(23) Gírio, F. M.; Fonseca, C.; Carvalheiro, F.; Duarte, L. C.; Marques, S.; Bogel-Łukasik, R. Hemicelluloses for Fuel Ethanol: A Review. *Bioresource Technology* **2010**, *101* (13), 4775–4800.

(24) Rao, J.; Lv, Z.; Chen, G.; Peng, F. Hemicellulose: Structure, Chemical Modification, and Application. *Progress in Polymer Science* **2023**, *140*, 101675.

(25) Harahap, B. Degradation Techniques of Hemicellulose Fraction from Biomass Feedstock for Optimum Xylose Production: A Review. *Jurnal Keteknikan Pertanian Tropis dan Biosistem* **2020**, *8*, 107-124.

(26) Kishani, S.; Vilaplana, F.; Xu, W.; Xu, C.; Wågberg, L. Solubility of Softwood Hemicelluloses. *Biomacromolecules* **2018**, *19* (4), 1245–1255.

(27) Huang, L.; Ma, M.-G.; Ji, X.-X.; Choi, S.-E.; Chuanling, S. Recent Developments and Applications of Hemicellulose From Wheat Straw: A Review. *Frontiers in Bioengineering and Biotechnology* **2021**, *9*.

(28) Upton, B. M.; Kasko, A. M. Strategies for the Conversion of Lignin to High-Value Polymeric Materials: Review and Perspective. *Chem. Rev.* **2016**, *116* (4), 2275–2306.

(29) Notley, S. M.; Norgren, M. Lignin: Functional Biomaterial with Potential in Surface Chemistry and Nanoscience. In *The Nanoscience and Technology of Renewable Biomaterials*; John Wiley & Sons, Ltd, 2009; pp 173–205.

(30) Liu, X.; Bouxin, F. P.; Fan, J.; Budarin, V. L.; Hu, C.; Clark, J. H. Recent Advances in the Catalytic Depolymerization of Lignin towards Phenolic Chemicals: A Review. *ChemSusChem* **2020**, *13* (17), 4296–4317.

(31) Lobato-Peralta, D. R.; Duque-Brito, E.; Villafán-Vidales, H. I.; Longoria, A.; Sebastian, P. J.; Cuentas-Gallegos, A. K.; Arancibia-Bulnes, C. A.; Okoye, P. U. A Review on Trends in Lignin Extraction and Valorization of Lignocellulosic Biomass for Energy Applications. *Journal of Cleaner Production* **2021**, *293*, 126123.

(32) Gellerstedt, G.; Pranda, J.; Lindfors, E.-L. Structural and Molecular Properties of Residual Birch Kraft Lignins. *Journal of Wood Chemistry and Technology* **1994**, *14* (4), 467–482.

(33) Katahira, R.; Elder, T. J.; Beckham, G. T. A Brief Introduction to Lignin Structure. In *Lignin Valorization*; Royal Society of Chemistry, 2018; pp 1–20.

2

(34) Windeisen, E.; Wegener, G. Lignin as Building Unit for Polymers. In *Polymer Science: A Comprehensive Reference*; Matyjaszewski, K., Möller, M., Eds.; Elsevier: Amsterdam, 2012; pp 255–265.

(35) Korányi, T. I.; Fridrich, B.; Pineda, A.; Barta, K. Development of 'Lignin-First' Approaches for the Valorization of Lignocellulosic Biomass. *Molecules* 2020, *25* (12), 2815.

(36) Andhika, D.; Kasim, A.; Asben, A.; Yusniwati, Y. Delignification of Lignocellulosic Biomass. *World Journal of Advanced Research and Reviews* 2021, *12*, 462–469.

(37) Chauhan, P. S. Role of Various Bacterial Enzymes in Complete Depolymerization of Lignin: A Review. *Biocatalysis and Agricultural Biotechnology* 2020, *23*, 101498.

(38) Sharma, V.; Tsai, M.-L.; Nargotra, P.; Chen, C.-W.; Sun, P.-P.; Singhania, R. R.; Patel, A. K.; Dong, C.-D. Journey of Lignin from a Roadblock to Bridge for Lignocellulose Biorefineries: A Comprehensive Review. *Science of The Total Environment* 2022, 160560.

(39) Haq, I.; Mazumder, P.; Kalamdhad, A. S. Recent Advances in Removal of Lignin from Paper Industry Wastewater and Its Industrial Applications – A Review. *Bioresource Technology* 2020, *312*, 123636.

(40) Vásquez-Garay, F.; Carrillo-Varela, I.; Vidal, C.; Reyes-Contreras, P.; Faccini, M.; Teixeira Mendonça, R. A Review on the Lignin Biopolymer and Its Integration in the Elaboration of Sustainable Materials. *Sustainability* 2021, *13* (5), 2697.

(41) Lora, J. H.; Glasser, W. G. Recent Industrial Applications of Lignin: A Sustainable Alternative to Nonrenewable Materials. *Journal of Polymers and the Environment* 2002, *10* (1), 39–48.

(42) Tomani, P. The Lignoboost Process. *Cellulose Chemistry and Technology* 2010, *44*, 53–58.

(43) Sjöström, E.; Alén, R. Lignin. In *Analytical Methods in Wood Chemistry, Pulping, and Papermaking*; Springer Science & Business Media, 1998; pp 77–120.

(44) Hubbe, M.; Alén, R.; Paleologou, M.; Kannangara, M.; Kihlman, J. Lignin Recovery from Spent Alkaline Pulping Liquors Using Acidification, Membrane Separation, and Related Processing Steps: A Review. *BioResources* 2019, *14*, 2300–2351.

(45) Laurichesse, S.; Avérous, L. Chemical Modification of Lignins: Towards Biobased Polymers. *Progress in Polymer Science* 2014, *39* (7), 1266–1290.

(46) Ringena, O.; Saake, B.; Lehnen, R. Isolation and Fractionation of Lignosulfonates by Amine Extraction and Ultrafiltration: A Comparative Study. 2005, *59* (4), 405–412.

(47) Kun, D.; Pukánszky, B. Polymer/Lignin Blends: Interactions, Properties, Applications. *European Polymer Journal* 2017, *93*, 618–641.

(48) Nadif, A.; Hunkeler, D.; Käuper, P. Sulfur-Free Lignins from Alkaline Pulping Tested in Mortar for Use as Mortar Additives. *Bioresource Technology* 2002, *84* (1), 49–55.

(49) Luo, H.; Abu-Omar, M. M. Chemicals From Lignin. In *Encyclopedia of Sustainable Technologies*; Abraham, M. A., Ed.; Elsevier: Oxford, 2017; pp 573–585.

(50) Ragauskas, A. J.; Beckham, G. T.; Biddy, M. J.; Chandra, R.; Chen, F.; Davis, M. F.; Davison, B. H.; Dixon, R. A.; Gilna, P.; Keller, M.; Langan, P.; Naskar, A. K.; Saddler, J. N.; Tschaplinski, T. J.; Tuskan, G. A.; Wyman, C. E. Lignin Valorization: Improving Lignin Processing in the Biorefinery. *Science* 2014, *344* (6185), 1246843.

(51) Chandel, A. K.; Garlapati, V. K.; Singh, A. K.; Antunes, F. A. F.; da Silva, S. S. The Path Forward for Lignocellulose Biorefineries: Bottlenecks, Solutions, and Perspective on Commercialization. *Bioresource Technology* **2018**, *264*, 370–381.

(52) Chandra, R. P.; Bura, R.; Mabee, W. E.; Berlin, A.; Pan, X.; Saddler, J. N. Substrate Pretreatment: The Key to Effective Enzymatic Hydrolysis of Lignocellulosics? In *Biofuels*; Olsson, L., Ed.; Advances in Biochemical Engineering/Biotechnology; Springer: Berlin, Heidelberg, 2007; pp 67–93.

(53) Nakagame, S.; Chandra, R. P.; Kadla, J. F.; Saddler, J. N. The Isolation, Characterization and Effect of Lignin Isolated from Steam Pretreated Douglas-Fir on the Enzymatic Hydrolysis of Cellulose. *Bioresource Technology* **2011**, *102* (6), 4507–4517.

(54) Vishtal, A.; Kraslawski, A. Challenges in Industrial Applications of Technical Lignins. *Bioresources* **2011**, *6*, 3547–3568.

(55) Mahmood, N.; Yuan, Z.; Schmidt, J.; Xu, C. (Charles). Depolymerization of Lignins and Their Applications for the Preparation of Polyols and Rigid Polyurethane Foams: A Review. *Renewable and Sustainable Energy Reviews* **2016**, *60*, 317–329.

(56) Garguiak, J. D.; Lebo, S. E. Commercial Use of Lignin-Based Materials. In *Lignin: Historical, Biological, and Materials Perspectives*; ACS Symposium Series; American Chemical Society, 1999; Vol. 742, pp 304–320.

(57) Huang, J.; Zhang, L. Effects of NCO/OH Molar Ratio on Structure and Properties of Graft-Interpenetrating Polymer Networks from Polyurethane and Nitrolignin. *Polymer* **2002**, *43* (8), 2287–2294.

(58) Hatakeyama, H.; Kosugi, R.; Hatakeyama, T. Thermal Properties of Lignin-and Molasses-Based Polyurethane Foams. *Journal of Thermal Analysis and Calorimetry* **2008**, *92*, 419–424.

(59) Sarkar, S.; Adhikari, B. Synthesis and Characterization of Lignin–HTPB Copolyurethane. *European Polymer Journal* **2001**, *37* (7), 1391–1401.

(60) Sahoo, S.; Seydibeyoğlu, M. Ö.; Mohanty, A. K.; Misra, M. Characterization of Industrial Lignins for Their Utilization in Future Value Added Applications. *Biomass and Bioenergy* **2011**, *35* (10), 4230–4237.

(61) Fang, W.; Yang, S.; Wang, X.-L.; Yuan, T.-Q.; Sun, R.-C. Manufacture and Application of Lignin-Based Carbon Fibers (LCFs) and Lignin-Based Carbon Nanofibers (LCNFs). *Green Chemistry* **2017**, *19* (8), 1794–1827.

(62) Poursorkhabi, V.; Abdelwahab, M. A.; Misra, M.; Khalil, H.; Gharabaghi, B.; Mohanty, A. K. Processing, Carbonization, and Characterization of Lignin Based Electrospun Carbon Fibers: A Review. *Frontiers in Energy Research* **2020**, *8*.

(63) Gonçalves, A. R.; Benar, P. Hydroxymethylation and Oxidation of Organosolv Lignins and Utilization of the Products. *Bioresour Technol* **2001**, *79* (2), 103–111.

(64) Arend, M.; Westermann, B.; Risch, N. Modern Variants of the Mannich Reaction. *Angew Chem Int Ed Engl* **1998**, *37* (8), 1044–1070.

(65) Matsushita, Y.; Yasuda, S. Reactivity of a Condensed–Type Lignin Model Compound in the Mannich Reaction and Preparation of Cationic Surfactant from Sulfuric Acid Lignin. *J Wood Sci* **2003**, *49* (2), 166–171.

(66) Khvan, A. M.; Abduazimov, B. B.; Abduazimov, Kh. A. Nitration of Lignin and Sorptive Properties of the Resulting Products. *Chemistry of Natural Compounds* **2002**, *38* (5), 471–472.

2

2

(67) Sawamura, K.; Tobimatsu, Y.; Kamitakahara, H.; Takano, T. Lignin Functionalization through Chemical Demethylation: Preparation and Tannin-Like Properties of Demethylated Guaiacyl-Type Synthetic Lignins. *ACS Sustainable Chem. Eng.* **2017**, *5* (6), 5424–5431.

(68) Ou, J.; Li, S.; Li, W.; Liu, C.; Ren, J.; Yue, F. Revealing the Structural Influence on Lignin Phenolation and Its Nanoparticle Fabrication with Tunable Sizes. *ACS Sustainable Chem. Eng.* **2022**, *10* (45), 14845–14854.

(69) Jiang, X.; Tian, Z.; Ji, X.; Ma, H.; Yang, G.; He, M.; Dai, L.; Xu, T.; Si, C. Alkylation Modification for Lignin Color Reduction and Molecular Weight Adjustment. *Int J Biol Macromol* **2022**, *201*, 400–410.

(70) Kelley, S. S.; Glasser, W. G.; Ward, T. C. Engineering Plastics from Lignin. XV. Polyurethane Films from Chain-Extended Hydroxypropyl Lignin. *J. Appl. Polym. Sci.* **1988**, *36* (4), 759–772.

(71) Silva, E. A. B. da; Zabkova, M.; Araújo, J. D.; Cateto, C. A.; Barreiro, M. F.; Belgacem, M. N.; Rodrigues, A. E. An Integrated Process to Produce Vanillin and Lignin-Based Polyurethanes from Kraft Lignin. *Chemical Engineering Research and Design* **2009**, *87* (9), 1276–1292.

(72) Chen, C.; Zhu, M.; Li, M.; Fan, Y.; Sun, R.-C. Epoxidation and Etherification of Alkaline Lignin to Prepare Water-Soluble Derivatives and Its Performance in Improvement of Enzymatic Hydrolysis Efficiency. *Biotechnology for Biofuels* **2016**, *9* (1), 87.

(73) Buono, P.; Duval, A.; Verge, P.; Averous, L.; Habibi, Y. New Insights on the Chemical Modification of Lignin: Acetylation versus Silylation. *ACS Sustainable Chem. Eng.* **2016**, *4* (10), 5212–5222.

(74) Liu, L.-Y.; Hua, Q.; Renneckar, S. A Simple Route to Synthesize Esterified Lignin Derivatives. *Green Chem.* **2019**, *21* (13), 3682–3692.

(75) Mei, Q.; Shen, X.; Liu, H.; Liu, H.; Xiang, J.; Han, B. Selective Utilization of Methoxy Groups in Lignin for N-Methylation Reaction of Anilines. *Chem. Sci.* **2019**, *10* (4), 1082–1088.

(76) Yang, S.; Zhang, Y.; Yuan, T.-Q.; Sun, R.-C. Lignin-Phenol-Formaldehyde Resin Adhesives Prepared with Biorefinery Technical Lignins. *J. Appl. Polym. Sci.* **2015**, *132* (36), 42493.

(77) Zhang, M.; Ogale, A. A. Carbon Fibers from Dry-Spinning of Acetylated Softwood Kraft Lignin. *Carbon* **2014**, *69*, 626–629.

(78) Bajwa, D. S.; Pourhashem, G.; Ullah, A. H.; Bajwa, S. G. A Concise Review of Current Lignin Production, Applications, Products and Their Environmental Impact. *Industrial Crops and Products* **2019**, *139*, 111526.

(79) Naseem, A.; Tabasum, S.; Zia, K. M.; Zuber, M.; Ali, M.; Noreen, A. Lignin-Derivatives Based Polymers, Blends and Composites: A Review. *International Journal of Biological Macromolecules* **2016**, *93*, 296–313.

(80) Sen, S.; Patil, S.; Argyropoulos, D. S. Thermal Properties of Lignin in Copolymers, Blends, and Composites: A Review. *Green Chem.* **2015**, *17* (11), 4862–4887.

(81) Liu, S.; Cheng, X. Application of Lignin as Antioxidant in Styrene Butadiene Rubber Composite. *AIP Conference Proceedings* **2010**, *1251* (1), 344–347.

(82) Xu, G.; Yan, G.; Zhang, J. Lignin as Coupling Agent in EPDM Rubber: Thermal and Mechanical Properties. *Polym. Bull.* **2015**, *72* (9), 2389–2398.

(83) Jagadale, S.; Chavan, D.; Rajkumar, K.; Shinde, D.; Patil, C. Lignin As a Plasticizer In Nitrile Rubber, It's Effect on Properties. *International Journal of Research in Engineering and Applied Sciences ISSN 2249-3905* **2016**, *Volume 6*, 78–84.

(84) Keilen, J. J.; Pollak, A. Lignin for Reinforcing Rubber. *Rubber Chemistry and Technology* **1947**, *20* (4), 1099–1108.

(85) Kumaran, M. G.; De, S. K. Utilization of Lignins in Rubber Compounding. *Journal of Applied Polymer Science* **1978**, *22* (7), 1885–1893.

(86) Botros, S. H.; Eid, M. A. M.; Nageeb, Z. A. Thermal stability and dielectric relaxation of natural rubber/soda lignin and natural rubber/thiolignin composites. *Journal of Applied Polymer Science* **2006**, *99* (5), 2504–2511.

(87) Košíková, B.; Gregorová, A. Sulfur-Free Lignin as Reinforcing Component of Styrene–Butadiene Rubber. *Journal of Applied Polymer Science* **2005**, *97* (3), 924–929.

(88) Barana, D.; Ali, S. D.; Salanti, A.; Orlandi, M.; Castellani, L.; Hanel, T.; Zoia, L. Influence of Lignin Features on Thermal Stability and Mechanical Properties of Natural Rubber Compounds. *ACS Sustainable Chem. Eng.* **2016**, *4* (10), 5258–5267.

(89) Ikeda, Y.; Phakkeeree, T.; Junkong, P.; Yokohama, H.; Phinyocheep, P.; Kitano, R.; Kato, A. Reinforcing Biofiller "Lignin" for High Performance Green Natural Rubber Nanocomposites. *RSC Advances* **2017**, *7* (9), 5222–5231.

(90) Mohamad Aini, N. A.; Othman, N.; Hussin, M. H.; Sahakaro, K.; Hayeemasae, N. Lignin as Alternative Reinforcing Filler in the Rubber Industry: A Review. *Frontiers in Materials* **2020**, *6*, 329–347.

(91) Yu, P.; He, H.; Jia, Y.; Tian, S.; Chen, J.; Jia, D.; Luo, Y. A Comprehensive Study on Lignin as a Green Alternative of Silica in Natural Rubber Composites. *Polymer Testing* **2016**, *54*, 176–185.

(92) Jiang, C.; He, H.; Jiang, H.; Ma, L.; Jia, D. M. Nano-Lignin Filled Natural Rubber Composites: Preparation and Characterization. *Express Polym. Lett.* **2013**, *7* (5), 480–493.

(93) Asrul. Lignin Filled Unvulcanised Natural Rubber Latex: Effects of Lignin on Oil Resistance, Tensile Strength and Morphology of Rubber Films; 2013.

(94) Yu, P.; He, H.; Jiang, C.; Wang, D.; Jia, Y.; Zhou, L.; Jia, D. M. Reinforcing Styrene Butadiene Rubber with Lignin-Novolac Epoxy Resin Networks. *Express Polymer Letters* **2015**, *9*, 36–48.

(95) Sagajllo, I. Lignin as a Compounding Ingredient for Natural Rubber. *Rubber Chemistry and Technology* **1957**, *30* (2), 639–651.

(96) Jiang, C.; He, H.; Yao, X.; Yu, P.; Zhou, L.; Jia, D. In Situ Dispersion and Compatibilization of Lignin/Epoxidized Natural Rubber Composites: Reactivity, Morphology and Property. *Journal of Applied Polymer Science* **2015**, *132* (23).

(97) Jiang, C.; He, H.; Yao, X.; Yu, P.; Zhou, L.; Jia, D. The Aggregation Structure Regulation of Lignin by Chemical Modification and Its Effect on the Property of Lignin/Styrene–Butadiene Rubber Composites. *Journal of Applied Polymer Science* **2018**, *135* (5), 45759.

(98) Li, Z.-X.; Kong, Y.-R.; Chen, X.-F.; Huang, Y.-J.; Lv, Y.-D.; Li, G.-X. High-Temperature Thermo-Oxidative Aging of Vulcanized Natural Rubber Nanocomposites: Evolution of Microstructure and Mechanical Properties. *Chin J Polym Sci* **2023**, *41* (8), 1287–1297.

(99) Setua, D. K.; Shukla, M. K.; Nigam, V.; Singh, H.; Mathur, G. N. Lignin Reinforced Rubber Composites. *Polymer Composites* **2000**, *21* (6), 988–995.

2

(100) Frigerio, P.; Zoia, L.; Orlandi, M.; Hanel, T.; Castellani, L. Application of Sulphur-Free Lignins as a Filler for Elastomers: Effect of Hexamethylenetetramine Treatment. *BioResources* **2014**, *9*.

(101) Bahl, K.; Jana, S. C. Surface Modification of Lignosulfonates for Reinforcement of Styrene–Butadiene Rubber Compounds. *Journal of Applied Polymer Science* **2014**, *131* (7), 1–9.

(102) Barana, D.; Orlandi, M.; Zoia, L.; Castellani, L.; Hanel, T.; Bolck, C.; Gosselink, R. Lignin Based Functional Additives for Natural Rubber. *ACS Sustainable Chem. Eng.* **2018**, *6* (9), 11843–11852.

(103) Bahl, K.; Swanson, N.; Pugh, C.; Jana, S. C. Polybutadiene-g-Polypentafluorostyrene as a Coupling Agent for Lignin-Filled Rubber Compounds. *Polymer* **2014**, *55* (26), 6754–6763.

(104) Mohamad Aini, N. A.; Othman, N.; Hussin, M. H.; Sahakaro, K.; Hayeemasae, N. Efficiency of Interaction between Hybrid Fillers Carbon Black/Lignin with Various Rubber-Based Compatibilizer, Epoxidized Natural Rubber, and Liquid Butadiene Rubber in NR/BR Composites: Mechanical, Flexibility and Dynamical Properties. *Industrial Crops and Products* **2022**, *185*, 115167.

(105) Shorey, R.; Gupta, A.; Mekonnen, T. H. Hydrophobic Modification of Lignin for Rubber Composites. *Industrial Crops and Products* **2021**, *174*, 114189.

(106) Hait, S.; De, D.; Ghosh, P.; Chanda, J.; Mukhopadhyay, R.; Dasgupta, S.; Sallat, A.; Al Aiti, M.; Stöckelhuber, K. W.; Wießner, S.; Heinrich, G.; Das, A. Understanding the Coupling Effect between Lignin and Polybutadiene Elastomer. *Journal of Composites Science* **2021**, *5* (6), 154–169.

(107) Cao, Z.; Liao, Z.; Wang, X.; Su, S.; Feng, J.; Zhu, J. Preparation and Properties of NBR Composites Filled with a Novel Black Liquor–Montmorillonite Complex. *Journal of Applied Polymer Science* **2013**, *127* (5), 3725–3730.

(108) Xiao, S.; Feng, J.; Zhu, J.; Wang, X.; Yi, C.; Su, S. Preparation and Characterization of Lignin-Layered Double Hydroxide/Styrene-Butadiene Rubber Composites. *Journal of Applied Polymer Science* **2013**, *130* (2), 1308–1312.

(109) Bahl, K.; Miyoshi, T.; Jana, S. C. Hybrid Fillers of Lignin and Carbon Black for Lowering of Viscoelastic Loss in Rubber Compounds. *Polymer* **2014**, *55* (16), 3825–3835.

(110) Liu, R.; Li, J.; Lu, T.; Han, X.; Yan, Z.; Zhao, S.; Wang, H. Comparative Study on the Synergistic Reinforcement of Lignin between Carbon Black/Lignin and Silica/Lignin Hybrid Filled Natural Rubber Composites. *Industrial Crops and Products* **2022**, *187*, 115378.

(111) Griffith, T. R.; MacGregor, D. W. Aids in Vulcanization of Lignin–Natural Rubber Coprecipitates. *Ind. Eng. Chem.* **1953**, *45* (2), 380–386.

(112) Wang, H.; Liu, W.; Huang, J.; Yang, D.; Qiu, X. Bioinspired Engineering towards Tailoring Advanced Lignin/Rubber Elastomers. *Polymers (Basel)* **2018**, *10* (9), 1033.

(113) Li, M.; Zhu, L.; Xiao, H.; Shen, T.; Tan, Z.; Zhuang, W.; Xi, Y.; Ji, X.; Zhu, C.; Ying, H. Design of a Lignin-Based Versatile Bioreinforcement for High-Performance Natural Rubber Composites. *ACS Sustainable Chem. Eng.* **2022**, *10* (24), 8031–8042.

(114) Peterson, A. A.; Vogel, F.; Lachance, R. P.; Fröling, M.; Michael J. Antal, J.; Tester, J. W. Thermochemical Biofuel Production in Hydrothermal Media: A Review of Sub- and Supercritical Water Technologies. *Energy Environ. Sci.* **2008**, *1* (1), 32–65.

(115) Wikberg, H.; Ohra-aho, T.; Pileidis, F.; Titirici, M.-M. Structural and Morphological Changes in Kraft Lignin during Hydrothermal Carbonization. *ACS Sustainable Chem. Eng.* **2015**, *3* (11), 2737–2745.

2

(116) Libra, J. A.; Ro, K. S.; Kammann, C.; Funke, A.; Berge, N. D.; Neubauer, Y.; Titirici, M.-M.; Fühner, C.; Bens, O.; Kern, J.; Emmerich, K.-H. Hydrothermal Carbonization of Biomass Residuals: A Comparative Review of the Chemistry, Processes and Applications of Wet and Dry Pyrolysis. *Biofuels* **2011**, *2* (1), 71–106.

(117) Erfani Jazi, M.; Narayanan, G.; Aghabozorgi, F.; Farajidizaji, B.; Aghaei, A.; Kamyabi, M. A.; Navarathna, C. M.; Mlsna, T. E. Structure, Chemistry and Physicochemistry of Lignin for Material Functionalization. *SN Appl. Sci.* **2019**, *1* (9), 1094.

(118) Funke, A.; Ziegler, F. Hydrothermal Carbonization of Biomass: A Summary and Discussion of Chemical Mechanisms for Process Engineering. *Biofuels, Bioproducts and Biorefining* **2010**, *4* (2), 160–177.

(119) A. Nicolae, S.; Au, H.; Modugno, P.; Luo, H.; E. Szego, A.; Qiao, M.; Li, L.; Yin, W.; J. Heeres, H.; Berge, N.; Titirici, M.-M. Recent Advances in Hydrothermal Carbonisation: From Tailored Carbon Materials and Biochemicals to Applications and Bioenergy. *Green Chemistry* **2020**, *22* (15), 4747–4800.

(120) Barbier, J.; Charon, N.; Dupassieux, N.; Loppinet-Serani, A.; Mahé, L.; Ponthus, J.; Courtiade, M.; Ducrozet, A.; Quoineaud, A.-A.; Cansell, F. Hydrothermal Conversion of Lignin Compounds. A Detailed Study of Fragmentation and Condensation Reaction Pathways. *Biomass and Bioenergy* **2012**, *46*, 479–491.

(121) Kang, S.; Li, X.; Fan, J.; Chang, J. Classified Separation of Lignin Hydrothermal Liquefied Products. *Ind. Eng. Chem. Res.* **2011**, *50* (19), 11288–11296.

(122) Hu, J.; Shen, D.; Wu, S.; Zhang, H.; Xiao, R. Effect of Temperature on Structure Evolution in Char from Hydrothermal Degradation of Lignin. *Journal of Analytical and Applied Pyrolysis* **2014**, *106*, 118–124.

(123) Padhye, L. P.; Bandala, E. R.; Wijesiri, B.; Goonetilleke, A.; Bolan, N. Hydrochar: A Promising Step Towards Achieving a Circular Economy and Sustainable Development Goals. *Frontiers in Chemical Engineering* **2022**, *4*.

(124) Islam, M. T.; Sultana, A. I.; Chambers, C.; Saha, S.; Saha, N.; Kirtania, K.; Reza, M. T. Recent Progress on Emerging Applications of Hydrochar. *Energies* **2022**, *15* (24), 9340.

(125) Sekar, P. Design of a Bio-Based Filler System for Tire Treads. PDEng thesis, University of Twente, The Netherlands, 2018.

2

3. Reinforcing effects of Hydrothermally Treated Kraft Lignin in an SSBR/BR blend
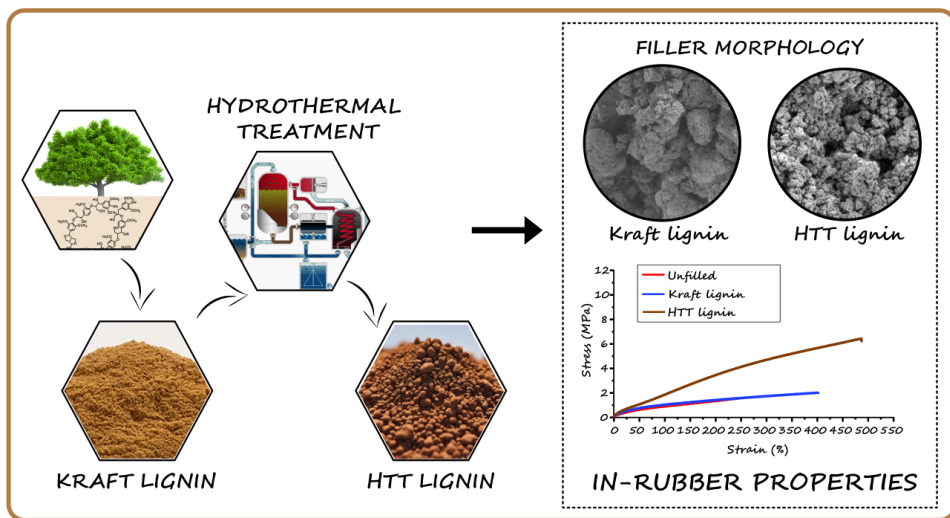
Impact of Hydrothermal Treatment on Physio-chemical and Reinforcing Properties of Lignin

This chapter examines the morphological, physical, and chemical differences between hydrothermally treated lignin and its initial feedstock, Kraft lignin. Furthermore, the reinforcing potential of the hydrothermally treated lignin was investigated in a blend of solution styrene butadiene rubber/ butadiene rubber (SSBR/BR) in relation to the initial feedstock Kraft lignin, conventional reinforcing fillers carbon black and silica[a]. The results demonstrate that on the one hand, hydrothermally treated lignin exhibits superior in-rubber performance compared to the Kraft lignin. The improvement was attributed to the physio-chemical changes induced by the hydrothermal process. On the other hand, the reinforcing effects of hydrothermally-treated lignin in the investigated rubber system are low compared to the reinforcing carbon black and silica fillers. This was ascribed to its relatively low surface area and still available polar functionality, which negatively affected its micro-dispersion in the used non-polar rubbers.

3

---

[a]Some of the figures (i.e., in-rubber data of carbon black-, silica-, HTT lignin-filled rubber compounds) discussed in this chapter were published[1]

3.1 Introduction

Non-reinforced rubber vulcanizates are seldomly utilized in practical applications as they are considered to be "too weak". The addition of finely divided particulate fillers to rubber enhances the performance of rubber composites, especially stiffness and strength properties such as tensile strength, abrasion, and tear resistance[2,3] This improvement in mechanical properties of the rubber by the inclusion of a second solid phase is termed as reinforcement.[2,3] Depending on the influence of filler on the rubber reinforcement, they are classified as reinforcing, semi-reinforcing, and non-reinforcing.[4] The origin of such reinforcement has been related to the chemical and/or physical interaction between the polymer and the filler.[2,3,5] The filler-polymer interaction is influenced by the degree of dispersion of the filler within the polymer matrix.[2,3,5] The expression "dispersion of filler" means the change in the physical nature of the fillers, i.e., reduction in filler cluster sizes leading to a spatial rearrangement by applying shear forces during mixing.[6] Depending on the size of generated clusters in the rubber matrix, the quality of filler dispersion can be classified as macro-(between 2 and 100 μm) and micro-(less than 2 μm) dispersion according to ASTM D3053.[7,8] Excessively deteriorated filler clusters do not reinforce the elastomer.[9] The reinforcing effect of filler on rubber strongly depends on the loading and filler characteristics such as particle size and surface area, structure, and surface chemistry.[10] These parameters govern the degree of rubber-filler and filler-filler interaction (dispersion). For example, when the primary particle size of the filler is in the range of 1000 to 8000 nm, the filler is categorized as "non-reinforcing" (e.g., soft clays); fillers with a size between 100 to 1000 nm are classified as "semi-reinforcing" (hard clays, precipitated calcium carbonates, zinc oxide); and fillers with a particle size of 10 to 100 nm are considered to be "reinforcing" filler.[3]

Carbon black, produced from partial combustion or thermal decomposition of petroleum hydrocarbons, and silica, produced by the precipitation process of a water-soluble sodium silicate (water-glass) with sulfuric acid, are the most widely used and dominant reinforcing fillers in rubber composites due to their high reinforcing effects. Currently, these fillers cannot meet the sustainability goals either due to their source of origin or due to the use of non-renewable chemicals during manufacturing. Therefore, to strive towards sustainability in rubber's value chain, the use of alternative fillers, in particular renewable fillers, is gaining significant attention.[11] In this context, the use of lignin as an alternative renewable filler has been explored by researchers, as discussed in **Chapter 2**.[12–16] Nevertheless, the practical application of lignin as a reinforcing filler in rubber is challenging. From the findings of the prior art, it is clear that the lack of strong interfacial interactions between lignin and rubber matrix due to lignin's polar functional groups and the presence of large particle size affects negatively the reinforcing effect of lignin in rubber. Thus, the filler characteristics of lignin need to be enhanced further to facilitate its compatibility and dispersion in the rubber matrix. As discussed in **Chapter 1**, **under section 1.1**, lignins with enhanced defined chemical and morphological properties for

application as filler material can be produced by hydrothermal treatment (HTT) process.[17,18] Thus, this thesis investigates the use of one particular lignin type, softwood Kraft lignin treated by SunCoal's hydrothermal process[19-21] as a filler for rubber application. The Kraft lignin obtained after applying the HTT process is termed hydrothermally treated (HTT) lignin.

This chapter aims to provide insights into the variation in (i) elemental composition, chemical structure, and morphology and (ii) reinforcement behavior of Kraft lignin before and after hydrothermal treatment. For the first part of the study (i), a comprehensive characterization of the HTT lignin was carried out using solid-state ^{13}C nuclear magnetic resonance (NMR), diffuse reflectance infrared Fourier transform spectroscopy (DRIFTS), and scanning electron microscopy (SEM). The results were compared to those of the initial feedstock softwood Kraft lignin. For the second part (ii), HTT lignin was used as a filler for a solution styrene-butadiene rubber/ butadiene rubber (SSBR/BR) blend. The resulting rheological, cure, mechanical, and morphological properties were analyzed and compared to blends containing Kraft lignin, commercially available reinforcing carbon black, and silica-filled compounds. For silica-filled compound, a silane coupling agent, bis-(triethoxysilylpropyl)tetrasulfide, was employed to improve the dispersion and compatibility of silica with the hydrophobic elastomer.[22,23]

3.2 Experimental

3.2.1 Materials

Softwood Kraft lignin and HTT lignin were provided by SunCoal Industries GmbH, Germany. Carbon black, N330 (CB), and silica, ULTRASIL®7000GR (S) were purchased from Orion Engineered Carbon and Evonik Industries AG, Germany, respectively. **Table 3.1** lists the differences in filler characteristics. Bis-(triethoxysilylpropyl)tetrasulfide (TESPT) was obtained from Evonik Industries AG, Germany, and used as a coupling agent. Functionalized solution-SBR (SPRINTAN^{TR} SLR 4602, Tg of 25 °C) with 21 wt.% styrene and 62 wt.% vinyl-butadiene configurations and neodymium catalyzed BR (BUNA®CB24, Tg of -107 °C) with 96 wt.% 1,4 cis-content were used as obtained from Synthos Deutschland GmbH, Schkopau and Arlanxeo Deutschland GmbH, Germany, respectively. Treated distillate aromatic extract oil (TDAE), VIVATEC® 500, was provided by Hansen & Rosenthal KG, Germany, and used as processing oil. Other ingredients such as (i) vulcanization/cure activators: zinc oxide (ZnO) and stearic acid (SA); (ii) curing agent: sulfur (S); and (iii) accelerators: N-tert-butyl-2-benzothiazolesulfenamide (TBBS), tetrabenzylthiuramdisulfide (TBzTD), 1,3-diphenylguanidine (DPG) were provided by Apollo Tires B.V, The Netherlands. Antidegradants 2,2,4-trimethyl-1,2-dihydroquinoline (TMQ), N-(1,3-dimethylbutyl)-N'-phenyl-p-phenylenediamine (6-PPD) were supplied by Flexsys, Belgium.

Table 3.1 Filler specifications provided by the supplier

Filler	Specific density (g/cm³)	BET specific surface area (m²/g)
HTT lignin (HL)	1.35	38
Kraft lignin (KL)	1.35	5
Carbon black (CB)	1.8	78
Silica (SL)	2.0	180

3.2.2 Characterization of the Lignins used in this study

3.2.2.1 Elemental compositions

The relative proportions of carbon (C), hydrogen (H), sulfur (S), and oxygen (O) were determined using a Thermo Scientific Flash 2000 series elemental analyzer. Calibration was done with acetanilide before the start of the test. The sample was weighed in tin capsules and fed into an oxidation/reduction reactor kept at a temperature of 900 – 1000 °C. The measurement was repeated three times for KL and HL, and the average value was reported in this study.

3.2.2.2 Structural analysis

^{13}C solid-state NMR spectra of lignins were generated on a Bruker 9.4 T (operating at 400.34 MHz for ^{1}H and at 100.67 MHz for ^{13}C) Avance III HD 400 spectrometer equipped with a 4 mm magic angle spinning (MAS) probe. ^{13}C cross-polarization (CP) MAS measurements were conducted at a spinning rate of 14 kHz, with a 90° pulse for ^{1}H of 2.4 µs and a contact time of 2 ms. ^{13}C spectra were internally referenced by the chemical shift of the methoxy peak of the lignin (δ = 56.1 ppm) and obtained with 1486 complex points with a spectral width of 295 ppm, with a relaxation delay of 2 s. They were acquired with a maximum of 30000 averages, with sufficient signal-to-noise ratio being ensured.

Diffuse Reflectance Infrared Fourier transform spectroscopy DRIFTS was used to evaluate the functional groups on the lignin surface. Spectra were recorded in the range 4000 to 400 cm^{-1} and averaged over 32 scans, using a resolution of 4 cm^{-1} on a Perkin-Elmer 100 spectrometer equipped with a deuterated triglycine sulfate (DTGS) detector. Potassium bromide powder, KBr (99 %, FTIR grade, Sigma-Aldrich) was used as a reference for background scanning and baseline correction. In addition, KBR was also used for the sample preparation. For this, KBR and lignin (in a ratio of 20:1) were mixed and ground together using a mortar and pestle. The obtained relative peak absorbance was normalized for all IR bands in each sample. The measurement was repeated three times for each sample. All tests were performed at room temperature.

3

3.2.2.3 Morphological study

SEM was performed on a Jeol JSM-7200F to observe the surface morphology of the lignin samples. The samples were mounted on a layer of colloidal graphite paste (isopropanol-based) and applied to a copper stub. Subsequently, the samples were dried in a vacuum oven for 2 hours at 40 °C and then surface coated with gold using a Jeol JFC-1300 sputter coater before analysis. The gold sputtering step was carried out to prevent charge accumulation on the sample during the analysis, which could lead to image artifacts.

3.2.3 Preparation of Rubber Compounds

The compound formulations for filled and unfilled compounds used throughout this investigation are shown in **Table 3.2**. It is similar to a typical passenger car tire tread compound.[22]

Table 3.2 Formulation for the compound studies (Amounts in parts per 100 rubber (phr))

	Ingredients	Unfilled	CBR[a]	STR[b]	HLR[c]	KLR[d]
Stage 1	SSBR	75	75	75	75	75
	BR	25	25	25	25	25
	Filler	-	80	80	80	80
	TESPT	-	-	6.2	-	-
	TDAE	33	33	33	33	33
	ZnO	2.5	2.5	2.5	2.5	2.5
	SA	2.5	2.5	2.5	2.5	2.5
	TMQ	2	2	2	2	2
	6-PPD	2	2	2	2	2
Stage 2	S	2.2	2.2	2.2	2.2	2.2
	TBBS	1.5	1.5	1.5	1.5	1.5
	TBzTD	0.5	0.5	0.5	0.5	0.5
	DPG	0.25	0.25	0.25	0.25	0.25

[a]**C**arbon **B**lack-filled **r**ubber, [b]TESPT silanized **S**ilica-filled **r**ubber, [c]**H**TT **L**ignin-filled **r**ubber, [d]**K**raft **L**ignin-filled **r**ubber

Two-stage mixing was performed for all the compounds using a tangential rotor internal mixer with a chamber volume of 390 cm³ (Brabender Plasticorder 350S). This way of mixing was selected as it was observed to be efficient in terms of time and achieving properties. For stage 1 mixing (masterbatch preparation), the mixer was operated at a fill factor of 70 %, a rotor speed of 50 rpm, and an initial set temperature of 50 °C till the ram sweep at 5:00. The detailed mixing procedure for unfilled and filled rubber compounds is shown in **Table 3.3**.

Table 3.3 Two-stage mixing procedure for unfilled and filled rubber compounds

	Mixing time (min: sec)	Rotor speed (RPM)	Action for unfilled rubber
	0:00 - 0:20	50	Open the ram and load rubbers
	0:20 - 1:20	50	Mix rubbers
	1:20 - 1:40	50	Add ZnO, SA, TMQ, and 6-PPD
Stage 1	1:40 - 2:40	50	Mix
	2:40 - 3:00	50	Ram sweep
	3:00 - 5:10	Variable	Mix
	5:10	-	Discharge at ~90 - 100 °C
	0:00 - 0:20	30	Add the masterbatch
	0:20 - 1:00	30	Mix
	1:00 - 1:10	30	Add S, TBBS, TBzTD, DPG
Stage 2	1:10 - 2:00	30	Mix
	2:00 - 2:10	30	Ram sweep
	2:10 - 5:00	30	Mix & discharge at ~90 - 100 °C

	Mixing time (min: sec)	Rotor speed (RPM)	Action for filled rubber
	0:00 - 0:20	50	Open the ram and load rubbers
	0:20 - 1:00	50	Mix rubbers
	1:00 - 1:20	50	1st part of filler (*½ silane)
	1:20 - 2:00	50	Mix
	2:00 - 2:20	50	2nd part of filler (*½ silane), TDAE
	2:20 - 3:00	50	Mix
	3:00 - 3:20	50	3rd part of filler
Stage 1	3:20 - 4:00	50	Mix
	4:00 - 4:20	50	4th part of filler, ZnO, SA, TMQ, and 6PPD
	4:20 - 5:00	50	Mix
	5:00 - 5:20	50	Ram sweep
	5:20 - 10:00	Variable	Mixing and silanization
	10:00	-	Discharge at ~140 - 150 °C after silanization
	0:00 - 0:20	30	Add the masterbatch
	0:20 - 1:00	30	Mix
	1:00 - 1:10	30	Add S, TBBS, TBzTD, DPG
Stage 2	1:10 - 2:00	30	Mix
	2:00 - 2:10	30	Ram sweep
	2:10 - 5:00	30	Mix & discharge at ~90 - 100 °C

The incorporation of fillers into the mixer was done in four equal parts, as reported in **Table 3.3**. This is because both the Kraft and HTT lignins have low bulk density. Thus, four subsequent steps facilitated easy incorporation and prevented material loss. The mixing conditions of the filled compounds, including carbon black and silica-filled rubber, were kept constant to avoid variation in the mixing sequence and its influence on rubber

properties. To carry out the modification reaction of silica by silane (the reaction is commonly known as silanization) in the rubber mixer, the mixture temperature was gradually increased after adding all the ingredients by adjusting the rotor speed. It is to be noted that TESPT (average S-rank of 3.8) in the STR compound can donate sulfur and can participate in rubber crosslinking/vulcanization; therefore, the compound was discharged between 140 - 150 °C to prevent premature crosslinks (pre-scorch). Apart from influencing the processing, the additional sulfur released from TESPT can result in an increase in crosslink density and, consequently, in an improvement of mechanical properties. A similar protocol was followed for other filled compounds to avoid mixing variations. After stage 1, all the compounds were sheeted out on a Schwabenthan Polymix80T 80 x 300 mm two-roll mill and kept overnight before the second mixing stage.

Stage 2 mixing: The addition of curatives was also carried out in the internal mixer operated at a fill factor of 70 %, a rotor speed of 30 rpm, and an initial set temperature of 50 °C. The rotor speed was relatively low to ensure a low mixing temperature to prevent pre-scorch. After the compounds were discharged, they were sheeted out on the two-roll mill operating with a gap width of 2.5 mm.

3.2.4 Compound Characterizations

3.2.4.1 Rheological and vulcanization properties

The rheological properties of the unfilled and different filled SSBR/BR compositions in terms of curing/vulcanization behavior and Payne effect were assessed with a Rubber Process Analyzer (TA Instruments, USA).

(a) Vulcanization behavior: The cure characteristics of the compounds were determined at 160 °C for 30 minutes at 1.667 Hz frequency and 6.98 % strain according to ISO 3417. The corresponding scorch time (ts_2) and optimum time of cure ($t_{c,90}$), the minimum (M_L) and maximum torque (M_H), and torque increase (ΔM) values were recorded. The rubber compounds were vulcanized in a Wickert laboratory press WLP 1600/5*4/3 at 160 °C and 100 bar pressure.

(b) Payne effect: The difference between the storage modulus (G') at small (0.56 %) and large strain amplitude (100 %), known as the Payne effect, was taken as an indication of the extent of filler-filler interaction in carbon black- and silica-filled compounds. [24–27] The storage moduli G' of the still uncured compounds were determined at 100 °C. The values were recorded under shear deformation with a strain sweep range of 0.56 - 100 % at a frequency of 1 Hz. The reported data are the average values of three specimens of each sample.

3.2.4.2 Apparent crosslink density

The apparent crosslink densities (CLD) of the rubber vulcanizates were measured by swelling experiments. Tensile sheets were used for this measurement. Prior to the swelling test, the cured samples were extracted in a Soxhlet apparatus with acetone for 48 h to remove low molecular weight polar substances like unreacted curatives or curing by-products. As the investigated lignins are partially soluble in acetone, their impact on weight loss was also studied. The extracted samples were then dried in a vacuum oven at 40 °C for 24 h and weighed. In comparison to the conventional filler, the observed change in weight of the lignin samples before and after acetone extraction is negligible. The acetone-extracted specimens were subsequently immersed in toluene at room temperature for one week. At the end of the immersion period, the weight of swollen vulcanizates was measured after removing the surface liquid with cellulose filter paper (pore size 1 μm). Afterward, the samples were dried in a vacuum oven for 24 h at 105 °C and 0.8 bar to obtain the dry weight. The apparent crosslink density per unit volume V_e (in moles per volume of rubber, mol/cm³) was calculated according to Flory-Rehner,[28] **equations (3.1) and (3.2)**:

$$V_e = \frac{-[\ln(1 - V_r) + V_r + \chi V_r^2]}{V_s (V_r^{\frac{1}{3}} - \frac{V_r}{2})} \qquad (3.1)$$

where the volume fraction of polymer in the swollen gel at equilibrium (V_r) can be calculated as:

$$V_r = \frac{m_r}{m_r + m_s(\frac{\rho_r}{\rho_s})} \qquad (3.2)$$

χ is the Flory-Huggins polymer-solvent interaction parameter (0.37 for SBR/toluene [29] is used for calculation considering the higher proportion of SSBR than BR in the formulation and because the polymer solubility parameter difference between SSBR and BR is minimal); V_s is the molar volume of the solvent (106.20 cm³/mol for toluene); m_r is the mass of the rubber network; m_s is the mass of the solvent in the swollen sample at equilibrium conditions; ρ_s and ρ_r are the densities of the solvent (0.867 g/cm³) and SSBR rubber (0.93 g/cm³, as provided by the supplier), respectively. The crosslink density was not corrected by the Kraus equation, which can distinguish the network formed by the rubber crosslinking and the rubber-filler interaction.[30] This is because the interaction parameter between filler and rubber (K constant) required for the Kraus equation was not determined experimentally by varying the filler loading.[30] Since all the filled compounds contain the same amount of 80 phr filler, the values can be mutually compared. Therefore,

the designation apparent crosslink density was used. However, due to the very different chemical nature of the fillers, this comparison has to be made with reserve. The given apparent crosslink density values are the average values of five specimens of every sample.

3.2.4.3 Morphological and Modulus mapping

The evaluation of filler micro-dispersion in the rubber matrix was carried out using atomic force microscopy (AFM). The choice for AFM over other microscopic techniques such as transmission or scanning electron microscopy (TEM or SEM) was due to the fact that along with the characterization of the sample morphology and filler micro-dispersion, also the mechanical properties of the surface, in particular, the elastic modulus can be evaluated. Besides, AFM does not require intensive sample preparation steps, and the images can be acquired in atmospheric conditions.[31] Thus, AFM was employed to study the bulk morphology and mechanical characteristics at the surface of the specimens with different filled vulcanizates.[32] The samples were cryo-fractured in liquid nitrogen. An exposed surface was measured in air at room temperature using a MultiMode 8 AFM instrument with a NanoScope V controller (Bruker) to obtain a series of images representing the topography and contact elastic modulus values (hereinafter called Young's modulus) of different filled vulcanizates.[32] The AFM was operated in the PeakForce Quantitative Nanomechanical Mapping mode (PF-QNM) to record force-distance curves, typically 262,144 per map. The curves were further processed in the NanoScope Analysis software (version 1.9). The ScanAsyst controlled parameters (scan rate, feedback loop, applied load, etc.) in the user interface of the NanoScope software (version 9.7) were set to "off" to use dedicated constant scanning parameters. The force-distance curves were collected following a sine-wave sample-tip trajectory with a frequency of 2 kHz and utilizing a peak-force amplitude value of 150 - 200 nm. Soft cantilevers were chosen to perform this study, with a nominal spring constant of 0.5 N/m and a silicon-made tip with a nominal radius of 8 nm (MikroMasch, HQ: NSC19/No Al). The AFM optical sensitivity (deflection sensitivity) was calculated based on the thermal tune method.[33] The Young's modulus was calculated by fitting the slope of the extended part of the force-distance curves with a contact mechanics model based on the Derjaguin, Muller, and Toporov (DMT) theory, [34] using the following **equation (3.3)**:

$$E = (F_L - F_{adh})\frac{3(1 - v^2)}{4}R^{-\frac{1}{2}}(z - d)^{-\frac{3}{2}} \qquad (3.3)$$

where F_L is the applied maximum force (load); F_{adh} is the adhesion force; v is the Poisson's ratio; R is the AFM tip radius; z is the position of the AFM scanner; d is the cantilever deflection. For the Poisson's ratio, a value close to 0.5, common for rubbery materials, was used.[35] The nominal spring constant and tip radius values were taken for the calculations. Thus, it should be noted that the calculated values of the elastic modulus are based on

these estimations. Other values needed for calculating Young's modulus based on the DMT theory were extracted from force-distance curves.

For each sample, the topology and elastic modulus images were collected from five different places over an area of 10 x 10 μm^2 and at a digital resolution of 512 pixels × 512 pixels. Log-Young's modulus maps, as the most contrasted, were processed by Bearing Analysis in the NanoScope Analysis software to export the threshold images of only two map colors (Filler versus matrix). Then, the filler cluster and the elementary particle sizes were measured individually using the ImageJ software, assuming a spherical shape. Around 200 clusters and elementary particles were counted for each sample.

3.2.4.4 Mechanical properties

The vulcanizates for tensile tests were cured in sheets of 90 x 90 x 2 mm^3 in the Wickert laboratory press for their respective optimum cure time ($t_{c,90}$) plus two minutes. The vulcanized sheets were die-cut to dumbbell-shaped specimens for the tensile tests. The tests were performed in a Zwick Z020 Universal Tensile Tester at a crosshead speed of 500 mm/min, according to ISO 37, method A. Five specimens were used for the evaluation of the tensile data. The mean values taken from these five specimens are reported.

The hardness of the samples was measured with a Zwick 3150 hardness tester, Shore A type, according to ISO 48 at 23 °C. The tests were carried out using cylindrical specimens of 6 mm thickness prepared for their respective optimum cure time ($t_{c,90}$) plus five minutes. Three specimens were used for the compound hardness evaluation, and the mean value was reported. Also, the standard deviation from these three specimens is reported as an error bar.

3.2.4.5 Dynamic mechanical properties

The dynamic mechanical performance of rubber compounds is paramount for many applications, particularly tires. The addition of filler changes the dynamic properties of rubber, both modulus and hysteresis. For a given polymer and cure system, the filler parameters and morphology play an essential role in a compound's dynamic properties and viscoelastic behavior.[36] The dynamic properties were evaluated by Dynamic Mechanical Analysis (DMA). For this test, circular-plate-shaped specimens of 10 mm diameter were die-cut from the cured sheets prepared for the tensile tests. A temperature sweep test was performed at 10 Hz frequency using a DMA Eplexor 9 (Netzsch Gabo Instrument GmbH) in double shear mode. The measurements were divided into two segments with different strains. The low strain of 1 % was applied in the low-temperature range (-35 to +10 °C) to avoid the compound's stiffness effect. In contrast, a strain of 3 % was used in the temperature range of +10 to 60 °C to investigate the dynamic properties at elevated temperatures where the rubber elasticity is more pronounced. Three specimens from each compound were used to evaluate the DMA data, and the mean value taken from these three specimens was reported.

3.3 Results and Discussion

3.3.1 Impact of Hydrothermal Treatment on Lignin Characteristics

The differences in the elemental composition C, H, S, O of Kraft (the initial feedstock for the HTT process) and the HTT lignin are depicted in **Figure 3.1.** It can be seen that the hydrothermal treatment of Kraft lignin leads to a reduction of O content and H/C ratio in lignin. This result indicates that the polarity of lignin has changed.
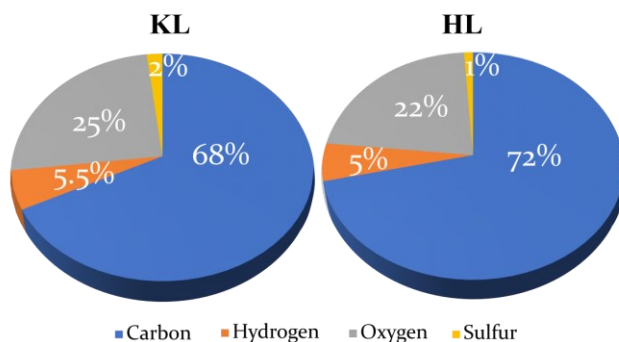

Figure 3.1 Elemental composition of Kraft (KL) and HTT (HL) lignin in weight percent (dry ash-free basis) used in this study

The change in the chemical structure of Kraft lignin after the HTT process was assessed by solid-state ^{13}C NMR spectroscopy. The spectra of the initial feedstock Kraft lignin and the obtained product, HTT lignin, are presented in **Figure 3.2 (a) and (b)**, respectively. Both materials show similar ^{13}C NMR spectra with few noticeable changes in the peak area, indicating that the core structure of lignin is almost unaffected by the hydrothermal process.
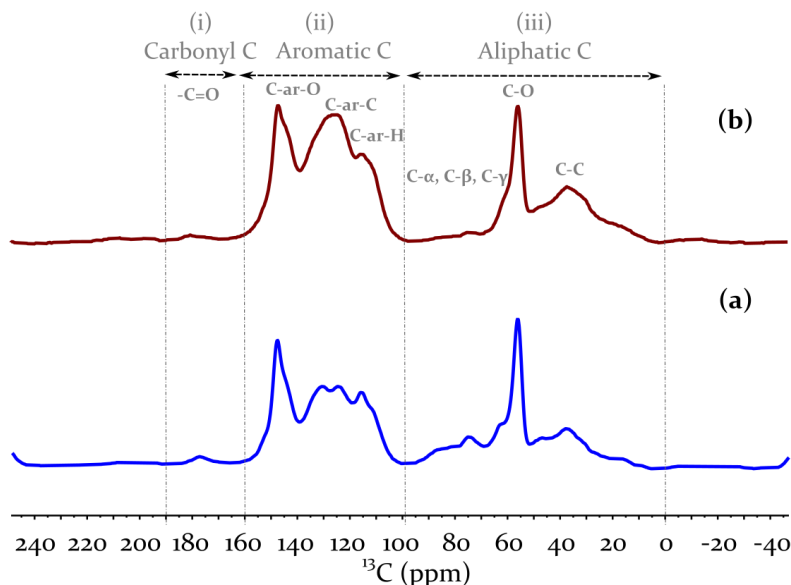
Figure 3.2 Normalized ^{13}C NMR spectra of (a) reference Kraft (KL) and (b) HTT lignin (HL)

Both the lignins exhibit three distinct zones of different chemical nature as follows: (i) 190 - 160 ppm corresponding to carbonyl carbons (C=O); (ii) 160 - 100 ppm is ascertained to three different environments of aromatic (ar) carbons: (a) oxygenated, C-ar-O – 160 - 140 ppm, (b) aromatic, C-ar-C – 140 - 123 ppm, and (c) hydrogen-bonded aromatic carbons, C-ar-H – 123 - 100 ppm; (iii) 100 - 20 ppm ascribed to alkyl carbons, in particular, 90 - 62 ppm related to aliphatic C-O lignin interunit linkages (β-O-4, α-O-4, β-5, C_Y-OR), 56 ppm corresponding to C in methoxy groups (C-ar-O-CH$_3$), which is a characteristic functional group of guaiacyl (G) and syringyl (S) lignin types, and 40 – 10 ppm corresponding to aliphatic CH$_2$ and CH$_3$ type (C-C) carbons.[37–40] The chemical structure of lignin can be found in **Chapter 2** (see **Figures 2.2 and 2.3**). **Table 3.4** summarizes the obtained variation in the chemical shifts of HL and KL. From the chemical shifts, it is possible to identify and distinguish the composition of lignin (G-and S-units). The presence of aromatic C-ar-H resonances at δ 115/111 and aromatic C-ar-C at δ 123/126 of Kraft and HTT lignin indicates that both the lignins are predominantly of G sub-units.[40] This is further evidenced by the resonance of aromatic carbons bound to the methoxy groups of lignin (C-ar-O-CH$_3$) in 147 - 148 ppm range.[40] The existence of significant proportions of G units is characteristic of softwood-type lignin.

3

Table 3.4 Proximate chemical shifts δ (in ppm) of carbon atoms in Kraft lignin (KL) and HTT lignin (HL) acquired from ^{13}C NMR spectra. The nature of the peak intensities is represented as S - Strong, M - Moderate, W - Weak

Assignment	δ KL	δ HL
Ester, COO-R	177 (M)	177 (W)
Aromatic C-O	147 (S)	148 (S)
Aromatic C-C	130 (S), 123 (S)	126 (S)
Aromatic C-H	115 (S)	111 (S)
C_β in β-O-4, C_α in β-5, β-β interunit linkages	85 (M)	-
C_α in β-O-4 interunit linkages	74 (S)	72 (W)
C_γ-OR	62 (S)	62 (W)
Aromatic-O-**C**H3	56 (S)	56 (S)
C_α and C_β in aliphatic-CH$_2$	37 (S)	36 (S)
C_γ in -CH$_3$	14 (W)	-

The slight reduction in peak height around 14 ppm corresponding to end alkyl-chain methyl groups, increase in the peak broadness between 20 - 45 ppm representing CH$_2$-type aliphatic carbon, the reduction in the peak intensity of oxygen-containing alkyl carbons, α-O-4 (72 ppm), and the absence of β-O-4 (85 ppm) along with the observed increase in aromatic carbon signals between 100-115 ppm indicates that the ether linkages are cleaved during the HTT process, resulting in different bonding arrangements of these subunits in HL compared to Kraft lignin.[41,40] Additionally, the decrease in the signals of esters and C_γ-OR of HL demonstrates that these groups are also eliminated during the treatment. The increase in aromatic carbon peaks between 120 - 135 ppm in HL suggests that larger aromatic domains are formed within the HTT lignin structure. Thus, the result shows that, unlike KL, HL has more aromatic C-C structures of G units connected via new linkages rather than the β-O-4 or α-O-4 present in Kraft lignin.

DRIFT analysis was performed to examine the variation in the surface functional groups due to the hydrothermal process. The DRIFT spectra of the initial feedstock (Kraft lignin) and HTT lignin are shown in **Figure 3.3**. The assignment of absorption bands was done based on the literature.[37-40,42] Softwood lignins are mainly composed of guaiacyl units (G). This is characterized by the vibrations observed at 1513 cm^{-1} (aryl ring stretch, asymmetric), 1463 cm^{-1} (CH deformation, asymmetric), 1271 cm^{-1} (aryl ring breathing mode; C-O stretch),

1151 and 1034 cm^{-1} (aromatic CH in-plane), and 855 cm^{-1} (aromatic C-H out-of-plane deformation).[43] The presence of these signals with changes in the intensity in HL suggests that the core ring structure of Kraft lignin subunits remains after the hydrothermal process. This is in line with the results of solid-state ^{13}C NMR spectroscopy.
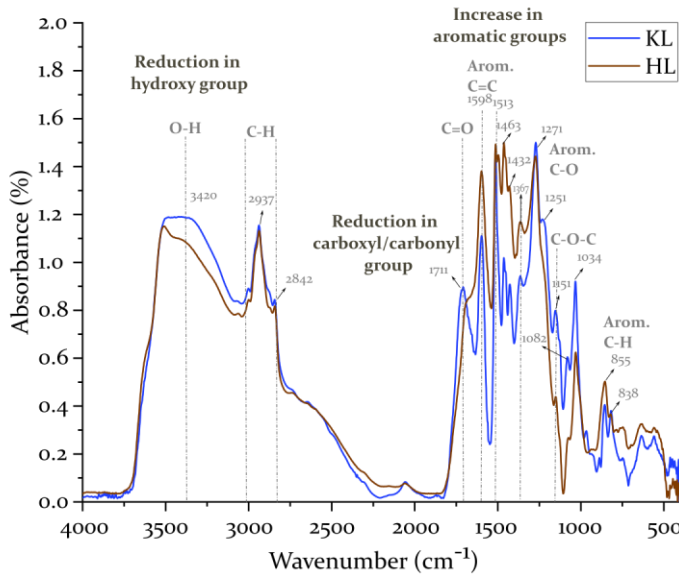

Figure 3.3 Normalized DRIFT spectra of reference Kraft and HTT lignin

The broadness of the peak in the region between 3200 - 3500 cm^{-1}, corresponding to –OH stretch, is reduced, and a decrease in the absorbance is observed after hydrothermal treatment. The absorption band between 2900 - 2800 cm^{-1} related to the C-H stretch of methyl and methylene group is not affected by the hydrothermal treatment. The increase in bands at 1598 cm^{-1} representing the symmetric aryl ring stretch (aromatic C=C skeleton) of lignin suggests that a higher content of aromatic structures was found in HL compared to KL. The decrease in the intensities at 1711, 1082, and 1034 cm^{-1}, corresponding to stretching vibrations in unconjugated C=O and C-O in secondary and primary alcohols, respectively, suggests the reduction in these functional groups in HL. Furthermore, the decrease in absorption bands at 1082 cm^{-1} (C-O deformation at C_β and aliphatic ether) and 1034 cm^{-1} (C-O deformation at C_α and aliphatic ether) demonstrates that the interunit ether linkages in HTT lignin are reduced compared to the Kraft lignin. These obtained results are in line with the elemental composition and NMR results. The reduction in oxygen-containing functionalities in HL makes it less hydrophilic than KL, thus can increase its compatibility with the hydrophobic rubber.

Morphological differences of KL and HL are presented in **Figure 3.4** at three different magnification levels. The presented SEM reveals that KL and HL have different morphologies. In particular, the clusters of HL are built with an irregular mixture of smooth and coarse particles, including fine pores in between. In contrast, KL clusters are

composed of smooth and larger particles. The existence of smaller particles and porous structures is minimal in these KL clusters. This indicates that the HTT process exposes more surfaces by breaking down the lignin aromatic structures into smaller units through a series of reactions such as hydrolysis, dehydration, etc.[44] In addition, the generation of porous morphologies could be attributed to the volatiles evaporation during the process, as described in the literature.[45,41] The presence of smaller particles and higher porosity in HL than in KL is expected to enhance the rubber interactions with HL compared to KL.
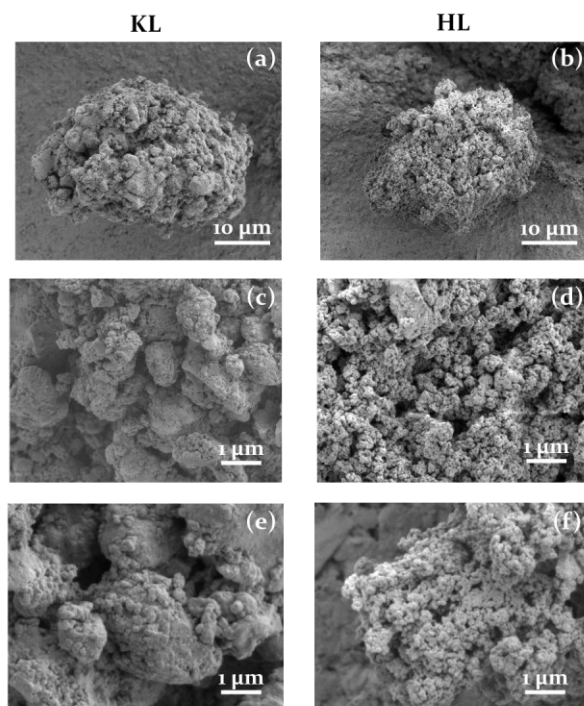
Figure 3.4 Microscopic images of Kraft (a, c, e) and HTT (b, d, f) lignin at different magnifications

3.3.2 Influence of HTT lignin on the in-rubber properties of SSBR/BR compared to Kraft lignin, CB, and silica

The observed differences in chemical composition, morphology, and average particle or fractal cluster size indicate that the interaction of the used lignins with rubber and their dispersion state in the rubber matrix vary remarkably and, eventually, will impact the reinforcing properties. The influence on the in-rubber performance is discussed in the present section.

3.3.2.1 Properties of HTT lignin versus Kraft lignin, CB, and silica as filler in an uncured SSBR/BR compound

Strain sweep analysis of uncured compounds, unfilled and filled with HTT lignin, Kraft lignin, CB, and Silica, were performed to investigate the change in the viscoelastic behavior. **Figure 3.5** shows that the unfilled compound has the lowest dynamic modulus value, G'. It is independent of the applied strain, up to 50 % strain amplitude (γ). Above this amplitude, a slight change in the modulus, i.e., the onset of strain-dependent modulus (non-linear), was observed. This effect could be caused by the disentanglement of the polymer chains by the applied strain, which leads to an orientation of the polymer chains in the direction of the applied force.[46] With the inclusion of filler, a remarkably higher modulus value is seen in the lower strain region, indicating the reinforcing power of the used filler types. This increase in modulus is a cumulative contribution of hydrodynamic, Payne (filler-filler), and interphasial (filler-rubber) reinforcement effects of the filler, besides the rubbery entanglement network. Hydrodynamic interaction is a volume effect where the increase in modulus results from the weighted average of the properties of the SSBR/BR rubber and the homogenously distributed filler particles. This effect is strain-independent as the filler particles, in general, are rigid and cannot undergo a shape change upon application of strain.[47] Nevertheless, these particles, when formed as structures, such as aggregates, agglomerates, or clusters due to physical interactions by Van der Waals forces or hydrogen bonding, exhibit a strain-dependent modulus behavior at a low oscillatory strain amplitude in the range from 0.1 % to ~10 %. This is known as the Payne effect.
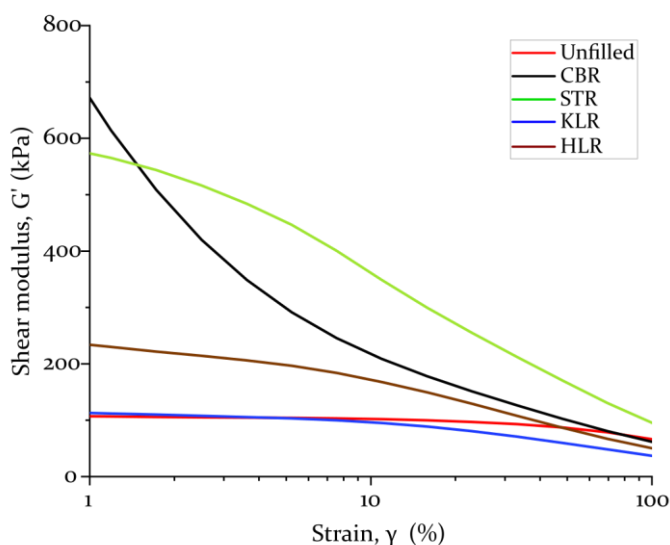
Figure 3.5 Shear modulus of unfilled and differently filled SSBR/BR uncured compounds as a function of strain amplitude γ at 100 °C and 1 Hz[1]

From **Figure 3.5**, it can be seen that in comparison with the unfilled compound, the compound filled with classical fillers CB (CBR) and silica (STR) exhibits an apparent non-linear viscoelastic behavior where a typical decrease in the dynamic modulus (G') with increasing strain amplitude takes place as a result of the breakage of the filler-filler network structures.[24–26] In the case of lignin fillers, Kraft lignin-filled compound (KLR) shows almost a linear viscoelastic behavior similar to the unfilled compound, whereas, for HTT lignin-filled compound (HLR), a moderate non-viscoelastic behavior can be observed. This indicates that the magnitude of the non-linear effect varies with the type of filler used, principally with the resulting filler network structure and strength inside the rubber matrix.

Of the investigated filler systems, KLR shows the lowest G' at low strain, i.e., almost no Payne effect. This indicates that KL exhibits the lowest filler-filler interactions among the other fillers (HL, CB, SL). Furthermore, the obtained modulus value is similar to the unfilled rubber, ascertaining that the other effects, like hydrodynamic and polymer-filler interaction, are negligible. This shows that Kraft lignin is not reinforcing. The HTT lignin curve lies between the reinforcing fillers (CB and SL) and KL or unfilled, demonstrating a moderate Payne effect. This suggests that the HTT lignin particles are dispersed far better than KL, establishing a percolation network in the rubber matrix to some extent. However, the HLR compound exhibits a significantly lower modulus than CB and SL-filled systems. It can be observed that compared to the other filled compounds, the Payne behavior of CB is different, and it exhibits a rapid reduction in modulus upon application of strain. This shows that, on the one hand, the CB filler network is highly percolating and susceptible to the applied strain as the network is based on weak Van der Waals forces. On the other hand, polar fillers like silica and lignin are associated with each other by hydrogen bonding and are less susceptible in the low-strain region. The higher G' at 100 % strain of uncured STR compared to other filled compounds suggests that the coupling between filler-silane-polymer occurred during mixing.

3.3.2.2 Cure properties of HTT lignin-filled versus Kraft-filled, CB-filled, and silica-filled SSBR/BR compounds

The influence of the used filler types on the vulcanization behavior of the SSBR/BR matrix can be seen in **Figure 3.6**.
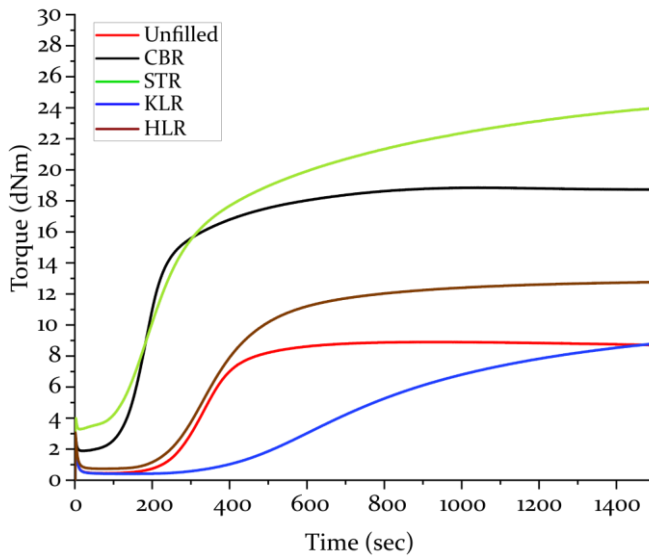
Figure 3.6 Cure behavior of unfilled and differently filled SSBR/BR compounds[1]

Table 3.5 summarizes all the characteristic parameters, i.e., the scorch time (ts_2), optimum cure time ($t_{c,90}$), ultimate state of cure (ΔM), minimum (M_L), and maximum (M_H) torque obtained from the cure curves of the compared samples. In addition, the apparent crosslink densities (CLD) achieved are also reported. The effect on the minimum torque value (M_L) indicates the different processing properties of the compounds filled with the filler systems investigated. Here, a similar tendency is observed for unfilled and examined lignin samples. The high M_L of the CBR and STR indicates an increased compound viscosity.

Table 3.5 Obtained cure parameters of unfilled and differently filled SSBR/BR

Description	Unfilled	CBR	STR	HLR	KLR
ts_2 (min)	4.8	2.2	2.1	4.7	7.8
$t_{c,90}$ (min)	7.9	7.4	18.6	11.3	20.5
M_H (dN.M)	8.9	18.9	25	12.9	8.8
M_L (dN.m)	0.4	1.9	3.3	0.7	0.4
$\Delta M, M_H\text{-}M_L$ (dN.m)	8.5	17.0	22.3	12.2	8.4
Apparent CLD ($\times 10^{-4}$ mol/cm^3)	1.52±0.02	4.24±0.12	4.38±0.14	1.89±0.08	1.59±0.02

3

KLR shows an extended scorch time associated with a slower cure rate and a more pronounced marching modulus than all other compounds. This indicates that Kraft lignin's surface adsorbs basic accelerators or curing aids, decelerating the vulcanization process, leading only to the same level of vulcanization as the unfilled rubber as represented by the low M_H and low apparent CLD values (**Table 3.5**). This suggests that adding KL does not impart filler-filler, filler-polymer, and polymer-polymer interaction in the matrix. This indicates that the reinforcing power of KL is low. This effect is significantly reduced after the hydrothermal treatment, indicating a reduced activity of the filler surface for the curing agents and vulcanization accelerators. Nevertheless, the observed apparent CLD and M_H values altogether are low in comparison to conventional fillers, giving an indication that accelerators are still adsorbed, leading to less interaction of filler to the rubber, a lower filler-filler interaction, and a lower apparent crosslinking of the rubber. CBR and STR demonstrate the highest M_H and apparent CLD values among the compared filled compounds, indicating the higher reinforcing power of CB and silica. In the case of STR, it can be attributed to the additional sulfur released from TESPT.

3.3.2.3 Mechanical properties of HTT lignin-filled versus Kraft lignin-filled, CB-filled, and silica-filled SSBR/BR vulcanizates

The mechanical behavior of the SSBR/BR rubber compounds filled with the investigated filler types is shown in **Figure 3.7**. The addition of reinforcing fillers generally improves tensile properties compared to the unfilled rubber. It is observed that carbon black and silica/silane-filled vulcanizates exhibit superior reinforcing properties. The addition of Kraft lignin does not improve the mechanical modulus and ultimate tensile strength of the SSBR/BR rubber compounds compared to CB- and SL-filled ones. KLR and unfilled rubber show nearly identical behavior up to 250 % elongation, and after that, KLR fails at a strain of 400 %. For HL-filled compounds, a moderate impact can be observed. Unlike KLR, HLR shows a higher modulus even at a lower strain than the unfilled rubber. This indicates that adding HL improves the reinforcing properties of SSBR/BR compared to KL. However, the reinforcing effect is lower compared to the conventional reinforcing fillers.
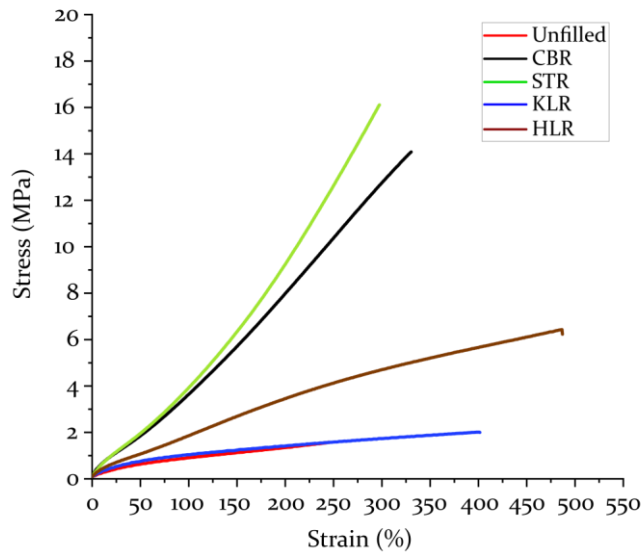
Figure 3.7 Tensile properties of unfilled and differently filled SSBR/BR vulcanizates[1]

Table 3.6 shows the hardness of all rubber composites. This is an indication of the compound's surface rigidity. Compared to KLR, the compound hardness of HLR is higher but lower than the compounds filled with the two conventional fillers, CB and SL.

Table 3.6 Compound hardness of unfilled and differently filled SSBR/BR vulcanizates[1]

Description	Unfilled	CBR	STR	HLR	KLR
Hardness (Shore A)	41±0.13	64±0.70	63±0.20	53±0.37	46±0.11

Figures 3.8 a, b, c display the temperature-dependent viscoelastic behavior of the cured compounds in terms of storage modulus (G'), loss modulus (G"), and loss factor (tan δ = G"/G') of the unfilled and filled compounds at 10 Hz frequency and strains of 1 % and 3 % respectively. The discontinuity of the lines in **Figure 3.8** is due to the higher strain applied from 10 °C onwards (see **Section 3.2.4**).
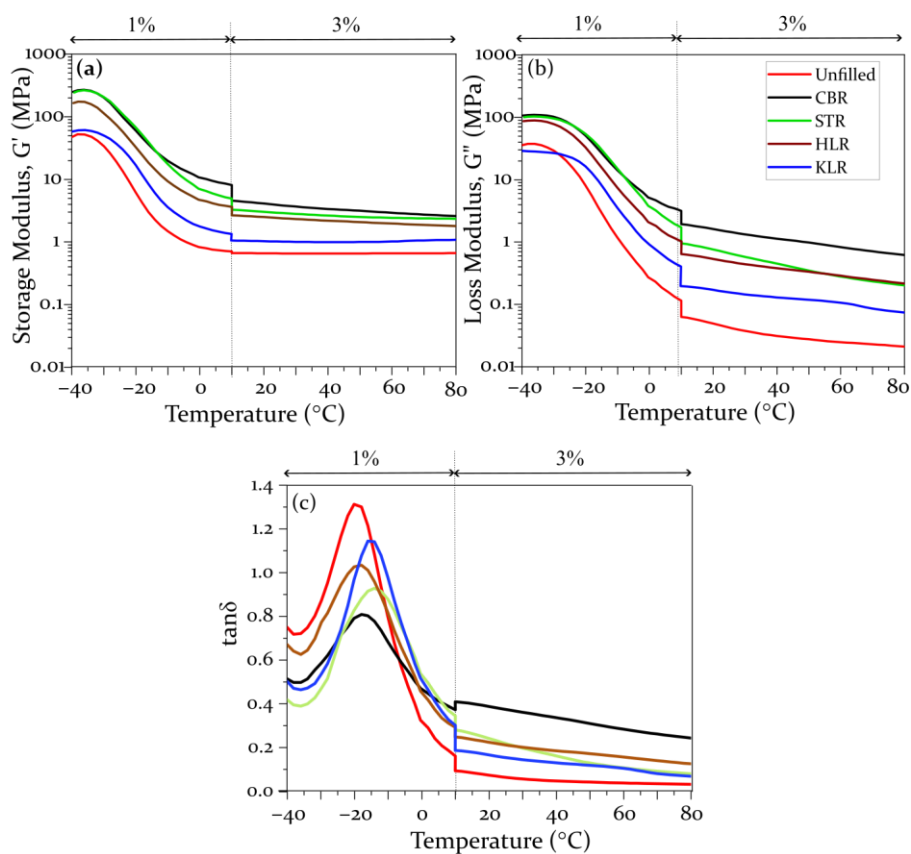
Figure 3.8 (a) Dynamic storage modulus (G'); (b) loss modulus (G"); and (c) tan δ as a function of temperature for unfilled and differently filled SSBR/BR vulcanizates[1]

Upon addition of the fillers, the dynamic storage moduli increase over the whole temperature range and vary in value depending on the type of filler used, respectively, with the extent of filler-filler and filler-polymer interactions. Among the different filled compounds, the G' of the silica-silane- and carbon black-filled compounds are the highest and indicate their high reinforcing potential. The HTT lignin-filled compound has lower moduli than the conventional reinforcing carbon black- and silica-filled ones, yet higher values than the Kraft lignin-filled compound. This indicates the higher interaction potential of HTT lignin with the selected polymer type compared to the untreated Kraft lignin.

The temperature position of the tan δ peak maximum can be used to quantify the glass transition temperature (T_g) and is associated with the segmental mobility or relaxation of polymer chains.[48] This relaxation phenomenon involves cooperative motions or internal frictions of polymer chains, which induces energy dissipation reflected by a maximum

tan δ value at that temperature.[49] It is observed that the different filled systems presented in **Figure 3.8 c** show a variation in the position of the tan δ peak with respect to temperature (shift in the T_g to a higher value) and its magnitude (decrease in its value) compared to the unfilled rubber. This signifies that the mobility and dynamics of the polymeric chain are changed depending on the filler type at a given filler load and polymer microstructure type. This variation is influenced by several factors, such as the nature of the interaction of the filler with the rubber, the degree of filler dispersion (filler-filler interaction) in the rubber matrix, and the degree of rubber crosslinking.[48,50] The T_g of the unfilled SSBR/BR compound is observed to be –19 °C and exhibits the maximum tan δ value. When silica is added, the T_g is shifted to a higher temperature of -13 °C, and a decrease in the height of the tan δ peak is observed; in other words, the segmental mobility of the polymer chain at the interface is restricted. This restriction in molecular movement reduces the compound hysteresis and could be related to the chemical coupling of the silica particles to the rubber molecule via the silane molecule and the increase in the degree of crosslinking as determined by the apparent CLD values (**Table 3.5**).[51] Conversely, the T_g exhibited by CB- and HL-filled compound shows no significant change (T_g =-18 °C) compared to the unfilled compound. This result indicates that the presence of CB or HL filler in SSBR/BR composites may not restrict the chain mobility to a larger extent due to their weak physical interaction with the polymer chains. But, depending on the degree of crosslinking and filler dispersion in the rubber, the height of peak tangent (tan δ) of CBR and HLR varies. The reduction in the tan δ peak height of CBR suggests a good filler dispersion is achieved in the rubber, thereby increasing the local interactions between the polymer chains and the filler interface compared to HLR. These interactions reduce the mobility of the polymer chains that participate in the molecular motions responsible for energy dissipation. A distinctive viscoelastic behavior is observed for the Kraft lignin-filled compound compared to the HL-filled one: a higher T_g of -15 °C and an increased tan δ peak. This can be attributed to the improper dispersion of KL particles in the rubber matrix, giving rise to vacant spaces and enabling the polymer chains to move or rotate freely, thereby increasing the energy dissipation compared to other fillers. The dispersion behavior of KL in the rubber matrix is presented in **Figure 3.10** and is discussed later. The lower peak height of HLR compared to the Kraft lignin-filled one indicates a moderate filler dispersion and distribution level and enhances its interaction with the polymer.

Above glass-transition temperature, the tan δ curve of the vulcanizates decreases with increasing temperature. A high tan δ value of the filled composites at 60 °C is related to the compound's energy dissipation (hysteresis) behavior resulting from the increased filler-filler interaction and the weak filler-polymer interaction.[50] The tan δ value of CBR at 60 °C is significantly higher than that of the other filled ones. This is mainly caused by the energy loss attributed to the weakening of CB filler networks and CB-rubber physical interactions upon temperature rise and cyclic deformation.[52] The presence of TESPT silane enables silica filler to attach to the rubber covalently, reducing the filler-filler

3

interaction; thereby, the compound's energy dissipation is lowered. Thus, STR exhibits a lower tan δ compared to CBR. At temperatures above 50 °C, the tan δ of the Kraft lignin-filled compound (KLR) coincides with the silica-silane-filled system (STR) and is lower than that for the HTT lignin-filled one (HLR) and much lower than for carbon black-filled compound (CBR). It is a result of a comparatively lower filler-filler interaction of KL. This is in line with the results of the uncured Payne effect (**Figure 3.5**). In the case of HLR, the tan δ curve above 50 °C lies between STR and CBR, demonstrating an intermediate energy dissipation behavior.

3.3.2.4 Morphological Properties of HTT lignin-filled versus Kraft lignin- and Silica-filled SSBR/BR vulcanizates

AFM was applied to examine the effects of hydrothermal treatment on the morphology and dispersion of lignin within the rubber matrix. Moreover, the AFM results of KLR and HLR were compared to those of an unfilled and an SL-filled compound (STR). CB-filled compound (CBR) was not considered. **Figures 3.9 and 3.10** represent the AFM height images (upper) and Young's modulus maps (lower) of the unfilled and filled vulcanizates. The height images represent the vulcanizates' bulk surface morphology, and Young's modulus maps describe the vulcanizates' local distribution of filler and stiffness. From both images, filler clusters are readily distinguished, with a bright contrast to the dark rubber matrix indicating a much higher modulus than the surrounding rubber material. The height image shows a flat and homogeneous surface for the unfilled vulcanizate (**Figure 3.9**), while for the filled systems, the surface is rough and distinctly dependent on the filler used. The bright spots in the unfilled rubber can be attributed to ZnO particles and can be neglected in the present context, as all the compounds contain ZnO. Detailed visual inspection of the micrographs reveals that the silica particles are well dispersed and evenly distributed throughout the rubber matrix. The visible particles are in the range of 100±50 nm.
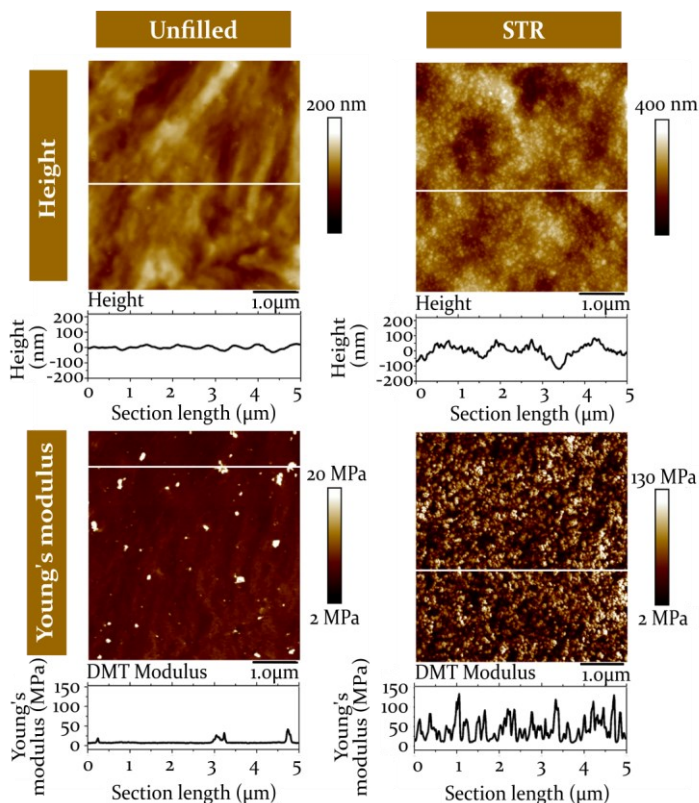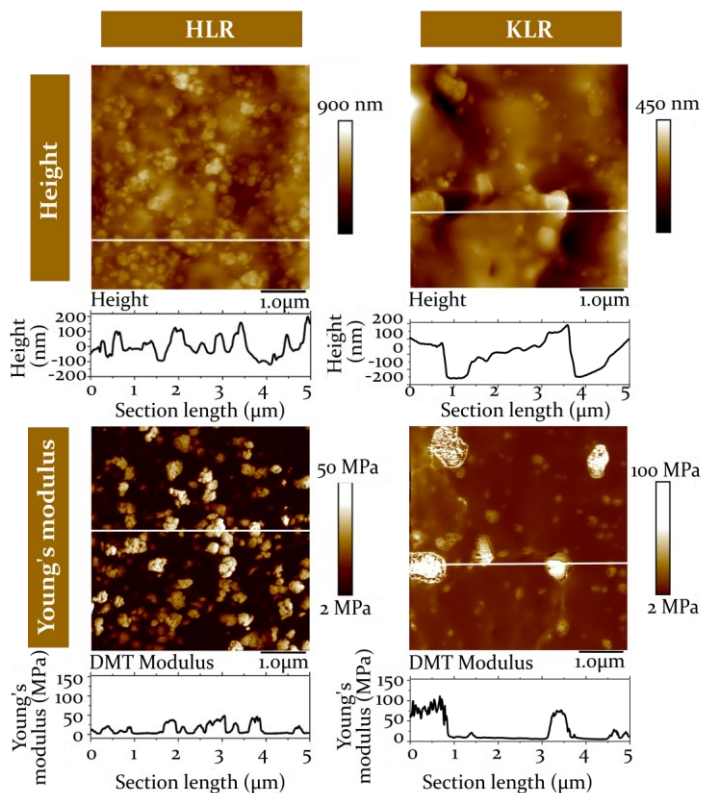
Figure 3.9 AFM height images (upper) and Young's modulus maps (lower) of cryo-fractured unfilled and silica-filled vulcanizates with their corresponding height and modulus profiles represented below. Scanning area: 5 x 5 μm². The cross-section profiles were taken along white lines and plotted on the same scale for data comparison

Contrarily, as shown in **Figure 3.10**, HTT lignin is built up of dominant clusters of 200±100 nm, comprising several elementary particles of 70±20 nm. This indicates that the HTT lignin is in-homogeneously distributed on the micro-scale level compared to silica filler. Nevertheless, the observed HL clusters in the rubber matrix are smaller than those of the filler clusters visualized by SEM (**Figure 3.4 b, d, f**) generated on pure filler material. This difference in cluster size may be attributed to the mechanical breakdown of the larger agglomerates by shear forces during rubber mixing. In opposition to this, the Kraft lignin-filled vulcanizate shows lumpy clusters of 200 - 500 nm and nearly missing micro-dispersion of the particles.

3

Figure 3.10 AFM height images (upper) and Young's modulus maps (lower) of cryo-fractured HTT lignin- and Kraft lignin-filled vulcanizates with their corresponding height and modulus profiles represented below. Scanning area: 5 x 5 µm². The cross-section profiles were taken along white lines and plotted on the same scale for data comparison

3.4 Conclusions and Recommendations

The reinforcing behavior of two different lignin types, untreated softwood Kraft and a hydrothermally-treated (HTT) softwood Kraft lignin, was investigated in an SSBR/BR rubber system, and the properties were compared with the conventional reinforcing fillers. The performed study highlights the advantages of hydrothermal treatment for lignin applications in rubber. The HTT lignin has a chemical composition and physical properties different from the initial softwood Kraft lignin feedstock. More specifically, the observed smaller particle sizes of the clusters of HTT lignin, lower content of oxygen-containing functional groups, and increased carbon content compared to Kraft lignin make HL more suitable for application in the selected rubber system. The results of the NMR analysis demonstrate that the changes achieved were caused by the cleavage of ether linkages and carbon side chain structures, leading to the formation of a compound with a higher content of aromatic structures. The obtained in-rubber properties of HTT lignin-

filled SSBR/BR vulcanizate are superior to the Kraft lignin-filled one. This is attributed to the strong interaction of the KL with the vulcanization chemicals and inhibition of the sulfur vulcanization process. Furthermore, the dispersion and distribution of HL in the rubber matrix are uniform compared to KL, contributing largely to the rubber reinforcement effects. The results of the performed studies show that hydrothermal treatment enhances Kraft lignin's filler characteristics, such as surface area and surface reactivity. As a result, a better compatibility between the lignin and polymer is achieved. Nevertheless, the reinforcing potential of HTT lignin in the investigated SSBR/BR system is lower than the used reference reinforcing fillers like N330 carbon black and ULTRASIL 7000GR silica. This is mainly attributed to its comparably low specific surface area and the presence of polar functional groups potentially adsorbing part of the basic vulcanization accelerators. Also, the micro-dispersion of HTT lignin in the rubber matrix is lower than that of conventional fillers.

The reinforcing properties of HTT lignin-filled rubber can be further enhanced by:

(i) Controlling its surface activity: increasing its interaction with rubber via chemical modification reactions and/or shielding the polar groups of lignin by the use of specific adsorption chemicals

(ii) Increasing the crosslink density by adjusting the cure system

(iii) Decreasing the particle size and/or increasing the specific surface area

(iv) Improving the micro-dispersion by using different mixing strategies

A combination of these strategies will result in high-end rubber applications of HTT lignin.

References

(1)   Sekar, P. Design of a Bio-Based Filler System for Tire Treads. PDEng thesis, University of Twente, The Netherlands, 2018.

(2)   Kraus, G. Reinforcement of Elastomers by Carbon Black. *Rubber Chemistry and Technology* **1978**, *51* (2), 297–321.

(3)   Edwards, D. C. Polymer-Filler Interactions in Rubber Reinforcement. *J Mater Sci* **1990**, *25* (10), 4175–4185.

(4)   Leblanc, J. L. Rubber–Filler Interactions and Rheological Properties in Filled Compounds. *Progress in Polymer Science* **2002**, *27* (4), 627–687.

(5)   Wang, M.-J.; Morris, M. Chapter 4 - Filler Dispersion. In *Rubber Reinforcement with Particulate Fillers*; Hanser, 2021; pp 177–192.

(6)   Gundlach, N.; Hentschke, R. Modelling Filler Dispersion in Elastomers: Relating Filler Morphology to Interface Free Energies via SAXS and TEM Simulation Studies. *Polymers* **2018**, *10* (4), 446.

(7)   ASTMD3053-Standard Terminology Relating to Carbon Black, 2015.

(8)   Lacayo-Pineda, J. Filler Dispersion and Filler Networks. In *Encyclopedia of Polymeric Nanomaterials*; Kobayashi, S., Müllen, K., Eds.; Springer: Berlin, Heidelberg, 2015; pp 771–776.

(9)   Jl, L. Some considerations on optimum mixing with respect to the full development of rubber - carbon black morphology. *Kautsch. Gummi Kunstst.* **2001**, *54* (6), 327–333.

(10) Wang, M.-J.; Morris, M. Chapter 5 - Effect of Fillers on the Properties of Uncured Compounds. In *Rubber Reinforcement with Particulate Fillers*; Hanser, 2021; pp 193–262.

(11) Chang, B. P.; Gupta, A.; Muthuraj, R.; Mekonnen, T. H. Bioresourced Fillers for Rubber Composite Sustainability: Current Development and Future Opportunities. *Green Chem.* **2021**, *23* (15), 5337–5378.

(12) Keilen, J. J.; Pollak, A. Lignin for Reinforcing Rubber. *Rubber Chemistry and Technology* **1947**, *20* (4), 1099–1108.

(13) Kumaran, M. G.; De, S. K. Utilization of Lignins in Rubber Compounding. *Journal of Applied Polymer Science* **1978**, *22* (7), 1885–1893.

(14) Setua, D. K.; Shukla, M. K.; Nigam, V.; Singh, H.; Mathur, G. N. Lignin Reinforced Rubber Composites. *Polymer Composites* **2000**, *21* (6), 988–995.

(15) Košíková, B.; Gregorová, A. Sulfur-Free Lignin as Reinforcing Component of Styrene–Butadiene Rubber. *Journal of Applied Polymer Science* **2005**, *97* (3), 924–929.

(16) Jiang, C.; He, H.; Yao, X.; Yu, P.; Zhou, L.; Jia, D. In Situ Dispersion and Compatibilization of Lignin/Epoxidized Natural Rubber Composites: Reactivity, Morphology and Property. *Journal of Applied Polymer Science* **2015**, *132* (23).

(17) Meisel, K.; Röver, L.; Majer, S.; Herklotz, B.; Thrän, D. A Comparison of Functional Fillers—Greenhouse Gas Emissions and Air Pollutants from Lignin-Based Filler, Carbon Black and Silica. *Sustainability* **2022**, *14* (9), 5393.

(18) Cha, Y.-L.; Alam, A.-M.; Park, S.-M.; Moon, Y.-H.; Kim, K.-S.; Lee, J.-E.; Kwon, D.-E.; Kang, Y.-G. Hydrothermal-Process-Based Direct Extraction of Polydisperse Lignin Microspheres from Black Liquor and Their Physicochemical Characterization. *Bioresource Technology* **2020**, *297*, 122399.

(19) Wittmann, T.; Richter, I. Method for Extracting Lignin from Black Liquor and Products Produced Thereby. US Patent 9902816B2, 2015.

(20) Wittmann, T. Method for Obtaining Stabilized Lignin Having a Defined Particle-Size Distribution from a Lignin-Containing Liquid. US20170247255A1, 2017.

(21) Wittmann, T.; Bergemann, K. Hydrothermal Treatment of Renewable Raw Material. US20200239697A1, 2020.

(22) Rauline, R. Rubber Compound and Tires Based on Such a Compound. EP0501227A1, 1992.

(23) Wolff, S. Chemical Aspects of Rubber Reinforcement by Fillers. *Rubber Chemistry and Technology* **1996**, *69* (3), 325–346.

(24) Payne, A. R. The Dynamic Properties of Carbon Black Loaded Natural Rubber Vulcanizates. Part II. *Journal of Applied Polymer Science* **1962**, *6* (21), 368–372.

(25) Payne, A. R.; Whittaker, R. E. Low Strain Dynamic Properties of Filled Rubbers. *Rubber Chemistry and Technology* **1971**, *44* (2), 440–478.

(26) Payne, A. R. A Note on the Conductivity and Modulus of Carbon Black-Loaded Rubbers. *Journal of Applied Polymer Science* **1965**, *9* (3), 1073–1082.

(27) Luginsland, H.-D.; Fröhlich, J.; Wehmeier, A. Influence of Different Silanes on the Reinforcement of Silica-Filled Rubber Compounds. *Rubber Chemistry and Technology* **2002**, *75*, 563–579.

(28) Flory, P. J. Thermodynamics of High Polymer Solutions. *J. Chem. Phys.* **1941**, *9* (8), 660–660.

(29) Soney, G.; Ninan, K.; Thomas, S. Effect of Degree of Crosslinking on Swelling and Mechanical Behaviour of Conventionally Vulcanised Styrene-Butadiene Rubber Membranes. *Polymers & Polymer Composites* **1999**, *7* (5), 345–353.

(30) Kraus, G. Swelling of Filler-Reinforced Vulcanizates. *Journal of Applied Polymer Science* **1963**, *7* (3), 861–871.

(31) Wang, C. C.; Donnet, J. B.; Wang, T. K.; Pontier-Johnson, M.; Welsh, F. AFM Study of Rubber Compounds. *Rubber Chemistry and Technology* **2005**, *78* (1), 17–27.

(32) Gojzewski, H.; van Drongelen, M.; Imre, B.; Hempenius, M. A.; Check, C.; Chartoff, R.; Wurm, F. R.; Vancso, G. J. AFM Monitoring of the Cut Surface of a Segmented Polyurethane Unveils a Microtome-Engraving Induced Growth Process of Oriented Hard Domains. *Polymer Testing* **2023**, *120*, 107961.

(33) Hutter, J. L.; Bechhoefer, J. Calibration of Atomic-force Microscope Tips. *Review of Scientific Instruments* **1993**, *64* (7), 1868–1873.

(34) Derjaguin, B. V.; Muller, V. M.; Toporov, Yu. P. Effect of Contact Deformations on the Adhesion of Particles. *Journal of Colloid and Interface Science* **1975**, *53* (2), 314–326.

(35) Ferencz, R.; Sanchez, J.; Blümich, B.; Herrmann, W. AFM Nanoindentation to Determine Young's Modulus for Different EPDM Elastomers. *Polymer Testing* **2012**, *31* (3), 425–432.

3

3

(36) Wang, M.-J. Effect of Polymer-Filler and Filler-Filler Interactions on Dynamic Properties of Filled Vulcanizates. *Rubber Chemistry and Technology* **1998**, *71* (3), 520–589.

(37) Huang, F.; Singh, P. M.; Ragauskas, A. J. Characterization of Milled Wood Lignin (MWL) in Loblolly Pine Stem Wood, Residue, and Bark. *J. Agric. Food Chem.* **2011**, *59* (24), 12910–

(38) Wang, S.; Ru, B.; Lin, H.; Sun, W.; Luo, Z. Pyrolysis Behaviors of Four Lignin Polymers Isolated from the Same Pine Wood. *Bioresource Technology* **2015**, *182*, 120–127.

(39) Borloluz, J.; Cemin, A.; Bonetto, L.; Ferrarini, F.; Esteves, V.; Giovanela, M. Isolation, Characterization and Valorization of Lignin from Pinus Elliottii Sawdust as a Low-Cost Biosorbent for Zinc Removal. *Cellulose* **2019**, *26*.

(40) Latham, K. G.; Matsakas, L.; Figueira, J.; Rova, U.; Christakopoulos, P.; Jansson, S. Examination of How Variations in Lignin Properties from Kraft and Organosolv Extraction Influence the Physicochemical Characteristics of Hydrothermal Carbon. *Journal of Analytical and Applied Pyrolysis* **2021**, *155*, 105095.

(41) Wikberg, H.; Ohra-aho, T.; Pileidis, F.; Titirici, M.-M. Structural and Morphological Changes in Kraft Lignin during Hydrothermal Carbonization. *ACS Sustainable Chem. Eng.* **2015**, *3* (11), 2737–2745.

(42) Gordobil, O.; Moriana, R.; Zhang, L.; Labidi, J.; Sevastyanova, O. Assesment of Technical Lignins for Uses in Biofuels and Biomaterials: Structure-Related Properties, Proximate Analysis and Chemical Modification. *Industrial Crops and Products* **2016**, *83*, 155–165.

(43) Otromke, M.; Shuttleworth, P. S.; Sauer, J.; White, R. J. Hydrothermal Base Catalysed Treatment of Kraft Lignin for the Preparation of a Sustainable Carbon Fibre Precursor. *Bioresource Technology Reports* **2019**, *5*, 251–260.

(44) Barbier, J.; Charon, N.; Dupassieux, N.; Loppinet-Serani, A.; Mahé, L.; Ponthus, J.; Courtiade, M.; Ducrozet, A.; Quoineaud, A.-A.; Cansell, F. Hydrothermal Conversion of Lignin Compounds. A Detailed Study of Fragmentation and Condensation Reaction Pathways. *Biomass and Bioenergy* **2012**, *46*, 479–491.

(45) Hu, J.; Shen, D.; Wu, S.; Zhang, H.; Xiao, R. Effect of Temperature on Structure Evolution in Char from Hydrothermal Degradation of Lignin. *Journal of Analytical and Applied Pyrolysis* **2014**, *106*, 118–124.

(46) Warasitthinon, N.; Genix, A.-C.; Sztucki, M.; Oberdisse, J.; Robertson, C. G. The Payne Effect: Primarily Polymer-Related or Filler-Related Phenomenon? *Rubber Chemistry and Technology* **2019**, *92* (4), 599–611.

(47) Goudarzi, T.; Spring, D. W.; Paulino, G. H.; Lopez-Pamies, O. Filled Elastomers: A Theory of Filler Reinforcement Based on Hydrodynamic and Interphasial Effects. *Journal of the Mechanics and Physics of Solids* **2015**, *80*, 37–67.

(48) Bashir, M. A. Use of Dynamic Mechanical Analysis (DMA) for Characterizing Interfacial Interactions in Filled Polymers. *Solids* **2021**, *2* (1), 108–120.

(49) Datta, J.; Parcheta, P.; Surówka, J. Softwood-Lignin/Natural Rubber Composites Containing Novel Plasticizing Agent: Preparation and Characterization. *Industrial Crops and Products* **2017**, *95*, 675–685.

(50) Warasitthinon, N.; Robertson, C. G. Interpretation of the Tanδ Peak Height for Particle-Filled Rubber and Polymer Nanocomposites with Relevance to Tire Tread Performance Balance. *Rubber Chemistry and Technology* **2018**, *91* (3), 577–594.

(51) Ueda, E.; Liang, X.; Ito, M.; Nakajima, K. Dynamic Moduli Mapping of Silica-Filled Styrene–Butadiene Rubber Vulcanizate by Nanorheological Atomic Force Microscopy. *Macromolecules* **2019**, 52 (1), 311–319.

(52) Neethirajan, J.; Parathodika, A. R.; Hu, G.-H.; Naskar, K. Functional Rubber Composites Based on Silica-Silane Reinforcement for Green Tire Application: The State of the Art. *Functional Composite Materials* **2022**, 3 (1), 7.

3

3

4. Use of Silanes as Surface Modifiers for Hydrothermally Treated Lignin
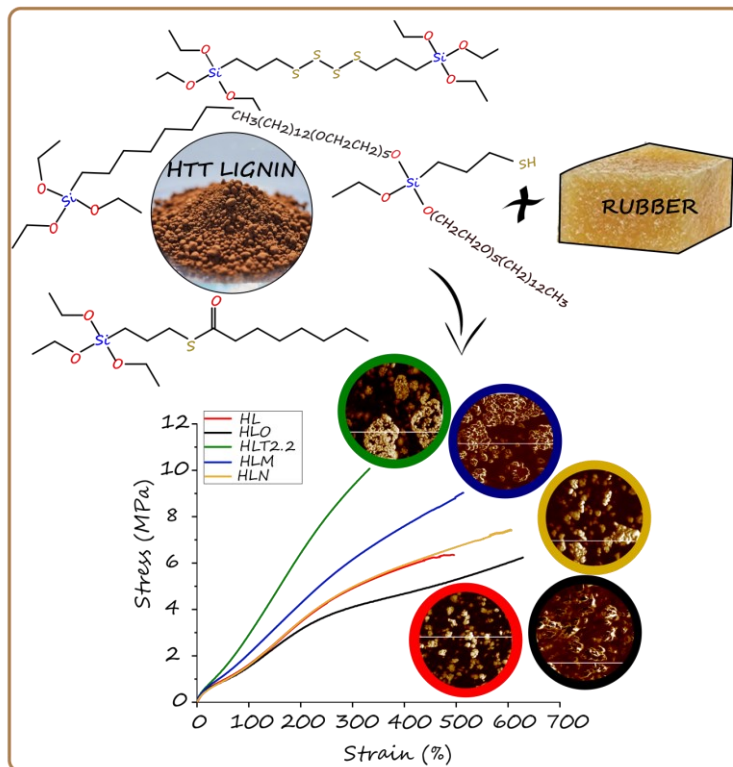
Impact of Silanes on the Reinforcing Behavior of Hydrothermally Treated Lignin

In this chapter, two different types of silanes were investigated as potential surface modifiers for hydrothermally treated lignin (HTT) in order to further improve its reinforcing properties in an SSBR/BR blend:

i.   mono-functional silane carrying only one ethoxy functionality

ii.   different bi-functional silanes[a] having an additional sulfur moiety

Modifications of HTT lignin using different silanes were carried out directly in the mixer. The influence of these silane modifications on the vulcanization behavior, the morphological characteristics as well as the mechanical and other in-rubber properties of HTT lignin-filled SSBR/BR were examined, and the results were compared.

Particular types of bi-functional silane-modified HTT lignins remarkably enhance the rubber properties compared to the mono-functionalized and unmodified ones. This reinforcement effect is related to the polymer-filler interactions as well as the HTT lignin morphology formed in the rubber matrix. Depending on the type of sulfur moiety of the bi-functional silanes, significant discrepancies in in-rubber properties and dispersion quality were observed. Especially, a silane with an inaccessible sulfur, 3-octanoylthio-1-propyltriethoxysilane (OTPTES), shows a negligible effect on the reinforcing and morphological behavior in an HTT lignin-filled rubber compound.

---

[a] Some of the figures (in-rubber data of bifunctional silanes modified HTT lignin-filled rubber compounds) presented in this chapter were already published in [1]

4.1 Introduction

Hydrothermal treatment (HTT) of Kraft lignin provides a carbonaceous material with enhanced filler characteristics such as smaller particle size, higher specific surface area, and a reduced number of oxygen-containing hydroxy and carboxy functionalities relative to the technical Kraft lignin used as feedstock. Besides, the reinforcing performance of the obtained HTT lignin in an SSBR/BR composite is superior to the technical Kraft lignin. However, the achieved in-rubber properties are lower than compounds filled with conventional reinforcing fillers such as carbon black or silica. The observed effects were due to the presence of still available polar groups on HTT lignin's surface, which negatively affect the compatibility including the type and extent of interactions with non-polar rubbers. Also, the lower specific surface area of HTT lignin compared to the investigated conventional types of reinforcing fillers, carbon black and silica hampers its contact with the rubber. Both facts negatively affect the micro-dispersion of HTT lignin within the polymer matrix. These shortcomings result in a mixture of HTT lignin and rubber that cannot withhold or transfer the applied stress, which is visible in reduced mechanical properties. This restricts the effective utilization of HTT lignin as a reinforcing filler for the investigated rubber. For this reason, it is of high interest to modify the surface of HTT lignin to overcome the polarity difference with the hydrophobic rubber. The presence of functional groups in HTT lignin, such as aromatic and aliphatic hydroxy, carboxy, etc., should allow the modification of its surface chemically to make it more suitable for application as reinforcing filler for non-polar rubbers.

The chemical functionalization using organosilane agents (R'Si(OR)$_3$) is one of the widely applicable techniques in the rubber industry to enhance the compatibility of hydrophilic fillers like silica and hydrocarbon rubber.[2–6] The silane molecules can be tailor-made to be used as shielding or coupling agents.

(a) Shielding silane agents consist of only one functionality (mono-functional) and are solely reactive toward the filler. They hydrophobize the filler surface as shown in **Figure 4.1 (a)**, thereby promoting physical interactions with the rubber.

(b) Coupling agents or bi-functional silanes chemically anchor the hydrophilic filler to the hydrophobic rubber with the two different reactive substituents (filler-reactive and rubber-reactive), as depicted in **Figure 4.1 (b)**. The working mechanism of this type of silane is as follows: (i) the alkoxysilyl group of the silane either directly or after hydrolysis attaches to the filler surface bearing polar groups (e.g. silica containing silanols) during mixing;[7,8] and (ii) the organo functionality, such as sulfide, mercapto, vinyl double bonds, etc., interacts with the rubber during vulcanization.[5–8] A chemical covalent bond between the rubber and the filler is formed by this type of reaction, resulting in a strong interfacial adhesion between the filler and polymer matrix.[9,10]
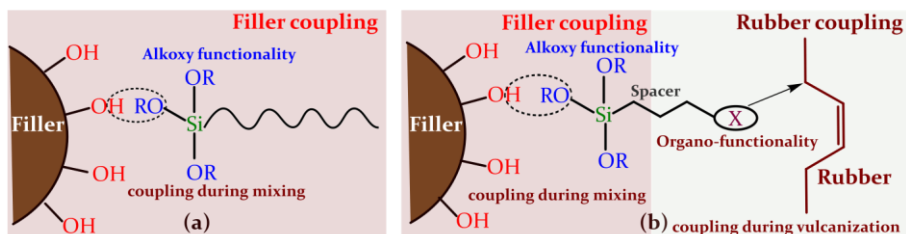
Figure 4.1 Representation of working principle of (a) shielding or mono- and (b) coupling or bifunctional silane agent with hydrophilic filler

Previous studies have shown the benefits of using different silane agents as surface modifiers for lignin. The addition of silanes resulted in a homogeneous dispersion of lignin in the studied non-polar rubbers and improved mechanical strength and dynamic properties.[11–13] Hait et. al and Liu et al. investigated bis(triethoxysilylpropyl)tetrasulfide for lignin modification in order to incorporate the lignin successfully in poly-butadiene (BR) and natural rubber (NR), respectively.[11,13] Shorey et al. used 3-(triethoxysilyl) propyl isocyanate to functionalize Kraft lignin and studied its potential in NR.[12]

In the present chapter, different silanes were investigated as modifying agents for HTT lignin:

(i)   mono-functional, octyltriethoxysilane (OCTEO) comprising three ethoxysilyl groups;

(ii)   bi-functional poly-sulfidic silane, bis(triethoxsilylpropyl)tetrasulfide (Si69®/TESPT) comprising of six ethoxysilyl groups and a polysulfide part;

(iii)   bi-functional shielded thiol silane, (3-mercaptopropyl) monoethoxypolyethersilane (Si363®/MPMEPS) consisting of a free mercapto group, one ethoxy group and two polymeric, amphiphilic substituents that act as a physical shield for the mercapto group;

(iv)   bi-functional blocked thiol silane, 3-octanoylthio-1 propyltriethoxysilane (NXT®/OTPTES) comprising of three ethoxysilyl groups and a highly reactive thiol group blocked (esterified) by using octanethionic acid.

The chemical structure and the role of each silane are provided in **Table 4.1**. In-situ modification was carried out to functionalize HTT lignin. For this, the silane was introduced together with the filler and other ingredients into the rubber during mixing. The behavior of HTT lignin filler in rubber after silane modification is described and explained in terms of processability, curing, filler-filler interactions, and mechanical properties. Furthermore, the evaluation of filler micro-dispersion in the rubber matrix was carried out to understand the coupling efficiency of the used silane.

Table 4.1 Chemical structures of the silane surface modifiers for HTT lignin in-situ modification

Silane	Chemical structure	Molecular weight (g/mol)	Ethoxy groups	Sulfur rank	Possible functions		
					Silanization	Coupling	Sulfur donation
OCTEO		276.5	3	0	X	-	-
Si69®/TESPT (reference)		532.5	6	3.8	X	X	X
Si363®/MPMEPS		987.5	3	0	X	X	-
NXT®/OTPTES		365	3	0	X	X	-

4

4.2 Experimental

4.2.1 Materials

As elastomers, end-chain functionalized solution-SBR (SPRINTAN[TR] SLR 4602) with 21 wt.% styrene and 62 wt.% vinyl-butadiene configurations and neodymium polymerized BR (BUNA CB24) with 96 wt.% cis-content were used, as obtained from Trinseo Deutschland GmbH, Schkopau and Arlanxeo Deutschland GmbH, Germany, respectively. HTT lignin with a BET specific surface area of 37 m²/g, specific density of 1.35 g/cm³, and an average particle size (d50) of 2.4 µm determined by static light scattering, was provided by SunCoal Industries GmbH, Germany. The silanes octylpropyltriethoxysilane, OCTEO; bis-(triethoxysilylpropyl)tetrasulfide, TESPT (Si-69®); (3-mercaptopropyl) monoethoxypolyethersilane, MPMEPS (Si363®) were purchased from Evonik Industries AG, Germany. 3-octonylthio-1-propyltriethoxysilane, OTPTES (NXT®) was obtained from Momentive Performance Materials GmBH, Germany. Treated distillate aromatic extract oil, VIVATEC® 500, was provided by Hansen & Rosenthal KG, Germany, and used as processing oil.

Other ingredients: vulcanization/cure activators zinc oxide (ZnO) and stearic acid (SA), and curing agents: sulfur-containing 1 wt.% of mineral oil (S) and N-tert-butyl-2-benzothiazolesulfenamide (TBBS), tetrabenzylthiuramdisulfide (TBzTD) accelerators were purchased from Sigma-Aldrich Chemie, Germany. Antidegradants 2,2,4-trimethyl-

1,2-dihydroquinoline (TMQ), N-(1,3-dimethylbutyl)-N'-phenyl-p-phenylenediamine (6- PPD) and the secondary accelerator 1,3 diphenylguanidine (DPG) were purchased from Flexsys, Belgium.

4.2.2 Preparation of Rubber Compounds

The compound formulation and the amount of silane used in the investigations are presented in **Table 4.2**.

Table 4.2 Rubber formulation

Ingredient	Amounts in parts per hundred rubber (phr)				
	HLO[a]	HLT2.2[b]	HLT1.5[c]	HLM[d]	HLN[e]
SSBR	75	75	75	75	75
BR	25	25	25	25	25
HTT lignin	80	80	80	80	80
OCTEO	6.4*	-	-	-	-
TESPT	-	6.2	6.2	-	-
MPMEPS	-	-	-	9+	-
OTPTES	-	-	-	-	8.5*
Sulfur	2.2	2.2	1.5	2.2	2.2

TDAE - 33 ; ZnO - 2.5; St. acid - 2.5; TMQ - 2; 6 PPD - 2; TBBS - 1.5; TBzTD - 0.5; DPG - 0.25

[a]OCTEO silane containing HTT Lignin filled rubber;
[b]TESPT (Si69®) silane containing HTT Lignin filled rubber;
[c]TESPT silane (Si69®) containing HTT Lignin filled rubber with sulfur correction;
[d]MPMEPS silane (Si363®) containing HTT Lignin filled rubber;
[e]OTPTES silane (NXT®) containing HTT Lignin filled rubber
+**Amount recommended by the supplier**
*****Adjusted to be equimolar and alkoxy equivalents to TESPT (Si69®) silane**

A reference compound containing HTT lignin without silane modification (HLR) was included to understand the influence of the silanes. The mixing formulation for this compound is the same as the one mentioned in **Chapter 3,** under **Table 3.2.** TESPT was taken as reference silane, and the amount applied is 6.2 phr in accordance with Michelin's green tire formulation independent of the filler's specific surface area and the available surface functional groups. As the molar mass and the number of ethoxy groups of the other used silanes differ from the TESPT (reference), the quantities of these silanes were adjusted to represent an equimolar quantity based on the ethoxy groups to the reference

silane except for MPMEPS. An equimolar adjustment of MPMEPS was not performed as it has a high molecular weight and would result in a maximum dosage of 23 phr. Furthermore, the findings of the supplier suggested that such a high amount is not required. Therefore, the amount investigated in an earlier work for silica fillers was applied.[14]

Table 4.3 Two-stage mixing procedure for silane-modified compounds

	Mixing time (min: sec)	Rotor speed (RPM)	Actions
Stage 1	0:00 - 0:20	50	Open the ram and load rubbers
	0:20 - 1:00	50	Mix rubbers
	1:00 - 1:20	50	1st part of filler, ½ silane
	1:20 - 2:00	50	Mix
	2:00 - 2:20	50	2nd part of filler, ½ silane, TDAE
	2:20 - 3:00	50	Mix
	3:00 - 3:20	50	3rd part of filler
	3:20 - 4:00	50	Mix
	4:00 - 4:20	50	4th part of filler, ZnO, St. acid, TMQ & 6PPD
	4:20 - 5:00	50	Mix
	5:00 - 5:20	50	Ram sweep
	5:20 - 10:00	Variable	Mixing and silanization
	10:00	-	Discharge at ~140 - 150 °C after silanization
Stage 2	0:00 - 0:20	30	Add the masterbatch
	0:20 - 1:00	30	Mix
	1:00 - 1:10	30	Add S, TBBS, TBzTD, DPG
	1:10 - 2:00	30	Mix
	2:00 - 2:10	30	Ram sweep
	2:10 - 5:00	30	Mix & discharge at ~90 - 100 °C

Taking into consideration the sulfur donating effect of TESPT (average S-rank of 3.8), an additional compound with a corrected lower sulfur amount was prepared for HTT lignin modified with TESPT (HLT1.5). This is because the sulfur donated by the TESPT can also participate in the rubber crosslinking/vulcanization. This can result in an increase in crosslink density and consequently, in an improvement of mechanical properties.[15,16] The amount of S in phr to compensate for the releasable sulfur of TESPT in the HLT1.5 compound was calculated relative to the weight fraction of S-atoms released from TESPT, commonly approximately 2 per molecule of TESPT, as displayed in **Table 4.2**. This should indicate if the observed reinforcement effects are due to the additional sulfur in the system or originate from the proper interaction of silane with filler and subsequent coupling of the TESPT silanized HTT lignin filler with the rubber.

All compounds were mixed according to the mixing procedure described in **Table 4.3**, except for the HLR compound, which was mixed according to the procedure described in **Chapter 3, Table 3.3** under **Section 3.2**. A two-stage mixing was performed using an internal mixer with tangential rotor geometry and a chamber volume of 390 cm³ (Brabender Plasticorder 350S). For the Stage 1 mixing (masterbatch preparation), the mixer was operated at a fill factor of 70 %, a rotor speed of 50 rpm, and an initial set temperature of 50 °C till the ram sweep at 5:00. Thereafter, the rotor speed was varied for the series in order to achieve the desired discharge temperature. Herewith, too high temperatures were avoided for MPMEPS- and TESPT silane-modified compounds in order to prevent premature scorch. As the used HTT lignin has low bulk density, it was incorporated in four equal parts, and this necessitated a long mixing time.

After Stage 1, all compounds were sheeted out on a Schwabenthan Polymix 80T 80 x 300 mm two-roll mill and kept overnight before the second mixing stage started. Stage 2: The mixing of curatives was also carried out in the internal mixer operated at a fill factor of 70 %, a rotor speed of 30 rpm, and an initial set temperature of 50 °C. After the compounds were discharged, they were sheeted out on the two-roll mill operating with a gap width of 2.5 mm.

4.2.3 Compound Characterizations

Investigations such as Payne (uncured), cure characteristics, mechanical properties, and morphological characteristics, as described in **Section 3.2.2** of **Chapter 3,** were performed. The compounds were also tested for their Mooney viscosities by using a Mooney viscometer 2000E (Alpha Technologies) at 100°C with a large rotor according to ISO 289. The value is represented as ML(1+4) 100 °C. The standard deviations of the results are assumed to be within ±1.5 Mooney points with 95 % confidence[17] for all compounds.

4.3 Results and Discussion

4.3.1 Influence of Silanization on the Compound Processability of HTT Lignin-filled SSBR/BR Compounds

The Mooney viscosities of the investigated compounds are presented in **Figure 4.2**.
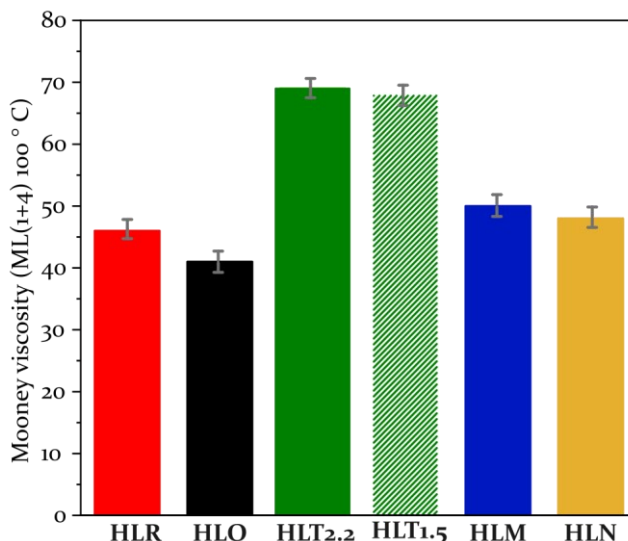
Figure 4.2 Mooney viscosity of HTT lignin- and different silane/HTT lignin-filled-SSBR/BR compounds[1]

The obtained result evidences that the use of silanes plays a significant role in the compound viscosity. The compound mixed with the mono-functional silane, OCTEO (HLO), has a lower Mooney viscosity compared to the HLR compound. This indicates that the introduction of OCTEO silane either hydrophobized the HTT lignin surface by reducing the filler-filler interaction or acted as a softener reducing the intermolecular attractive forces between the rubber chains in the filled compound. In contrast, the addition of bi-functional silanes increases the compound viscosity of HTT lignin-filled rubber compounds, depending on the type and chemical structure of the used silane. The tetrasulfide silane (TESPT) containing compounds with and without sulfur correction (HLT2.2 and HLT1.5) show the highest viscosities, followed by the MPMEPS-(HLM) and OTPTES-containing ones (HLN). This is in contrast to the silica-silane system, where the addition of silane generally reduces the compound viscosity by interacting with the silica's surface silanol groups and decreasing the filler-filler interaction.[3] As the measured discharged temperatures were in the range between 140 - 150 °C for the coupling between HTT lignin-TESPT during mixing, the high viscosity observed for HLT2.2 and HLT1.5 compounds could be interpreted in terms of two predominant reactions, which may take place simultaneously as presented in **Scheme 4.1**. The proposed reaction scheme is partly based on the silica-silane coupling mechanism.[8]

Scheme 4.1 Presumed mechanism of coupling of TESPT to HTT lignin during mixing (note: the proposed reaction mechanism was based on the first assumption)
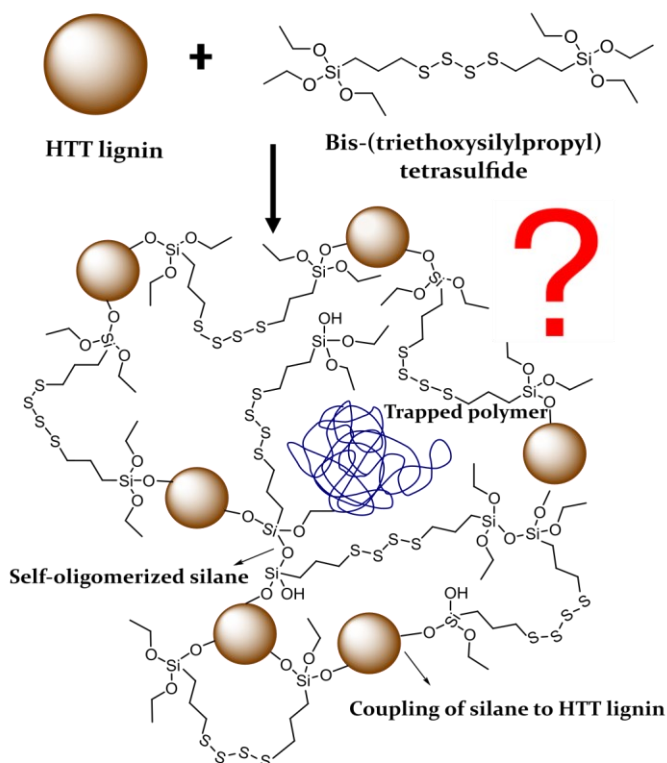
First, a coupling reaction could occur, forming strong chemical/physical linkages (covalent/hydrogen bonding) between the silane and HTT lignin. Second, the silane hydrolysis could be followed by condensation reactions resulting in covalent linkages between two silanes. TESPT silane containing six ethoxy functionalities could self-condense with other silane molecules bound to the HTT lignin surface and could connect these lignin particles. This kind of filler networking could be the reason for the increased compound viscosity, but may additionally trap rubber molecules and restrict their relative motion. As MPMEPS and OTPTES contain only three ethoxy functionalities, the extent of condensation could be lower, resulting in a comparatively lower degree of polymer chain restriction. Further, unlike for TESPT, it is assumed that the steric effect induced by long alkoxy chains of MPMEPS and the octanoyl group of OTPTES also plays a role in the lower compound viscosity.

The differences observed in the Mooney viscosities in **Figure 4.2** correspond to the results of the Payne effect (uncured) of modified HTT lignins, as depicted in **Figure 4.3**.
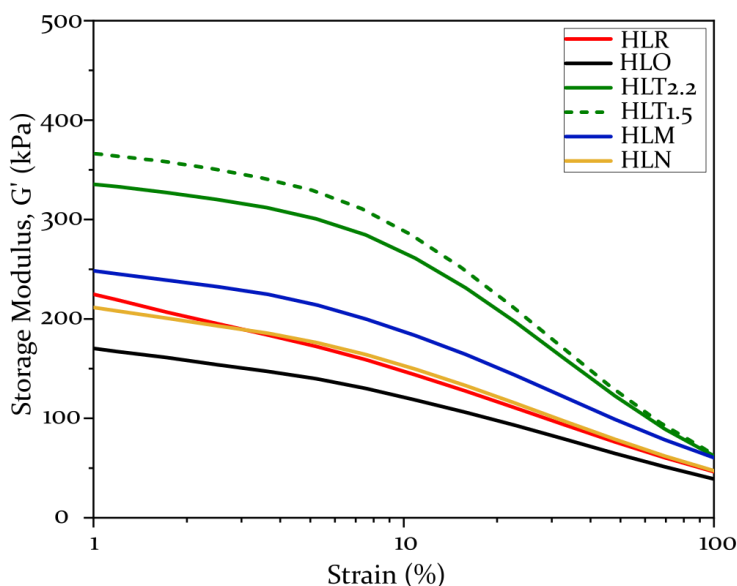
Figure 4.3 Payne effect (uncured) of HTT lignin and different silane/HTT lignin-filled SSBR/BR compounds[1]

The magnitude of the non-linear effect varies with the type of silane, respectively, the resulting filler network structure and strength in the rubber matrix. In general, the increase in shear modulus (G') at low and high strains can be related to filler-filler and filler-polymer interactions, respectively. The addition of the bifunctional TESPT silane, on the one hand, shows a significant increase in the G' of the compounds (HLT2.2 and HLT 1.5) at low and high strain compared to the unmodified HTT lignin-filled compound (HLR). This trend is also observed for the HLM, but the influence is comparatively minimal. OTPTES silane does not show any influence on the G' at low and high strain. On the other hand, the addition of monofunctional OCTEO silane lowers the G' at low strain. This observation is in contrast to what happens in the silica-silane system in which the addition of any type of silane (mono- or bi-functional) reduces the degree of silica networking, thereby lowering the G' at low strain.[18] The strong paradoxical effects observed in HLT2.2 and HLT1.5 could be attributed to the formation of filler interactions, as explained earlier. Another possible aspect contributing to an increased modulus at low strain could be the trapping of rubber molecules within the formed network (**Scheme 4.1**), leading to an increase in the effective volume fraction of the filler. Upon increasing the strain amplitude, the lowering of G' is related to the breakage of the formed filler network, releasing the trapped rubber molecules. This effect is more pronounced in the case of HLT2.2 and HLT1.5 due to the chemical structure of TESPT, respectively, to the higher number of ethoxy functionalities (six groups) prone to self-condensation or oligomerization reaction. Given the number of ethoxy functionalities, the degree of

oligomerization is minimal in the HLO, HLM, and HLN compounds, and the resulting networks are weaker, leading to a lower modulus at low strain. Conversely, the presence of long alkyl chains in MPMEPS, OTPTES, and OCTEO silane can increase the hydrophobation effect in the respective HTT lignin-filled compounds, lowering the G' at low strain.

Assuming there is a correlation between Payne effect data and the degree of micro-dispersion[19], an increase in Payne effect for HLT2.2, HLT1.5, HLM versus HLR, HLN, HLO could eventually be related to poor micro-dispersion of HTT lignin originating from the above-mentioned concept of networking of HTT lignin particles within the rubber matrix. To evaluate the micro-dispersion, AFM investigations were carried out which are described in **Section 4.3.3**.

4.3.2 Influence of Silanization on the Cure Properties of HTT Lignin-filled SSBR/BR Compounds

Figure 4.4 displays the cure behavior of different silane-modified and unmodified HTT lignin-filled compounds.
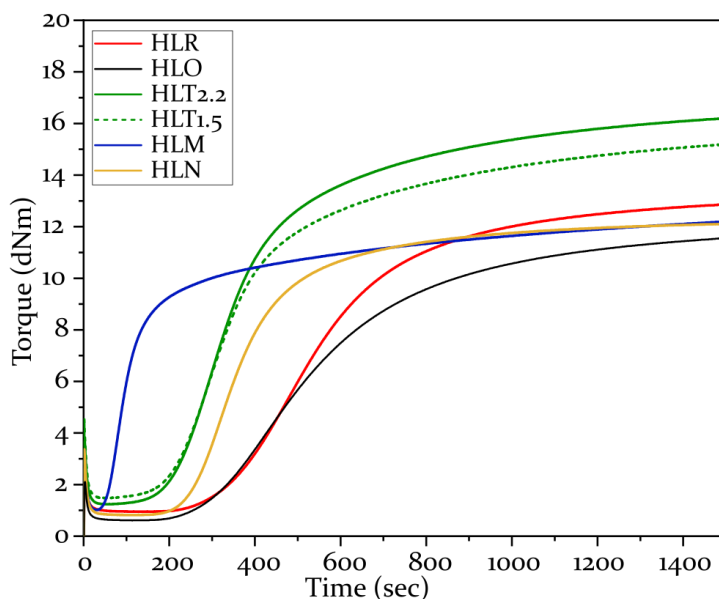
Figure 4.4 Cure behavior of HTT lignin and different silane/HTT lignin-filled SSBR/BR compounds[1]

The addition of certain silanes decreases the rather long scorch time of the compound. This suggests that TESPT, MPMEPS, and OTPTES cover the surface of HTT lignin and inhibit the adsorption of the basic accelerators facilitating the availability and mobility of the accelerators. This improvement in kinetics is achieved without affecting the processability of compounds with TESPT and OTPTES silane. For the MPMEPS silane-containing compound (HLM), the scorch safety is inferior. In other words, the time

available to initiate the cure reaction is short due to the presence of free thiol groups, which are very reactive to the vinyl functionalities of the rubber.[20] In comparison to this, the superior scorch safety of the OTPTES silane-containing compound (HLN) is related to the hindrance offered by the blocking end-group on the reactive thiol-functionality. The cure parameters obtained from the rheogram are tabulated in **Table 4.4.** A higher minimum M_L and a higher maximum torque M_H for both HLT1.5 and HLT2.2 were observed. The increase in M_H is an indication of the cumulative contribution from polymer-polymer interaction (crosslink density), HTT lignin-silane-polymer coupling, and filler-filler networking. In addition, as described earlier, the sulfur-donating behavior of TESPT during vulcanization also increases the M_H. The additional crosslinks formed in the TESPT-modified HTT lignin compound (HLT2.2) and their impact on M_H can be distinguished from unmodified and other silane-containing HTT lignin compounds with the help of the reduced sulfur formulation: HLT1.5, which accounted for the sulfur that is possibly released from TESPT. It shows the tendency of TESPT to couple HTT lignin to the polymer chains. The reduction in stiffness of the HLM, HLN, and HLO vulcanizates could be related to the lower contribution of filler-polymer and filler-filler networks in comparison to TESPT compounds.

Table 4.4 Obtained cure parameters of HTT lignin and different silane/HTT lignin-filled SSBR/BR

Description	HLR	HLO	HLT2.2	HLT1.5	HLM	HLN
t_{S_2} (min)	4.9	4.8	3.7	3.5	0.9	4.0
$t_{c,90}$ (min)	11.3	10.7	14.1	13.6	8.5	8.8
M_H (dN.m)	12.9	11.6	16.2	15.2	12.0	12.0
M_L (dN.m)	0.7	0.6	1.2	1.1	0.9	0.8
$\Delta M, M_H-M_L$ (dN.m)	12.2	11.0	15.0	14.1	11.1	11.2

4.3.3 Influence of Silanization on the Morphological Characteristics of HTT Lignin-filled SSBR/BR Vulcanizates

AFM was applied to examine the filler morphology and dispersion within the rubber matrix of the cured samples in order to understand the effects of surface modification of the HTT lignin. A clear distinction in the micro-dispersion of HTT lignin in the presence of different silanes can be identified in **Figures 4.5 and 4.6**.
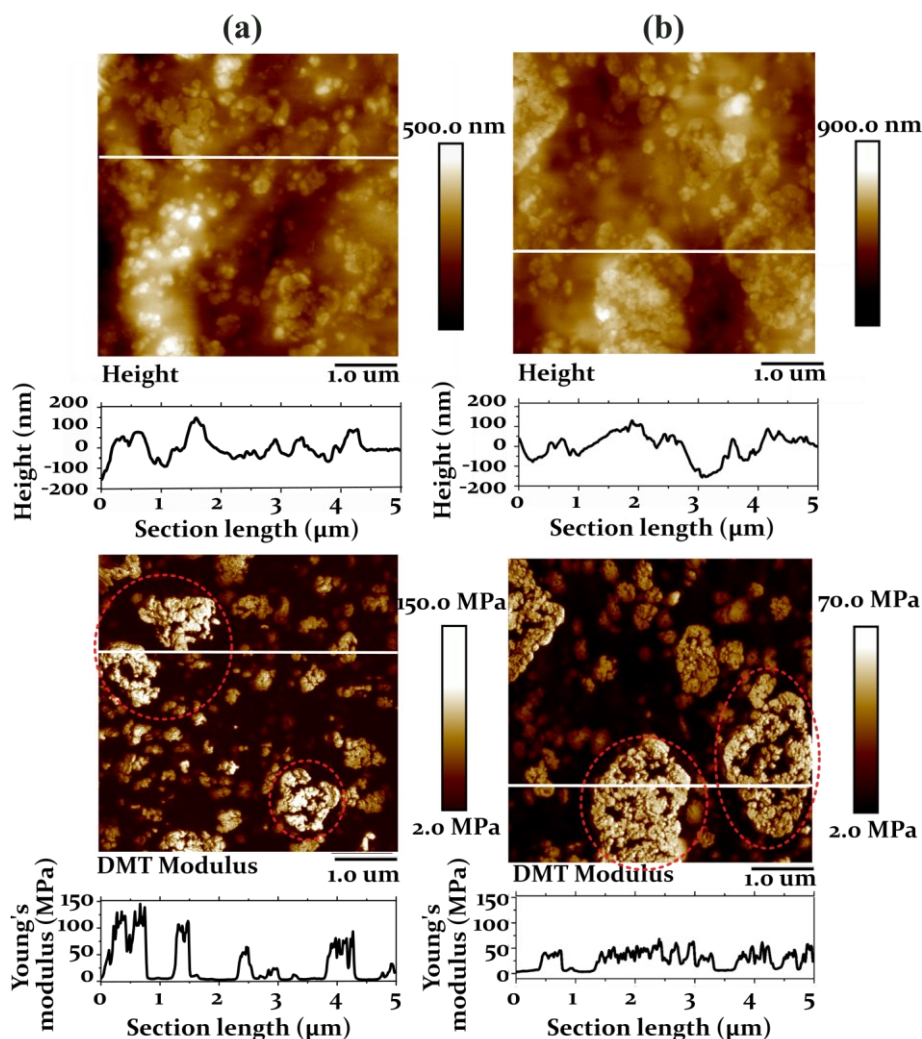
4
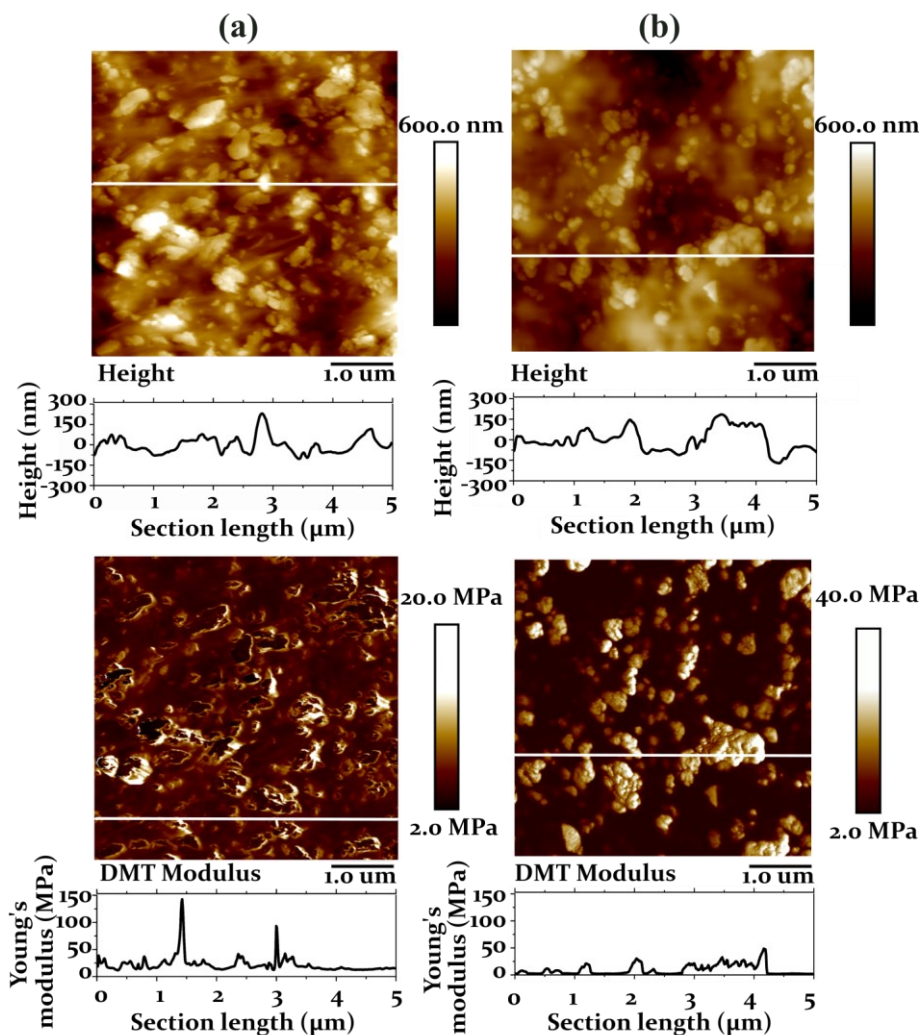
Figure 4.5 AFM height images (top) and Young's modulus maps (bottom) of cryo-fractured vulcanizates: (a) HLO; and (b) HLN with their corresponding height and modulus profiles represented below. Scanning area: 5 x 5 µm². The cross-section profiles were taken along the white lines and plotted on the same scale for data comparison

From the obtained topography depicted in **Figures 4.5 and 4.6**, two different classes of filler structures with varying particle sizes can be distinguished: (I) clusters of 200±100 nm similar to HLR morphology as described in **Chapter 3** under **section 3.3.2.4** and (II) larger clusters of HTT lignin of 0.5 - 3 µm with trapped rubber, which is termed as sponge-like lignin textures (see red dotted circles). Based on the observed contrast difference between rubber (dark color) and HTT region (bright color) in Young's modulus map (presented in **Figure 4.6**), signifying the variation in mechanical properties of the two regions, the presence of trapped rubber can be detected in the larger HTT lignin clusters. HLO and HLN vulcanizates (**Figure 4.5 (a) and (b)**) fall under class (I), representing a similar

morphology as the unmodified HTT lignin compound **(see Chapter 3, Figure 3.11)**. Thus indicating that these silanes act as a softener, causing slippage during mixing. The reduction in shear forces impacts the dispersion of the filler particles negatively.

Figure 4.6 AFM height images (top) and Young's modulus maps (bottom) of cryo-fractured vulcanizates: (a) HLM and (b) HLT1.5 with their corresponding height and modulus profiles represented below. Scanning area: 5 x 5 μm². The cross-section profiles were taken along the white lines and plotted in the same scale for data comparison [Red-dotted circles denote sponge-like HTT lignin textures]

Conversely, the application of MPMEPS and TESPT results in a heterogeneous distribution of the filler consisting of both types of filler structure: classes (I) and (II), demonstrated in **Figure 4.6 (a) and (b)**. As anticipated from the other data, the presence of HTT lignin network structures in these silane-containing vulcanizates confirms that these silanes promote higher filler-filler interactions and negatively affect the filler micro-dispersion. The class II filler structure, the sponge-like lignin textures, seems to be comprised of small and stiff primary particles in the range of 20 - 100 nm clustered together and partially packed with rubber inside. Further, depending on the silane type, the size of the filler structure and sponge-like textures varies. For instance, HLM vulcanizate includes an HTT lignin cluster with dimensions of 0.5 - 1 μm, different from the HLT1.5 with 2 - 3 μm. These lignin networks are built of primary particles ranging between 20 – 80 ±20 nm. The formation of sponge-like lignin structures in HLT1.5 and HLM vulcanizates could be a result of two different reactions taking place simultaneously: (i) during mixing, the silane interacts with the surface of the filler facilitating dispersion of the lignin clusters by shear forces into smaller particles, and (ii) connecting these broken clusters as a result of silane condensation or oligomerization of unreacted ethoxy and/or alkoxy groups, which in turn trap rubber in-between the developing sponge-like textures (refer to **Scheme 4.1**).

Having assumed that the formation of sponge-like filler textures is due to the condensation reaction, the absence of these structures in OCTEO and OTPTES vulcanizates having the same alkoxy functionalities as MPMEPS raises uncertainty about the reaction mechanism. This indicates that the mechanism of coupling between silanes and HTT lignin is different from that of the silica-silane system and needs further investigations which is covered in **Chapter 5**.

4.3.4 Influence of Silanization on the Mechanical Properties of the HTT Lignin-filled SSBR/BR Vulcanizates

Figure 4.7 presents the stress-strain behavior of the different compounds after curing. Among all the investigated compounds, the TESPT silane-containing ones perform best in terms of mechanical properties. It appears that the presence of larger sponge-like textures, as demonstrated in **Figure 4.5 (b),** does not impart inferior properties in comparison to the other silanes. In contrast to this, it is apparent that the sulfur-donating nature of TESPT plays a major role in the stress-stress properties in the HLT2.2 vulcanizate by increasing the polymer-polymer interaction, i.e. crosslinking density, in comparison to the HLT1.5.
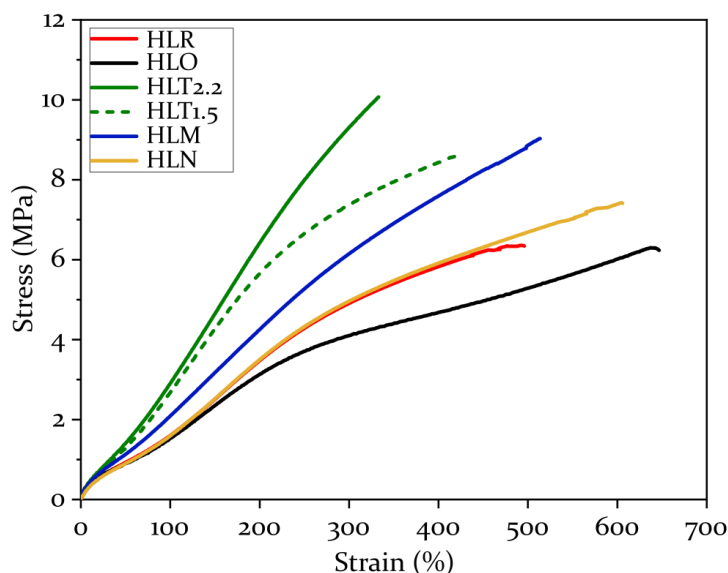
Figure 4.7 Stress-Strain properties of differently silane/HTT lignin-filled SSBR/BR vulcanizates

From the result of the HLT1.5 vulcanizate, the sole impact of silanization on the mechanical properties can be understood. It can be assumed from this result that TESPT couples to HTT lignin, enhancing the filler-polymer interaction, and thus the reinforcing properties of the HTT lignin. Apart from this, the HTT lignin sponge-like textures can also contribute to the overall reinforcement. Nevertheless, the observed low tensile strength of 10 MPa suggests that the poor dispersion of HTT lignin causes local stress concentration sites adversely affecting the strength properties of TESPT silane-containing compounds. HLM shows higher reinforcing properties than the unmodified HTT lignin. Surprisingly, the blocked thiol silane (OTPTES) containing vulcanizate, HLN exhibits identical properties to the unmodified one. It seems that this silane does not couple to HTT lignin and therefore, the filler-polymer interaction is low in comparison to the other coupling agents. This is in line with the results of the Payne effect and AFM. Similarly, the addition of the mono-functional OCTEO to the HTT lignin-filled compound (HLO) shows a decrease in modulus and an increase in elongation at break. This result indicates that OCTEO shields the surface of lignin effectively, thereby reducing the filler-filler interaction. However, this result, in combination with the AFM findings, implies that the surface is not covered by OCTEO, but it induces a plasticizing effect which leads to inferior mechanical behavior.

4.4 Conclusions and Recommendations

The potential of mono-functional and bi-functional silanes as surface modifiers for HTT lignin was investigated in this chapter. The study highlights that the use of bifunctional silanes, TESPT and MPMEPS, enhances the in-rubber properties compared to the mono-functional, OCTEO silane. The positive effects of the thiol silane reveal that a coupling reaction occur between HTT lignin and the silane promoting the filler-polymer interaction. This confirms that a chemical coupling of HTT lignin with the polymer is a prerequisite for enhancing the physical properties of rubber for exploiting HTT lignin as a reinforcing filler. Besides, other interesting but opposing effects compared to the silica-silane system such as an increase in the Payne effect, Mooney viscosity, and formation of filler clusters confirm that the filler-filler interaction has also increased. This worsens the micro-dispersion of HTT lignin in the rubber matrix, which is one of the important factors in achieving good rubber reinforcement properties. Surprisingly, the results from the vulcanizate containing the blocked thiol silane, OTPTES (NXT®), and HTT lignin affirm that no clustering of the filler by the reaction of two attached silane molecules and/or no coupling between filler and polymer occurs in the presence of this silane. Thus, the properties achieved in this case are similar to the unmodified HTT lignin. This peculiar behavior of OTPTES compared to the other two bi-functional silanes, TESPT and MPMEPS, is difficult to interpret and this questions the reactivity of the ethoxy functional groups of the silane towards HTT lignin.

Therefore, to widen the scope of HTT lignin as a reinforcing filler in the presence of bi-functional silanes, it is important to clarify and understand the ambiguities such as:

(i) The cause for sponge-like lignin textures when using certain bifunctional silanes

(ii) The reactivity of ethoxysilyl groups of the silane towards the HTT lignin

(iii) The role of polysulfide and/or thiol groups for the in-rubber properties of HTT lignin

In order to explore the above-discussed challenges, the coupling mechanism of HTT lignin and sulfur-containing silanes needs to be elucidated.

References

(1) Sekar, P. Design of a Bio-Based Filler System for Tire Treads. PDEng thesis, University of Twente, The Netherlands, 2018.

(2) Rauline, R. Rubber Compound and Tires Based on Such a Compound. EP0501227A1, 1992.

(3) Luginsland, H.-D.; Fröhlich, J.; Wehmeier, A. Influence of Different Silanes on the Reinforcement of Silica-Filled Rubber Compounds. Rubber Chemistry and Technology 2002, 75, 563–579.

(4) Luginsland, H.-D.; Röben, C. The Development of Sulphur-Functional Silanes as Coupling Agents in Silica-Reinforced Rubber Compounds. Their Historical Development over Several Decades. International Polymer Science and Technology 2016, 43 (4), 1–6.

(5) Reuvekamp, L. A. E. M.; Brinke, J. W.; Swaaij, P. J.; Noordermeer, J. W. M. Effects of Time and Temperature on the Reaction of TESPT Silane Coupling Agent during Mixing with Silica Filler and Tire Rubber. Rubber Chemistry and Technology 2002, 75 (2), 187–198.

(6) Ansarifar, A.; Saeed, F.; Ostad Movahed, S.; Wang, L.; Ansar Yasin, K.; Hameed, S. Using a Sulfur-Bearing Silane to Improve Rubber Formulations for Potential Use in Industrial Rubber Articles. Journal of Adhesion Science and Technology 2013, 27 (4), 371–384.

(7) Goerl, U.; Hunsche, A.; Mueller, A.; Koban, H. G. Investigations into the Silica/Silane Reaction System. Rubber Chemistry and Technology 1997, 70 (4), 608–623.

(8) Hunsche, A.; Görl, U.; Müller, A.; Knaack, M.; Göbel, T. Investigations Concerning the Reaction Silica/Organosilane and Organosilane/Polymer. Part 1: Reaction Mechanism and Reaction Model for Silica / Organosilane. KGK-Kautschuk und Gummi Kunststoffe 1997, 50, 881–889.

(9) Okel, T. A.; Waddell, W. H. Silica Properties/Rubber Performance Correlation. Carbon Black-Filled Rubber Compounds. Rubber Chemistry and Technology 1994, 67 (2), 217–236.

(10) Wang, M.-J. Effect of Polymer-Filler and Filler-Filler Interactions on Dynamic Properties of Filled Vulcanizates. Rubber Chemistry and Technology 1998, 71 (3), 520–589.

(11) Hait, S.; De, D.; Ghosh, P.; Chanda, J.; Mukhopadhyay, R.; Dasgupta, S.; Sallat, A.; Al Aiti, M.; Stöckelhuber, K. W.; Wießner, S.; Heinrich, G.; Das, A. Understanding the Coupling Effect between Lignin and Polybutadiene Elastomer. Journal of Composites Science 2021, 5 (6), 154–169.

(12) Shorey, R.; Gupta, A.; Mekonnen, T. H. Hydrophobic Modification of Lignin for Rubber Composites. Industrial Crops and Products 2021, 174, 114189.

(13) Liu, R.; Li, J.; Lu, T.; Han, X.; Yan, Z.; Zhao, S.; Wang, H. Comparative Study on the Synergistic Reinforcement of Lignin between Carbon Black/Lignin and Silica/Lignin Hybrid Filled Natural Rubber Composites. Industrial Crops and Products 2022, 187, 115378.

(14) Klockmann, O.; Hasse, A. A New Rubber Silane for Future Requirements - Lower Rolling Resistance; Lower VOCs. KGK-Kautschuk und Gummi Kunststoffe 2007, 60 (3), 82–84.

(15) Luginsland, H. Reactivity of the Sulfur Chains of the Tetrasulfane Silane Si 69 and the Disulfane Silane TESPD. Kautschuk Gummi Kunststoffe 2000, 53, 10–19.

(16) Sengloyluan, K.; Sahakaro, K.; Dierkes, W. K.; Noordermeer, J. W. M. Reinforcement Efficiency of Silica in Dependence of Different Types of Silane Coupling Agents in Natural Rubber-Based Tire Compounds. KGK-Kautschuk und Gummi Kunststoffe 2016, 69 (5), 44–53.

4

(17) Niemiec, S. A Review of Factors Affecting Precision in Mooney Viscosity Measurement. Polymer Testing 1980, 1 (3), 201–209.

(18) Fröhlich, J.; Niedermeier, W.; Luginsland, H.-D. The Effect of Filler–Filler and Filler–Elastomer Interaction on Rubber Reinforcement. Composites Part A: Applied Science and Manufacturing 2005, 36 (4), 449–460.

(19) Jin, J.; Kaewsakul, W.; Noordermeer, J. W. M.; Dierkes, W. K.; Blume, A. Macro- and Micro-Dispersion of Silica in Tire Tread Compounds: Are They Related? Rubber Chemistry and Technology 2021, 94 (2), 355–375.

(20) Sato, M. Reinforcing Mechanisms of Silica / Sulfide-Silane vs. Mercapto-Silane Filled Tire Tread Compounds. PhD Thesis, University of Twente, The Netherlands, 2018.

4

5. Paradox of Rubber Reinforcement of Silane-Modified Hydrothermally Treated Lignin
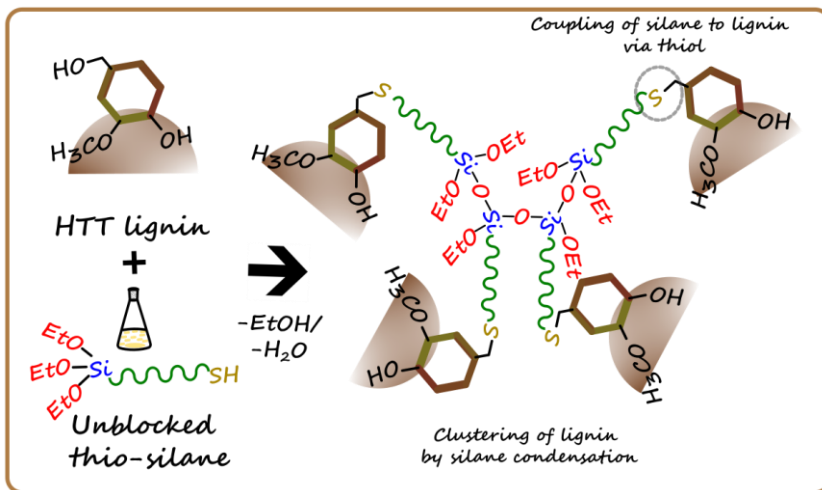
Reactivity Study of HTT lignin/Silane and Elucidation of the Coupling Reaction by using Model Studies[a]

The use of specific silane coupling agents enhances the in-rubber properties of HTT lignin-filled SSBR/BR compounds. However, these types of reactive sulfur-containing silanes result in the formation of large filler clusters within the rubber matrix, as observed by Atomic Force Microscopy and discussed in **Chapter 4**. In contrast, the addition of blocked mercapto silanes does not improve the mechanical properties of the HTT lignin-filled rubber compound, and the filler morphology remains similar to that of unmodified HTT lignin, with a cluster size of ±200 - 500 nm. This difference in the behavior of the reactive and the blocked sulfur-containing silanes raises uncertainties regarding their potential as coupling agents for HTT lignin. Thus, the present chapter addresses the existing ambiguities by elucidating the coupling mechanism of HTT lignin and silane modifiers. This was done by modifying HTT lignin and its model representatives, vanillyl alcohol and guaiacol, using modifiers that bear specific silane functionalities: alkoxy and thiol, and the combination of both groups in a round-bottom flask without solvents. Extensive Nuclear Magnetic Resonance (NMR) investigations were conducted on the reaction products of different modified HTT lignin and modified HTT lignin model substances. These investigations demonstrated that for the coupling reaction to occur, the presence of the aliphatic hydroxy (-OH) groups on the α-carbon of the aromatic ring (namely the OH at the benzylic carbon) in combination with the hydroxy group at the para-position of the aromatic ring is essential. Based on the observations, the underlying and most favorable mechanisms involved in the coupling between HTT lignin and silane are discussed. The reaction involves a chemical coupling between the thiol group of the silane and the formed reactive quinone methide intermediate of HTT lignin through Michael addition. Astonishingly, ethoxysilyl groups of silane and/or the hydrolyzed silane (silanol) are unreactive towards HTT lignin. Instead, the silanol (-SiOH) groups either condense with another silanol and/or with the ethoxysilyl group (-SiOEt), leading to the oligomerization of silane. It is supposed that both the reactions: (i) coupling between silane and lignin via the sulfur moiety and (ii) condensation of silanes via the SiOH/SiOEt moieties, lead to the formation of HTT lignin clusters evidenced by AFM measurements.

5.1 Introduction

The previous chapter discussed the use of different silane agents as in-situ surface modifiers for the HTT lignin filler in an SSBR/BR blend. It was observed that the use of specific sulfur-containing silane coupling agents, e.g., bis (triethoxsilylpropyl) tetrasulfide (TESPT) and 3-thiopropyl-(di-tridecyl pentaethoxylate)monoethoxysilane (MPMEPS), can significantly enhance the reinforcing performance of HTT lignin filler in SSBR/BR compound than the unmodified one. This led to the conclusion that these silane coupling agents cover surface active sites of HTT lignin, which are polar in nature. Thus, the hydrophilicity is reduced, and the filler-polymer interaction is enhanced, one of the main prerequisites for rubber reinforcement. Therefore, the degree of dispersion, a further important reinforcement criterion, could be expected to be enhanced. However, the morphological studies carried out using AFM to discern the dispersion quality of the HTT lignin filler in the rubber matrix reveal a formation of large filler clusters of 2 - 3 µm in size in the presence of reactive sulfur-silanes contrary to the unmodified as well as chemically blocked sulfur silane (3-octanoylthio-1 propyltriethoxysilane, OTPTES) modified ones. This kind of filler cluster formation affects the degree of dispersion and distribution of HTT lignin in the rubber. Subsequently, the reinforcing properties of HTT lignin in the presence of reactive sulfur silane lead to a semi-reinforcing behavior compared to the high-reinforcing carbon black and silica used as a filler. These findings are opposite to those observed for silica filler, where the addition of any silane coupling agents generally enhances the filler-rubber compatibility and improves its dispersion in the rubber matrix.[2,3] The reasons for the improved reinforcing effect of HTT lignin and the formation of the filler clusters when using specific silane coupling agents (TESPT and MPMEPS) and for the non-existing impact on the reinforcing properties of the HTT lignin-filled rubber compound when using OTPTES are obscure. This led to a debate about whether, in general, the alkoxy groups of the silane are capable of reacting with HTT lignin or if other reaction pathways occur for HTT lignin and silane coupling agents. This necessitated the need to investigate the coupling mechanism of HTT lignin and the silane in depth.

To gain more profound knowledge about the coupling mechanism of HTT lignin and the reactive sulfur-bearing silanes, two different modification approaches were followed to understand the reactivity of the silanes with HTT lignin. As the reaction mechanism may involve the participation of different functional groups of HTT lignin (aliphatic and phenolic hydroxy, carboxylic acid groups, aldehydes, and ketones) and also of the silane, model studies were used in this study to gain insight into the phenomenon. First, the model studies used for this work are discussed, followed by the modification approaches. Vanillyl alcohol (VA) and guaiacol (G) (**Figure 5.1, A, B**) were used as model substances for HTT lignin. These substances are simplified guaiacyl-type lignin representative sub-structures, frequently occurring in lignins,[4] with either phenolic or a combination of phenolic and aliphatic hydroxy functional groups that are potential sites for

modifications. In order to clarify whether the reaction of silane to HTT lignin occurs via the (un)hydrolyzed alkoxysilyl group (as expected) or differently via the reactive sulfur moieties, in this study, modifier was chosen accordingly to bear: (i) only the alkoxy group (**Figure 5.1, C**), (ii) only the thiol group (**Figure 5.1, D**), and (iii) the combination of both functionalities (**Figure 5.1, E**). Thus, for this investigation, trimethylethoxy silane (TMES), 1-hexanethiol (HT), and 3-mercaptopropyltriethoxysilane (MPTES) were selected as modifiers. Two modifications were carried out to elucidate the reaction mechanism: (i) reactions between HTT lignin and the chosen surface modifiers and (ii) reactions between the selected HTT lignin model substances and the selected surface modifiers. The following characterization tools were used for analyzing the different modified HTT lignins and modified lignin model substances respectively: (i) standard solid-state analytical techniques such as thermogravimetric analysis (TGA), solid-state carbon and silicon nuclear magnetic resonance (^{13}C and ^{29}Si SSNMR), and (ii) one- and two-dimensional liquid ^{1}H - ^{13}C NMR. Due to the solubility limitations of HTT lignin, liquid-state characterization techniques were excluded for the modified HTT lignin samples.
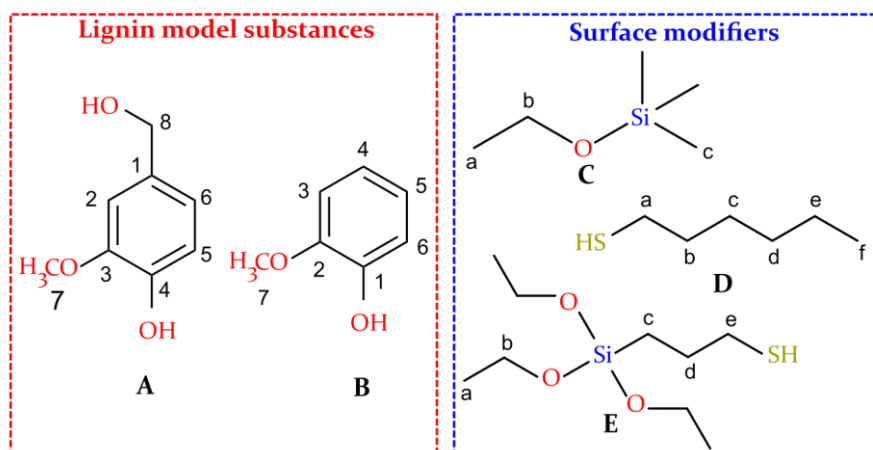
Figure 5.1. Chemical structures and numbering of the HTT lignin model substances: (A) vanillyl alcohol (VA), (B) guaiacol (G); and surface modifiers: (C) monofunctional silane, trimethylethoxysilane (TMES), (D) a simple aliphatic thiol, 1-hexanethiol (HT), (E) bifunctional silane, 3-mercaptopropytriethoxysilane (MPTES)

5.2 Experimental Section

5.2.1 Materials

Commercially available materials were purchased and used as received without further purification or pre-treatment unless otherwise stated. HTT lignin (pH 8.7) with a BET specific surface area of 47 m²/g was provided by SunCoal Industries GmbH, Germany. The supplier also specified that the available surface-accessible acidic hydroxy group of HTT lignin is 0.32 mmol/g. TMES (98 %); HT (95 %); MPTES (≥ 80 %); VA (98 %); G (98 %); deuterated dimethyl sulfoxide (DMSO-d6, 99.96 % atom D); deuterated chloroform (CDCl$_3$, 99.8 % atom D) were acquired from Merck KGaA, Germany.

5.2.2 Modification Procedure

5.2.2.1 Reaction of HTT lignin with different surface modifiers

All modification reactions were performed with the same quantity of HTT lignin (2 g, 0.64 mmol hydroxy groups) and modifiers (8.46 mmol) without any solvent. The amount of modifier was added in excess to the available hydroxy groups present in the mixture to improve the wetting of HTT lignin. The described protocol is identical for all modifying agents. HTT lignin and the modifier were added to a 100 ml flask. The reaction mixture was refluxed and heated under constant stirring in an oil bath at 160±5 °C for one hour. After this, the reaction product was extracted in a Soxhlet unit with acetone for 24 h to remove the unreacted and physically adsorbed modifier. Afterwards, it was placed in a vacuum oven at a temperature of 80 °C for 24 h to remove the solvent. In order to confirm that the Soxhlet extraction can efficiently remove the unreactive and physically adsorbed silane, further experiments were performed without this additional purification and subsequent drying step.

5.2.2.2 Reaction of HTT lignin model substances with different surface modifiers

Equimolar quantities (3 mmol) of VA or G and TMES were placed in a 5 ml glass ampoule and sealed with a rubber septum without any solvent. The filled ampoule was immersed in an oil bath at 160±5 °C, and the reaction was carried out for one hour under continuous stirring. After this, the reaction was stopped immediately by quenching the ampoule in liquid nitrogen. An identical procedure was followed for HT and MPTES. No post-treatment steps were applied. Control experiments with lignin model substances VA and G without silane were performed under identical conditions to check if side reactions like decomposition or oxidation were taking place and to neglect their impact on the analysis of the modified samples. The control samples are labeled as VA-160 and G-160.

5

5.2.3 Characterization Methods

5.2.3.1 Thermogravimetric analysis (TGA)

To distinguish between the physical and chemical grafting of the different surface modifiers to HTT lignin, the modified samples before and after extraction were subjected to thermal analysis using a TGA 550 analyzer, TA Instruments, USA. Approximately 5 to 8 mg of the sample was placed in a platinum pan, and all samples were first heated isothermally at 30 °C under a nitrogen atmosphere for 10 mins, followed by gradient heating from 30 to 600 °C at a rate of 15 °C/min. After incubating at 600 °C for 15 min under nitrogen atmospheric conditions, the samples were further heated from 600 to 900 °C at a heating rate of 15 °C/min under air atmosphere. Finally, the samples were kept under isothermal conditions at 900 °C for 15 min in an atmosphere of air.

5.2.3.2 Solid-state NMR

^{13}C SSNMR spectra of differently modified HTT lignins were obtained with a Bruker 9.4 T Avance III HD 400 spectrometer equipped with a 4 mm magic angle spinning (MAS) probe (operating at 400.34 MHz for ^{1}H and at 100.67 MHz for ^{13}C). ^{13}C cross-polarization (CP) MAS measurements were conducted at a spinning rate of 14 kHz, with a 90° pulse for ^{1}H of 2.4 µs and a contact time of 2 ms. ^{13}C spectra were internally referenced by the chemical shift of the methoxy peak of the lignin (δ = 56.1 ppm) and acquired with 1486 complex points with a spectral width of 295 ppm and a relaxation delay of 2 s and a maximum of 30000 averages. A sufficient signal-to-noise ratio was ensured during the measurement.

^{29}Si SSNMR spectra of TMES- and MPTES-modified HTT lignins were obtained with a Bruker 14.1 T Avance Neo spectrometer equipped with a 2.5 mm magic angle spinning (MAS) probe (operating at 600.16 MHz for ^{1}H, and at 119.23 MHz for ^{29}Si). ^{13}C CP MAS measurements were conducted at a spinning rate of 6 kHz, with a 90° pulse for ^{1}H of 1.94 µs and a contact time of 5 ms. ^{29}Si spectra were externally referenced by the downfield peak of the Q8M8 (trimethylsilyl ester of the double four-ring silicate) reference sample (δ = 12.4 ppm) and acquired with 768 complex points with a spectral width of 381 ppm and a relaxation delay of 15 s, and 17920 averages. All the SSNMR spectra were zero-filled, apodized with an exponential window function, subjected to phasing, and Fourier transformed using MestreNova.

5.2.3.3 Liquid state NMR:

Approximately 10 - 15 mg of each model reaction mixture and each control sample were dissolved in 0.5 ml DMSO-d6 to be analyzed by NMR. The prepared solutions were characterized by ^{1}H, ^{13}C, ^{1}H - ^{13}C heteronuclear single quantum coherence (HSQC) and heteronuclear multiple bond correlation (HMBC) NMR. Experiments were conducted on two different magnets: a Bruker 14.1 T Avance NEO spectrometer equipped with a 5 mm BBO solution state probe (operating at 600.16 MHz for ^{1}H) and a Bruker 9.4 T Avance III spectrometer equipped with a 5 mm BBFO solution state probe (operating at 400.13 MHz

for ^{1}H). Both spectrometers were equipped with a 50 G/cm gradient unit on the z-axis. All experiments were performed at room temperature. [1]H experiments were measured with a spectral width of 20 ppm, centered at 6.17 ppm, with 16 averages and 32768 complex points, and a relaxation delay of 2 s. All ^{13}C experiments were measured with a fully decoupled inverse gated sequence, with a spectral width of 262 ppm, centered at 110 ppm, with 1024 averages, acquired with 32768 complex points, and a relaxation delay of 2 s. All ^{1}H - ^{13}C HSQC experiments were fully decoupled and performed with double Insensitive Nuclei Enhancement by Polarization Transfers (INEPT) tuned to J = 140 Hz, employing echo/anti-echo gradient selection and two phase-cycled scans per t1 point, with a total of 128 complex t1 points, a spectral width of 13 ppm in the direct dimension, and 210 ppm in the indirect one, and a relaxation delay of 2 s. ^{1}H - ^{13}C HMBC experiments were performed using gradient coherence selection optimized for long-range couplings tuned to J = 4 Hz to ensure that [4]J and [5]J coupling could be observed. The acquisition was performed in magnitude mode, with 8 phase cycled averages per t1 point, with a total of 128 t1 points, a spectral width of 13 ppm in the direct dimension and 220 ppm in the indirect one, and a relaxation delay of 2 s.

All spectra were zero-filled twice on either one or two dimensions. All spectra were processed with Bruker Top-spin, with the 1D being apodized with an exponential window function, while 2D spectra were apodized with a sine bell (HMBC) and a squared sine bell (HSQC) window function. The ^{1}H and ^{13}C spectra were referenced to the solvent's proton and carbon peaks, respectively.[5] The assignment was performed with the NMRFAM-SPARKY software package.[6] Assignments were performed using all the spectra acquired while cross-referencing these with the Spectral DataBase for Organic Compounds (SDBS).[7] Specific peaks and cross peaks were displayed in the spectra to elucidate the chemical structures.

To investigate if there is a formation of any solution-state structures, diffusion ordered spectroscopy (DOSY) measurements were performed with a stimulated echo and LED sequence using bipolar gradient pulse pairs.[8] DOSY spectra were obtained with a 3 ms gradient length (δ) and with a diffusion time (Δ) of 200 ms, with 32 linearly varying gradient intensities, employing eight averages. The temperature was kept constant at 25 °C, with an airflow of 450 l/h. The obtained ^{1}H spectra are referenced to the DMSO solvent proton peak, and the peak assignments are performed identically to the methods described above. DOSY data were zero-filled, apodized with an exponential window function, subject to phasing, Fourier transformed, and subsequently processed with an exponential fitting using MestreNova. The obtained structures' molecular weights were estimated using the Stokes-Einstein equation[9], assuming a spherical shape for the formed structures and room temperature viscosities and densities for DMSO.[9]

5.3 Results and Discussion

5.3.1 Preliminary Confirmation of the Coupling Reaction between HTT lignin and the used chemicals

TGA measurements were performed on unextracted and extracted samples to investigate whether the chosen modifiers are physically or chemically grafted to HTT lignin. The TGA data (depicted in **Figure 5.2 (a) and (b)**) shows an insignificant mass loss for TMES-modified HTT lignin before and after extraction. In contrast, a significant mass loss below 300 °C is observed for the unextracted HT- and MPTES-modified samples compared to the extracted ones. This is related to the decomposition of low molecular weight residues and non-chemically bonded compounds.

(a) **(b)**
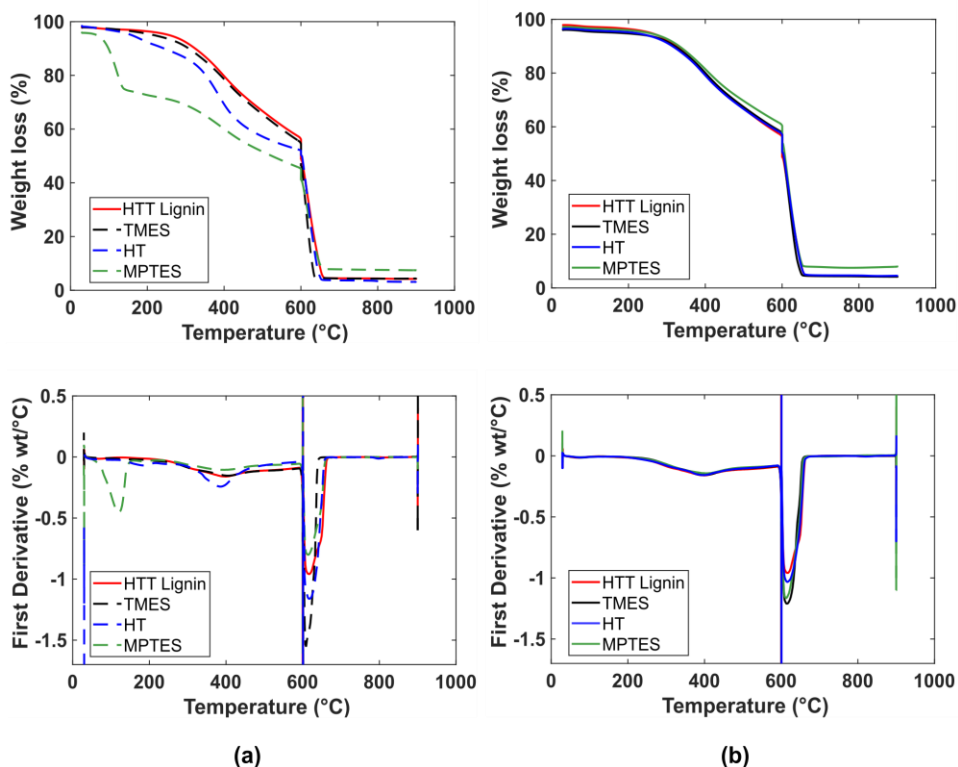
Figure 5.2 TGA (top) and Derivative TGA (DTGA, bottom) curves of differently modified HTT lignin: (a) before extraction and (b) after extraction. TMES – TMES-modified HTT lignin; HT – Hexane thiol-modified HTT lignin; MPTES – MPTES-modified HTT lignin [Note: The straight lines in the D-TGA plots represent the behavior due to isothermal conditions]

For the extracted samples, the thermal stability of all modified HTT lignin samples is similar to the unmodified ones in this temperature range. This implies the absence of an unreactive and/or physically adsorbed modifier on the HTT lignin surface. In the range

between 600 - 900 °C under the air atmosphere, it is observed that MPTES-modified lignin samples (**Figure 5.2 (a) and (b)**) show a higher residual content of 7 % compared to the other modified and unmodified HTT lignin samples (4 - 5 %). This signifies that the MPTES-modified HTT lignin sample contains more thermally stable carbonaceous and/or inorganic matter. This might be attributed to a higher degree of chemical functionalization of HTT lignin by MPTES and/or the presence of oligomerized MPTES silane on the filler surface formed due to the hydrolysis and condensation of ethoxysilyl functionalities. This supposition is discussed later in this section using the ^{13}C NMR and ^{29}Si NMR measurements results.

^{13}C SSNMR measurements investigated the chemical grafting of silane (after extraction) on the modified extracted samples compared to unmodified HTT lignin (**Figure 5.3**). Most of the spectral features observed are common to HTT lignin. These signals are qualitatively ascribed to protonated and non-protonated aromatic carbons (C=C; O-C=C) ranging between 100 to 160 ppm and to the aliphatic carbons (CH$_x$, where x= 1 - 3) occurring between 0 to 80 ppm. More specifically, the prominent peak at 56 ppm denotes aliphatic O-CH$_3$.[10,11]
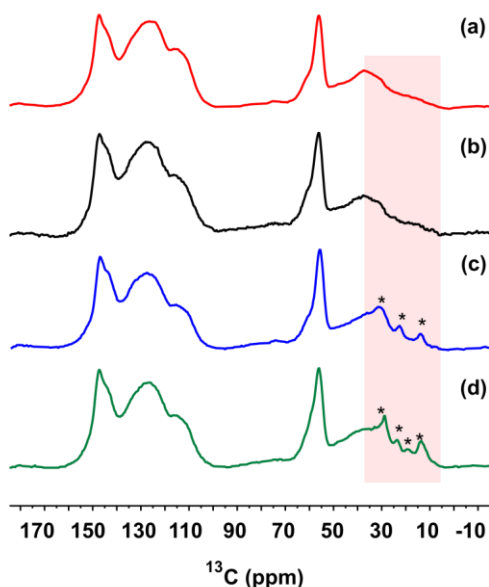
Figure 5.3 Solid-state ^{13}C NMR spectra of (a) unmodified HTT lignin; (b) TMES-modified; (c) HT-modified; and (d) MPTES-modified-HTT lignin after acetone extraction [The asterisk symbol '' represents the additionally observed peaks]*

The ^{13}C NMR result of TMES-modified HTT lignin (see **Figure 5.3 b**) shows no spectral changes relative to HTT lignin. Further, the ^{29}Si NMR measurement does not show any signal for this sample (see **Figure 5.4 a**). Therefore, it may be concluded that TMES is not coupled to the HTT lignin. Thus, the use of an ethoxy functionality of the silane is not a viable way to modify HTT lignin. In the case of HT- and MPTES-modified HTT lignin

samples **(Figure 5.3 c, d)**, additional carbon peaks (represented by the asterisk (*) symbol) are observed in the region between 10 - 35 ppm. This represents the characteristic aliphatic chain carbons of MPTES and HT (see **Table 5.1**), even though there is a clear spectral overlap with the signals of HTT lignin. This confirms that HT and MPTES are chemically grafted to the HTT lignin surface, indicating that the coupling via the thiol (-SH) functionality is viable. But, for the MPTES-modified sample, this inference should be taken with reserve. This is because of the presence of another functionality, i.e., the triethoxy silyl groups, that can undergo self-condensation upon hydrolysis. These self-condensed structures might physically adsorb on the HTT lignin surface and give rise to ^{13}C NMR signals in the region between 10 - 40 ppm. In order to evaluate if the self-condensation reaction occurred, ^{29}Si NMR measurement was performed additionally for the MPTES-modified HTT. The result is presented in **Figure 5.4 (b)**.

Table 5.1 Experimental chemical shift (δ) and assignment of ^{13}C resonances of the investigated surface modifiers in CDCl$_3$ at 25 °C

Modifiers	δ ^{13}C (ppm)					
	a*	b*	c*	d*	e*	f*
TMES	18.2	58.28		-	-	-
HT	23.76	33.41	27.5	30.75	22	13.63
MPTES	18.2	58.28	9.5	27.5	27.65	-

*the label numbering is explained in **Figure 5.1**

The appearance of spectral peaks in the range between -50 to -80 ppm in **Figure 5.4b** demonstrates the presence of self-condensed products in MPTES-modified HTT lignin. The peak for Si-O-C bonds formed between HTT lignin and MPTES via the ethoxysilyl group is not observed. This affirms that the condensation reaction of MPTES silane occurs but is not a coupling reaction between MPTES and HTT lignin via (un)hydrolyzed ethoxysilyl groups of silane. The degree of condensation in MPTES is represented by the "T^i" notation where "i" denotes the number of bridging oxygens surrounding the silicon atom, as depicted in **Figure 5.5**.[12]
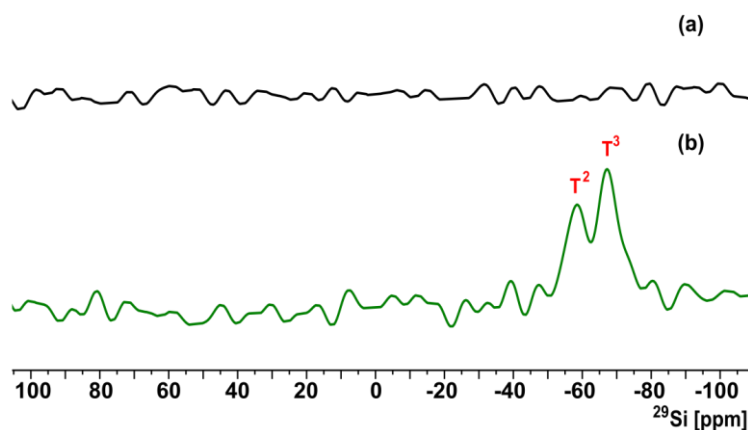
Figure 5.4 Solid state ^{29}Si NMR spectrum of (a) TMES- and (b) MPTES-modified HTT lignin after extraction acquired under MAS conditions [T2 – linear and T3 - three-dimensional oligomerized silanes]

Due to the low signal-to-noise ratio, only the linear (T^2 = -55 ppm) and three-dimensional Si-O-Si oligomeric peaks (T^3 = -68 ppm) are visible in the ^{29}Si spectra. However, the hydrolyzed silane moieties (T^0) and dimeric units (T^1), which generally show a peak below -50 ppm, are not easily distinguishable or identifiable. From these observations, it could be concluded that the oligomerized silane formed is mainly composed of linear and three-dimensional Si-O-Si structures.

All these qualitative analyses exclude that a modification of HTT lignin by MPTES occurred by the ethoxysilyl (or silanol) moiety. Furthermore, they demonstrate that these moieties are involved in self-condensation reactions. However, it is still unclear if the observed peaks are caused by the reaction of HTT lignin with the thiol group of MPTES and/or by the condensed siloxane structures physically adsorbed on the HTT lignin surface.

5
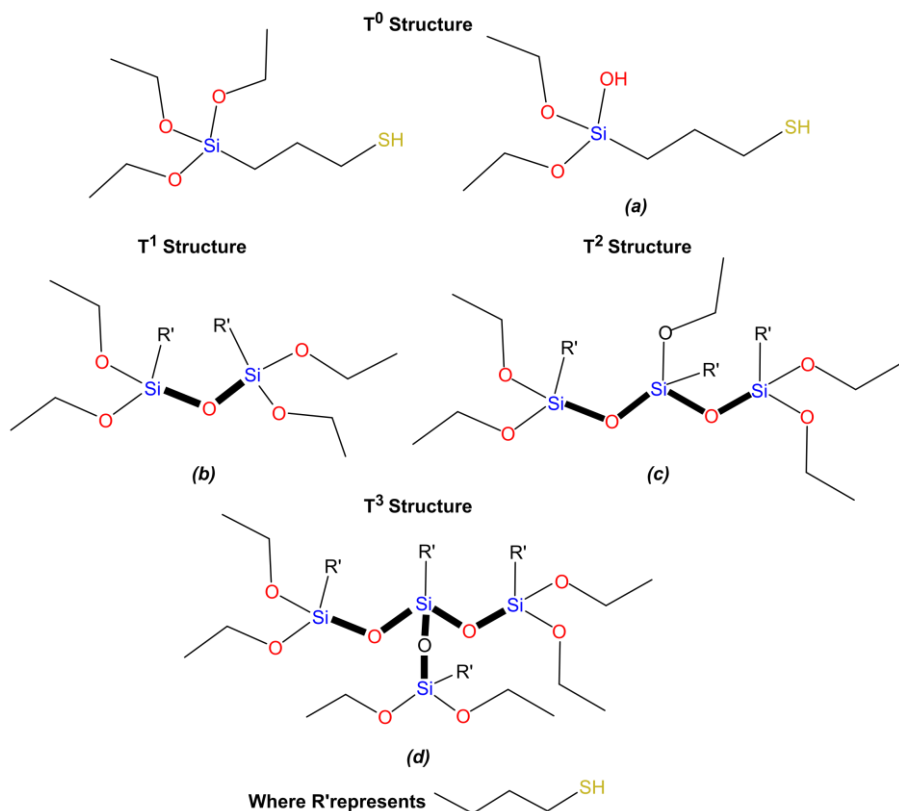
Figure 5.5 Schematic chemical representation of T^i structures (a) silanol; (b) dimer; (c) linear trimer; and (d) three-dimensional structure of MPTES[13]

5.3.2 Understanding the Reactivity of Functional Groups with HTT lignin using Model studies

5.3.2.1 Control studies with the chosen lignin models

Detailed model studies using lignin model substances and different surface modifiers (shown in **Figure 5.1**) were performed to confirm further the results of a reaction between HTT lignin and the modifying agents. Since it is known that the lignin model vanillyl alcohol undergoes condensation and oxidation reactions[14,15], an initial study was performed with VA alone (VA-160) to investigate whether VA is stable under the chosen reaction conditions or not. The NMR results of VA-160 (**Figure 5.6**) confirm the presence of an oxidation product, vanillin (V), and a condensation product, 4,4'-(oxybis(methylene))bis(2-methoxyphenol), which is an 8-O-8 dimer of vanillyl alcohol (DVA). Therefore, both have to be considered as possible side products in the reaction of VA with surface modifiers.
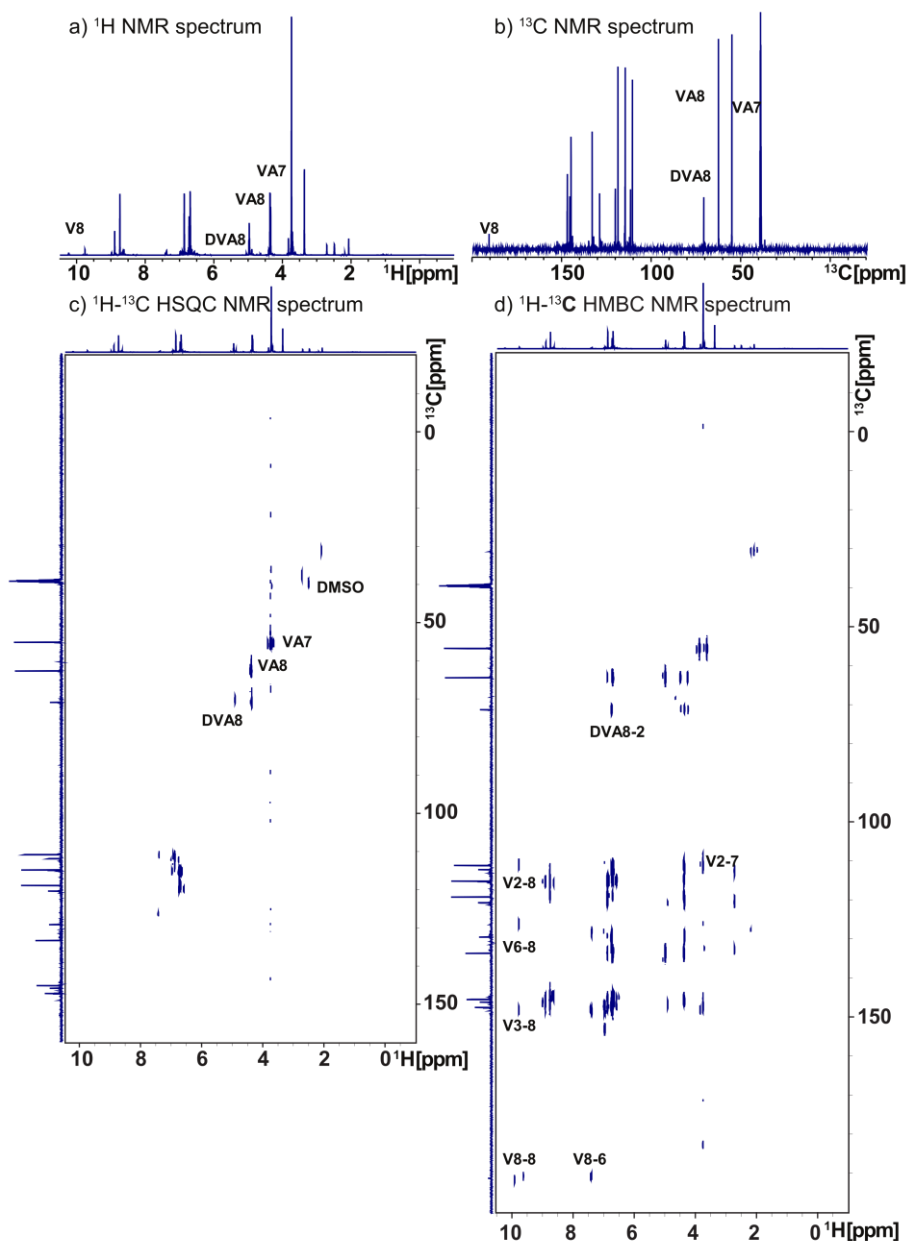
Figure 5.6 Solution one- and two-dimensional NMR spectra of vanillyl alcohol (VA) heated at 160 °C (V – vanillin; DVA – dimerized vanillyl alcohol (4,4'-(oxybis(methylene))bis(2-methoxyphenol)) [Carbon to proton, e.g., 2-8 represents C2 and H8]

The structures of V and dimers of VA are shown in **Scheme 5.1**. The 4-O-8 dimer type, which is the most commonly occurring condensed product of VA as presented in **Scheme 5.1**, was not identified under the applied reaction conditions.

Scheme 5.1 Possible reaction products of vanillyl alcohol (VA) at 160 °C: Vanillin (V) and dimers (8-O-8, 4-O-8) [The structures highlighted in green denote the identified reaction products]
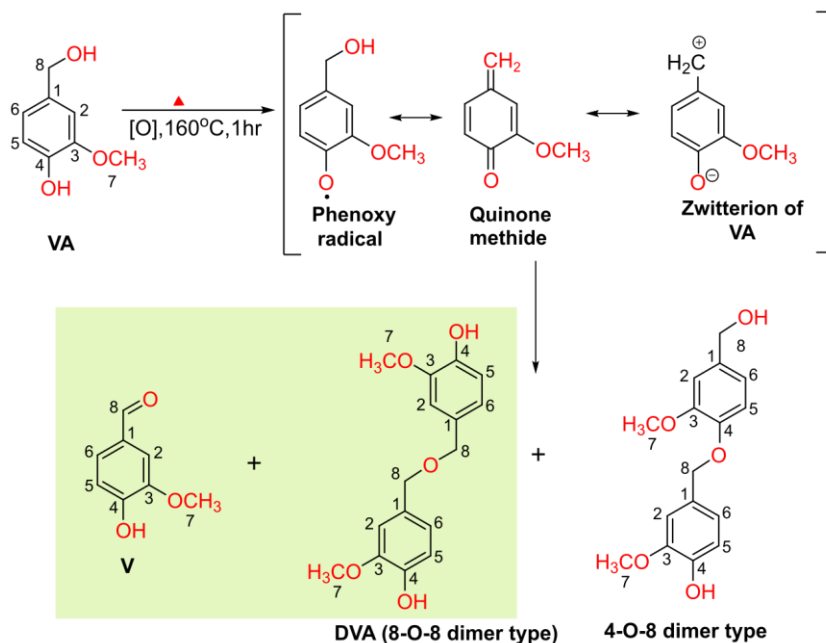
All the reactions mentioned above happen specifically at the carbon in position 8 (C8) of VA (refer to **Figure 5.1 A** for the numbering). Thus, based on the C8-OH/C8=O and C8-OH/C8-O-C8 ratios, the proportions of V and DVA were quantified as 9 and 13 %, respectively, and reported in **Table 5.2**. The formation of vanillin and DVA at 160 °C without any solvent was expected due to either the generation of a resonance-stabilized benzylic carbocation or quinone methide intermediates (QM) by the oxidation of VA to a phenoxy radical as described in earlier findings.[14–17] Since the carbocation of VA or QM intermediates is highly unstable and reactive; it is difficult to identify and quantify them. Therefore, they do not appear in the spectra. Nevertheless, this study indicates that if there is a formation of such intermediates being electron acceptor species, they can offer a wide range of reactivities, meaning VA can react with different modifiers.[14,18–21]

Table 5.2. Summarized estimations of the conversion of HTT Lignin Model (LM) substances upon heating at 160 °C: G or VA (labeled as LM), NI – Not Identifiable

Products / Reactants	Remaining LM (%)	Oxidized LM (%)	Condensed LM (%)
VA-160	78	9	13
G-160	100	NI	NI

In a similar control study performed with guaiacol at 160 °C (G-160), no condensation or oxidation products could be identified in the ^{13}C spectra shown in **Figure 5.7**. This indicates that under the given reaction conditions, guaiacol is stable, and side reactions like oxidation or condensation, as observed for VA, are negligible in the guaiacol system.
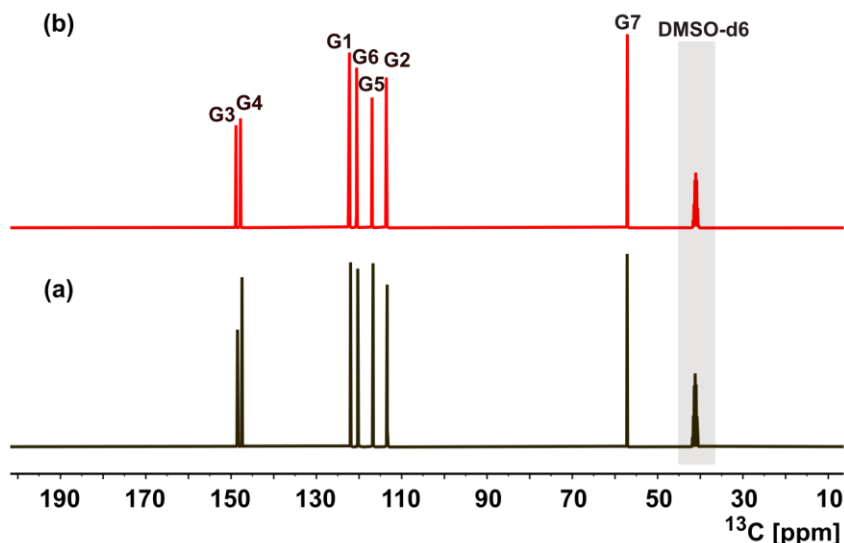
Figure 5.7 Solution ^{13}C NMR spectra of (a) pure guaiacol (G) and (b) guaiacol heated at 160 °C (G- 160) [The carbon numbering is provided in Figure 5.1]

5.3.2.2 Reactivity study with the lignin model and surface modifiers

5.3.2.2.1 Reactivity study 1: lignin model, vanillyl alcohol, and different surface modifiers

Having sorted out the side reactions of the lignin model substances under the chosen conditions, the occurrence of the preferred coupling reaction between the lignin model substances and the surface modifiers was investigated by different 1D and 2D NMR measurements. The summary of all the relative proportions of the main reaction products as a result of coupling is reported in **Table 5.3**. This quantification was performed on clearly distinct and identifiable resonances that were found in the same position in the molecules. The proportions of the products in the reaction mixtures of vanillyl alcohol and TMES silane (VA+TMES) were determined by the ratios of C8 (**Figure 5.1 A**). For the reaction products of vanillyl alcohol and hexane thiol (VA+HT), the proportions were estimated by the ratio of the integrals of the C7 of vanillin (V7) and VA-HT7 ^{13}C peaks. In the case of VA+MPTES, in which no oxidized and condensed VA was observed, the outcome is considered quantitative for only having the remaining starting material or product.

Table 5.3. Summarized estimations of the conversion of HTT lignin model substance: VA with different surface modifiers: TMES, HT, and MPTES (labeled as X). NI – Not Identifiable; VA8 – reaction occurring at carbon 8 of VA; OEt- ethanol

Products / Reactants	Remaining VA (%)	Oxidized VA (%)	Condensed VA (%)	VA8-X (%)	VA8-OEt (%)
VA+TMES	68	6	13	NI	13
VA+HT	NI	7	NI	93	
VA+MPTES	NI	NI	NI	100	NI

Vanillyl alcohol reacts with the modifiers under the applied conditions, suggesting that the hydroxymethyl functionality is vital for the modification. The ^{13}C spectra of the reaction products of VA with and without the three modifying agents are shown in **Figure 5.8**.

As identified in the spectra of the VA control sample (VA-160, **Figure 5.6**), the condensation and oxidation products around δ 72 and 190 ppm, respectively, could also be observed in the reaction between VA with TMES, as depicted in **Figures 5.8 b and 5.9**. Further, the HMBC spectra demonstrated in **Figure 5.9** suggest the presence of trimethyl silanol, TMSOH, in the reaction mixture, signifying that TMES hydrolyzed under the subjected reaction conditions. The identification of the product formed because of the reaction between ethanol (EtOH) and VA in carbon position 8 (VA-OEt8, **Figure 5.9 a, d**) further confirmed TMES hydrolysis. This indicates that ethanol, a byproduct of TMES hydrolysis, also reacts with VA. This can be considered as another side reaction. This reaction does not significantly change the amount of other side products (dimer or vanillin). Besides the side reactions, no direct coupling products of TMES-VA or TMSOH-VA could be found. Although the findings of Nathan et al. reported the trans-etherification reaction between the primary aliphatic alcohol of VA and ethoxy of silane, it could not be detected in this study.[22] Thus, it can be concluded that TMES or TMSOH are less reactive towards VA than short aliphatic hydroxy nucleophiles like ethanol.
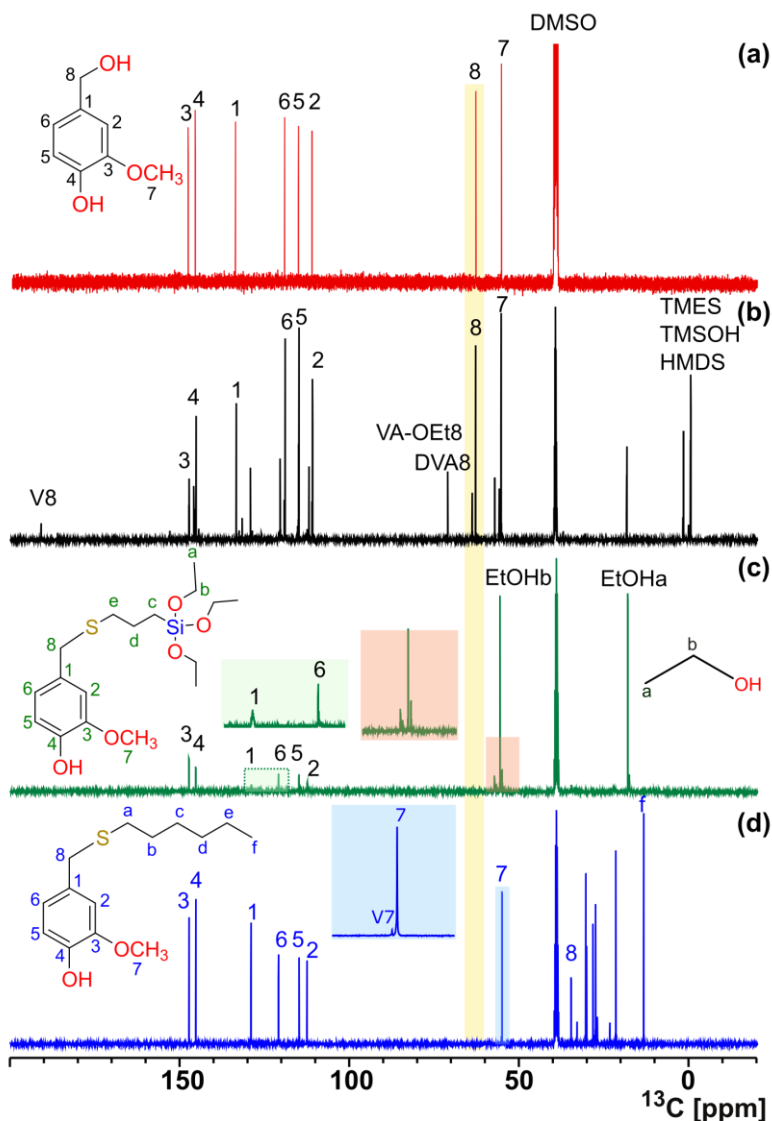
Figure 5.8 Liquid state ^{13}C NMR spectra of (a) pure vanillyl alcohol (VA) and the reaction products of vanillyl alcohol (VA) obtained after reaction at 160±5 °C with (b) TMES, (c) MPTES, and (d) HT (V- Vanillin; DVA-Dimerized VA; EtOH (a,b)- Ethanol). The data was acquired in DMSO-d6 at room temperature; (a) was performed at 14.1 T, whereas (b) and (c) were performed at 9.4 T
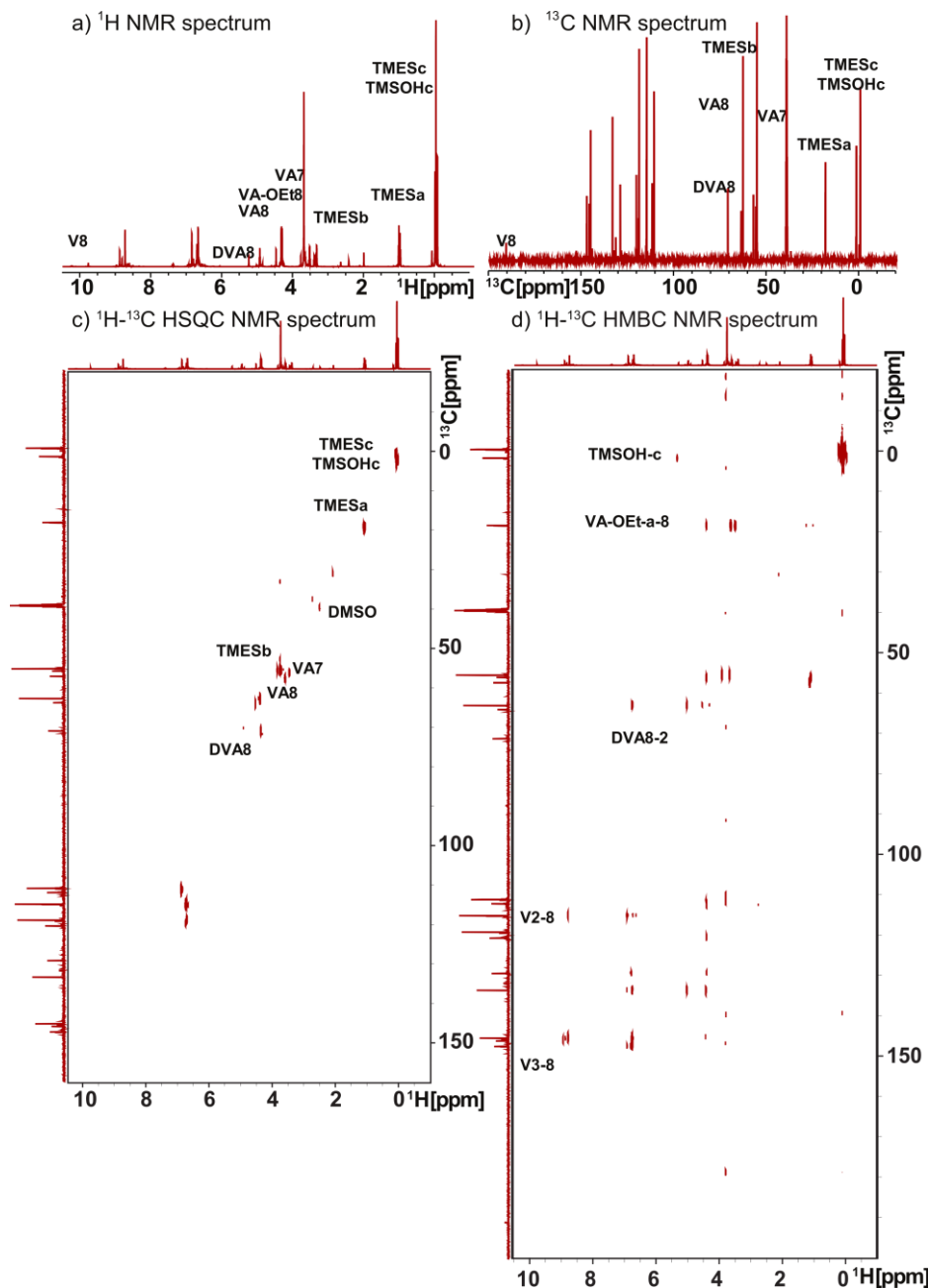
Figure 5.9 One- and two-dimensional liquid-state NMR spectra resulting from the reaction of vanillyl alcohol (VA) with trimethylethoxysilane (TMES) at 160±5 °C [The hydrogen and carbon numbering is the same as in Figure 5.1. The peak assignments are provided in SI S1, (i)]

The reaction of VA with HT results in a direct coupling and can be identified in **Figure 5.8** by the disappearance of the aliphatic hydroxy carbon in position 8 at ~62 ppm. Furthermore, a direct coupling between the sulfur atom of HT and VA can be identified via HMBC (the cross peak between carbon 8 of VA and the proton in position 'a' of HT in **Figure 5.10**) and occurred at a high conversion rate (~93 %, **Table 5.3**). The chemical structure of the formed products is shown in **Scheme 5.2**. In addition, the findings highlight that the coupling reaction between VA and HT is highly preferred compared to side reactions like oxidation and condensation, unlike TMES.

Scheme 5.2 Reaction products of vanillyl alcohol and hexane thiol at 160 °C
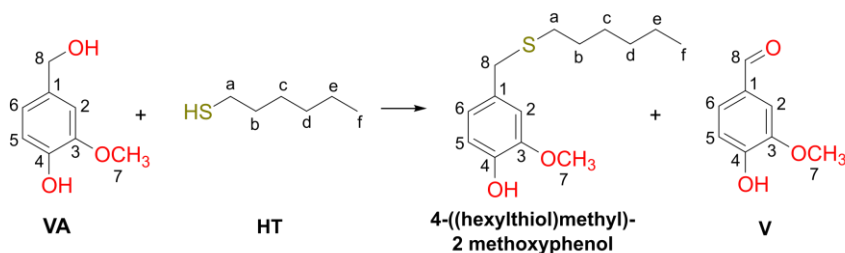
The reactivity of thiols toward VA was also evaluated by using the MPTES modifier. **Figure 5.8** shows that the intensity of the spectrum is significantly lower than those of the other modified HTT lignin spectra. This could be observed due to increased broader lines (which can also be observed in the ¹H spectrum, as presented in **Figure 5.11**). Furthermore, the peak corresponding to the aliphatic hydroxy carbon in position 8 is absent in the ¹³C spectrum. This indicated a conversion, which was observed by an HMBC correlation between the carbon 8 of the VA moieties and the proton at position 'c' of the MPTES one.

5
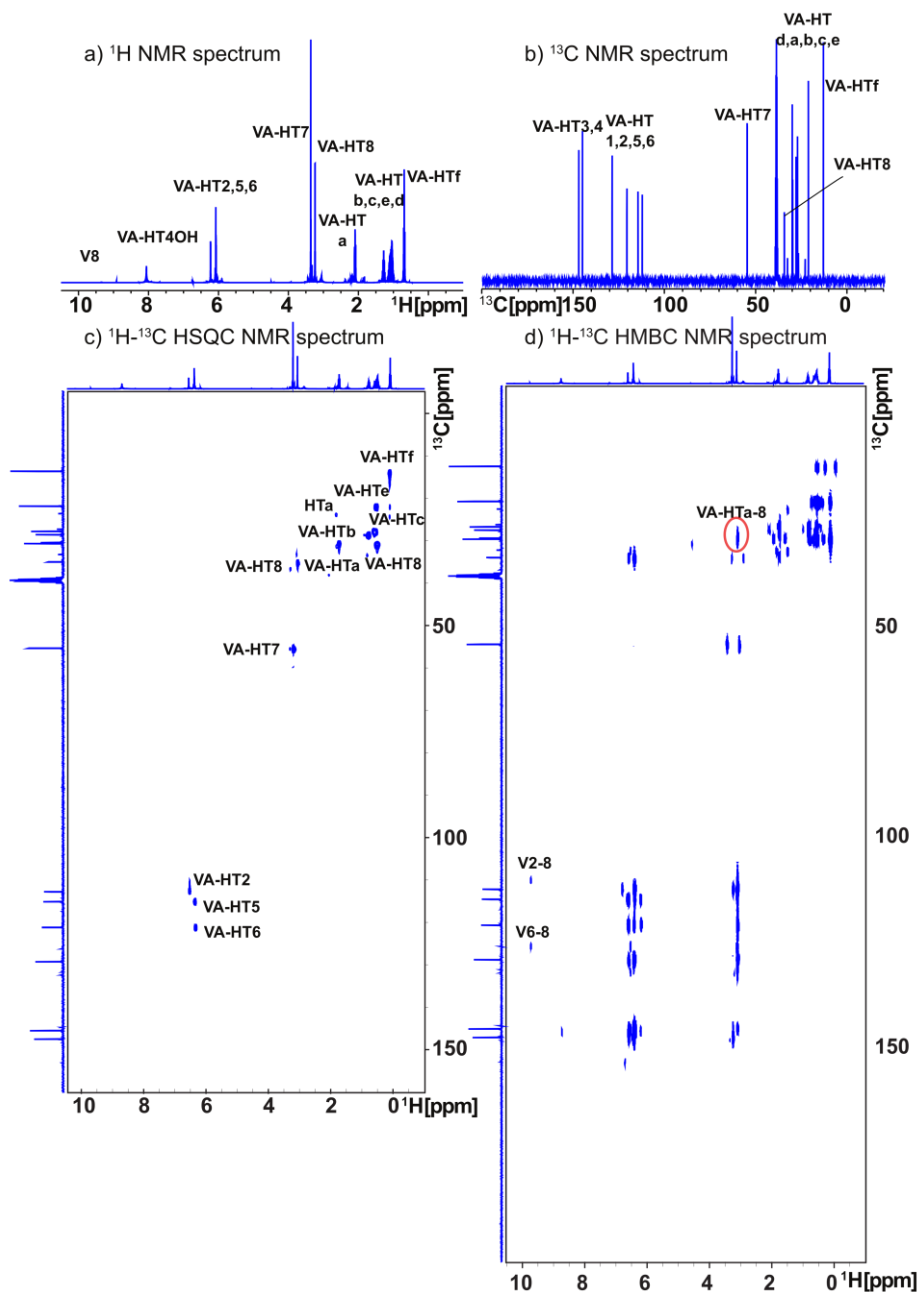
Figure 5.10 One- and two-dimensional liquid-state NMR spectra resulting from the reaction of vanillyl alcohol (VA) with hexanethiol (HT) at 160±5 °C [The hydrogen and carbon numbering is the same as in Figure 5.1. The peak assignments are provided in SI S1, (ii)]
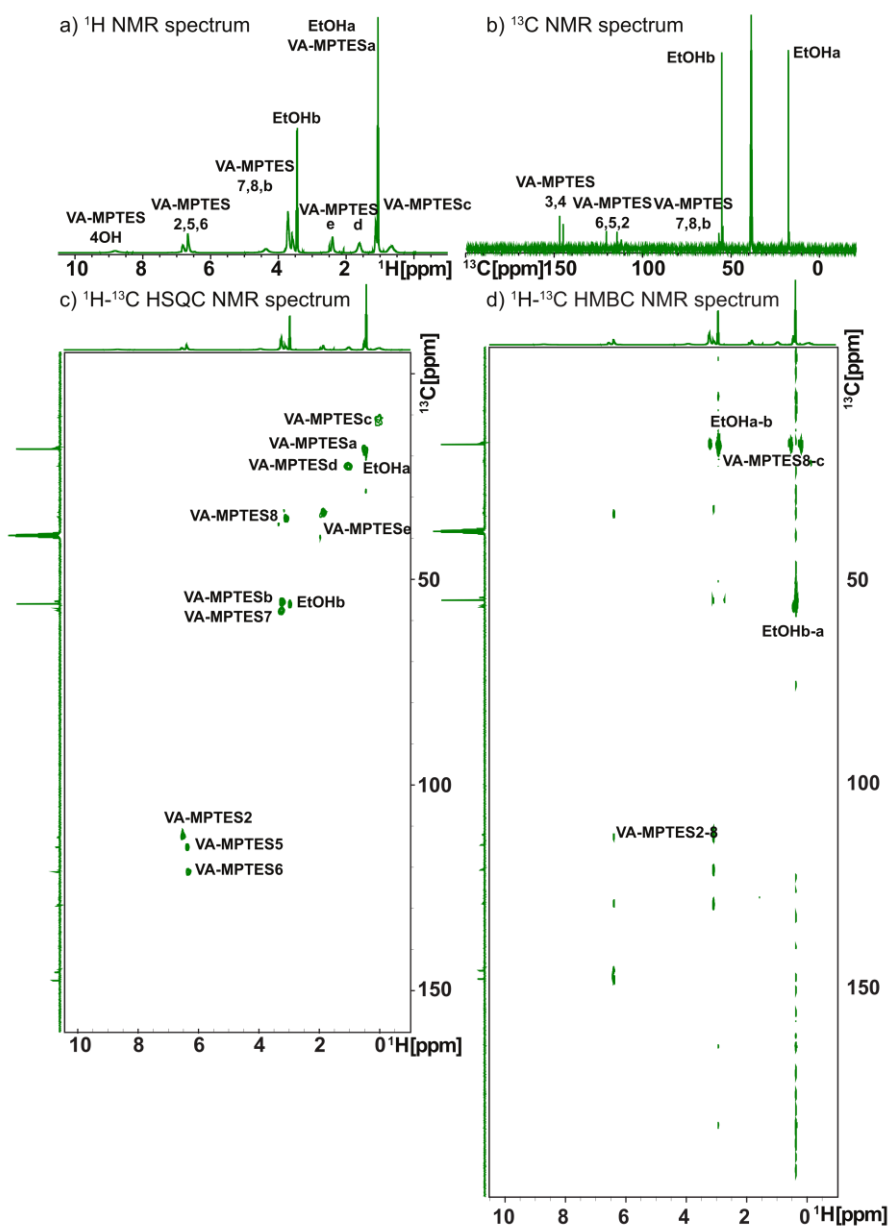
***Figure 5.11** One- and two-dimensional liquid-state NMR spectra resulting from the reaction of vanillyl alcohol (VA) with mercaptopropyltriethoxysilane (MPTES) at 160±5 °C [The hydrogen and carbon numbering is the same as in Figure 5.1. The peak assignments are provided in SI S1, (iii)]*

No clear leftovers of VA nor its derivatives at these temperatures could be observed, demonstrating a high selectivity towards MPTES and having an approximately quantitative conversion. Furthermore, the formation of free ethanol could be observed, corresponding to ~58 % of the total amount in the system (considering all the CH_2 protons at position b from MPTES or derivatives, which were integrated). All these observations indicate a high reactivity of MPTES towards VA. In addition, the observed broader spectral lines suggest the presence of large structural moieties. This was further assessed and confirmed by DOSY NMR (**Figure 5.12**), which reports the diffusivity of molecules in solution. It is possible to observe herein slow diffusing molecules that are incorporated in the coupled VA-MPTES structure, with a diffusion coefficient of ~5.8±1.1 x 10^{-11} m²/s, besides the fast diffusing ones, such as ethanol. The molecular weights of these structures are estimated to be between 11 and 35 kDa, based on the Stokes-Einstein equation.[9] This indicates oligomerized structure(s) of MPTES coupled to VA, as shown in **Scheme 5.3**.
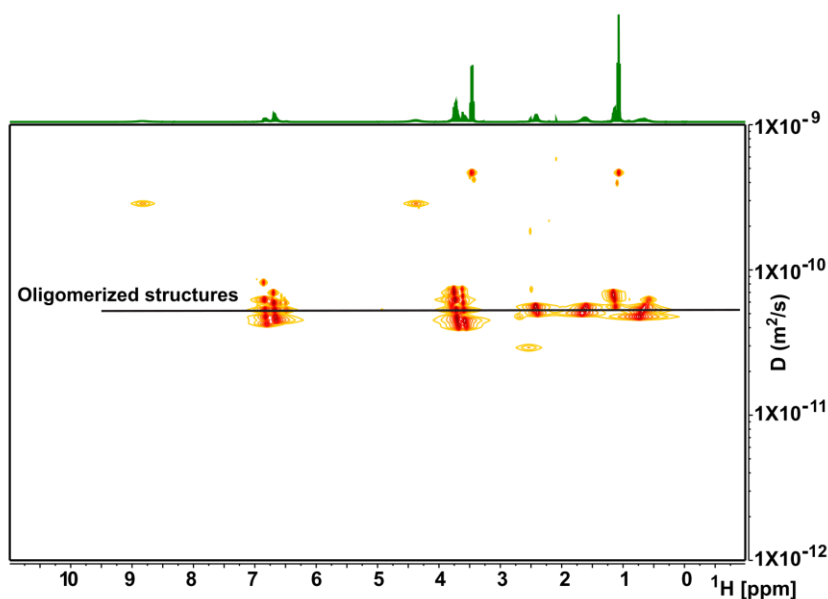
Figure 5.12 Diffusion Ordered Spectroscopy (DOSY) liquid-state NMR spectrum resulting from the reaction of vanillyl alcohol (VA) with MPTES at 160±5 °C

Scheme 5.3 depicts the oligomerized structure(s) of MPTES coupled to VA formed due to the condensation reaction of silanol or alkoxysilyl group. Alternatively, the condensation of VA molecules via etherification could have occurred; however, the respective structures were not identified in the spectra.

Scheme 5.3 Proposed reaction mechanism of vanillyl alcohol and MPTES at 160 °C
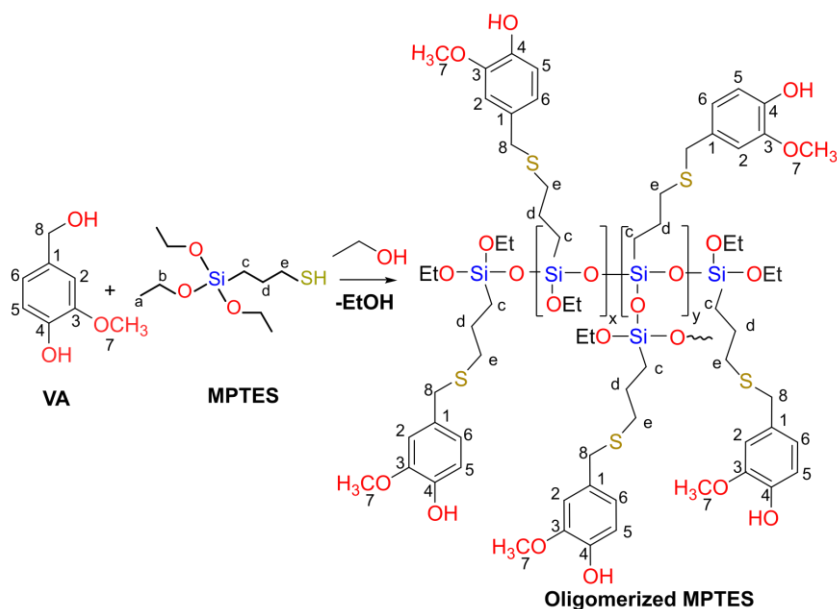
5.3.2.2.2 Reactivity study 2: lignin model, guaiacol, and different surface modifiers

Unlike VA, the study with the lignin model guaiacol did not show any reaction products with the modifiers, as shown in **Supporting information (SI) Figure S5.1 - S5.3**. **Table 5.4** summarizes the conversion of guaiacol in the presence of different surface modifiers. In the case of the reaction carried out with TMES, hydrolyzed TMES, i.e., trimethylsilanol (TMSOH) and the condensed TMES, hexamethyldisiloxane (HMDS) were identified in addition to the signals of G and TMES (see **SI, Figure S5.1**). Contrarily, hydrolyzed and condensed or oligomerized products of MPTES were not detected in the G+MPTES mixture (see **SI**, **Figures S5.3 and S5.4**). Overall, the investigations carried out with guaiacol emphasize that no reaction occurs between the selected functionalities, ethoxy (and/or generated silanol) and thiol, with the phenolic OH or any other reactive sites of the guaiacol molecule.

Table 5.4. Summarized estimations of the conversion of HTT Lignin Model (LM) substances: G or VA (labeled as LM), with different surface modifiers: TMES, HT, and MPTES (labeled as X). NI – Not Identifiable; LM8 –reaction occurring at carbon 1 of lignin model substances; OEt- ethanol

Products / Reactants	Remaining G (%)	Oxidized G (%)	Condensed G (%)	G1-X (%)	G1-OEt (%)
G+TMES	100	NI	NI	-	-
G+HT	100	NI	NI	-	-
G+MPTES	100	NI	NI	-	-

5.3.2.2.3 Elucidating the coupling reaction between the model lignin and different surface modifiers

For the model reaction carried out between guaiacol and the different modifiers, no reaction products could be identified. In the case of vanillyl alcohol and different modifiers, different reaction products were identified. The reaction of VA with surface modifiers occurs at the C8 position. This indicates that the presence of a hydroxymethyl in para-position to the phenolic -OH group is a prerequisite for the coupling reaction to occur. From these observations, the following reaction mechanism can be postulated using the concept of "hard" and "soft" electrophile-nucleophile chemistry (hard and soft acid and base concept).[23,24] Under the conditions of the used reaction, the vanillyl alcohol can be converted to electrophilic p-quinone methide intermediates (QM) by elimination of water,[15,18] as shown in **Scheme 5.4**.

Scheme 5.4 Proposed coupling mechanism of thiol to vanillyl alcohol. Heterolytic cleavage of vanillyl alcohol (VA) leading to quinone methide (QM) with subsequent rearrangement of the carbenium ions of QM followed by a thiol attack
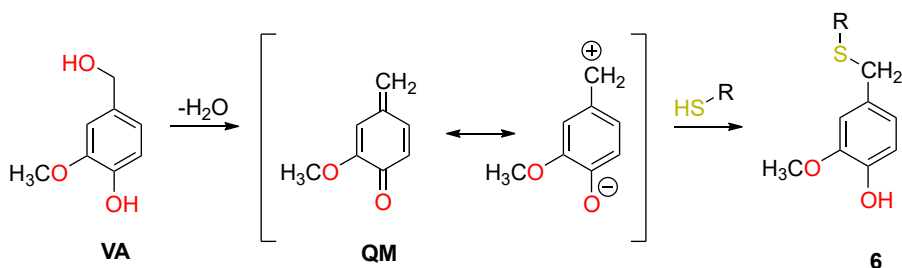
The highly reactive QM can undergo resonance stabilization, resulting in a polar zwitterion, which is susceptible to nucleophilic attack.[19,21] As QM and the resulting carbocation of the zwitterion are soft electrophiles, the reactivity of this reaction depends significantly on the chemical hardness/softness of the nucleophiles, as recognized

before.[19] Based on the experimental observations, the nucleophilic reactivity towards these QMs and/or the resulting carbocations of the zwitterion decreases in the following order:

-CH₂-SH (thiols) > -CH₂-OH (aliphatic hydroxy from another VA or ethanol) >> -Si-OH (silanols)

Thus, on the one hand, 1-hexanethiol, being a soft nucleophile, can undergo addition with QM, leading to a thioether formation (6, outlined in **Scheme 5.4**).[18-20] On the other hand, due to the comparatively lower polarizability of silanol groups under the given pH value, the reaction of TMES with QM is very slow and unfavorable in the presence of thiols and ethanol (the by-product of the silane hydrolysis) as shown in **Scheme 5.5**. Thus, TMES or MPTES do not react with VA via the silanol functionality, as demonstrated by the results of the VA/TMES and VA/MPTES experiments.

Scheme 5.5 Reaction products of vanillyl alcohol (VA) and trimethylethoxysilane (TMES) at 160 °C
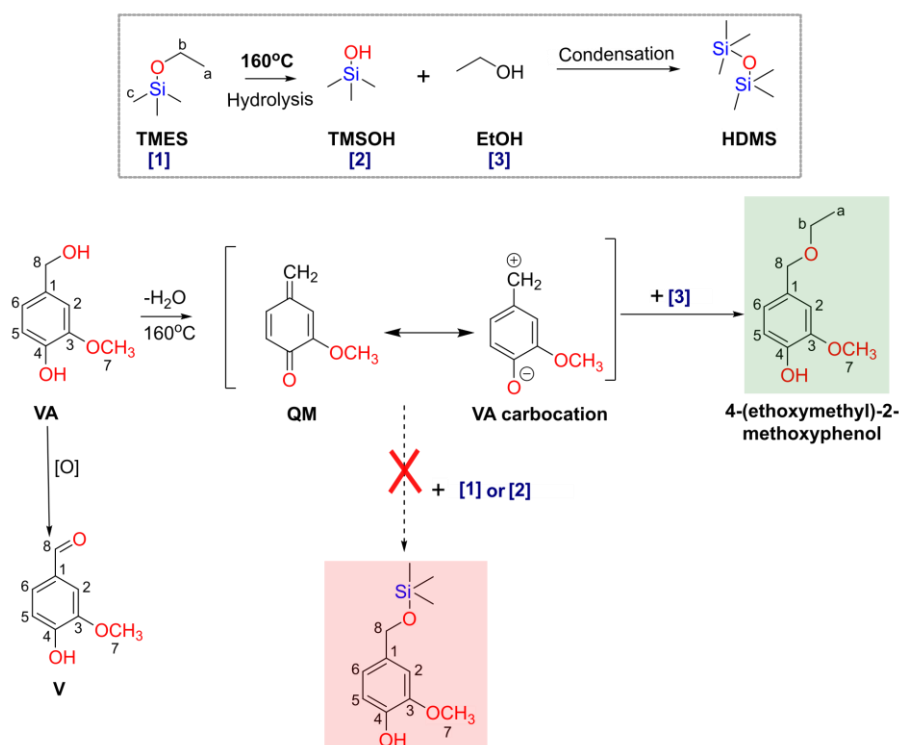
Though the proposed reaction scheme (**Scheme 5.4**) fits well with the results obtained, the formation of QM is still not confirmed. Further studies are required to prove this reaction pathway.

5.3.3 Unraveling the Coupling Mechanism of HTT lignin and Sulfur-bearing silanes

The ^{13}C NMR, ^{29}Si SSNMR, and all the liquid NMR data reveal that the thiol functionality plays a vital role in the coupling reaction with HTT lignin and its model substances. The data also demonstrates that both alkoxysilyl and silanol (hydrolyzed alkoxysilyl) functionalities of the silane are less reactive to VA or HTT lignin and are involved in the self-condensation reaction.[13] The occurrence of the coupling reaction via thiol and the self-condensation reaction of silane can be evidenced by the ^{13}C NMR of HT- (**Figure 5.3**) and ^{29}Si NMR of the MPTES-modified HTT lignin, respectively (**Figure 5.4, b**). Besides, the DOSY NMR spectra (**Figure 5.12**) of the model study carried out between VA and MPTES further confirm the formation of relatively large structures in the reaction product. This highlights that the reactivity of silane to HTT lignin is different. This is in contrast to the originally expected mechanism based on the silica-silane interaction, where (un)hydrolyzed alkoxysilyl groups are predominantly involved in the coupling reactions. Additionally, it is apparent from the model study that the thiol reacts with the benzylic carbon through a nucleophilic addition reaction (**Scheme 5.4**). Based on the proposed reaction pathway of the lignin model substances and thiol outlined in **Scheme 5.4**, the possible coupling reaction between HTT lignin and the silane, e.g., MPTES, is exemplified using **Scheme 5.6.** This involves the following reactions:

(a) A coupling reaction leading to a covalent thioether bond between HTT lignin and unblocked sulfur silanes: a result of the generation of quinone methide or a carbocation electrophile from the available benzylic hydroxy groups of the HTT lignin. Both favor a nucleophilic addition reaction with the thiol-functionalized silane.

(b) Condensation reaction between the (un)hydrolyzed silane grafted via the thiol functionality to the HTT lignin and another thiol-modified HTT lignin containing the (un)hydrolyzed silane molecule. Thus resulting in the clustering of HTT lignin particles.

In the case of silane hydrolysis followed by condensation, hydrolysis can occur either by the moisture available on the surface of HTT lignin (5 %) or by the water generated during the coupling reaction of HTT lignin with the thiol. These silanols can condense either with another silanol group or with an ethoxy silane already attached to the HTT lignin. It is unclear if the hydrolysis step occurs before, after, or parallel to the coupling reactions. For simplicity, it is assumed in **Scheme 5.6** that this reaction occurs after the coupling. It is to be noted that a direct condensation of silanes is also possible without a hydrolysis step.

Scheme 5.6 Coupling reaction hypothesis for HTT lignin-MPTES silane: (a) Benzylic hydroxy groups of HTT lignin favoring the addition of MPTES through the possible formation of quinone methide intermediate (which might be a concerted one); (b) Condensation of hydrolyzed silane leading to the formation of HTT lignin filler network
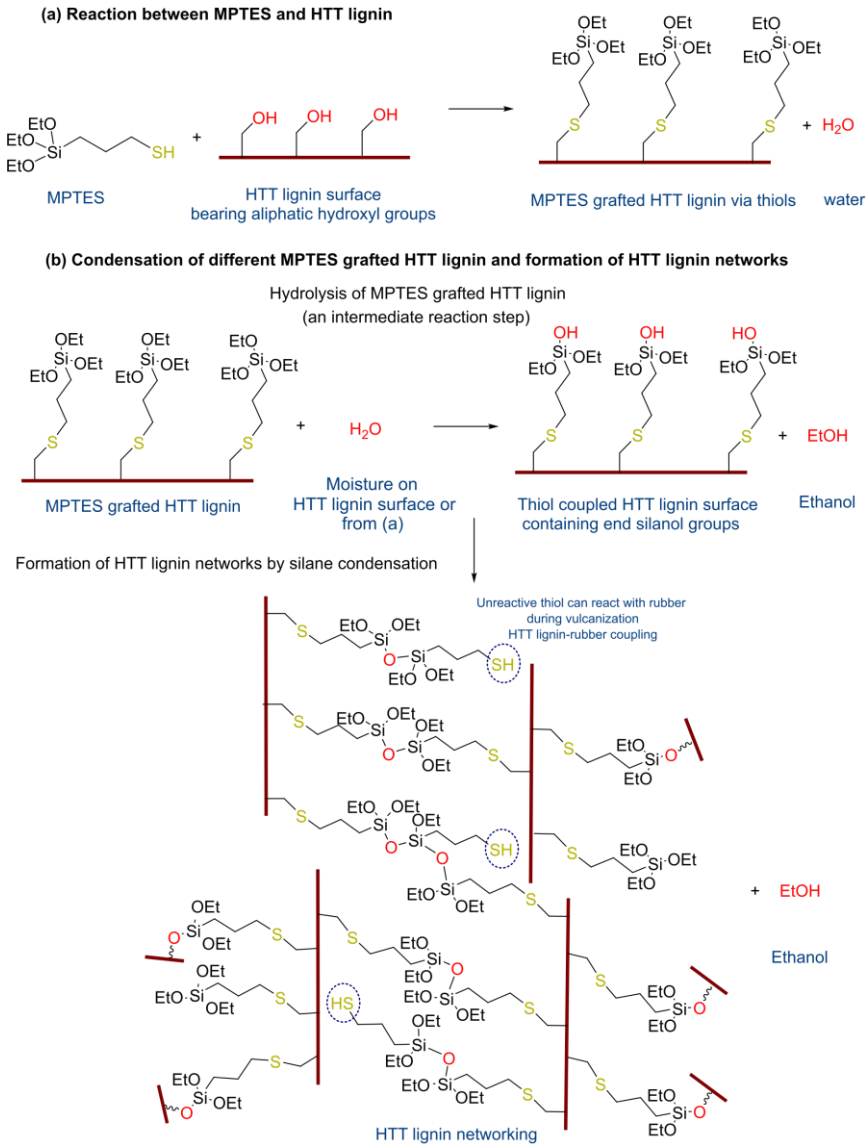
In earlier work, it was reported that both the quinone methide formation (which leads to the coupling) and the silane condensation (oligomerization of partially hydrolyzed and/or unhydrolyzed alkoxysilanes) reactions are highly favorable in a basic environment[14,18,25,26] This means that HTT lignin with a pH of 8.7 promotes both of the above-described reactions.

The proposed coupling scheme can be extended to the other silane-containing HTT lignin-filled rubber compounds. For the TESPT-HTT lignin-rubber system and the MPMEPS-HTT lignin-rubber system, reaction schemes are depicted in **Schemes 5.7 and 5.8**. This scheme fits very well with the experimental data discussed in **Chapter 4**: increased uncured Payne effect, high Mooney viscosity, improved mechanical properties, etc.[27] From the experiments, it is clear that the formation of HTT lignin cluster in TESPT and MPMEPS-modified HTT lignin arises due to the oligomerization of (un)hydrolyzed ethoxysilyl groups of the silane, and the enhanced mechanical properties originate from the grafting as a result of a chemical "thioether" bond formed between HTT lignin and the thiol groups of the silane. In the case of OTPTES, the observed inferior in-rubber properties (as presented in **Chapter 4**) are assumed to be due to the lack of coupling reaction between the filler and the silane. This could be caused by the presence of esterified sulfur (or blocked thiol) in the silane, which is not reactive to the HTT lignin. The de-esterification or deblocking reaction of OTPTES occurs mainly during the curing of the rubber compound, where the ester part of the molecule splits off and exposes the highly reactive monosulfane or thiol group. This reaction is thermally initiated and boosted by amine accelerators (e.g. diphenyl guanidine) in the rubber compound.[28] Thus, the presence of esterified sulfur in this silane hinders its coupling with HTT lignin during mixing and the subsequent condensation reaction, leading to the formation of a sponge-like filler structure (refer to **Chapter 4**, **Figure 4.5 b**).

In summary, the specific reactivity of silanes with determined reactive surface groups of the HTT lignin is the leading factor for the formation of sponge-like filler clusters, and it plays a vital role in the rubber reinforcement of HTT lignin filler. It is also to be noted that the coupling and condensation reaction varies depending on the silane type.

Scheme 5.7 Postulated coupling reaction between HTT lignin and TESPT silane and rubber: (1) possible decomposition of TESPT during mixing (the highly reactive species presented in the scheme can react with rubber/accelerators); (2) Possible formation of quinone methide intermediate; (3) Chemical coupling of silane to HTT lignin via the thiol/sulfide moiety; (4) Condensation of hydrolyzed silane leading to formation of sponge-like HTT lignin filler networks and coupling of rubber to HTT lignin via remaining thiol groups
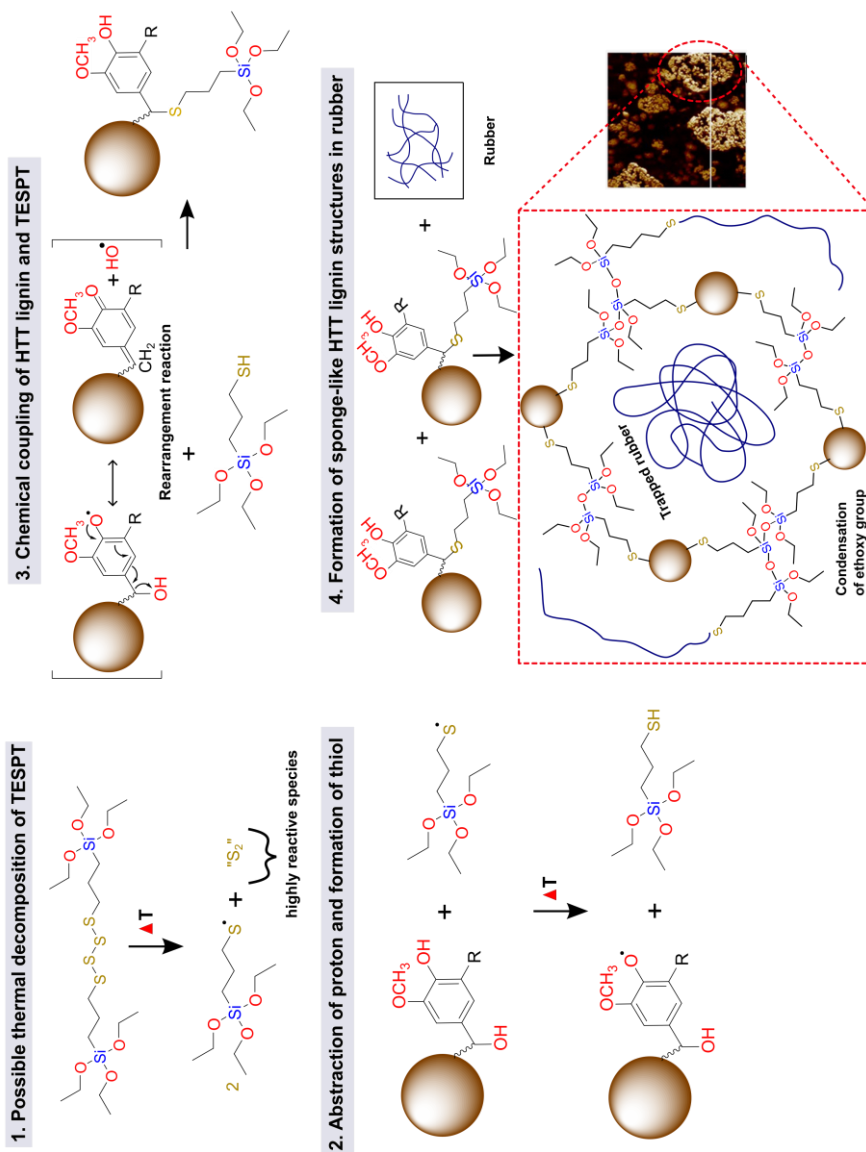
Scheme 5.8 Postulated mechanism of coupling between HTT lignin, MPMEPS, and rubber: (a) benzylic hydroxy groups of HTT lignin allowing the addition of MPMEPS free thiol group to the formed quinone methide intermediate; (b) Condensation of hydrolyzed silane leading to the formation of HTT lignin network and hypothesis of rubber-HTT lignin coupling via thiol groups
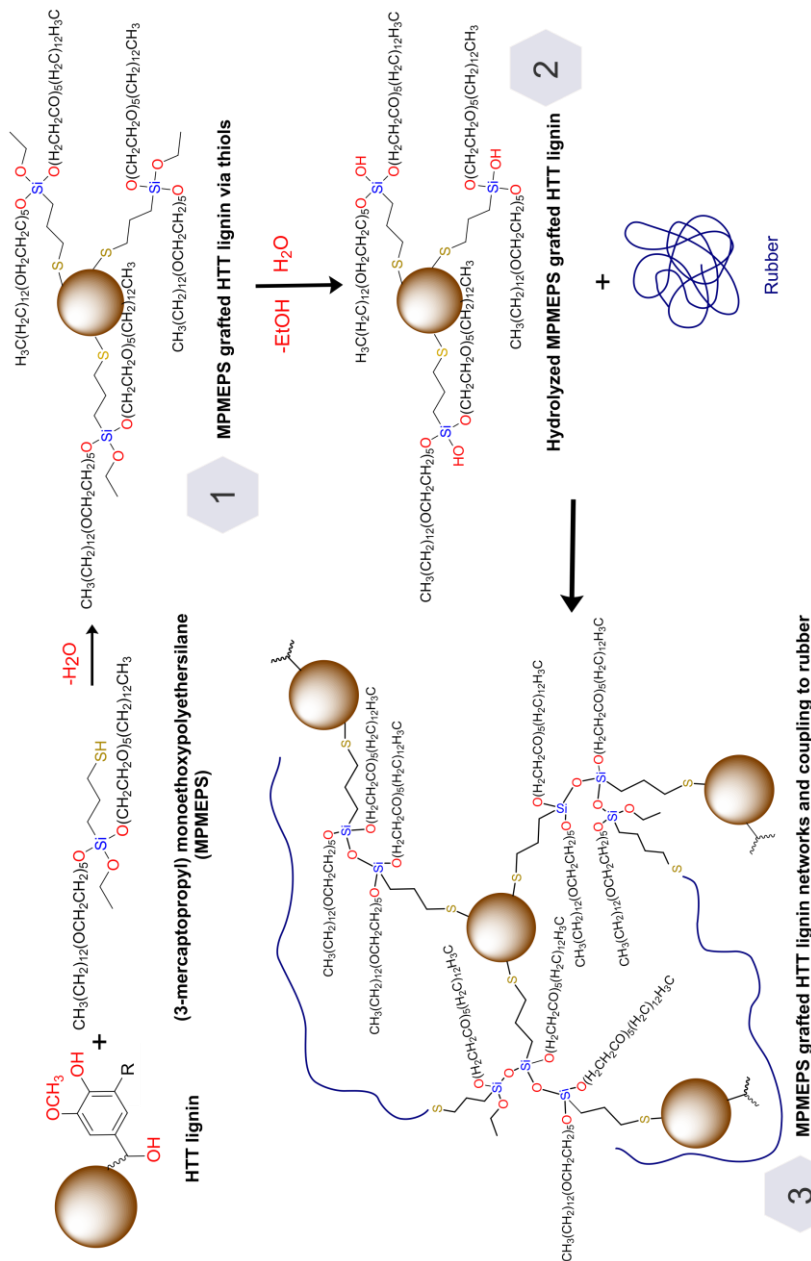
5.4 Conclusions

The possible coupling reaction between HTT lignin and different organosilane coupling agents was explored through parallel studies conducted with HTT lignin and its model substances (vanillyl alcohol and guaiacol) with different surface modifiers. A comprehensive NMR investigation of the different modified lignin model substances enabled a better understanding of the possible reactions between HTT lignin and the functional silanes selected for this study. From these studies, the following conclusions are derived:

(i) Silane is coupled to HTT lignin via the thiol functionality. Under the investigated conditions, the aliphatic hydroxy groups in the α-position on the aromatic ring, in combination with the para-hydroxy group of HTT lignin, are identified as pivotal moieties for the coupling reaction. Thus, HTT lignin and silane coupling results in a thioether covalent bond (-C-S-) rather than -Si-O-C interfacial bonds.

(ii) The (un)hydrolyzed alkoxysilyl groups of the silane are primarily involved in the self-condensation reaction rather than in the coupling reaction with the functional groups of HTT lignin. The former reaction is mainly responsible for the formation of sponge-like lignin clusters in reactive sulfur-silane-containing HTT lignin-filled rubber compounds. Furthermore, this condensation reaction creates siloxane (-Si-O-Si-) bonds within the rubber matrix.

Based on this gained knowledge, a new mechanistic model for sulfur silane and HTT lignin was proposed as the existing reaction mechanism of the silica-silane coupling model cannot be directly transferred to the current system. This unprecedented reaction model provided a straightforward explanation for the formation of sponge-like lignin textures in the TESPT silane-modified HTT lignin-filled rubber compound. It also justifies the previously obtained results for Mooney viscosity, uncured Payne effect, and mechanical properties of HTT lignin containing different sulfur silanes. In particular, the less reinforcing behavior of the OTPTES (NXT®) containing HTT lignin-filled rubber compound is due to the restriction in the coupling reactions. The findings also suggest that if an ethoxy-end chain-functionalized SSBR is used in a formulation, a filler-polymer coupling can be achieved to a lesser extent by condensation between ethoxy groups of silane and the end-chain-functionalized SSBR.

To summarize, the findings suggest that the clustering of HTT lignin can be prevented if triethoxysilyl groups are absent. Furthermore, it indicates that a molecule with thiol functionality can be utilized as a potential surface modifier for HTT lignin. However, the thiol functionality is also reactive to rubber. Thus, it is still unclear to which extent the thiol moieties participate in the coupling reaction with the filler and/or with the rubber. Further studies can be conducted to clarify this ambiguity and evaluate the potential of reinforcing the rubber using the HTT lignin-thiol system.

5

Supporting Information

S1 Peak Assignments for the reaction of vanillyl alcohol (VA) with different surface modifiers:

(i) Peak Assignments for VA-TMES heated at 160 °C:

^{1}H NMR (600 MHz, DMSO) δ 10.24 (s, 1H), 9.78 (s, 1H), 8.90 (s, 5H), 8.83 (s, 3H), 8.75 (s, 10H), 7.02 – 6.91 (m, 4H), 6.90 – 6.86 (m, 17H), 6.84 (d, J = 1.9 Hz, 4H), 6.79 – 6.63 (m, 48H), 5.29 (s, 3H), 4.99 (t, J = 5.7 Hz, 11H), 4.53 (s, 5H), 4.44 – 4.35 (m, 42H), 3.84 (s, 3H), 3.79 – 3.68 (m, 79H), 3.59 (q, J = 7.0 Hz, 12H), 3.46 (qd, J = 7.0, 4.9 Hz, 11H), 3.39 (s, 10H), 2.08 (s, 3H), 1.08 (dt, J = 19.8, 7.0 Hz, 34H), 0.18 (d, J = 3.3 Hz, 6H), 0.08 (d, J = 15.4 Hz, 84H).

^{13}C NMR (151 MHz, DMSO) δ 190.99, 147.48, 147.44, 147.41, 147.38, 146.01, 145.66, 145.33, 144.61, 144.53, 133.51, 132.64, 131.78, 129.34, 128.77, 126.10, 120.79, 120.59, 120.49, 119.39, 119.12, 115.43, 115.36, 115.33, 115.25, 115.16, 115.06, 112.86, 112.67, 112.10, 111.21, 111.06, 110.83, 110.71, 71.24, 64.06, 63.05, 57.41, 56.11, 55.71, 55.60, 55.58, 55.54, 55.51, 37.21, 18.58, 18.50, 2.01, 1.82.

(ii) Peak Assignments for VA-HT heated at 160 °C:

^{1}H NMR (400 MHz, DMSO) δ 8.85 (s, 1H) – **VA-HT4OH**, 6.86 (d, J = 1.8 Hz, 1H) – **VA-HT2**, 6.76 – 6.63 (m, 2H) – **VA-HT5,6**, 3.74 (s, 3H) – **VA-HT7**, 3.79 – 3.68 (m, 1H), 3.61 (s, 2H) – **VA-HT8**, 2.41 – 2.32 (m, 2H) – **VA-HTa**, 1.54 – 1.42 (m, 2H) – **VA-HTb**, 1.40 – 1.14 (m, 6H) – **VA-HTc,e,d**, 0.91 – 0.80 (m, 3H) – **VA-HTf**.

^{13}C NMR (101 MHz, DMSO) δ 147.45 – **VA-HT3**, 145.46 – **VA-HT4**, 129.25 – **VA-HT1**, 121.18 – **VA-HT2**, 120.86, 115.37, 115.14 – **VA-HT5**, 112.79 – **VA-HT6**, 55.70 – **V7**, 55.51 – **VA-HT7**, 38.04, 35.22 – **VA-HTd**, 33.46, 30.91 – **VA-HTa**, 30.82, 30.67, 28.80 – **VA-HTb**, 28.59, 28.03 – **VA-HTc**, 27.51, 23.85, 22.09 – **VA-HTe**, 13.89 – **VA-HTf**.

(iii) Peak Assignments for VA-MPTES heated at 160 °C:

^{1}H NMR (400 MHz, DMSO) δ 8.82 (s, 1H) – **VA-MPTES4OH**, 6.84 – 6.76 (m, 1H) – **VA-MPTES2**, 6.71 – 6.61 (m, 2H) – **VA-MPTES5,6**, 4.37 (s, 2H), 3.72 (s, 4H), 3.77 – 3.67 (m, 1H), 3.67 (s, 1H), 3.65 (s, 1H), 3.45 (q, J = 7.0 Hz, 4H) – **EtOHb**, 2.47 – 2.36 (m, 3H), 1.66 – 1.51 (m, 3H), 1.19 – 1.10 (m, 1H), 1.06 (t, J = 7.0 Hz, 6H) – **EtOHa**, 0.62 (s, 1H) – **VA-MPTESc**.

^{13}C NMR (101 MHz, DMSO) δ 147.48 – **VA-MPTES3**, 145.49 – **VA-MPTES4**, 145.46, 129.15 – **VA-MPTES1**, 121.16 – **VA-MPTES6**, 115.15 – **VA-MPTES5**, 112.72 – **VA-MPTES2**, 57.74 – **VA-MPTES7**, 57.68, 57.27, 56.12 – **EtOHb**, 55.71 – **VA-MPTESb**, 55.50, 35.09 – **VA-MPTES8**, 33.77 – **VA-MPTESe**, 22.60 – **VA-MPTESd**, 18.57 – **EtOHa**, 18.32, 18.22, 18.19 – **VA-MPTESa**, 10.51 – **VA-MPTESc**.

S2 Peak Assignments for the reaction of guaiacol (G) with different surface modifiers:

(i) G+TMES

^{1}H NMR (600 MHz, DMSO) δ 9.27 (s, 1H) – **G1OH**, 7.32 (m, 1H) – **G3**, 7.22 – 7.12 (m, 3H) – **G4,5,6**, 4.17 (s, 3H) – **G7**, 4.01 (q, J = 7.0 Hz, 2H) – **TMESb**, 1.52 (t, J = 7.0 Hz, 3H) – **TMESa**, 0.48 (s, 9H), 0.44 (s, 1H) – **TMESc**.

^{13}C NMR (151 MHz, DMSO) δ 147.65 – **G1**, 146.60 – **G2**, 121.95, 120.87 – **G5**, 120.73, 120.56, 119.12 – **G4**, 115.56 – **G6**, 112.46, 112.32 – **G3**, 57.36 – **G7**, 56.04, 55.51 – **TMESb**, 55.22, 30.64, 18.54, 18.45 – **TMESa**, 1.96, 1.78 – **TMSOHa**, 0.33, -0.18, -0.37 – **TMESc**.

(ii) G+HT

^{1}H NMR (400 MHz, DMSO) δ 8.86 (s, 1H) – **G1OH**, 6.94 – 6.84 (m, 1H) – **G3**, 6.82 – 6.68 (m, 3H) – **G4,5,6**, 3.75 (s, 3H) – **G7**, 2.46 (q, J = 7.4 Hz, 2H) – **HTa**, 2.18 – 2.06 (m, 1H), 1.60 – 1.46 (m, 2H) – **HTb**, 1.35 – 1.16 (m, 6H) – **HTc,d,e**, 0.86 (t, J = 6.9 Hz, 3H) – **HTf**.

^{13}C NMR (101 MHz, DMSO) δ 147.66 – **G1**, 146.62 – **G2**, 120.86 – **G5**, 119.11 – **G4**, 115.56 – **G6**, 112.27 – **G3**, 55.50 – **G7**, 33.43 – **HTb**, 30.79 – **HTd**, 27.49 – **HTc**, 23.82– **HTa**, 22.08 – **HTe**, 13.87 – **HTf**.

(iii) G+MPTES

^{1}H NMR (400 MHz, DMSO) δ 8.86 (s, 1H) – **G1OH**, 6.94 – 6.85 (m, 1H) – **G3**, 6.82 – 6.69 (m, 3H) – **G4,5,6**, 3.80 – 3.70 (m, 9H) – **MPTESb + G7**, 2.47 (t, J = 6.7 Hz, 2H) – **MPTESe**, 2.20 (d, J = 7.6 Hz, 1H), 1.66 – 1.54 (m, 2H) – **MPTESd**, 1.15 (t, J = 7.0 Hz, 9H) – **MPTESa**, 0.72 – 0.61 (m, 2H) – **MPTESc**.

^{13}C NMR (101 MHz, DMSO) δ 147.66 – **G1**, 146.62 – **G2**, 120.87 – **G5**, 119.12 – **G4**, 115.56 – **G6**, 112.29 – **G3**, 57.72 – **MPTESb**, 55.50 – **G7**, 27.33 – **MPTESd**, 26.82 – **MPTESe**, 18.18 – **MPTESa**, 9.03 – **MPTESc**.

5
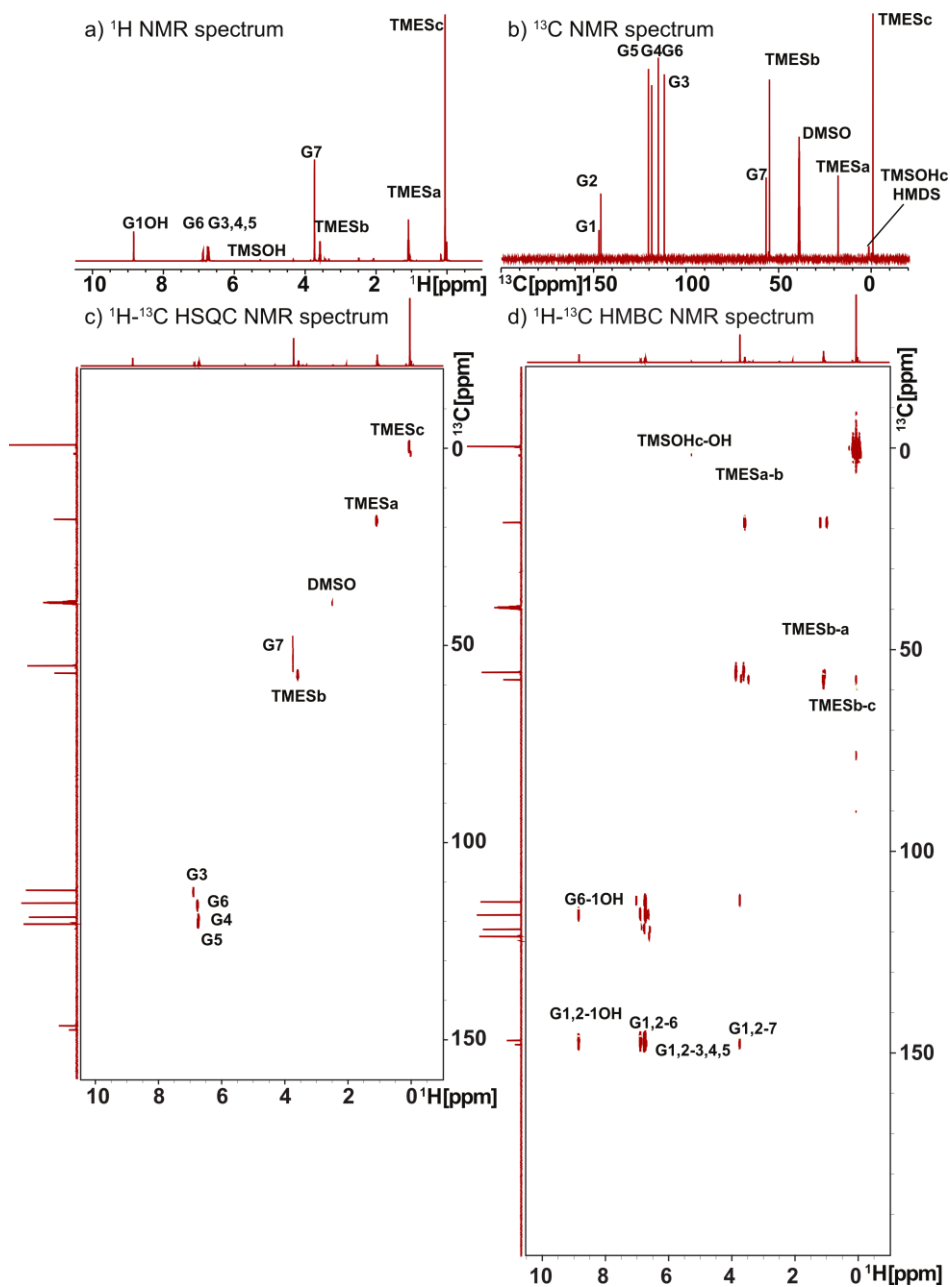
Figure S5.1 One- and two-dimensional liquid-state NMR spectra resulting from the reaction of guaiacol (G) with trimethylethoxysilane (TMES) at 160±5 °C [All data were acquired in DMSO-d6 at 14.1 T at room temperature]
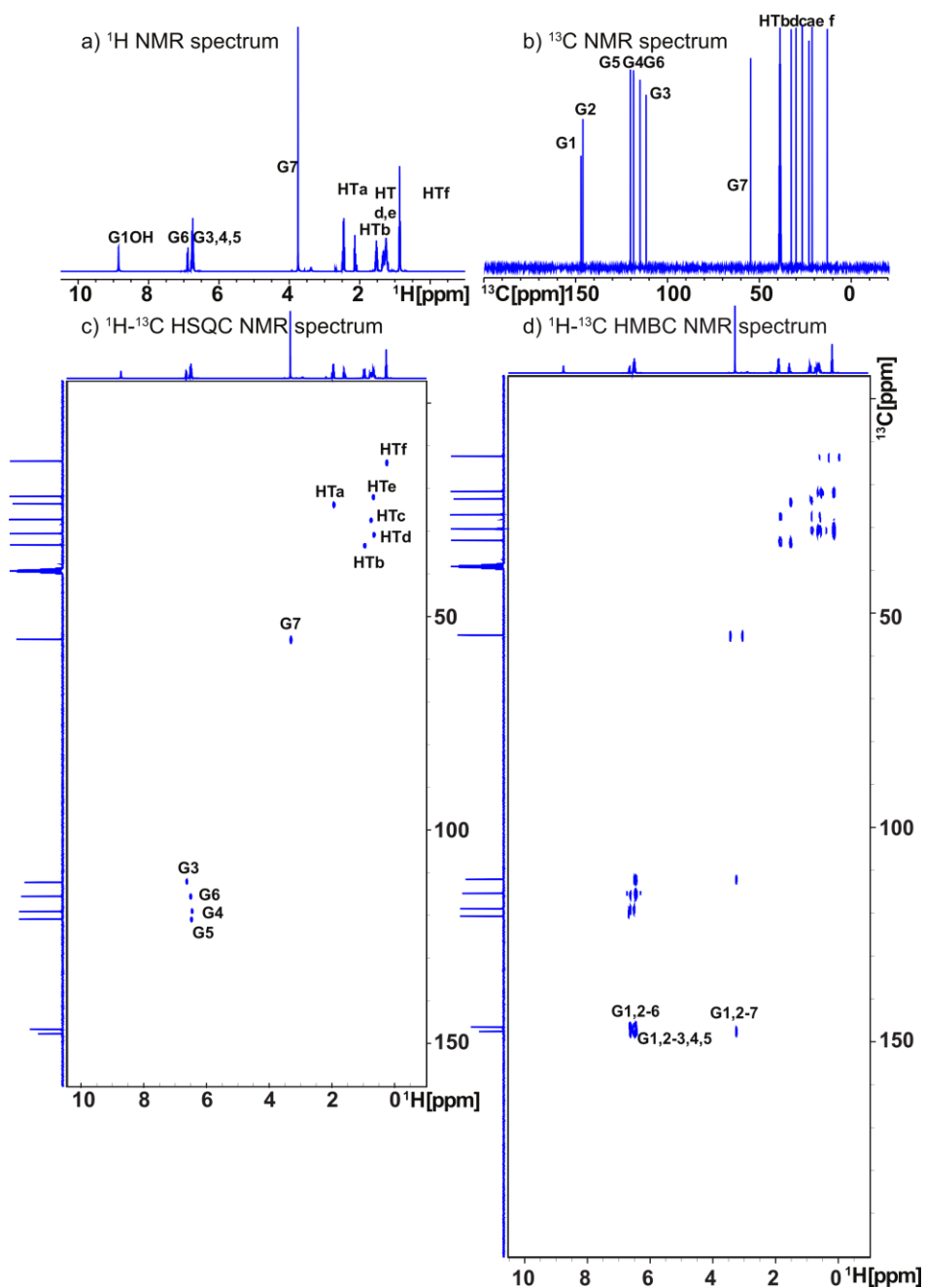
Figure S5.2 One- and two-dimensional liquid-state NMR spectra resulting from the reaction of guaiacol (G) with hexane thiol (HT) at 160±5 °C [All data were acquired in DMSO-d6 at 14.1 T at room temperature]
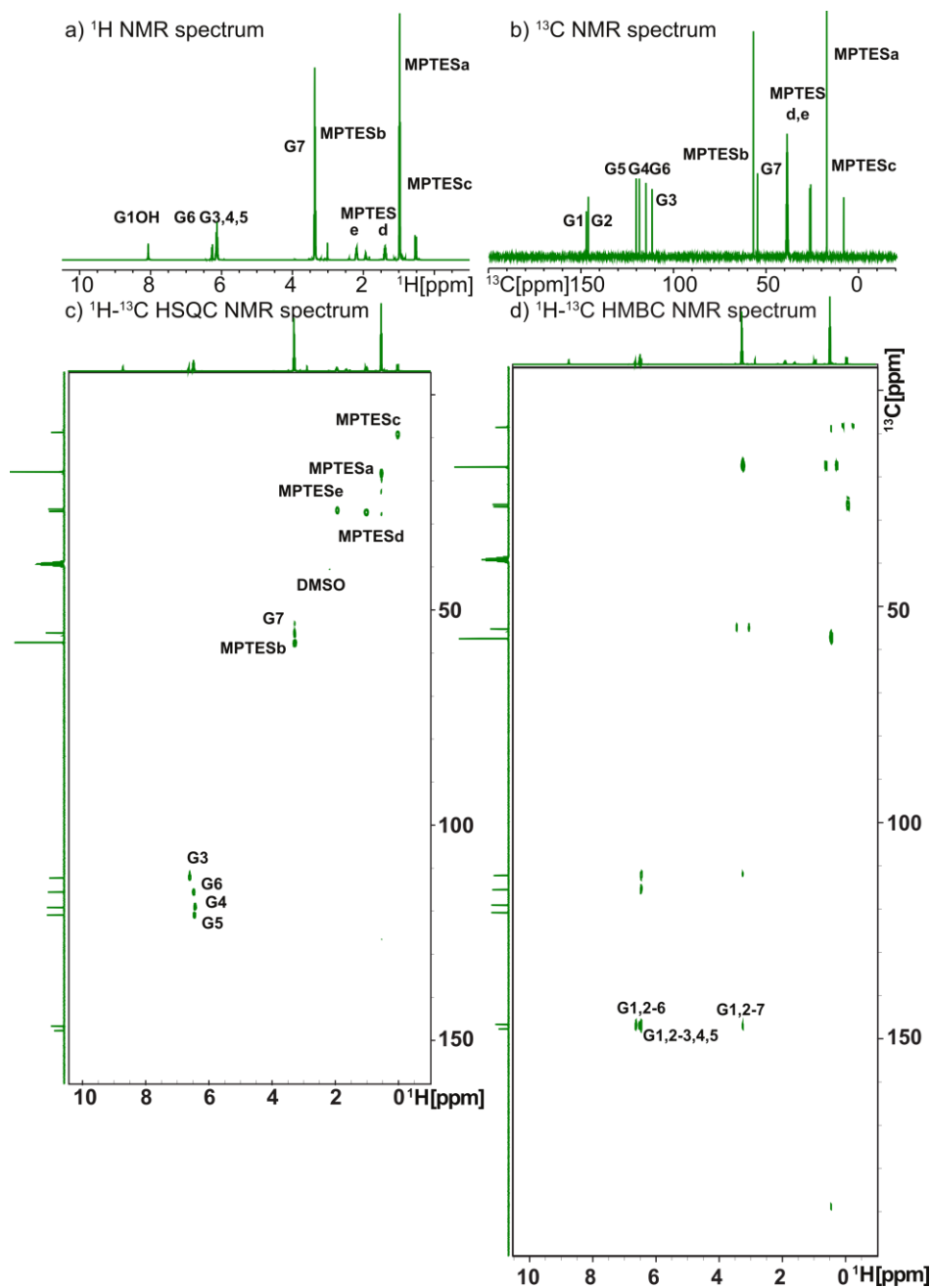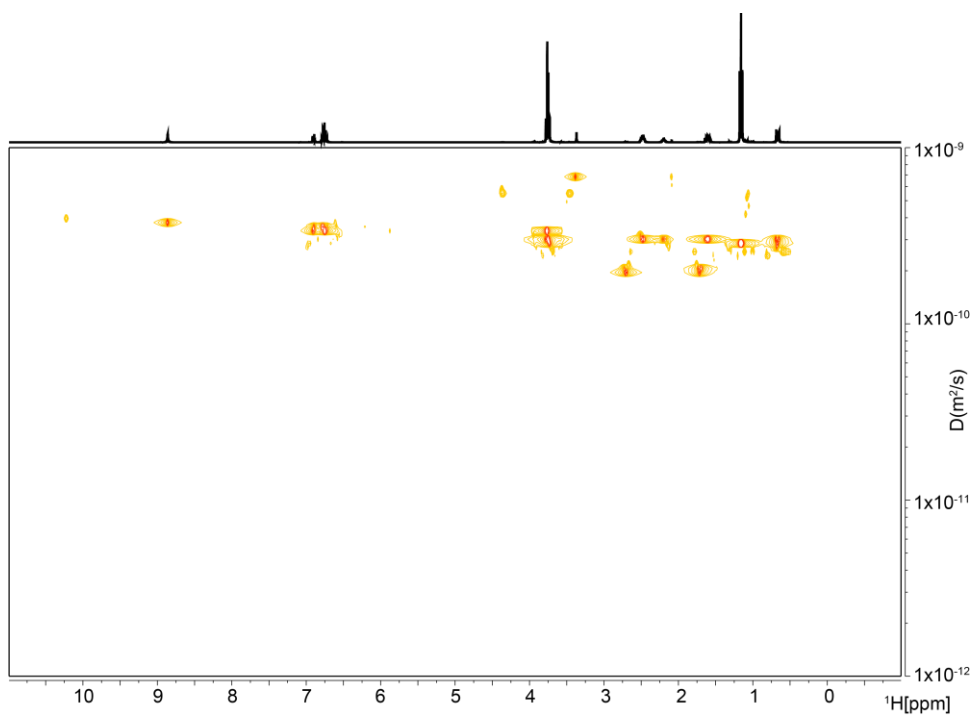
Figure S5.3 One- and two-dimensional liquid-state NMR spectra resulting from the reaction of guaiacol (G) with mercaptopropyltriethoxysilane (MPTES) at 160±5 °C [All data were acquired in DMSO-d6 at 14.1 T at room temperature]

Figure S5.4 Diffusion Ordered Spectroscopy (DOSY) liquid-state NMR spectrum resulting from the reaction of guaiacol (G) with MPTES at 160±5 °C [The data were acquired in DMSO-d₆ at 9.4 T at 25 °C]

5

References

(1)   Sekar, P.; Martinho, R. P.; Talma, A. G.; Gojzewski, H.; Stücker, A.; Schwaiger, B.; Podschun, J.; Blume, A. Horizons in Coupling of Sulfur-Bearing Silanes to Hydrothermally Treated Lignin toward Sustainable Development. ACS Sustainable Chem. Eng. 2023, 11 (48), 16882–16892.

(2)   Sengloyluan, K.; Sahakaro, K.; Dierkes, W. K.; Noordermeer, J. W. M. Reinforcement Efficiency of Silica in Dependence of Different Types of Silane Coupling Agents in Natural Rubber-Based Tire Compounds. KGK-Kautschuk und Gummi Kunststoffe 2016, 69 (5), 44–53.

(3)   Lee, G. M.; Yoo, J. W.; Lee, K. B. Enhancement of Dispersion of Silica Modified with a Silane Coupling Agent in a Rubber Composite. J. Chem. Eng. Japan 2014, 47 (2), 159–164.

(4)   Balakshin, M.; Capanema, E.; Santos, R.; Chang, H.-M.; Jameel, H. Structural Analysis of Hardwood Native Lignins by Quantitative 13C NMR Spectroscopy. Holzforschung 2015, 70.

(5)   Fulmer, G. R.; Miller, A. J. M.; Sherden, N. H.; Gottlieb, H. E.; Nudelman, A.; Stoltz, B. M.; Bercaw, J. E.; Goldberg, K. I. NMR Chemical Shifts of Trace Impurities: Common Laboratory Solvents, Organics, and Gases in Deuterated Solvents Relevant to the Organometallic Chemist. Organometallics 2010, 29 (9), 2176–2179.

(6)   Lee, W.; Tonelli, M.; Markley, J. L. NMRFAM-SPARKY: Enhanced Software for Biomolecular NMR Spectroscopy. Bioinformatics 2015, 31 (8), 1325–1327.

(7)   Spectral Database for Organic Compounds. https://sdbs.db.aist.go.jp (National Institute of Advanced Industrial Science and Technology) (accessed 2022-09-01).

(8)   Wu, D. H.; Chen, A. D.; Johnson, C. S. An Improved Diffusion-Ordered Spectroscopy Experiment Incorporating Bipolar-Gradient Pulses. Journal of Magnetic Resonance, Series A 1995, 115 (2), 260–264.

(9)   Li, W.; Chung, H.; Daeffler, C.; Johnson, J. A.; Grubbs, R. H. Application of 1H DOSY for Facile Measurement of Polymer Molecular Weights. Macromolecules 2012, 45 (24), 9595–9603.

(10) Baccile, N.; Laurent, G.; Babonneau, F.; Fayon, F.; Titirici, M.-M.; Antonietti, M. Structural Characterization of Hydrothermal Carbon Spheres by Advanced Solid-State MAS 13C NMR Investigations. J. Phys. Chem. C 2009, 113 (22), 9644–9654.

(11) Calucci, L.; Rasse, D. P.; Forte, C. Solid-State Nuclear Magnetic Resonance Characterization of Chars Obtained from Hydrothermal Carbonization of Corncob and Miscanthus. Energy Fuels 2013, 27 (1), 303–309.

(12) Peeters, M. P. J.; Wakelkamp, W. J. J.; Kentgens, A. P. M. A 29Si Solid-State Magic Angle Spinning Nuclear Magnetic Resonance Study of TEOS-Based Hybrid Materials. Journal of Non-Crystalline Solids 1995, 189 (1), 77–89.

(13) Brochier Salon, M.-C.; Belgacem, M. N. Hydrolysis-Condensation Kinetics of Different Silane Coupling Agents. Phosphorus, Sulfur, and Silicon and the Related Elements 2011, 186 (2), 240–254.

(14) Hemmingson, J. A.; Leary, G. The Self-Condensation Reactions of the Lignin Model Compounds, Vanillyl and Veratryl Alcohol. Aust. J. Chem. 1980, 33 (4), 917–925.

(15) Komatsu, T.; Yokoyama, T. Revisiting the Condensation Reaction of Lignin in Alkaline Pulping with Quantitativity Part I: The Simplest Condensation between Vanillyl Alcohol and Creosol under Soda Cooking Conditions. Journal of Wood Science 2021, 67 (1), 45–57.

5

(16) Shevchenko, S. M.; Apushkinsky, A. G.; Zarubin, M. Y. On Regioselectivity of the Reaction of P-Quinone Methides with p-Hydroxybenzyl Alcohols. Wood Sci.Technol. 1992, 26 (5), 383–392.

(17) Lahtinen, M.; Heinonen, P.; Oivanen, M.; Karhunen, P.; Kruus, K.; Sipilä, J. On the Factors Affecting Product Distribution in Laccase-Catalyzed Oxidation of a Lignin Model Compound Vanillyl Alcohol: Experimental and Computational Evaluation. Org. Biomol. Chem. 2013, 11 (33), 5454–5464.

(18) Leary, G. J. Quinone Methides and the Structure of Lignin. Wood Sci. Technol. 1980, 14 (1), 21–34.

(19) Coles, B. Effects of Modifying Structure on Electrophilic Reactions with Biological Nucleophiles. Drug Metab Rev 1984, 15 (7), 1307–1334.

(20) Bolton, J. L.; Turnipseed, S. B.; Thompson, J. A. Influence of Quinone Methide Reactivity on the Alkylation of Thiol and Amino Groups in Proteins: Studies Utilizing Amino Acid and Peptide Models. Chemico-Biological Interactions 1997, 107 (3), 185–200.

(21) Toteva, M. M.; Richard, J. P. The Generation and Reactions of Quinone Methides. Adv Phys Org Chem 2011, 45, 39–91.

(22) Ferrandin-Schoffel, N.; Haouas, M.; Martineau-Corcos, C.; Fichet, O.; Dupont, A.-L. Modeling the Reactivity of Aged Paper with Aminoalkylalkoxysilanes as Strengthening and Deacidification Agents. ACS Appl. Polym. Mater. 2020, 2 (5), 1943–1953.

(23) Pearson, R. G. Hard and Soft Acids and Bases—the Evolution of a Chemical Concept. Coordination Chemistry Reviews 1990, 100, 403–425.

(24) LoPachin, R. M.; Geohagen, B. C.; Nordstroem, L. U. Mechanisms of Soft and Hard Electrophile Toxicities. Toxicology 2019, 418, 62–69.

(25) Arkles, B.; Steinmetz, J.; Zazyczny, J.; Mehta, P. Factors Contributing to the Stability of Alkoxysilanes in Aqueous Solution. Journal of Adhesion Science and Technology 1992, 6, 193–206.

(26) Brinker, C. J. Hydrolysis and Condensation of Silicates: Effects on Structure. Journal of Non-Crystalline Solids 1988, 100 (1–3), 31–50.

(27) Sekar, P.; Noordermeer, J. W. M.; Anyszka, R.; Gojzewski, H.; Podschun, J.; Blume, A. Hydrothermally Treated Lignin as a Sustainable Biobased Filler for Rubber Compounds. ACS Appl. Polym. Mater. 2023, 5 (4), 2501–2512.

(28) Sato, M. Reinforcing Mechanisms of Silica / Sulfide-Silane vs. Mercapto-Silane Filled Tire Tread Compounds. PhD Thesis, University of Twente, The Netherlands, 2018.

5

5

6. Investigation of Thiols as a Potential Surface Modifier for Hydrothermally Treated Lignin
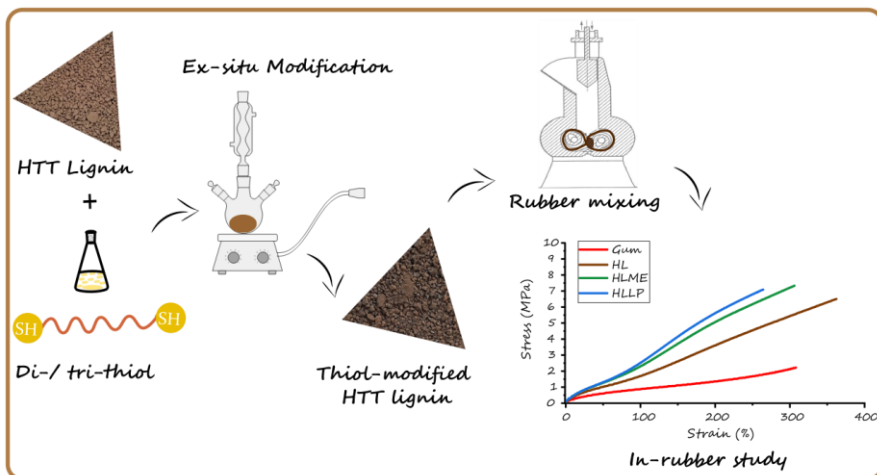
A Feasibility Study on the Reinforcing Behavior of Thiol-modified Hydrothermally Treated (HTT) Lignin

In the present chapter, two different thiol-containing molecules, 1,2-bis(2- mercaptoethoxy) ethane and a liquid polysulfide polymer with thiol end groups, were investigated as surface modifiers for HTT lignin to improve its compatibility with non-polar rubbers. An ex-situ modification was carried out, and the impact of the modified HTT lignins on the processability, cure, and mechanical properties of the solution styrene butadiene rubber was studied in comparison to carbon black N330 and the unmodified HTT lignin. The thiol-modified lignins showed pronounced improvement in the curing and mechanical properties of solution styrene butadiene rubber compared to the unmodified one. The results revealed that the thiol modification effectively modified the surface of HTT lignin, contributing to better compatibility between the filler and rubber. The tensile properties of both the thiol-modified HTT lignins are still lower than the reinforcing carbon black, indicative of a lower degree of polymer-filler interaction.

6

6.1 Introduction

The application of the hydrothermally treated (HTT) lignin with a BET specific surface area of 37 m²/g, along with reactive sulfur-containing silane modifiers such as bis(triethoxysilyl)propyl tetrasulfide (TESPT), improves the mechanical properties of solution styrene butadiene/butadiene rubber blend. This is attributed to the combined effect of (i) the chemical coupling established between TESPT and HTT lignin and (ii) the trapped rubber within the clusters of HTT lignin particles, as discussed in **Chapter 5**. However, the resulting in-rubber properties are relatively lower than those of the rubber compounds filled with reinforcing carbon black and silica. It is supposed that it is observed due to the inferior micro-dispersion of HTT lignin particles caused by the condensation of the triethoxysilyl groups of TESPT that are grafted to the HTT lignin surface, as depicted in **Chapter 5, Scheme 5.7**. This ultimately limits the enhancement of mechanical properties in a TESPT-HTT lignin-filled rubber, as achieving optimal filler dispersion is one of the crucial parameters in obtaining desired in-rubber properties for end-use applications.[1,2] To address the dispersion issues caused by silane coupling agents containing reactive sulfur or thiol groups and to simultaneously improve the compatibility of HTT lignin with rubber, an alkoxysilyl-free modifier can be utilized. Thus, the present study aims to investigate a surface modifier with thiol "-SH" functionality, which demonstrated reactivity towards HTT lignin at 160 °C, as outlined in **Chapter 5**. However, the thiol functionality can already react with the vinyl groups of the rubber (and to a lesser extent to the cis-double bonds) at 90 °C.[3] This introduces uncertainty regarding the extent to which thiol moieties participate in coupling with the HTT lignin filler and/or with the rubber. To understand the reactivity between the thiol and HTT lignin at 90 °C, a model kinetic study was conducted between vanillyl alcohol (VA) and hexane thiol (HT) by varying time ranging between 0 and 60 minutes. The ¹³C NMR results (presented in **Supporting Information (SI)**, **Figure S6.1**) demonstrate that the peaks corresponding to VA-thiol coupling appeared only around 60 minutes, indicating a slow reactivity between thiol and VA at 90 °C. Therefore, an ex-situ type of modification (outside the mixer without rubber and other ingredients) was carried out using two different thiol-based coupling agents, as listed below:

(a) 1,2-Bis(2-mercaptoethoxy)ethane (MEE), a molecule containing two free -SH functionalities, where thiol functionalities can react with HTT lignin and/or with rubber. The thiol functionalities are highlighted in yellow in **Figure 6.1 (a)**.

(b) Liquid polysulfide polymer with thiol end groups (LPST), a molecule containing one -SH at each alkyl chain end (highlighted in yellow in **Figure 6.1, (b)**) and disulfides in its main chain (highlighted in pink in **Figure 6.1, (b)**), where the thiol groups are expected to react with HTT lignin and/or rubber, and the disulfides can participate in rubber vulcanization and can chemically couple the lignin to rubber.
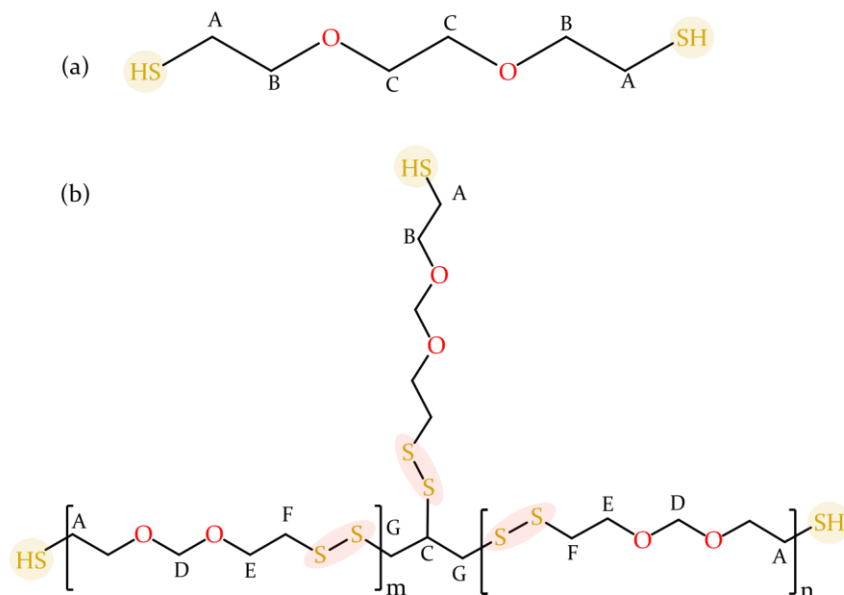
Figure 6.1. Chemical structures of the selected thiols: (a) 1,2-bis(2-mercaptoethoxy) ethane (MEE); and (b) liquid polysulfide polymer with thiol end groups (LPST), where m + n = 4.3 [The capital letters represent the different carbons of the thiols]

This approach is assumed to avoid any reaction between the modifier and rubber during mixing and can increase the coupling yield between HTT lignin and thiol. In order to facilitate the coupling between HTT lignin and rubber, an appropriate temperature has to be selected for modification. While a lower temperature of 90 °C yields lower reactivity of thiol to VA, a higher temperature of 160 °C leads to increased reactivity. Therefore, a moderate temperature of 110 °C was chosen for thiol-HTT lignin modification.

Prior to the in-rubber study, the thiol-modified HTT lignins were characterized using ^{13}C NMR and DRIFTS to confirm the reaction between thiol and the HTT lignin. Sulfur elemental analysis was also performed to validate the reaction. Furthermore, the effect of thiol modification on the thermal properties of HTT lignin was analyzed. Finally, the reinforcing behavior of the prepared thiol-modified HTT lignins was investigated in non-polar solution styrene butadiene rubber (SSBR) and was compared with unmodified HTT lignin and the commercially available reinforcing carbon black N330.

6.2 Experimental Section

6.2.1 Materials

Solution-SBR (SPRINTAN® SLR 4601) with 21 wt.% styrene and 62 wt.% vinyl-butadiene content was used, as obtained from Synthos Deutschland GmbH, Schkopau. HTT lignin with a BET specific surface area of 47 m²/g and a specific density of 1.35 g/cm³, and an average particle size (d50) of 1.1 µm determined at 12000 Ws by static light scattering was provided by SunCoal Industries GmbH, Germany. Further, the amount of surface-accessible acidic hydroxy groups of the HTT lignin was specified by the supplier as 0.32 mmol/g. Carbon black N330 (CB) with a BET specific surface area of 78 m²/g and a specific density of 1.8 g/cm³ was provided by Orion Engineered Carbon. 1,2-Bis(2-mercaptoethoxy) ethane (MEE) was purchased from Sigma-Aldrich Chemie, Germany. The liquid polysulfide polymer with thiol end groups, LPST (Thioplast® G44, M_n- 1016 g/mol), was provided by Nouryon Polymer Specialities, Germany. The treated Distillate Aromatic Extract (TDAE) oil, VIVATEC®500, was supplied by Hansen & Rosenthal KG, Germany, and used as processing oil. The vulcanization/cure activators zinc oxide (ZnO) and stearic acid (SA), curing agent: sulfur-containing 1 wt.% of mineral oil (S) and accelerators, N-tert-butyl-2-benzothiazolesulfenamide (TBBS) and tetrabenzylthiuramdisulfide (TBzTD) were purchased from Sigma-Aldrich Chemie, Germany. Deuterated chloroform (CDCl₃; anhydrous, ≥ 99.8 atom % D) and deuterated dimethyl sulfoxide (DMSO-d6; anhydrous, 99.9 atom % D) were purchased from Merck Chemicals, Netherlands.

6.2.2 Preparation of thiol-modified HTT lignins using the selected thiols and their characterization

6.2.2.1 Ex-situ modification protocol for thiol-modified HTT lignin

As stated in **Chapter 5**, the coupling of thiol to HTT lignin is proposed to occur via the formation of a quinone methide, which requires 4-(hydroxymethyl)phenol structures (i.e., a hydroxy group in the α-position on the aromatic ring in combination with the para-hydroxy group). Therefore, the amount of thiol modifier needed for surface modification depends on the quantity of these structures in the HTT lignin. Since distinctly quantifying these structures in HTT lignin was challenging, for this first study, the amount of thiol modifier was taken solely based on the contents of the available surface-accessible acidic hydroxy (-OH) groups provided by the supplier. It is assumed that these -OH groups are part of the 4-(hydroxymethyl)phenol structures present in HTT lignin and that the amount of thiol modifier applied would adequately cover the hydroxy groups of HTT lignin. For the surface modification, the number of thiols (-SH) was taken equivalent to the surface accessible acidic OH groups of HTT lignin (i.e., the molar ratio of -OH to -SH is around one). Considering the different numbers of -SH groups per molecule in the two selected modifiers, the quantity of MEE and LPST was taken 1/2 and 1/3 of moles of -OH

of HTT lignin, respectively, to compare the hydrophobation effects. **Table 6.1** presents the quantities of filler and thiol used for the modification reaction.

Table 6.1 Quantity of thiols and HTT lignin taken for ex-situ modification

Description	MEE	LPST
Molecular weight (g/mol)	182.30	1016
No. of -SH functionalities in the modifier	2	3
Amount of HTT lignin used for modification (g)	40	40
Amount of surface accessible -OH groups in HTT lignin (mmol)	12.80	12.80
Amount of thiol modifier used for modification*(mmol)	6.42	4.26
Amount of thiol modifier used for modification (g)	1.17	4.33
Obtained variant	HLM	HLLP

*Thiol equimolar to surface accessible hydroxy groups of HTT lignin (0.32 mmol/g) and thiol equivalent

6

The thiol modification of HTT lignin was performed by suspending the desired quantity of the filler (40 g) in 100 ml toluene in a round-bottomed flask equipped with a magnetic stirrer, a thermometer, and a condenser unit. This mixture was heated to 110 °C. The desired quantity of thiol was added, and the reaction mixture was heated under reflux for 1 h. The resulting mixture was transferred to a Soxhlet apparatus to extract unreacted thiol modifiers (MEE/LPST) and possible reaction by-products using toluene for 12 h. After extraction, the obtained products were dried in an oven under vacuum at a temperature of 80 °C for 24 h. The modified HTT lignins (HLM and HLLP) that were obtained were characterized and used for the rubber study.

6.2.2.2 Characterization of the thiol-modified HTT lignins

The thermogravimetric analysis (TGA) was carried out using a TGA 550 analyzer, TA Instruments. About 5 - 10 mg of the respective modified and unmodified lignin sample was weighed in a tared platinum pan for the measurement. The oven was first programmed isothermally at 30 °C for 10 mins, followed by gradient heating from 30 to 600 °C at a rate of 15 °C/min. The samples were measured under a nitrogen (N_2) atmosphere set at a flow rate of 20 mL/min. Three replicates for each sample were done to check the repeatability of the measurement. As the replicate deviation was minimal, a representative weight loss (thermogravimetric, TGA) and its first derivative (DTGA) curve

were selected and used. In addition to the modified as well as unmodified lignin samples, the thermal degradation behavior of pure MEE and LPST was also analyzed by setting the oven to a gradient heating program, starting from room temperature to 600 °C at the heating rate of 15 °C/min under N_2 atmosphere.

Elemental sulfur was determined according to DIN 51724-3 (Method A: Combustion process) using a LECO SC 832 analyzer. Approximately 300 - 400 mg of the sample was weighed in a glazed porcelain boat and placed in the furnace heated to > 1250±25 °C with an oxygen-rich environment. By burning the sample in an oxygen carrier furnace, the carbon, sulfur, and hydrogen in the sample were converted to oxides of carbon (CO, CO2), sulfur dioxide (SO2), and moisture (H_2O), respectively. Subsequently, the gaseous combustion products flow through anhydrone tubes, where moisture is extracted from them. The remaining purified gas stream concentration was detected separately by a non-dispersive infrared (NDIR) detector. The control software evaluates the sulfur amount from the detected SO_2 concentration and uses samples' calibration data with known composition.

The DRIFT measurement of the un- and thiol-modified HTT lignins was performed according to the procedure described in **Chapter 3 under section 3.2.2.2**. All DRIFT spectra were normalized according to the aromatic skeleton vibration band of lignin at 1600 cm^{-1}. The measurement was repeated three times for each sample. In addition to these lignin spectra, the FTIR spectra of pure MEE and LPST were recorded using an Attenuated Total Reflection (ATR) unit in the range 4000 to 600 cm^{-1} and averaged over 16 scans, using a resolution of 4 cm^{-1} on a Thermo Fisher Scientific Nicolet 8700 spectrometer equipped with a deuterated triglycine sulfate (DTGS) detector. Baseline correction and normalization procedures were performed on the spectra using the Spectrum software.

The solid-state ^{13}C NMR of the thiol-modified HTT lignins was performed according to the protocol described in **Chapter 3, section 3.2.2.2**. The liquid ^{13}C NMR of pure MEE was carried out in deuterated chloroform ($CDCl_3$) to identify its characteristic peaks, according to the procedure described in **Chapter 5, section 5.2.3.3**. In the case of LPST, the liquid ^{13}C NMR measurement was performed in deuterated dimethyl sulfoxide (DMSO-d6) using an identical protocol described in **Chapter 5, section 5.2.3.3**.

The specific surface area (SSA) measurement of thiol-modified HTT lignins was determined by multi-point Brunauer-Emmett-Teller (BET) procedure using a 3P meso BK222 surface analyzer. Before the measurement, the samples were degassed at 150 °C for 2 h under vacuum to remove any physically adsorbed substances from the surface like water molecules. The nitrogen adsorption/desorption isotherms of the degassed samples were obtained at a set temperature of –196.15 °C and with different pressures. The measurement was repeated three times, and the average was reported.

6

6.2.3 Preparation of rubber compounds and characterization techniques

6.2.3.1 Mixing protocol for the unfilled and different filled SSBR compounds

A simplified rubber formulation without a blend system and anti-degradants, as described in **Table 6.2**, was used in this study.

Table 6.2 Formulation for the compound studies (Amounts in parts per 100 rubber (phr))

	Ingredients	UFR[a]	CBR[b]	HLR[c]	HLMR[d]	HLLPR[e]
Stage 1	SSBR	100	100	100	100	100
	Filler	0	40	40	41*	43*
	TDAE	0	4	4	4	4
	ZnO	3	3	3	3	3
	SA	2	2	2	2	2
Stage 2	S	2	2	2	2	2
	TBBS	1.2	1.2	1.2	1.2	1.2
	TBzTD	0.3	0.3	0.3	0.3	0.3

[a]**Un**filled **r**ubber (UFR); [b]**C**arbon **b**lack-filled **r**ubber (CBR); [c]**H**TT **L**ignin-filled **r**ubber (HLR); [d]1,2- **B**is(2- **m**ercapto**e**thoxy)**e**thane modified **H**TT **L**ignin-filled **r**ubber (HLMR); [e]**L**iquid **P**oly**s**ulfide with **t**hiol end group modified **H**TT **L**ignin-filled **r**ubber (HLLPR)

*Adjusted amount by assuming 100 % conversion

6

Mixing ingredients was carried out in a Plastograph internal mixer (Brabender, Germany) of 50 ml volume. The compounds were mixed in two stages using a conventional mixing technique (mixing ingredients in a rubber mixer). The protocol for mixing is provided in **Table 6.3**. Stage 1 involves the masterbatch mixing, and the ingredients were added to the mixer with an initial temperature of 50 °C, rotor speed of 50 rpm, and a fill factor of 70 %. The amount of carbon black and HTT lignin was 40 phr. The content of thiol-modified HTT lignins was adjusted assuming 100 % yield, i.e., all the thiols added reacted with the HTT lignin surface. To avoid the crumbling of rubber in the small mixer, all the ingredients were slowly added in the first 2 minutes and mixed for another 4 minutes. The compounds were discharged at around 100 °C after 6 minutes. The compounds were then sheeted on a Schwabenthan Polymix80T 80x300 mm two-roll mill and kept for 16 hours before stage 2.

Table 6.3: Two-stage mixing procedure for unfilled and different filled compounds

	Mixing time (min: sec)	Rotor speed (RPM)	Actions
Stage 1	0:00 - 2:00	50	Add rubber, filler*, TDAE, ZnO, SA
	2:00 - 6:00	Variable**	Mix and discharge at ~100 °C
Stage 2	0:00 - 1:00	30	Add the masterbatch
	1:00 - 1:10	30	Add S, TBBS, TBzTD
	1:10 - 3:00	Variable**	Mix and discharge at ~90-100 °C

* Carbon black/ unmodified-/modified HTT lignin

**Rotor speed was varied accordingly to maintain the discharge temperature

The second mixing step (stage 2), the addition of curatives, was also done in the same small mixer. The initial mixing temperature for this step was also set to 50 °C with a fill factor of 70 %. After 3 minutes, the compounds were discharged at 90 - 100 °C.

6.2.3.2 Characterization of the unfilled and different filled SSBR compounds

The following studies were performed for the rubber compounds: Investigation of the Payne effect (uncured compounds), rheological and mechanical properties of cured rubber compounds with pre-modified lignin versus rubber compounds without filler, with HTT lignin and carbon black. For the investigations of the cured compounds, the compounds were cured on a Wickert laboratory press at 160 °C and 100 bar for t_{90}.

The procedures of these measurements can be found in **Chapter 3**, **under section 3.2.4**.

6.3 Results and Discussion

6.3.1 Impact of the selected thiols on the properties of HTT lignin

TGA-DTGA thermograms of unmodified (HL) and thiol-modified HTT lignins (HLM and HLLP) are shown in **Figure 6.2 a**. It is observed that both modified HTT lignins show slightly lower mass loss (~7 %) up to 250 °C compared to the unmodified one (~9 %). This indicates that the amount of moisture on the HTT lignin surface is decreased either due to the modification reaction or the thermal treatment during modification. Unlike the weight loss onsets observed in **Figure 6.2 b** for pure MEE and LPST at about 165 °C and 242 °C, respectively, no significant thermal degradation was observed for all materials up to 300 °C.
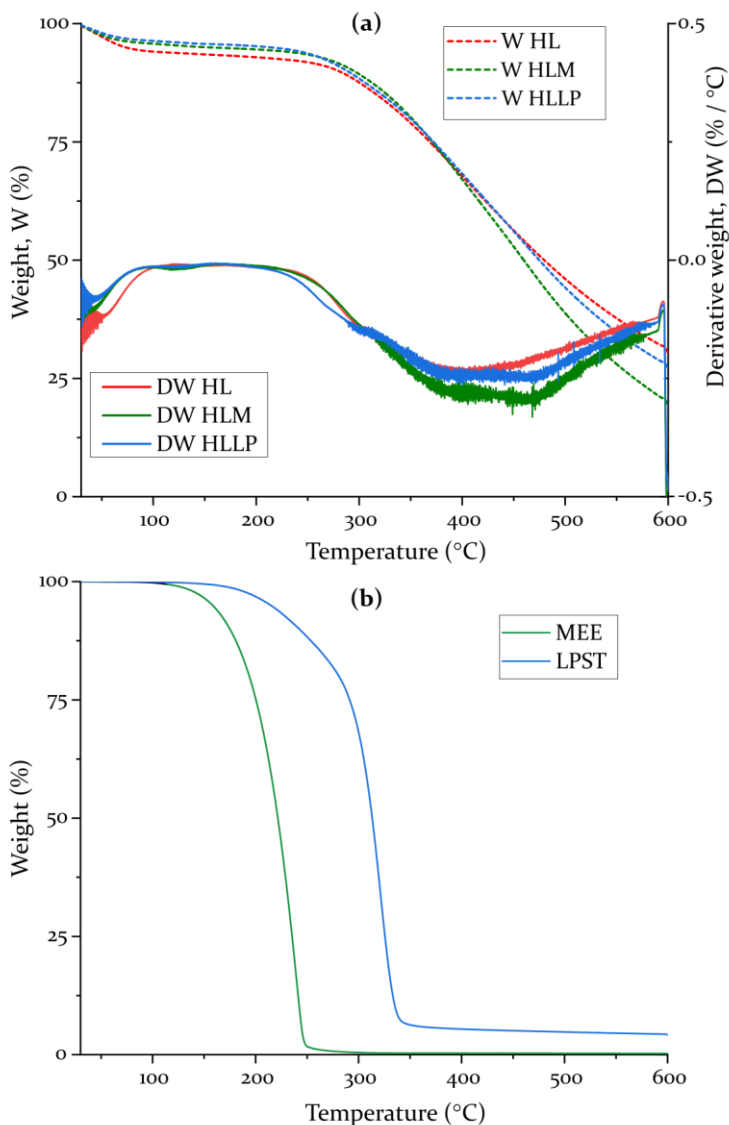
Figure 6.2 (a) TGA and DTGA thermograms of unmodified (HL) and modified HTT lignins (HLM, HLLP); (b) TGA of pure 1,2-bis(2-mercaptoethoxy)ethane (MEE) and liquid polysulfide polymer with thiol end groups (LPST)

For MEE-modified lignin (HLM), this observation is in line with the respective DTGA curve. This suggests the absence of unreacted MEE in HLM. However, for the LPST-modified sample (HLLP), the DTGA curve displays a minor change in weight loss in the region between 220 - 280 °C. This is attributed to the skeletal breakdown of the LPST caused by the presence of sulfide groups.[4,5] This observed change could be caused either by the residual unreacted LPST or the chemically grafted LPST to the HTT lignin surface. At around 300 °C, all materials degrade significantly. Between 300 - 350 °C, HLPP behaves

similarly to HL, while the degradation of HLM is enhanced more. At temperatures above 400 °C, the weight loss is more significant for HLM when compared to HLLP and HL. At 600 °C, the observed total weight losses are 79 % for HLM, 72 % for HLLP, and 68 % for HL. The higher weight loss observed for HLM and HLLP than HL could potentially be attributed to the thermal instability of the ether bonds (C-O) of MEE or LPST and/or to the cleavage of formed thioether bonds (C-S) between HTT lignin and the modifier.[6] HTT lignin modified with LPST is observed to be more thermally stable than the MEE thiol-modified sample. This could be due to the following reasons: (i) the presence of long-chain chemical structures of LPST (**Figure 6.1**) and (ii) a lower extent of grafting of LPST compared to MEE molecules.

The elemental sulfur (S) present in the HTT lignin before and after modification was determined and reported in **Table 6.4**. It can be observed that HTT lignin itself contains about 0.91 % sulfur, which was introduced during the initial Kraft pulping process. This value is found to be higher for the thiol-modified HTT lignin samples (see **Table 6.4**). This, along with the TGA data, provides evidence that the grafting of thiol to the HTT lignin surface has taken place. In order to evaluate the degree of grafting, the percent yield of sulfur introduction by modification was calculated. For this, first, the theoretical maximum sulfur content (S_T) that can be achieved at 100 % conversion in the modified HTT lignin is determined using **equation (6.1)**,

$$Theoretical\ sulfur\ content, S_T(\%) = \frac{(W_F * x) + (W_T * y)}{W_F + W_T} \qquad \textbf{(6.1)}$$

where W_F and W_T are the weight of HTT lignin and the thiol modifier (in grams), respectively, used for modification; x and y represent the sulfur content in HTT lignin and the used thiol modifier (in %), respectively. Subsequently, the yield is evaluated by using **equation (6.2)**,

$$Conversion\ yield\ (\%) = \frac{S_E}{S_T} * 100 \qquad \textbf{(6.2)}$$

where S_E is the experimental sulfur content of modified HTT lignins (HLM or HLLP); S_T represents the theoretical sulfur content at 100 % conversion of modified HTT lignin.

Table 6.4 Sulfur (S) elemental content of un- and thiol-modified HTT lignin

Samples	Theoretical S content at 100 % conversion (%)	Experimental S content (%)	Conversion yield (%)	Increase in S content after modification (%)
HL	0.91*	0.91	-	-
HLM	1.88	1.30	69	0.4
HLLP	4.99	2.03	41	1.12

*The experimental S value was taken as a theoretical one for HTT lignin (HL)

The data reported in **Table 6.4** shows that the S yield obtained for HLM is relatively higher than that obtained for HLLP. This indicates that the degree of grafting of MEE to HTT lignin is higher than LPST. This result is in line with the TGA results, where HLM demonstrated lower thermal stability after 400 °C than HLLP and the unmodified HTT lignin. Thus, it can be inferred that the amount of thiol grafted onto the surface of HTT lignin depends on the type of modifier used and negatively impacts the thermal degradation properties of HTT lignin. The lower conversion yield of both the modifiers can be interpreted in two ways: (i) the reaction conditions are inadequate to achieve a complete conversion, and/or (ii) the quantity of thiol added might be higher than that of the available 4-(hydroxymethyl)phenolic structures in HTT lignin.

The DRIFT spectra of the un- and modified HTT lignins are depicted in **Figure 6.3**. The bands (presented in the **SI**, **Figure S6.2, and S6.3**) at 2850 cm⁻¹, 2560 cm⁻¹, and 1200 – 1000 cm⁻¹ corresponding to C-H stretching, S-H stretching, and C-O stretching, respectively, are characteristics of MEE and LPST. Evidence of thiol modification can be found through the loss of the absorption band of thiol (ν-S-H around 2560 cm⁻¹) and a decrease in the peak absorbance of the hydroxy group (ν-OH between 3600 - 3100 cm⁻¹). However, interpreting the disappearance of thiol signals can be challenging in this case, as it overlaps with a shoulder of the HTT lignin signal (as shown in **Figure 6.3**). Nonetheless, the decrease in the peak absorbance of the hydroxy group observed in HLM and HLLP compared to HL may suggest that MEE and LPST are attached to the surface of HTT lignin.
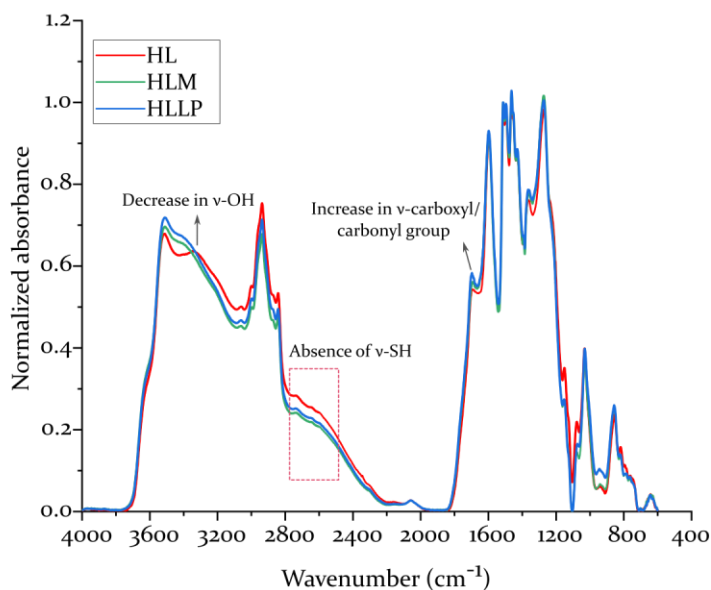
Figure 6.3. DRIFT spectra of unmodified and different thiol-modified HTT lignins

In addition to these observed signals, in the case of HLLP, an increase in the absorption band of the carbonyl / carboxylic group (C=O) around 1700 cm^{-1} is detected. The C=O signal is not a characteristic of LPST, as seen in **Figure S6.3**. This indicates that the polyether chains of LPST underwent oxidation, resulting in characteristic formates.[7] The existence of these structures is evidenced further by ^{13}C NMR results.

Figure 6.4 presents ^{13}C NMR spectra of thiol-modified and unmodified lignin, which provides insights into the structural changes caused by thiol modification. The spectral changes of HTT lignin are described in detail in **Chapter 3**, **section 3.3.1.**

6
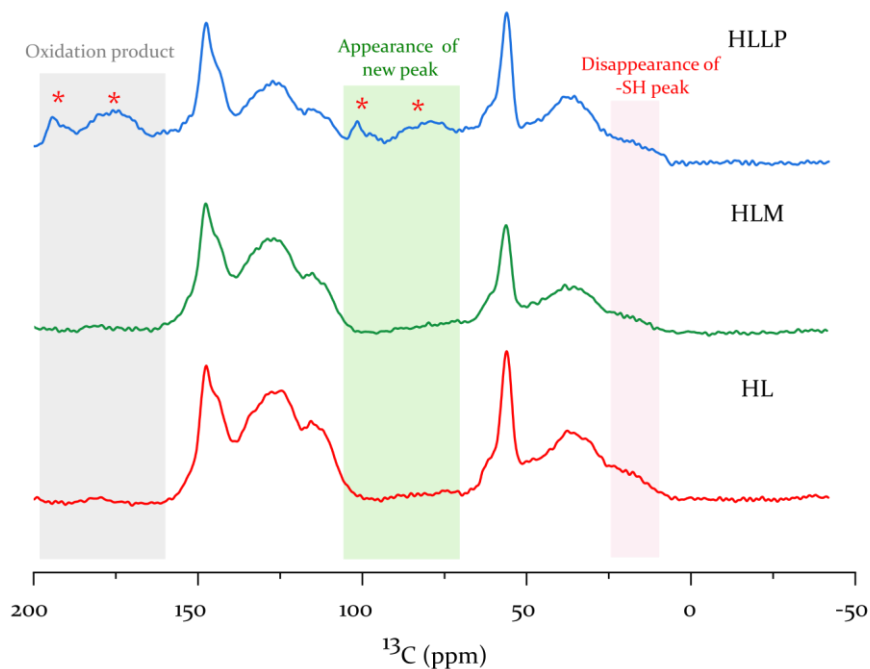
Figure 6.4 Solid state ¹³C NMR of unmodified- (HL) and different thiol-modified lignins (HLM and HLLP). The red asterisk "" denotes the peaks not characteristic of HTT lignin.*

6

To better interpret and compare the obtained spectra of the modified HTT lignins, the ¹³C NMR spectra of pure MEE display three characteristic peaks corresponding to the carbon atom close to the thiol (carbon A) and the aliphatic carbons of ether (carbon B and C), as shown in **Figure 6.5 (i)**. In contrast, LPST exhibits six significant characteristic signals, as shown in **Figure 6.5 (ii)**: (a) three from the polyether chains (carbon D – 95.4 ppm, E – 66.1 ppm, F – 38.8 ppm); (b) one from the methylene carbon in α position of the terminal thiol group (carbon A with a chemical shift of 24 ppm); (c) one from the carbon adjacent to the oxygen (carbon B – 69.7 ppm); and the carbon closer to the disulfides (carbon C - 31.6 ppm and G – 40.8 ppm). The peak assignments of LPST were performed based on the earlier works of Mahon et al. and Chemtob et al.[8,9]
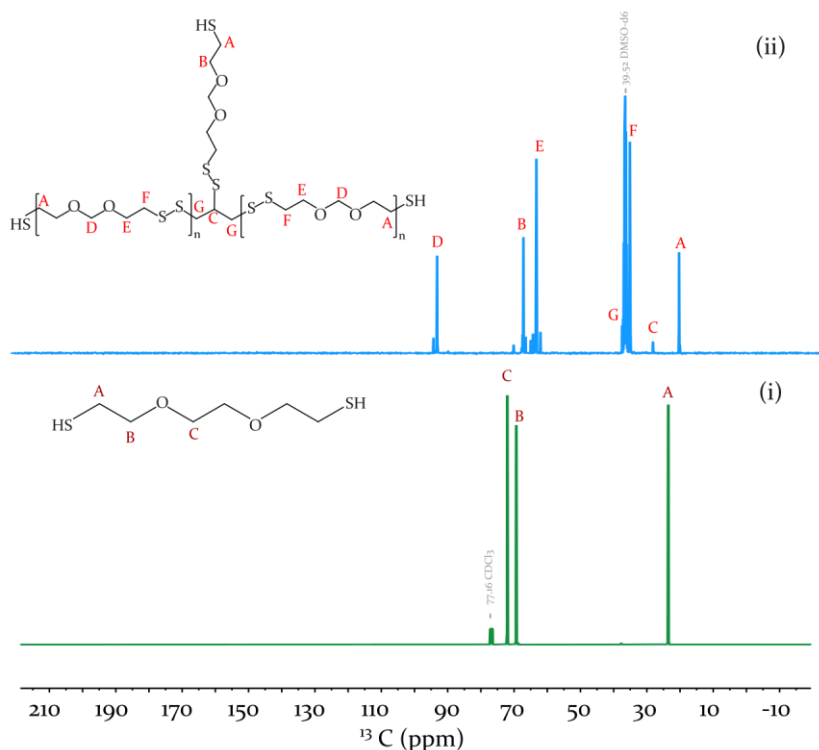
Figure 6.5 Liquid state ¹³C NMR of pure (i) 1,2-Bis(2-mercaptoethoxy)ethane (MEE); and (ii) Liquid polsulfide (LPST)

The carbon signal assigned to C-SH (carbon A) could not be identified in the spectra of HLM (**Figure 6.4**), indicating the absence of thiol moieties in the HLM sample. This observation, along with the findings of other analyses, suggests that the thiol moiety of MEE has reacted with HTT lignin. However, due to the signal overlap of the predominant peaks of HTT lignin with the chemical grafting ones, both HTT lignin and HLM spectra look similar. Therefore, it is impossible to give further interpretations of these data.

In the case of the HLLP sample, the absence of a peak around 24.5 ppm representing the methylene carbon adjacent to thiol (carbon A, refer to **Figure 6.5 ii**) and the appearance of new peaks (marked with a star in **Figure 6.4**) between 60 - 100 ppm corresponding to the carbon signals of the polyether chains of LPST (refer to **Figure 6.5 ii**) indicate the occurrence of a modification reaction.[8,9] This result is in line with the sulfur analysis and further evidence of the coupling between LPST and HTT lignin. The signals from the carbon neighboring to the disulfides of LPST arising around 31.6 ppm (carbon C) and 41 ppm (carbon G) appear to overlap with the carbon signals from HTT lignin, therefore, they cannot be identified in the spectrum. Besides the LPST characteristic peaks, other peaks between 160 - 200 ppm are also present in **Figure 6.4**. This spectral range can be assigned to the carbonyl-group (C=O) and is in line with the absorption peak observed at

1700 cm⁻¹ in the DRIFT spectra (refer to **Figure 6.3**) of HLLP. This confirms that the ether groups of LPST underwent oxidation (a possible side reaction) under the applied reaction conditions.[7,9] This further suggests that in the case of the HLLP sample, in addition to the LPST long chain structures, fragments of it formed as a result of oxidation are also attached to the HTT lignin surface. It is difficult to interpret the chemical structure of formed LPST with the performed measurements, and it is beyond the scope of the current study. However, a possible reaction product that could be created during the reaction between LPST and HTT lignin is illustrated using **Scheme 6.1**. The red highlighted ones in **Scheme 6.1 (a)** are polyether chains of LPST that can undergo oxidation. For simplicity, it is only shown in the scheme that one of them underwent oxidation, forming formate. However, in practice, it is possible that all of the polyether chains can undergo oxidation.

It is important to note that the peaks related to oxidation are not found in HLM spectra, indicating either the absence of side reactions during modification or a possible removal of the oxidation products during toluene extraction.

6

Scheme 6.1. Possible reaction between LPST and HTT lignin showing (a) oxidation of polyether chains of LPST and (b) the possible reaction between oxidized LPST and HTT lignin

(a) Possible oxidation of polyether chains of LPST
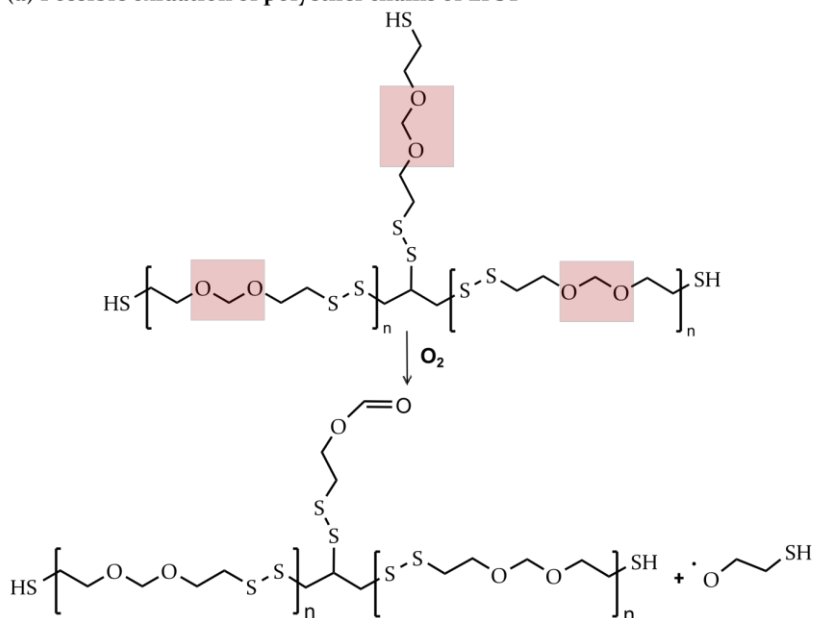
(b) Reaction between HTT lignin and oxidized LPST

6
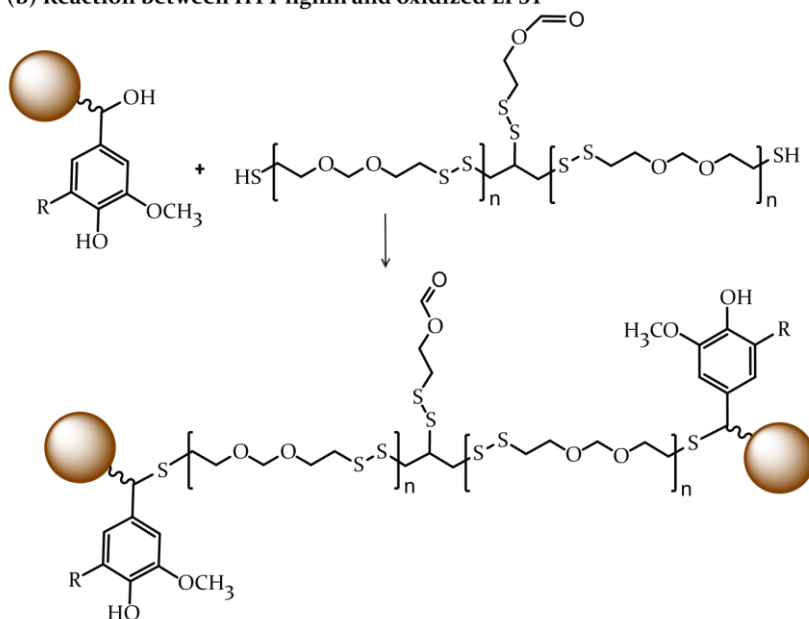
Based on the conducted analyses, it is likely that both the modifiers used were successfully grafted to the surface of HTT lignin. The sulfur analysis revealed that the grafting efficiency of MEE is higher than that of LPST. This difference could be due to the oxidation of LPST under the used reaction conditions, which was confirmed by the DRIFT and ^{13}C NMR results. Furthermore, the findings from ^{13}C NMR indicated that neither of the modified HTT lignins contained a thiol group. This suggests that the thiol moieties are highly reactive to HTT lignin, even at a moderate temperature of 110 °C. The probable reaction that can occur between HTT lignin and thiol is illustrated in **Scheme 6.2** using MEE thiol. Two possible ways of thiol reaction with HTT lignin are proposed, which can also be extended to LPST:

a) both the thiol groups grafting to the same HTT lignin particle, forming a U-shape;
b) the coupling of two HTT lignins to the same thiol modifier resulting in clustering of HTT lignin.

Scheme 6.2 Possible reactions involved in HTT lignin-thiol modifier coupling leading to complete consumption of thiols: (a) thiol moieties grafting to the same HTT lignin particle; (b) thiol moieties grafting to two different HTT lignin particles
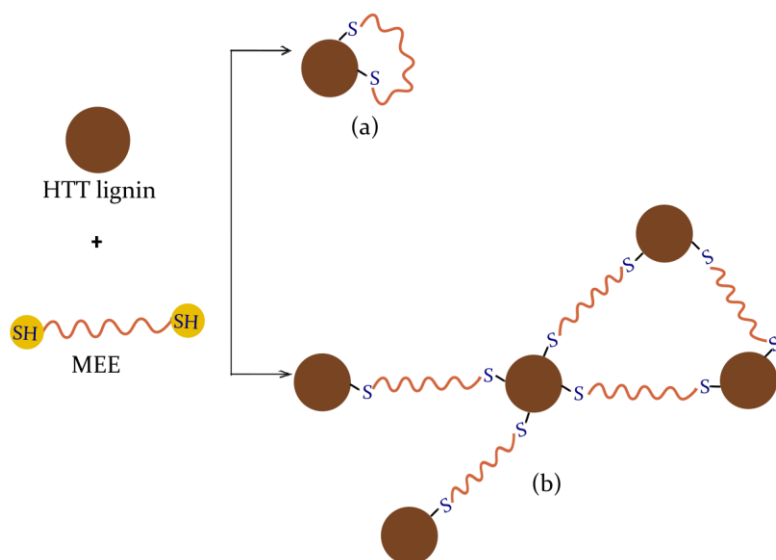
Given that the thiol functionalities of the grafted modifiers (i.e., 69 % MEE; 41 % LPST) were utilized entirely in modifying the filler, there is no possibility of a coupling reaction between HTT lignin and rubber via thiol when using MEE-modified HTT lignin as a filler. However, with LPST-modified HTT lignin (HLLP), disulfides in LPST could potentially facilitate a chemical coupling of HTT lignin and rubber in the HLLP compound. The impact of both modified HTT lignins on the in-rubber properties is investigated further.

6.3.2 Impact of the selected thiols on the in-rubber properties of HTT lignin-filled SSBR compound

Figure 6.6 shows the Payne effect of the uncured carbon black-(CB), unmodified HTT lignin-(HL), and thiol-modified HTT lignin (HLM, HLLP)-filled SSBR compounds. A typical linear viscoelastic behavior with no change in the shear modulus with the application of strain amplitude is observed for the unfilled SSBR (UFR) compound. A noticeable difference in the Payne effect curves is seen for all filled compounds. For all the HTT lignin-filled compounds (HLR, HLMR, HLLPR), as the strain increases, a gradual decline in the shear modulus is observed up to 10 %, followed by a sudden drop in the modulus between 10 – 100 % strain. In the case of CBR, a continuous decline of the modulus is observed even at small strain values, i.e., 1 %. This phenomenon is attributed to the destruction of the filler-filler network upon application of high strain. The obtained curve varies depending on the nature of the bonding between the filler particles. Carbon black develops a filler-filler network via a weak van der Waals bonding, whereas HTT lignin particles containing the different hydroxy groups can interact with each other by hydrogen bonding.[10] Thus, a distinctive behavior is seen between HL- and CB-filled compounds.
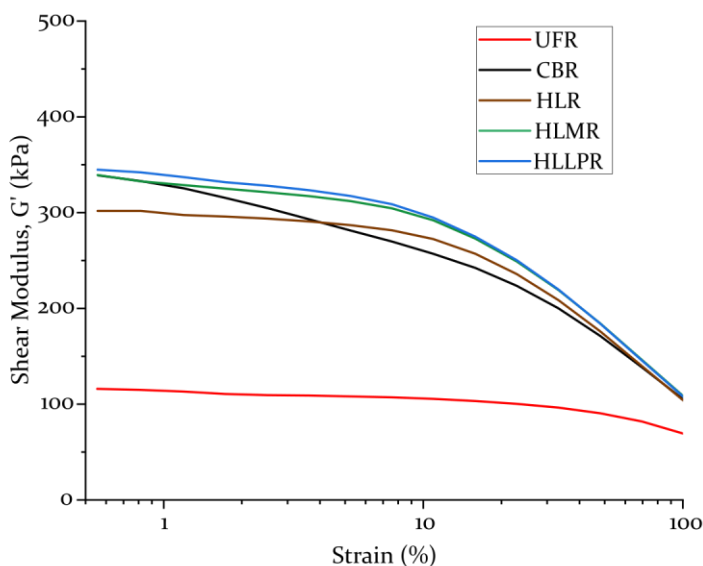
Figure 6.6 Payne effect curves of the unfilled and different filled uncured SSBR compounds

The unmodified HTT lignin-filled compound (HLR) shows the lowest G' value at low strain among the filled compounds. This indicates, on the one hand, that the filler-filler interaction is less than the thiol-modified HTT lignin-filled compounds, or a good filler dispersion is achieved in the polymer matrix. On the other hand, both the thiol-modified

HTT lignin-filled compounds demonstrate a higher G' at low strain than the unmodified one and CB-filled rubber. This indicates that the thiol-modified HTT lignin generates a strong filler-filler network in the rubber matrix, which could be explained by the reaction scheme postulated in **Scheme 6.2 (b)**. The nearly identical G' at 100 % strain of the modified HTT lignin compounds compared to the CBR and HLR suggest that a stable chemical polymer-filler interaction is not formed during mixing. This could also be due to the absence of thiol in the modified HTT lignin to react with the vinyl groups of SSBR during mixing.

The cure properties of different unmodified HTT lignin-, thiol-modified HTT lignin-, and CB-filled compounds are shown in **Figure 6.7**. All the filled compounds demonstrate a decreased scorch safety and higher minimum (M_L) and maximum torque (M_H) compared to the unfilled ones. This is observed due to the increase in filler-filler and filler-polymer interaction upon the addition of the filler, which varies depending on the filler type.
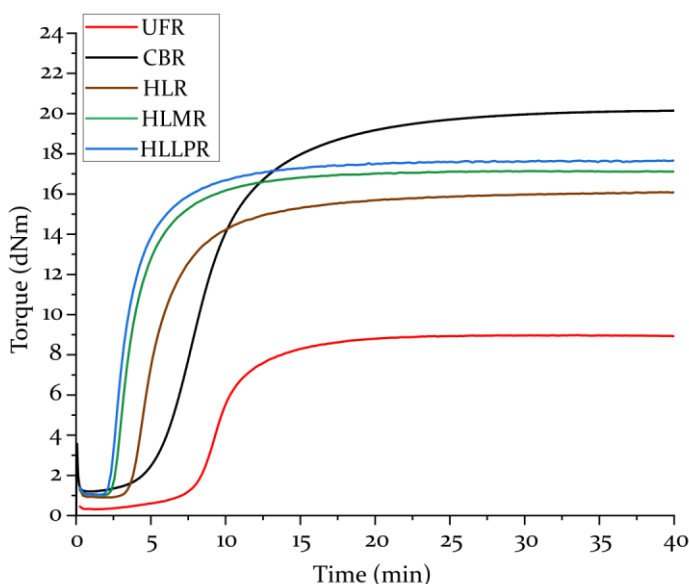
Figure 6.7 Curing curves of the unfilled and different filled SSBR compounds

A notable difference in the cure kinetics, i.e., a decrease in scorch safety and a slight increase in the cure rate, is observed between the modified and unmodified HTT lignin-filled compounds. This signifies that thiol modification enhances the vulcanization of the SSBR composite. Both the modified HTT lignin compounds also show higher M_H values compared to the unmodified which could be either due to the increase in filler-filler interactions (refer to **Figure 6.6**) and/or the increase in polymer-filler and polymer-polymer interactions due to the modification. Given the grafting efficiency of the modifiers (refer to **Table 6.4**), the cure characteristics of HLMR and HLLPR are observed to be very similar. This indicates that the disulfides of LPST probably participated in the

chemical coupling reaction between HTT lignin and the polymer chains during vulcanization. However, due to the low level of grafting of LPST, the achieved filler-polymer interaction in HLLPR could be relatively lower than for CBR, leading to a reduced M_H value.

Figure 6.8 shows the tensile properties of SSBR composites containing CB, unmodified, and modified HL. For the vulcanizates containing MEE- and LPST-modified HL, a higher tensile modulus is observed than the unmodified HL one.
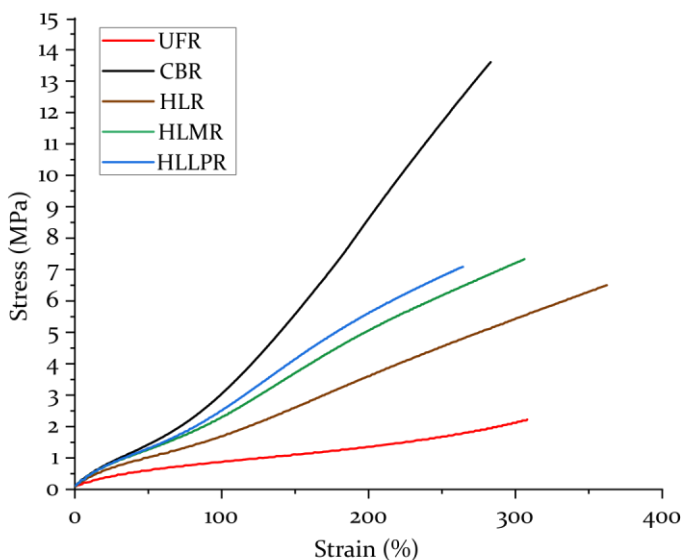
Figure 6.8 Mechanical properties of the unfilled and different filled SSBR vulcanizates

Similarly, a lower elongation at break is seen for the modified HL compounds, indicating that a more rigid network is formed (as depicted in **Scheme 6.2 (b)**) due to the modification affecting the flexibility and elasticity. This is in line with the results of the uncured Payne effect (high G' at low strain) and the cure data (high M_H). This suggests that the thiol modification improved the reinforcing effects of HTT lignin. The mechanical properties of both thiol-modified HTT lignin-filled vulcanizates remain similar, regardless of the difference in their respective grafting amounts (refer to **Table 6.4**). This could be due to the participation of disulfides of grafted LPST in the coupling of HTT lignin to rubber. This might enhance the mechanical properties of HLLPR equivalent to HLMR. Nevertheless, the achieved tensile strength and modulus are lower compared to CBR. The significant difference in the mechanical properties between thiol-modified and CB vulcanizates could be due to the following reasons:

(i) lack of strong interaction between rubber and filler in the former case, as no thiol moieties were detected in HLMR, and in the case of HLLPR, there was less grafting of LPST;

(ii)   poor micro-dispersion of modified HTT lignin filler within the rubber matrix due to the clustering of filler;

(iii)   lower BET surface area of the modified HTT lignins (HLM – 53 m²/g and HLLP – 48 m²/g) compared to N330 CB (78 m²/g), which can reduce the contact point between the filler and rubber, reducing their physical interaction.

6.4 Conclusions and Recommendations

The study investigated the use of thiol-based coupling agents, 1,2-Bis(2-mercaptoethoxy)ethane (MEE) and liquid polysulfide polymer with thiol end groups (LPST) as an alternative surface modifier to silanes to enhance the reinforcing capability of HTT lignin in SSBR. The analytical studies performed on modified HTT lignins indicate that MEE and LPST are grafted to the HTT lignin surface under ex-situ reaction conditions. Approximately 69 % of the added MEE and 41 % of added LPST underwent a coupling reaction with the HTT lignin. The lower grafting efficiency of LPST could be attributed to its oxidation, as evidenced by the presence of carbonyl groups in DRIFT and ^{13}C NMR spectra. Furthermore, no thiol moieties could be detected in the ^{13}C NMR spectra of the resulting modified HTT lignin samples. This suggested that the "thiol moieties" in both MEE and LPST modifiers have entirely reacted with the HTT lignin at a moderate temperature of 110 °C and that it is unavailable to couple the filler to the rubber. The modified lignins were then incorporated in a solution of styrene butadiene rubber using a conventional mixing procedure. The results revealed that the thiol modification of HTT lignin positively influenced the overall properties of the rubber compounds. Especially, the improved cure properties and increased tensile modulus of modified lignins demonstrated that the thiol modification has changed the polarity of HTT lignin compared to the unmodified lignin composites. Despite the difference in the MEE and LPST grafting amount, there is no significant difference in the in-rubber properties of both modified HTT lignins. This suggested that the disulfide moiety in LPST can enhance the coupling between filler and polymer. Although the thiol modification positively influences the overall in-rubber properties of HTT lignin-filled vulcanizates compared to the unmodified one, the obtained strength properties are still lower than those of the reinforcing carbon black (N330)-filled compound. Based on these results, it can be inferred that the less reinforcing effect of thiol-modified HTT lignins can be attributed to several factors. Firstly, the increased filler-filler networks in the modified lignin could affect the dispersion and decrease interaction with the polymer chains. Secondly, MEE-modified filler lacks thiols, and LPST-modified filler has fewer disulfides, which inhibits an effective chemical coupling with the polymer chains. Finally, the lower surface area of the filler (HLLP = 48 m²/g and HLM = 53 m²/g Vs. CB = 78 m²/g) negatively impacts the filler-polymer interaction, thus resulting in a reduced reinforcing effect.

In order to effectively utilize thiol coupling agents, further investigations are required to overcome the existing challenges. On the one hand, MEE displayed better grafting efficiency than LPST, but due to its high reactivity to HTT lignin, no thiol moieties were left for coupling reaction with rubber. On the other hand, disulfide moiety in LPST can enhance coupling with rubber, but it underwent oxidation during the ex-situ modification, resulting in less grafting. To improve the efficacy of MEE and LPST modification, milder reaction conditions, such as variations in time and temperature, can be implemented to prevent side reactions.

An alternative bifunctional thiol modifier can be exploited as a coupling agent to increase the coupling efficiency between HTT lignin and thiol. For instance, NXT™ Z 45 is one of the promising modifiers, as it contains reactive mercapto- and shielded thiocarboxylate functional groups. The mercapto group can interact with lignin during ex-situ modification, while the thioester group can interact with rubber during vulcanization, promoting filler-polymer interaction. Another effective approach would be to employ a thiol modifier with a different rubber reactive functionality, such as double bonds like conjugated, allylic, or vinylic groups, to enable interaction between filler and polymer. Other alternative bifunctional modifiers, aside from thiol, can be explored as a coupling agent for HTT lignin. This could potentially lead to enhanced reinforcing properties of HTT lignin-filled rubber.

6

Supporting Information
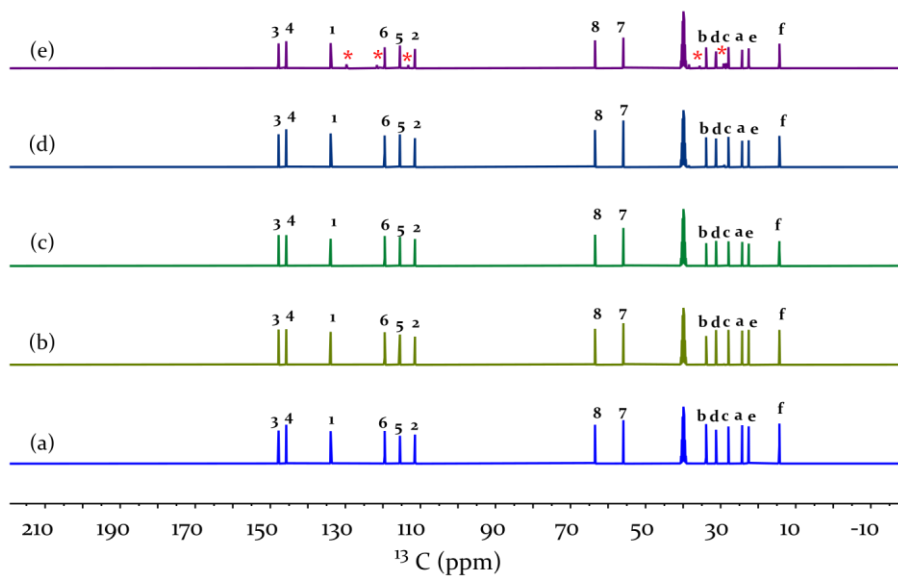
Figure S6.1 ^{13}C NMR spectra of reaction products of vanillyl alcohol (VA) and hexane thiol (HT) obtained at 90 °C for different reaction times: (a) 0, (b) 5, (c) 15, (d) 30, and (e) 60 minutes. The red asterisk "*" denotes the peaks characteristic of VA-HT coupling

6
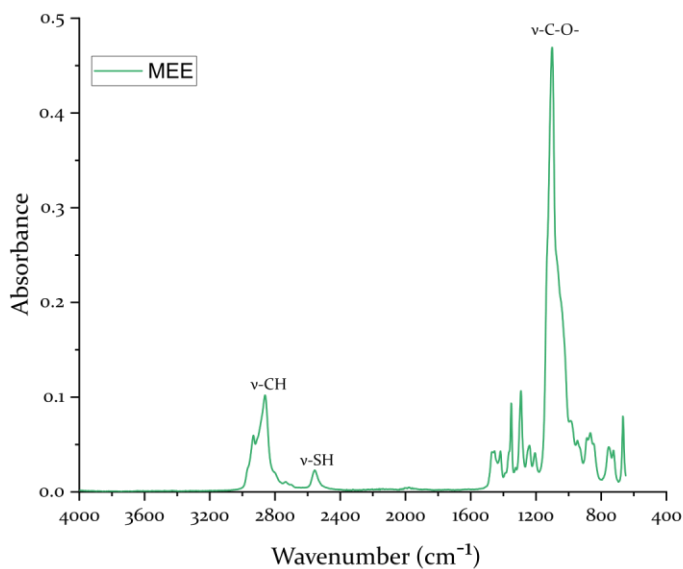
Figure S6.2. ATR-IR spectrum of 1,2-Bis(2-mercaptoethoxy)ethane (MEE)
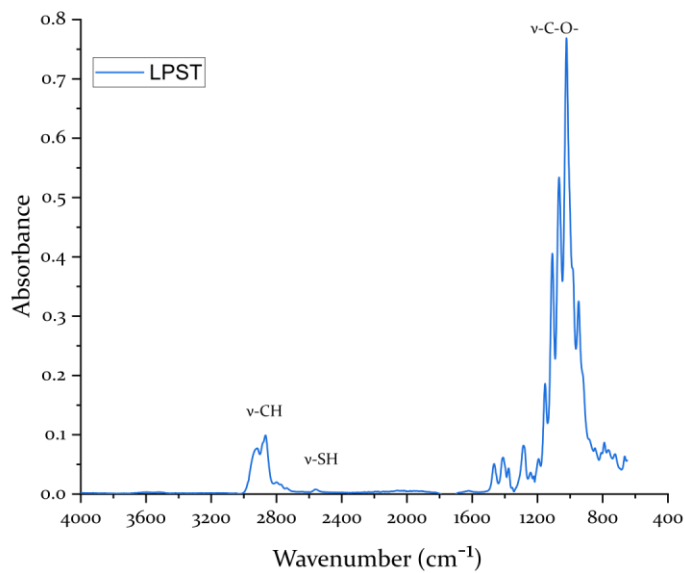
Figure S6.3. ATR-IR spectrum of Liquid Polysulfide (LPST)

References

(1) Boonstra, B. B.; Medalia, A. I. Effect of Carbon Black Dispersion on the Mechanical Properties of Rubber Vulcanizates. Rubber Chemistry and Technology 1963, 36 (1), 115–142.

(2) Sahakaro, K. Mechanism of Reinforcement Using Nanofillers in Rubber Nanocomposites. In Progress in Rubber Nanocomposites; Thomas, S., Maria, H. J., Eds.; Woodhead Publishing Series in Composites Science and Engineering; Woodhead Publishing, 2017; pp 81–113.

(3) Sato, M. Reinforcing Mechanisms of Silica / Sulfide-Silane vs. Mercapto-Silane Filled Tire Tread Compounds. PhD Thesis, University of Twente, The Netherlands, 2018.

(4) Ellson, G.; Carrier, X.; Walton, J.; Mahmood, S. F.; Yang, K.; Salazar, J.; Voit, W. E. Tough Thiourethane Thermoplastics for Fused Filament Fabrication. J of Applied Polymer Sci 2018, 135 (6), 45574.

(5) Shirsath, N. B.; Gupta, G. R.; Gite, V. V.; Meshram, J. S. Studies of Thermally Assisted Interactions of Polysulphide Polymer with Ionic Liquids. Bull Mater Sci 2018, 41 (2), 63.

(6) Federle, S. Sesquiterpenes as Building Blocks for the Synthesis of Bio-Based Polymers. PhD Thesis, University of Bath, England, 2021.

(7) Chemtob, A.; Feillée, N.; Vaulot, C.; Ley, C.; Le Nouen, D. Self-Photopolymerization of Poly(Disulfide) Oligomers. ACS Omega 2019, 4 (3), 5722–5730.

(8) Chemtob, A.; Feillée, N.; Ley, C.; Ponche, A.; Rigolet, S.; Soraru, C.; Ploux, L.; Nouen, D. Oxidative Photopolymerization of Thiol-Terminated Polysulfide Resins. Application in Antibacterial Coatings. Progress in Organic Coatings 2018, 121, 80–88.

(9) Mahon, A.; Kemp, T. J.; Coates, R. J. Thermal and Photodegradation of Polysulfide Pre-Polymers: Products and Pathways. Polymer Degradation and Stability 1998, 62 (1), 15–24.

(10) Mohamad Aini, N. A.; Othman, N.; Hussin, M. H.; Sahakaro, K.; Hayeemasae, N. Hydroxymethylation-Modified Lignin and Its Effectiveness as a Filler in Rubber Composites. Processes 2019, 7 (5), 315.

6

7. Use of Epoxy as a Non-silane-based Surface Modifier for Hydrothermally Treated Lignin
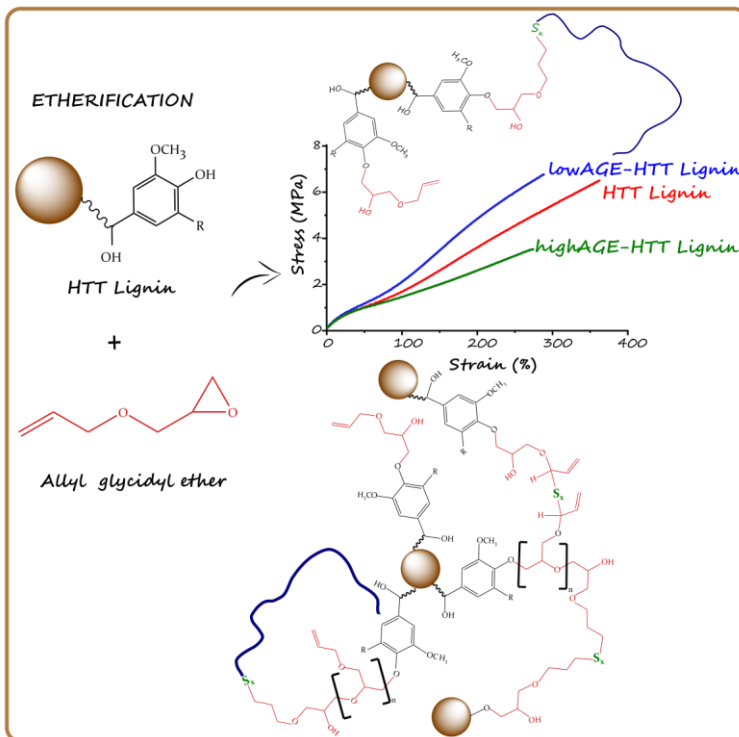
Reactivity Study of HTT lignin/Allyl glycidyl ether and Their Application in Rubber

The present chapter discusses the modification of HTT lignin using different non-silane-based mono- and bi-functional modifiers. It focuses primarily on understanding the potential of functionalized epoxides as an alternative non-silane-based surface modifier for HTT lignin. The initial ^{13}C nuclear magnetic resonance studies using vanillyl alcohol as a model substance for lignin and the epoxide allyl glycidyl demonstrated that the reaction conditions strongly influence the reactivity. A reaction in the presence of a catalyst at high temperature led to a ring-opening reaction of epoxy and subsequent coupling to vanillyl alcohol via the phenolic hydroxyl groups. With this gained knowledge, two modified HTT lignins were prepared by varying the quantities of allyl glycidyl ether. These samples were characterized by ^{13}C solid-state nuclear magnetic resonance, DRIFT spectroscopy, thermogravimetric analysis, and X-ray diffraction measurements. The results demonstrated that the allyl glycidyl ether is grafted to the HTT lignin surface via the phenolic hydroxyl groups. It was shown that oligomerized or homopolymerized allyl glycidyl ethers are formed with modified HTT lignin when a high content of epoxide agent is used. The coupling efficiency was further evidenced through the achieved in-rubber properties of allyl glycidyl ether modified-HTT lignin-filled styrene butadiene rubber. The in-rubber studies reveal that the mechanical properties of allyl glycidyl ether modified-HTT lignin-filled vulcanizates can be drastically changed by varying the content of allyl glycidyl ether. The vulcanizate containing modified HTT lignin with a low allyl glycidyl ether content exhibited improved in-rubber performance compared to the unmodified ones. In contrast, the addition of HTT lignin modified with high allyl glycidyl ether content deteriorated the in-rubber properties. It is presumed that the two side reactions of AGE, (i) homo-polymerization or oligomerization via epoxy group during modification and (ii) self-crosslinking via the grafted allyl groups during vulcanization, negatively affect the filler properties of HTT lignin, and, thereby, reduces the filler-polymer and polymer-polymer interaction compared to the unmodified HTT lignin.

7

7.1 Introduction

The reinforcing potential of hydrothermally treated (HTT) lignin in solution styrene butadiene rubber and butadiene rubber blend (SSBR/BR) is higher than the initial feedstock, Kraft lignin, as discussed in **Chapter 3**. Additionally, **Chapters 4 and 6** demonstrated that the reinforcing properties of HTT lignin-filled rubber compounds can be enhanced further by using silane-based surface modifiers containing reactive sulfur moieties and thiol coupling agents. However, the reinforcing effects of HTT lignin with these modifiers were lower than the conventional reinforcing carbon black. The limitations in enhancing the mechanical properties offered by these surface modifiers were discussed in detail in **Chapter 6**. To address the challenges posed by silane- and thiol-based surface modifiers, the present study aimed to identify alternative surface modifiers for HTT lignin that could potentially produce high-performance rubber composites. As part of this study, three different chemical modification reactions were explored for HTT lignin: (i) esterification, (ii) etherification, and (iii) urethanization. For each reaction category, a mono-functional additive (i.e., an agent containing only a filler reactive group) was selected, and the feasibility of reaction with HTT lignin was studied. Hexanoic anhydride, epoxy decane, and hexyl isocyanate were used as modifiers to perform esterification, etherification, and urethanization reactions on the surface of HTT lignin, respectively. These screening experiments have confirmed that all three selected modifiers chemically couple with HTT lignin. This is supported by the presence of C=O in esterified and urethanized HTT, as well as the presence of C-O-C in etherified HTT lignin, as demonstrated in the DRIFT results (presented in **Supporting information (SI)**, **Figure S7.1**). Thus, chemical modifications of HTT lignin through esterification, etherification, and urethanization reactions have been identified as viable alternatives. However, the technical availability of safe-to-use anhydride- or isocyanate-based coupling agents, i.e., carbonic acid anhydride and/or an isocyanate with a second functionality that can potentially couple the filler with the SSBR polymer, pose a significant challenge. Therefore, the present chapter primarily focuses on the etherification of HTT lignin using an epoxide-based coupling agent, which can efficiently graft to the surface of HTT lignin and introduces a second functionality that can couple the filler with the rubber. The etherification reaction of HTT lignin is carried out using allyl glycidyl ether (AGE) as an epoxide agent, a bifunctional molecule consisting of an end-terminated epoxy (filler reactive functionality) and an allyl group (sulfur reactive one[1] that can participate in the vulcanization reaction and can couple filler to the polymer). The structure of this molecule is shown in **Figure 7.1**. It has been studied extensively for the surface treatment of cellulose.[2,3] A recent study demonstrated that modification of Kraft lignin by dodecyl glycidyl ether hydrophobized its surface and improved its thermal properties.[4] The present study aimed to modify HTT lignin using AGE to enhance the rubber properties and to understand (i) the coupling mechanism determining optimum coupling conditions for HTT lignin and AGE and (ii) evaluate the potential coupling of the introduced allyl group to the polymer chain by vulcanization.
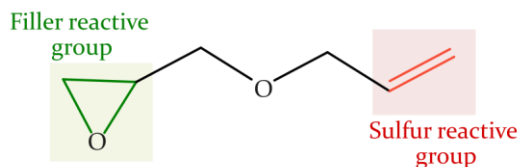
7

Figure 7.1 Chemical structure of the epoxide bifunctional agent, allyl glycidyl ether (AGE)

A preliminary model study using vanillyl alcohol (VA) as a model substance for HTT lignin and allyl glycidyl ether (AGE) was performed to understand which functional group (aliphatic and aromatic hydroxyl) is involved in the coupling reaction. Furthermore, the study aimed to identify the optimum reaction conditions for modifying HTT lignin with allyl glycidyl ether. For this purpose, an initial screening study was performed to understand the impact of temperature on the reaction rate between VA and AGE. The reaction was carried out for 1 h in a glass ampoule at three different temperatures (40 °C, 75 °C, and 150 °C), followed by ^{13}C NMR analyses. The result (presented in **SI**, **Figure S7.2**) indicated that the epoxy ring opening did not occur at the investigated temperatures. Also, no new peaks indicating a possible coupling product were identified, except for the side reaction products of VA at high temperatures. Since also at 150 °C the reaction did not proceed, the use of a catalyst was considered. Typically, the reaction between an epoxide ring and hydroxy groups can be accelerated by adding catalysts like Lewis bases.[5,4] Therefore, another screening study of VA and AGE was performed with different catalysts such as triethyl amine (TEA), 1-methylimidazole (1-MIM), potassium carbonate (K_2CO_3), sodium hydrogen carbonate ($NaHCO_3$), and diphenyl guanidine (DPG). The reactions with catalysts were carried out at 75 °C for 1 h, followed by ^{13}C NMR analysis. The results of this study are presented in **SI, Figure S7.3**. The study revealed that the addition of a catalyst triggers the reaction between VA and AGE. In particular, TEA, 1-MIM, and K_2CO_3 initiate the reaction and yield higher conversion than the other two catalysts (DPG, $NaHCO_3$). When comparing the efficiency of the reaction initiated by these three catalyzing agents, the efficiency decreases in the following order: 1-MIM > K_2CO_3 > TEA. This effect could be related to the nucleophilicity of the catalysts.[6] Thus, 1-MIM was identified as an effective catalyst for the VA-AGE reaction. Furthermore, the study indicated that along with the catalyst, a higher temperature or a longer reaction time is required to enhance the reaction yield. Therefore, a temperature of 150 °C and the 1-MIM catalyst were selected to identify the functional groups involved in the VA and AGE coupling reaction. The outcome of this study will be covered in the present chapter.

Following the preliminary investigations, an ex-situ modification of HTT lignin using two different concentrations of AGE (low and high) in the presence of 1-MIM catalyst and the characterization were undertaken. Finally, the impact of AGE-modified HTT lignins in solution styrene butadiene rubber compound was studied in terms of curing, filler-filler interactions, and mechanical properties and compared to the unmodified HTT lignin-filled rubber compound.

7.2 Experimental Section

7.2.1 Materials

7.2.1.1 Model study

Commercially available materials were purchased and used as received without further purification or pre-treatment unless otherwise stated. HTT lignin (pH 8.7) with a BET specific surface area of 47 m²/g was provided by SunCoal Industries GmbH, Germany. Allyl glycidyl ether (AGE, ≥ 99 %), vanillyl alcohol (VA, 98 %), deuterated dimethyl sulfoxide (DMSO-d6, 99.96 % deuterium atom), triethylamine (TEA, ≥ 99.5 %), 1- methylimidazole (1-MIM, 99 %), anhydrous pyridine (py, 99.8 %), potassium carbonate (K_2CO_3, ≥ 99 %) and sodium hydrogen carbonate ($NaHCO_3$, ≥ 99.7 %) were acquired from Merck KGaA, Germany. Diphenyl guanidine (DPG) was provided by Flexsys, Belgium.

7.2.1.2 In-rubber study

The same ingredients, as discussed in **Chapter 6**, were obtained and used as received.

7.2.2 Modification procedure

7.2.2.1 Reaction of Vanillyl alcohol with AGE with and without 1-MIM catalyst

Equimolar quantities (3 mmol) of VA and AGE were placed in a 5 ml glass ampoule and sealed with a rubber septum without any solvent. The filled ampoule was immersed in an oil bath at 150±5 °C, and the reaction was carried out for an hour under continuous stirring. No post-treatment steps were applied to the reacted mixtures. After this, the reaction was stopped immediately by quenching the ampoule in liquid nitrogen. A similar procedure was followed for the VA, AGE, and catalyst. 3 mmol of VA and 0.15 mmol of 1- MIM catalyst (the amount of catalyst was 5 % of the molar quantities of VA) were taken in a 5 ml glass ampoule and mixed together for 10 mins, followed by the addition of 3 mmol of AGE and sealing the ampoule with a rubber septum without any solvent. The rest of the procedure is identical to the VA+AGE mixture without a catalyst. A mixture of equimolar amounts of VA and AGE was prepared as a control at room temperature to identify the respective characteristic peaks.

7.2.2.2 Pre-modification of HTT lignin with AGE

Liquid-phase modification was carried out to improve the wetting behavior of HTT lignin. For this purpose, an inert, aromatic hydrocarbon solvent, xylene, was selected with a boiling point of 140 °C. Based on the screening study, 1-MIM was used as the catalyst for the modification reaction. 40 g of HTT lignin (12.8 mmol of surface accessible acidic hydroxyl (-OH) groups) and 1-MIM (0.64 mmol; corresponding to 5 % of the surface accessible hydroxyl groups) were added to a 250 ml flask (equipped with a thermometer) containing 100 ml xylene. The reaction mixture was heated under constant stirring in an oil bath to 140±5 °C under N_2 and refluxed using a condenser. After achieving an

7

equilibrium temperature, the desired quantities of AGE (12.8 mmol; taken equimolar to the amount of surface accessible -OH groups) were added to the reaction mixture. The modification was carried out for 3 h. At the end of the reaction, the product was extracted in a Soxhlet unit with acetone for 24 h to remove the unreacted and physically adsorbed AGE and the catalyst. Afterwards, it was placed in a vacuum oven at a temperature of 80 °C for 24 h to remove the solvent.

To understand the impact of AGE dosage on the modification reaction, an additional variant containing a higher amount of AGE (10 times the molar amount of phenolic -OH group, i.e., 128 mmol) than the previous one was prepared using the same protocol described above. A catalyst quantity corresponding to 5 % of the surface -OH groups was employed in this study to promote the formation of phenolate anions in HTT lignin, as opposed to the ring-opening and oligomerization of AGE. A summary of quantities used for the two modifications is listed in **Table 7.1**.

Table 7.1 Quantity of allyl glycidyl ether (AGE) and HTT lignin taken for ex-situ modification

Variant	Amount of HTT lignin (g)	Amount of catalyst (g)	Amount of AGE (g)
HTT Lignin +AGE-eq	40	0.05	1.46
HTT Lignin +AGE-10	40	0.05	14.61

7.2.3 Preparation of rubber compound

The preparation of the rubber compounds was done in a Plastograph internal mixer (Brabender, Germany) of 50 ml, and the mixing protocol is the same as that described in **Chapter 6, section 6.2.4**. The formulation used for the study is identical to the one described in **Chapter 6, Table 6.2**, except for the amount of unmodified and AGE-modified HTT lignin filler added to the rubber. It was kept constant (40 phr). The compound containing unmodified HTT lignin is termed HLR, and the ones having modified HTT lignin with equimolar and ten times higher quantity are addressed as HLAGE-eq and HLAGE-10, respectively.

7.2.4 Characterization Methods

7.2.4.1 Characterization of the VA/AGE with and without catalyst

Approximately 10 - 15 mg of each model mixture (with and without catalyst) and pure AGE as reference were dissolved in 0.5 ml DMSO-d6 to be analyzed by NMR. The prepared solutions were characterized by ^{13}C NMR, as discussed in **Chapter 5, section 5.2.3.3**.

The ^{13}C spectra were referenced to the solvent's carbon peak.[7] Assignments were performed by cross-referencing the spectra with the Spectral Database for Organic Compounds (SDBS).[8]

7.2.4.2 Characterization of the AGE-modified HTT lignins

The impact of the modification on the thermal degradation, surface functionalities, crystallinity, surface area, and particle size was studied for the AGE-modified HTT lignins after extraction.

The thermal analysis was carried out using a TGA 550 analyzer, TA Instruments, according to the procedure described in **Chapter 6, section 6.2.5.1**. Three replicates for each lignin sample were done to check the repeatability of the measurement. As the replicate deviation was minimal, a representative weight loss (thermogravimetric, TG) and its first derivative (DTG) curve were selected and used in this thesis.

The specific surface area (SSA) measurement of AGE-modified HTT lignins was determined by multi-point Brunauer-Emmett-Teller (BET) procedure using a 3P meso BK222 surface analyzer. Before the measurement, the samples were degassed at 150 °C for 2 h under vacuum to remove any physically adsorbed substances from the surface like water molecules. The nitrogen adsorption/desorption isotherms of the degassed samples were obtained at a set temperature of –196.15 °C and with different pressures. The measurement was repeated three times, and the average was reported.

DRIFT spectroscopy measurements of the un- and AGE-modified HTT lignins were performed according to the procedure described in **Chapter 3, section 3.2.2.2**. All IR spectra were normalized according to the aromatic skeleton vibration band of lignin at 1600 cm^{-1}. The measurement was repeated three times for each sample. In addition, the FTIR spectrum of pure AGE was obtained on a Thermo Fisher Scientific Nicolet 8700 spectrometer equipped with a deuterated triglycine sulfate (DTGS) detector in attenuated total reflection (ATR) mode. The spectrum was averaged over 16 scans in the range between 4000 to 600 cm^{-1} at a resolution of 4 cm^{-1}. A baseline correction and normalization procedures were performed on the spectra using the Spectrum software.

The solid-state ^{13}C NMR of the AGE-modified HTT lignins was performed according to the protocol described in **Chapter 3, section 3.2.2.2**.

A powder X-ray diffraction (XRD) study was carried out to characterize the crystal structure of the un- and AGE-modified samples. The XRD analysis was recorded with a D8 Bruker discover diffractometer using an Eiger 2R 500K detector, operating at 40 kV and 40 mA with a Cu-Kα radiation (λ= 1.5544 Å). Scans were performed in a step-scanning mode (Coupled 2Θ/Θ) over a diffraction angle 2Θ ranging from 3° to 74° at a scan rate of 2 deg/min.

7.2.4.3 Characterization of the AGE-modified HTT lignin-filled SSBR compounds

The Payne effect behavior (both uncured and cured), rheological and mechanical properties, and the apparent crosslink density (CLD) were measured for both the unmodified and pre-modified HTT lignin-containing rubber compounds based on the procedure described in **Chapter 3, section 3.2.4**. To investigate the vulcanizates, the compounds were cured in a Wickert laboratory press at 160 °C and 100 bar at the curing time t_{90}.

7

7.3 Results and Discussion

This section is divided into three sub-sections, which will discuss (i) the characterization of the AGE-modified lignin model (vanillyl alcohol), (ii) AGE-modified HTT lignin, and (iii) the behavior of AGE-modified HTT lignin in rubber.

7.3.1 Understanding the coupling reaction of HTT lignin and allyl glycidyl ether using model studies

The ^{13}C NMR spectra of pure AGE and the resultant product mixture of AGE and vanillyl alcohol with and without 1-MIM catalyst are depicted in **Figure 7.2**. In the presence of a 1-MIM catalyst, the following changes in the spectra are observed in **Figure 7.2 d**: (i) the disappearance of epoxy carbon peaks (Ce and Cf); (ii) the appearance of a new secondary alcohol peak (Ce*) around ~71 ppm in the ^{13}C NMR spectra; (iii) the appearance of new peaks (Cd*, Cf*) between 65 - 75 ppm; (iv) a shift of the carbon peak of aromatic hydroxy from 145 ppm (C4, **Figure 7.2 c**) to 147 ppm (C4*, **Figure 7.2 d**); (v) a shift of the aromatic carbon peaks C3 (147 ppm), C5 (115 ppm), C1 (133.5 ppm) (**Figure 7.2 c**) to new positions C3* (149 ppm), C5* (113 ppm), C1* (135.5 ppm), respectively (**Figure 7.2 d**). The observed peak changes (i, ii) suggest the occurrence of an epoxy ring-opening reaction, and (iii - v) indicate the coupling reaction between VA and AGE. The shift in aromatic carbon peaks (iv, v) and the presence of aliphatic hydroxy (C8 and C8*) in the same position at ~62 ppm suggests that the phenolic hydroxy group is preferably involved in the coupling reaction rather than the aliphatic hydroxy group. This differs from the thiol modification, where 4-hydroxymethyl phenolic structures are necessary for coupling.

Apart from the coupling reaction with VA, AGE can also undergo side reactions such as self-polymerization and isomerization of the pendant allyl group to cis- or trans-configuration, etc.[9,10] From the results of ^{13}C NMR, it can be noticed that the peak position of the allylic double bonds are not altered indicating that this functionality is not affected by the applied reaction conditions. Similarly, the presence of the secondary alcohol (e* in **Figure 7.2 d**) and the absence of line broadening demonstrates that the self-oligomerization of AGE has not occurred under the used conditions.

7
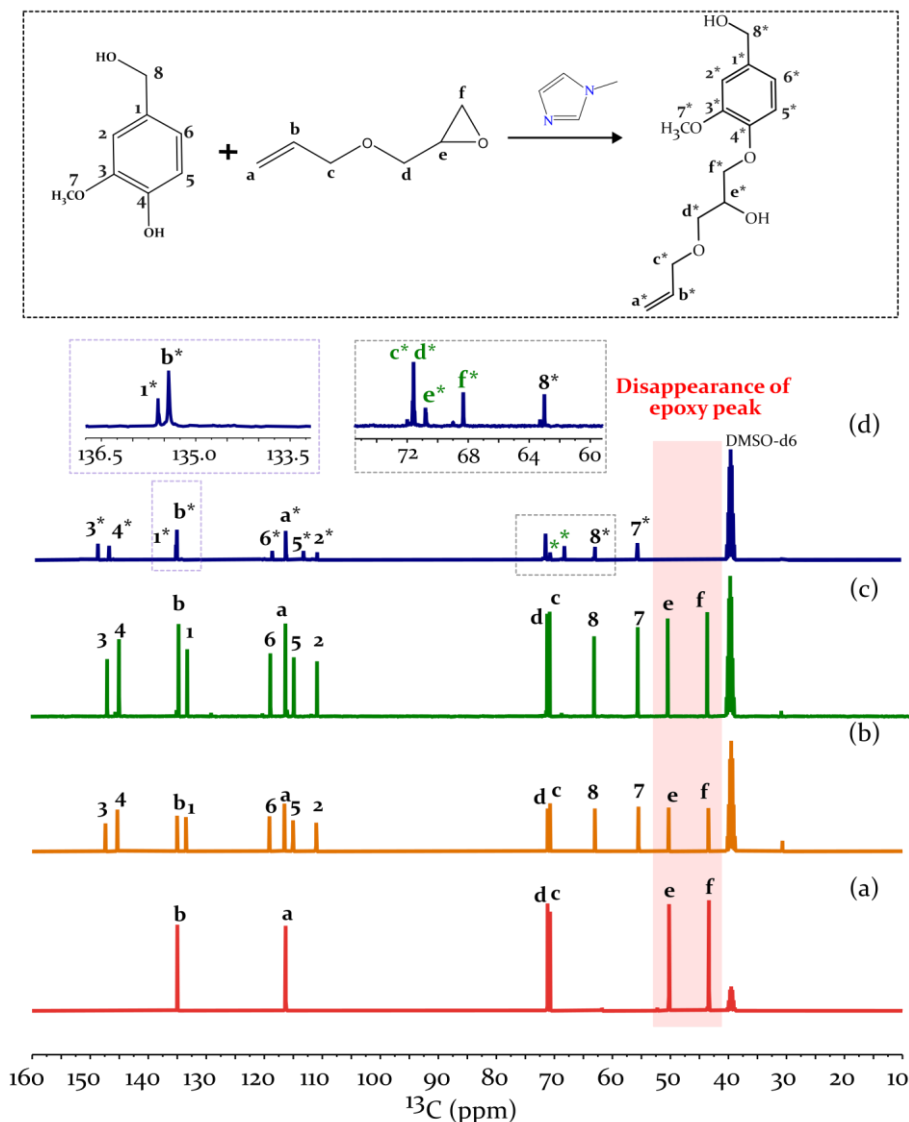
Figure 7.2 ^{13}C NMR spectra of (a) pure allyl glycidyl ether (AGE); (b) a mixture of vanillyl alcohol (VA) and allyl glycidyl ether (AGE); (c) reaction product of VA and AGE without 1-methylimidazole (1-MIM) catalyst after 1 h at 150 °C; (d) reaction product of VA and AGE with 1-MIM catalyst after treatment for 1 h at 150 °C

From the results, it can be postulated that the reaction of imidazole-catalyzed VA-AGE proceeds via the salt formation of the phenolic -OH with the imidazole, followed by the ring-opening of epoxide by the generated anion.[11,12] The possible reaction pathway of coupling is shown in **Scheme 7.1**.

Scheme 7.1 Simplified mechanism of coupling between vanillyl alcohol (VA) and allyl glycidyl ether (AGE) in the presence of 1-methylimidazole (1-MIM)
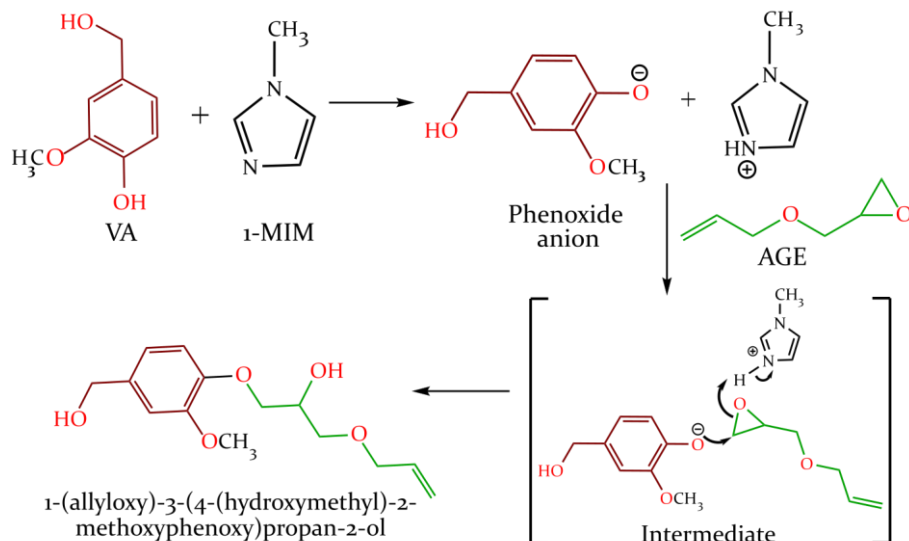
7.3.2 Impact of AGE pre-modification on HTT lignin properties

The TGA study of the AGE- and un-modified HTT lignin reveals the difference in the thermal degradation behavior corresponding to %weight loss and thermal stability at various temperature ranges. The curves of the obtained thermograms TG (weight loss as a function of temperature) and DTG (rate of weight loss at the corresponding temperature range) are presented in **Figure 7.3**. The initial mass percentages for all samples in **Figure 7.3** were found to be around 97-98 % instead of 100 %, which arises due to the false calibration of the instrument. Considering that all the studied samples have a similar calibration error, comparing them on a relative basis is acceptable. Upon heating, it is noticeable that the unmodified HTT lignin (HL) exhibits a two-step thermal degradation profile compared to the modified HTT lignins. The first step of HL degradation is relatively minimal and can be observed between the temperature ~135 and 240 °C, denoted by a weak shoulder-like peak in the DTG curve. This can be attributed to lignin's breakdown of the propanoid side chain.[4,13] A maximum degradation of HL is found in the second step, occurring between ~250 and 450 °C, represented by a broad peak in the DTG curve. This is associated with the fragmentation of the interunit linkages and the breaking of ether bonds in lignin.[13,14]
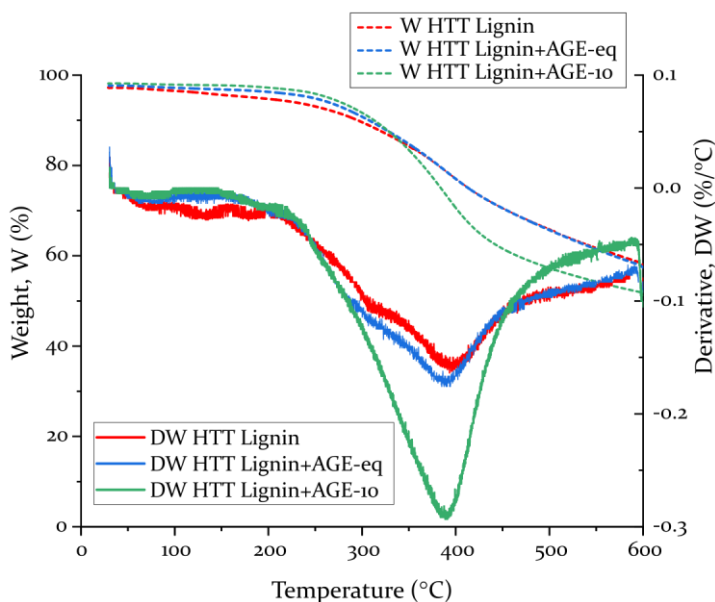
Figure 7.3 TG and DTG thermograms of un- and AGE-modified HTT lignin recorded under nitrogen atmosphere

The mass profile of allyl glycidyl ether (**Figure 7.4**) suggests that AGE is volatile at ambient temperature; around 80 °C, it evaporates with no residue at 110 °C. The high thermal stability of AGE-modified HTT lignins below 120 °C suggests that the extraction process has efficiently removed the unreacted AGE molecules in the modified lignin samples. Even though both the modified samples have a similar course of thermal degradation until ~300 °C, with increasing temperature, a faster rate of degradation and a higher weight loss (~47 % at 600 °C) is observed for the HTT lignin modified with a higher AGE content (HTT Lignin+AGE-10). In contrast, HTT lignin modified with a lower quantity of AGE (HTT Lignin+AGE-eq) shows similar thermal stability to HL in this region and displays a weight loss of ~39 % at 600 °C. The observed weight losses for modified and unmodified HTT lignin based on the TGA result are presented in **Table 7.2**. The thermal degradation of HTT lignin after modification is 2 % higher for HTT lignin+AGE-eq and 10 % higher for HTT lignin+AGE-10 compared to unmodified HTT lignin.
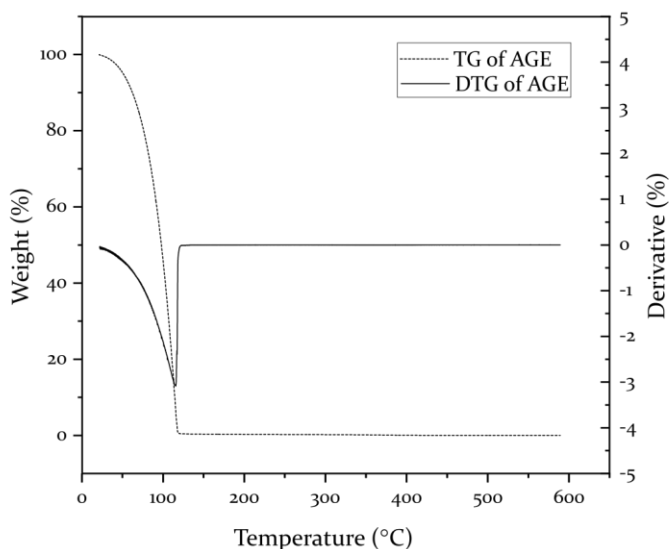
Figure 7.4 TG and DTG thermogram of pure allyl glycidyl ether

Taking into account the thermal decomposition of HTT lignin after modification (i.e., is higher by 2 % and 10 % for HTT lignin+AGE-eq and HTT lignin+AGE-10, respectively) and the quantities of the AGE modifier used for modification (3.4 % of AGE in HTT lignin+AGE-eq and 26.7 % of AGE in HTT lignin+AGE-10), it is determined that the quantity of AGE grafted to the HTT lignin is 57 % (7.3 mmol) for HTT lignin+AGE-eq and as 37 % (47 mmol) for HTT lignin+AGE-10. When compared to the available hydroxyl groups of HTT lignin (12.8 mmol), it is clear that HTT lignin modified with a high AGE content contains a significantly (2.7 times) higher quantity of AGE than that of the hydroxyl groups. This can be interpreted in two ways:

(i) There is a higher degree of grafting of AGE to the HTT lignin surface, which means that the phenolic-OH available in the bulk of HTT lignin is also reactive to AGE

(ii) Under the used reaction condition, the AGE grafted to the HTT lignin surface could have undergone a side reaction, such as homo-polymerization or self-oligomerization via the epoxy ring opening. Although the aforementioned reaction was not observed in the model system conducted at a temperature 10 °C higher, in this case, it might have been caused by adding an excess amount of AGE to the available phenolic-OH groups of HTT lignin. Further investigations with high AGE and model lignin compound, VA, are required to confirm this hypothesis.

As a result, the higher degradation observed with HTT lignin+AGE-10 could be related to the decomposition of grafted AGE and/or the destruction of the oligomerized or polymerized layer grafted on the lignin surface. Previous studies reported that the degradation observed in the range between 350 to 500 °C is related to the destruction of the oligomer or polymer chains formed by AGE.[15,16] In the case of HTT lignin modified with a low amount of AGE, the observed high thermal stability could be due to a lower grafting degree and/or significantly less and/or no formation of oligomers of AGE.

Table 7.2 Weight loss behavior of different HTT lignins

Samples	Initial weight loss at 300 °C (%)	Final weight loss at 600 °C (%)	Mass loss between 300-600 °C (%)
HTT Lignin	4	39	35
HTT Lignin+AGEeq	2	39	37
HTT Lignin+AGE10	2	47	45

To understand how the AGE modification affects the surface area of HTT lignin, the BET surface area was determined and is reported in **Table 7.3**. Generally, the specific surface area correlates with the primary particle size of a filler.[17] The smaller the average particle diameter of the filler, the higher the achieved surface area.[17] There is no significant difference in the specific surface area between the unmodified and modified HTT lignin with low AGE content. In contrast, HTT lignin modified with high AGE content shows a relatively lower surface area than the other samples. The relative surface area is reduced by approximately 50 %. This drastic reduction in the surface area of HTT lignin+AGE-10 could be due to the high grafting degree of AGE or the presence of homo-polymerized or oligomerized AGE structures grafted on the surface of HTT lignin. Such a layer could lead to an increase in the particle size of the filler. This can alter the surface morphology and chemistry and, thus, the interaction with the elastomer.

Table 7.3 Specific surface area (SSA) of un- and AGE-modified HTT lignins determined using N_2 Brunauer-Emmett-Teller (BET) measurement

Samples	SSA values (m^2/g)
HTT Lignin	47±0.05
HTT Lignin + AGE-eq	46±0.05
HTT Lignin+AGE-10	24±0.05

7

To elucidate the chemical structural changes of HTT lignin before and after modification, FTIR of the pure AGE, un- and AGE-modified samples were conducted. The obtained spectra are presented in **Figure 7.5**. The ATR-FTIR spectrum of the pure AGE displays the following characteristic absorption peaks: (i) 3100 cm^{-1} and 990 cm^{-1} representing =C-H tension vibration of alkene; (ii) 2997 cm^{-1} and 2850 cm^{-1} corresponding to asymmetric and symmetric C-H stretching vibrations, respectively; (iii) 1680 - 1650 cm^{-1}, 995 cm^{-1} and 930 cm^{-1} associated with C=C tension vibration; (iv) 1470 cm^{-1} asymmetric flexion vibration of the C-H; (v) 1350 - 1300 cm^{-1} denotes torsion and wagging vibration of methylene; (vi) 1253 cm^{-1}, 913 cm^{-1} and 845 cm^{-1} relating to oxirane ring breathing, antisymmetric and symmetric deformation, respectively.[18–20] The main peaks of unmodified HTT lignin can be found around 1600 cm^{-1}, 1515 cm^{-1}, and 1460 cm^{-1}, representing the aromatic skeleton vibration, C-H deformations (coupled with aromatic skeletal vibrations), and C-H deformations (asymmetric in methyl, methylene, and methoxyl group), respectively.[21] As also stated in **Chapter 3, section 3.3.1**, the vibrations of HTT lignin at 1271 cm^{-1}, 1034 cm^{-1} and 838 cm^{-1} are related to the guaiacyl unit.[21] The detailed peak assignment of different functionalities in HTT lignin is described in **Chapter 3**.

The grafting of AGE to HTT lignin can be evidenced by the following changes in the modified HTT lignin: (i) the absence of characteristic peaks of epoxy at 1253, 913, and 845 cm^{-1}, (ii) an increase in the absorption band around 3300 - 3400 cm^{-1} related to the stretching vibrations of -OH group[22] and C-O stretching vibrations of secondary alcohol around 1270 cm^{-1}, (iii) decrease in the adsorption bands around 3600 cm^{-1} corresponding to the phenolic hydroxy group[23] and (iv) increase in the vibrations in the region between 1000 - 1100 cm^{-1} associated with ether moieties. These changes suggest that the epoxy ring opening reaction occurred, and the phenolic hydroxy groups are involved in the coupling reactions with AGE, resulting in an ether bond (C-O-C). Further changes observed in the spectra of the AGE-modified HTT lignin sample are the increase in absorption of C-H stretching (3100 - 2850 cm^{-1}), C=C around 1690 - 1660 cm^{-1} and 990 cm^{-1}, asymmetric flexion of C-H at 1465 cm^{-1}, and =C-H at 924cm^{-1} related with vinyl groups of AGE compared to unmodified HTT lignin:[20,24,25] Notably, for HTT lignin modified with high AGE content, significant changes are observed in these characteristic peaks. Conversely, the low AGE-modified sample shows only a slight effect on the corresponding peaks, indicating a minor alteration in the structure of the HTT lignin. This difference could be related to the degree of grafting of AGE to the HTT lignin.
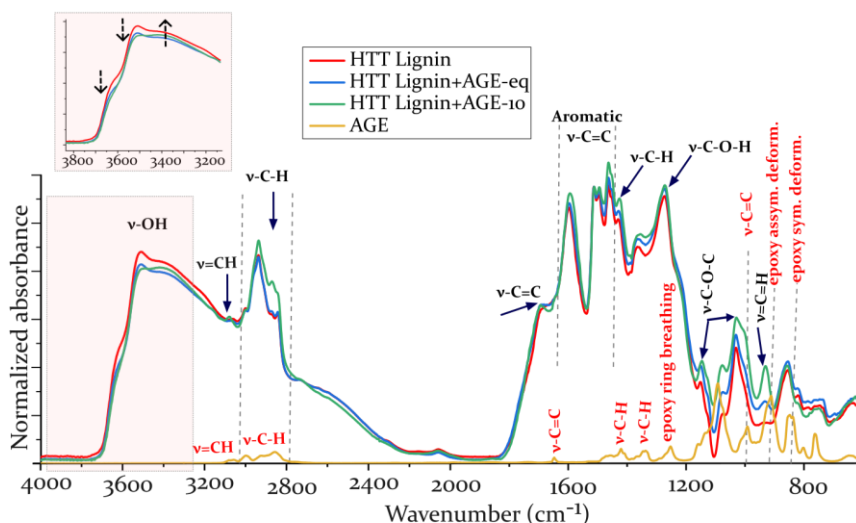
Figure 7.5 ATR-FTIR spectra of AGE and DRIFT spectra of unmodified and AGE-modified HTT lignins. The HTT lignin spectra were normalized with respect to the peak of the aromatic carbon band (1600 - 1500 cm⁻¹)

The ^{13}C NMR spectra of unmodified and AGE-modified HTT lignin presented in **Figure 7.6** further demonstrate the change in the chemical structure due to the AGE modification. Detailed descriptions of the ^{13}C spectral changes in HTT lignin can be found in **Chapter 3**, **section 3.3.1.** In the ^{13}C NMR spectra of AGE-modified HTT lignins, the peak corresponding to the epoxy ring (carbon e and f in the chemical structure in **Figure 7.2**) could not be identified between 40 - 50 ppm. Additionally, three new peaks corresponding to the carbon resonances of AGE (carbon a*- 115 ppm, carbon b*- 135 ppm, and carbon c*, f*, e*, d*- 64 - 80 ppm, in the chemical structure in **Figure 7.2**) are observed upon modification. Minor changes in the aromatic carbon peaks of HTT lignin are apparent when modified with a low AGE content. However, when modified with an HTT lignin with high AGE content, significant changes in the aromatic carbon peak intensity are observed, with an additional new peak around 152 ppm corresponding to the ether formation. These findings are consistent with other analyses (liquid ^{13}C NMR of model study and DRIFT), indicating that the catalyst-activated epoxy ring-opening reaction can attach to the HTT lignin. Based on the observed peak intensities, it can be concluded that the impact of AGE on the chemical structure of HTT lignin depends upon the quantity of AGE grafted onto the lignin.
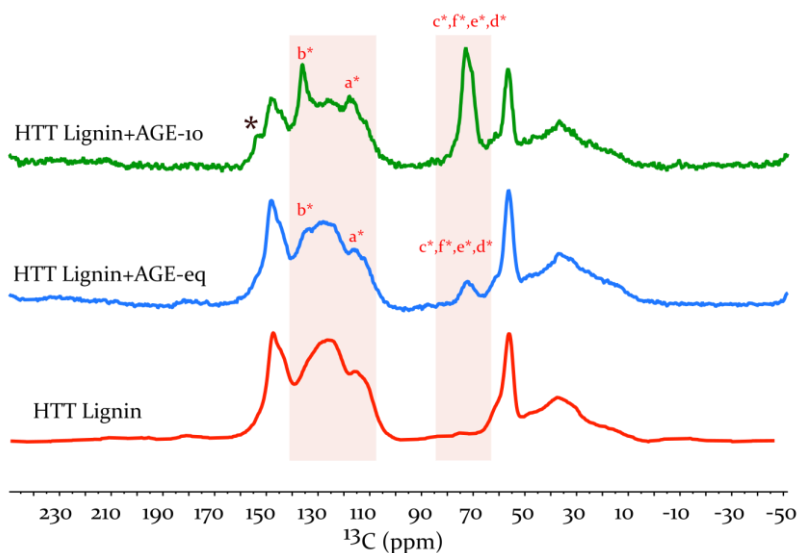
Figure 7.6 Solid state ^{13}C NMR spectra of un- and AGE-modified HTT lignins. The labels (a*, b*, c*, d*, e*, f*) denote the resonances due to carbon atoms in the AGE {The asterisk * represents the resonance due to AGE-HTT lignin coupling}

The XRD profiles of unmodified and AGE-modified HTT lignin powder samples are shown in **Figure 7.7**. The data reveals the variations in the phase characteristics of HTT lignin due to modification. It can be observed that all the lignin samples demonstrate two broad peaks in the range between 12° to 32° (region I) and between 34° to 47° (region II).[26] By functionalizing HTT lignin with a high concentration of AGE (HTT Lignin+AGE-10), a significant increase in the peak intensity of region I is observed compared to the unmodified HTT lignin. In contrast, such a drastic change in the peak intensities is not observed for HTT lignin modified with a low AGE content. This indicates that incorporating a high AGE content for modification changes the stacking of the HTT lignin. The observed change in stacking may be attributed to the scattering effect caused by AGE functionalization and/or an oligomerized or homopolymerized epoxy formed on the HTT lignin surface.[3]
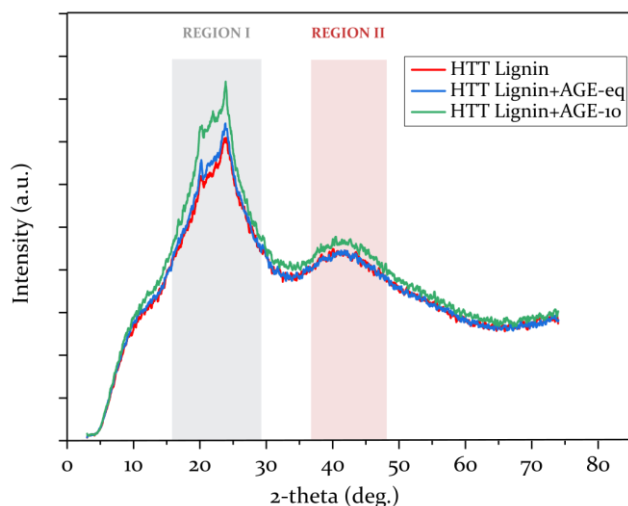
Figure 7.7 X-ray diffraction curves of un- and AGE-modified HTT lignins

The conducted studies have clearly demonstrated that the chemical grafting of AGE to the HTT lignin surface has taken place. Similar to the model study, the coupling reaction with AGE involves phenolic hydroxyl groups. When HTT lignin is modified with high AGE content, thermal decomposition behavior and phase characteristics of the HTT lignin are significantly altered. Furthermore, the surface area of the HTT lignin modified with a high AGE content is drastically changed compared to the unmodified one. This indicates either a high degree of AGE grafting or the formation of homopolymerized or oligomerized AGE structures via the secondary -OH groups generated by the epoxy ring-opening reaction. The reaction scheme of AGE and HTT lignin in the presence of high AGE content is proposed in **Scheme 7.2**. In contrast, HTT lignin modified with low AGE content demonstrated no change in the physical properties of HTT lignin.

7

Scheme 7.2 Possible reactions of AGE with HTT lignin in the presence of 1-MIM catalyst: (A) grafting and (B) homo-polymerization or self-oligomerization of AGE on the HTT lignin surface
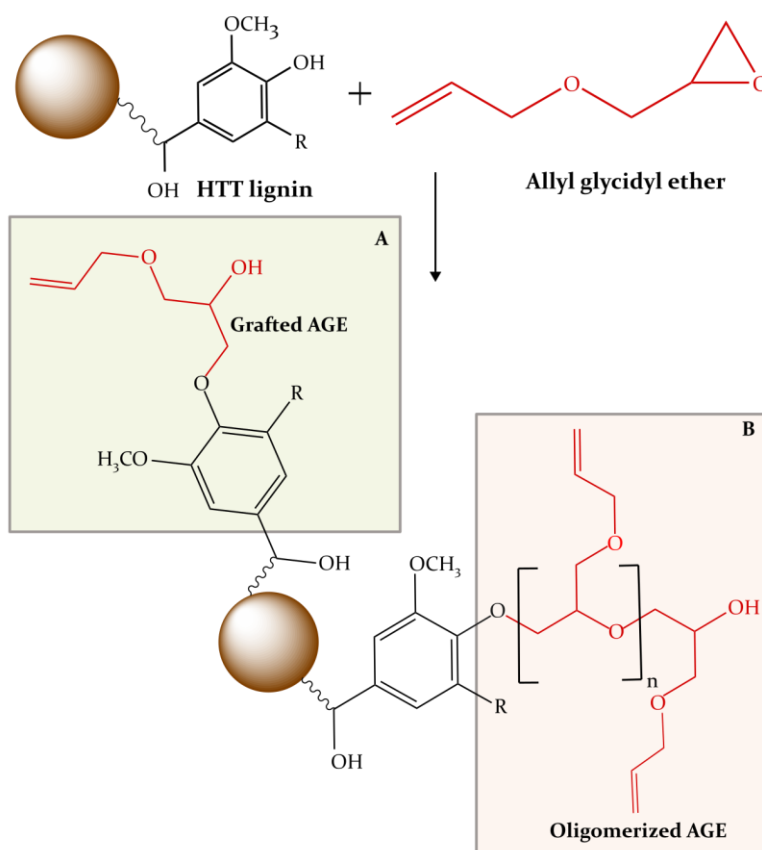
7.3.3 Impact of AGE pre-modification on in-rubber properties

In-rubber studies were performed to understand the behavior and influence of two different AGE-modified HTT lignins on the reinforcing properties.

A comparison of the Payne effect behavior of the different HTT lignin-filled compounds in the uncured state is presented in **Figure 7.8**. The storage moduli (G') of all the filled compounds at low and high strains show no difference in whether they are modified or not. It was expected for HLAGE-10 that a lower Payne effect (calculated from the difference in storage moduli of low and high strain) would be achieved compared to HLAGE-eq and HLR due to the increased shielding effect offered by grafting and side reactions of AGE. However, all samples have a similar Payne effect. This similar Payne effect indicates that the functionalization of HTT lignin using AGE does not introduce any secondary filler structure. Consequently, the filler-filler interaction is not increased in the rubber matrix. Furthermore, it indicates that the modification of HTT lignin by AGE does

not change the existing filler-filler interaction. Thus indicating that the level of dispersion of the filler particles in all the compounds falls within a similar range.
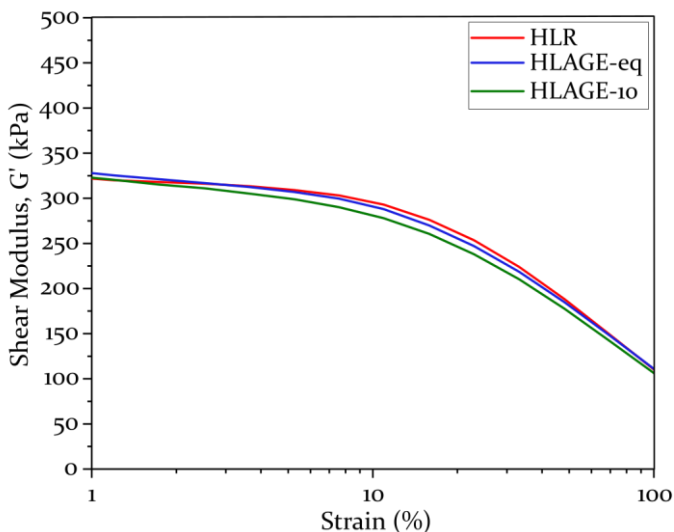
Figure 7.8 Payne (uncured) behavior of un- and AGE-modified HTT lignin-filled SSBR compounds

The unchanged G' value at 100 % strain of the modified compounds compared to that of the unmodified one suggests that the coupling reaction between the allyl groups on the modified filler and the rubber molecules has not occurred during mixing. Thus, all the compounds exhibit the same level of filler-polymer interaction.

The curing characteristics of compounds containing un- and AGE-modified HTT lignins are depicted in **Figure 7.9**. It can be observed that the AGE modification has a significant impact on the cure behavior of HTT lignin-filled rubber, resulting in a decrease in scorch time and an increase in the cure kinetics. This effect could be due to the following reasons:

(i) the surface modification reduces the adsorption of curing chemicals, and

(ii) the presence of allyl groups on the HTT lignin can initiate and participate in the crosslinking process.

The scorch safety of the compounds increases in the following order:

HLAGE-10 < HLAGE-eq < HLR

This finding provides further evidence that AGE molecules effectively cover the surface of HTT lignin. The results of the cure parameters for unmodified and AGE-modified HTT lignins are listed in **Table 7.4**.
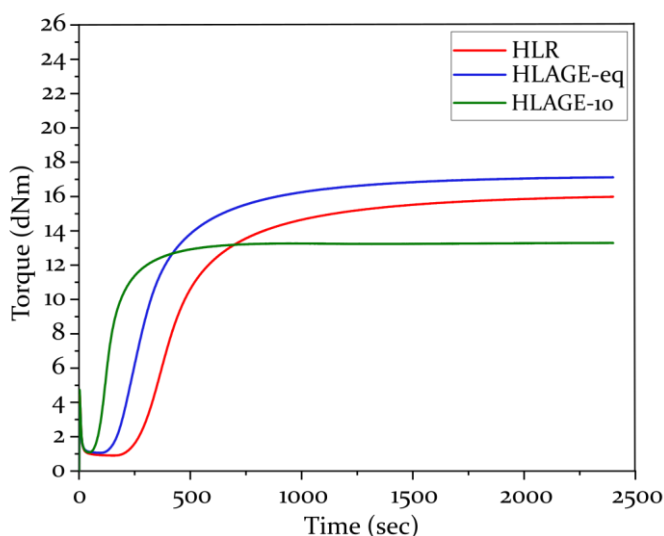
Figure 7.9 Cure properties of un- and AGE-modified HTT lignin-filled SSBR compounds

Table 7.4 Obtained cure parameters and apparent CLD by swelling of different HTT lignin-filled SSBR vulcanizates

Description	HLR	HLAGE-eq	HLAGE-10
t_{S_2} (min)	5.2	3.3	1.7
$t_{c,90}$ (min)	15.8	12.5	5.2
M_H (dN.M)	16	17	13
M_L (dN.m)	0.9	1.1	1.1
$\Delta M, M_H-M_L$ (dN.m)	15.1	15.9	11.9
Apparent CLD ($x10^{-4}$ mol/cm³)	2.02±0.04	2.22±0.02	1.52±0.04

Between the modified HTT lignin-filled compounds, the ones modified using a low AGE content (HLAGE-eq) exhibit the highest maximum torque (M_H). This indicates that HLAGE-eq displays an increased filler-polymer and/or polymer-polymer interaction compared to the compound containing un- and modified-HTT lignin with high AGE content (HLAGE- 10). The reduction in the M_H for HLAGE-10 could be attributed to two reasons: (i) the presence of a high concentration of reactive sites (allyl groups), which can consume the available sulfur and connect two allyl groups, thereby affecting the rubber crosslinking[1]; (ii) the formed homo-polymerized or oligomerized AGE on the lignin surface, which alters the surface activity of the filler and generates fewer connection

points for interaction with rubber, thus reducing physical filler-polymer interactions. The possible coupling of HTT lignin modified with high AGE to the rubber during vulcanization is depicted in **Scheme 7.3**.

Scheme 7.3 Possible mechanism of coupling between modified HTT lignin using high AGE content and the rubber during vulcanization
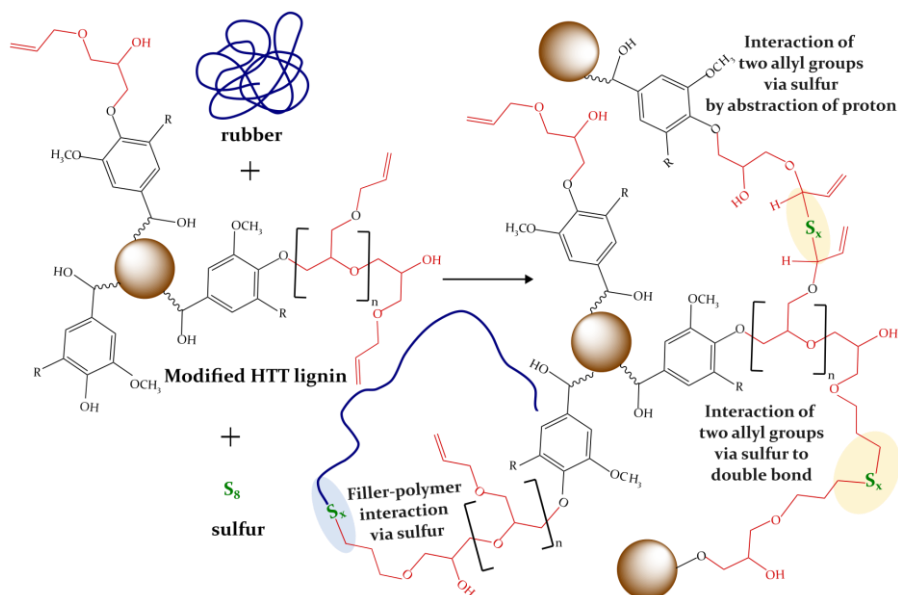
Table 7.4 also reports the apparent CLD value determined by swelling in toluene, which reveals that HLAGE-10 has a lower value than HLR and HLAGE-eq. This finding is consistent with the achieved M_H value (see **Table 7.4**), implying that the grafted allyl groups and/or the presence of an oligomerized or homopolymerized layer of AGE have a detrimental impact on the interactions between the polymer-polymer and filler-polymer. Conversely, the higher apparent CLD of HLAGEeq compared to HLR suggests that the grafted allyl groups did not consume sulfur for self-crosslinking and that the allyl moieties only play a role in the chemical coupling of the filler to the polymer without drastically affecting the filler-polymer filler-filler and polymer-polymer interactions. The significant difference between HLAGEeq and HLAGE-10 could be due to the difference in the grafting density of the AGE.

The stress-strain curves of the vulcanizates of SSBR with 40 phr filler loading of different lignins are shown in **Figure 7.10**. The HTT lignin modified with a low AGE-filled compound shows a significant increase in the modulus and a decrease in elongation at break compared to the unmodified one. This indicates that a strong interaction between HTT lignin and the rubber is achieved with the AGE modification. These findings suggest that grafting fewer allyl groups on the HTT lignin surface leads to minor or negligible self-

crosslinking reactions. This is in line with the results of the apparent CLD and maximum torque M_H. However, the achieved tensile strength of HLAGE-eq (7 MPa) did not change substantially compared to the HLR compound. This could be related to the degree of dispersion of the modified HTT lignin in the rubber matrix. It is expected that a better dispersion of filler can lead to a higher reinforcement.[27] As the surface area of the modified and unmodified HTT lignins (refer to **Table 7.3**) and the formed filler clusters in the rubber matrix (refer to **Figure 7.8**) are similar, the quality of dispersion of the filler might be unaffected. Thus, the achieved tensile strength seems to be similar.
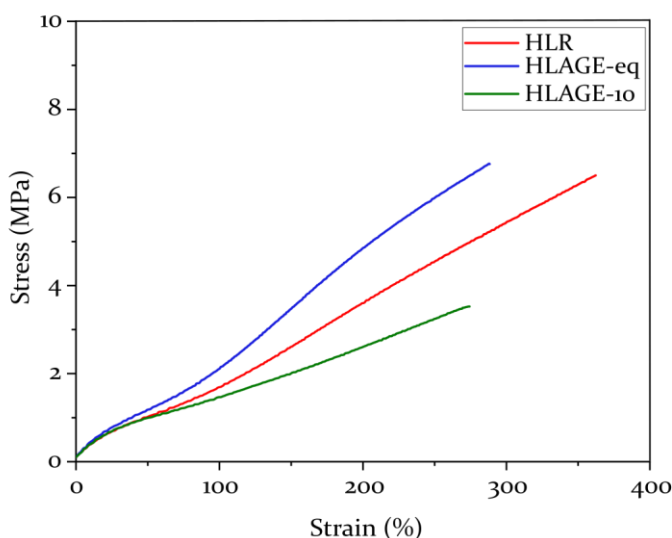
Figure 7.10 Stress-strain properties of different HTT lignin-filled SSBR vulcanizates

In the case of the vulcanizate containing modified HTT lignin with high AGE content, there is an appreciable reduction in modulus, tensile strength, and elongation at break. The obtained mechanical properties of HLAGE-10 are in line with the results of the achieved maximum torque (M_H) and apparent CLD values (**Table 7.4**). The decrease in tensile modulus and tensile strength of HLAGE-10, when compared to HLR, can be explained by the two theories: (i) self-crosslinking of allyl groups in the presence of sulfur[1] can reduce the chemical filler-polymer and polymer-polymer interaction; (ii) the low specific surface area of the modified lignin (**Table 7.3**) as a result of oligomerized or homopolymerized AGE can reduce the number of access points for the rubber, which in turn can reduce the physical and/or chemical interactions between filler and elastomer chains. The comparatively shorter elongation at break could be due to the following reasons: (a) a lower number of formed crosslinks (apparent CLD values in **Table 7.4**); (b) the formation of more mono-sulfidic crosslinks instead of di- or poly-sulfidic linkages; and (c) a combination of a and b. The mono-sulfidic type of crosslinking could be formed due to higher concentrations of allyl groups in the HLAGE-10 compared to HLAGE-eq. Further studies are needed to evaluate the distribution of different types of crosslinks in the modified and unmodified HTT lignin-filled compounds. The modification of HTT

lignin with a high AGE content has a substantial impact on the filler-filler, filler-polymer, and cross-linking of the rubber chains and, hence, on the rubber performance of AGE-modified HTT lignin (HLAGE-10). This is most likely due to two side reactions of AGE when used in high concentration: (i) oligomerization or homopolymerization of AGE on the HTT lignin surface during modification and (ii) self-crosslinking of AGE in the rubber matrix during rubber vulcanization.

Furthermore, it is also found that the obtained mechanical properties of the AGE-modified HTT lignin-filled vulcanizate (HLAGE-eq) are significantly lower than those of the reinforcing carbon black, CB (N330) filled vulcanizate, as discussed in **Chapter 6**. This is due to the difference in the primary particle size (surface area N330 - 78 m²/g vs HTT lignin+AGE-eq – 46 m²/g) and the different surface chemistry of the compared fillers. The lower reinforcing power of HLAGE-eq compared to the reinforcing CB, N330, suggests that further improvement in filler characteristics (particle size, structure, and surface chemistry) is required.

7.4 Conclusions and Recommendations

The potential of allyl glycidyl ether (AGE) as a non-silane coupling agent for HTT lignin was explored in this chapter. The initial study conducted using a lignin model substance, vanillyl alcohol (VA), and AGE in the presence of 1-methylimidazole (1-MIM) catalyst demonstrates that the ring opening reaction of epoxy occurs and AGE couples to the phenolic hydroxyl groups of VA. This study was further extended to modify HTT lignin filler. Two different concentrations (low and high) of AGE were employed to etherify HTT lignin. This was followed by the characterization and mixing of the pre-modified lignins in solution styrene butadiene rubber (SSBR) to evaluate their reinforcing performance. The characterization of AGE-modified HTT lignin revealed that AGE is grafted to the HTT lignin surface at both concentrations. However, when a high AGE content is used to functionalize HTT lignin, the thermal stability and phase characteristics of HTT lignin are much more affected than those observed for a low amount. In addition to this, the obtained surface area of modified HTT lignin with high AGE content is significantly lowered compared to the unmodified and modified HTT lignin with low AGE content. When the high AGE-modified HTT lignin is added to SSBR as a filler, it profoundly influences the obtained in-rubber properties. In particular, the apparent crosslink density and mechanical properties of HTT lignin-filled SSBR vulcanizates (HLAGE-10) are negatively affected. These observed effects are supposed to be caused by the high grafting of AGE or the formed oligomerized and/or homopolymerized AGE on the surface of HTT lignin at increased AGE concentration. It was conceptualized that the presence of a high amount of AGE containing allyl groups consumes the available free sulfur in the rubber compound and uses it to crosslink itself rather than coupling the filler to the rubber. This results in a reduction of the chemical filler-polymer interaction and rubber crosslinking. In contrast, the addition of pre-modified HTT lignin prepared with low AGE content (HLAGE-eq) demonstrated better cure and mechanical properties than the unmodified HTT lignin and HLAGE-10. The positive effects of the HLAGE-eq were attributed to the

7

chemical coupling between HTT lignin and rubber via the allyl groups of grafted AGE, leading to increased filler-polymer interaction.

Nevertheless, the achieved rubber reinforcement is still lower than the reinforcing carbon black (N330). This is mainly due to the still significantly lower specific surface area of HTT lignin (46 m²/g) compared to carbon black (78 m²/g) and due to the difference in surface chemistry of both fillers. These factors strongly influence the interfacial interaction between HTT lignin and the rubber and the resulting in-rubber performance. It was assumed that a higher AGE content would lead to better reinforcing properties of HTT lignin-filled compound; surprisingly, the results of the HLAGE-10 study show the opposite effect. This may be observed due to two unfavorable reactions: (i) the self-oligomerization of AGE via the formed secondary alcohol on the HTT lignin surface during modification and (ii) the self-crosslinking of the grafted AGE on the lignin surface via the free sulfur during vulcanization.

Further optimization studies are needed to identify the correct quantity of AGE that can efficiently change the surface chemistry of the HTT lignin, which at the same time does not generate oligomerized and crosslinked structures of AGE. The following studies can be carried out with AGE agent to enhance the mechanical properties of HTT lignin further filled SSBR:

- Identify the optimum amount of AGE required for modification of HTT lignin. A series of experiments varying the AGE concentrations (between equimolar to 10 times the molar amount of hydroxyl groups of HTT lignin) in the presence of 1-MIM.

- Use a different catalyst than 1-methylimidazole, for example, a secondary imidazole, 2-methylimidazole, or an adjustment of the catalyst amount that can result in 100 % grafting of AGE to HTT lignin when an equimolar quantity is used.

- As the allyl groups of AGE are assumed to consume sulfur for self-crosslinking reaction, a sulfur content optimization study can be performed for the HLAGE-10 compound to enhance the mechanical properties.

Other epoxide-type coupling agents, such as epoxidized polybutadiene and Thioplast®EPS polysulfides, can be investigated as alternative surface modifiers for HTT lignin.
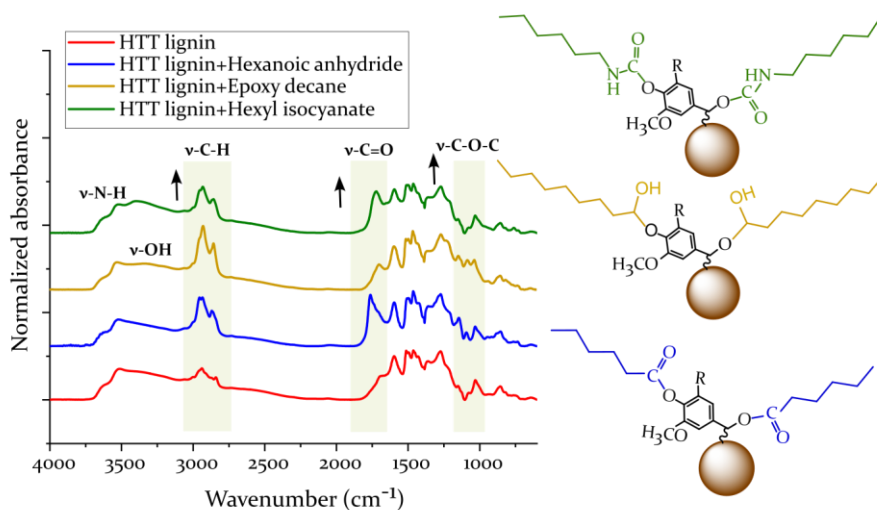
7

Supporting Information

Figure S7.1 DRIFT spectra of unmodified-, hexanoic anhydride-, epoxy decane-, and hexyl isocyanate-modified HTT lignins
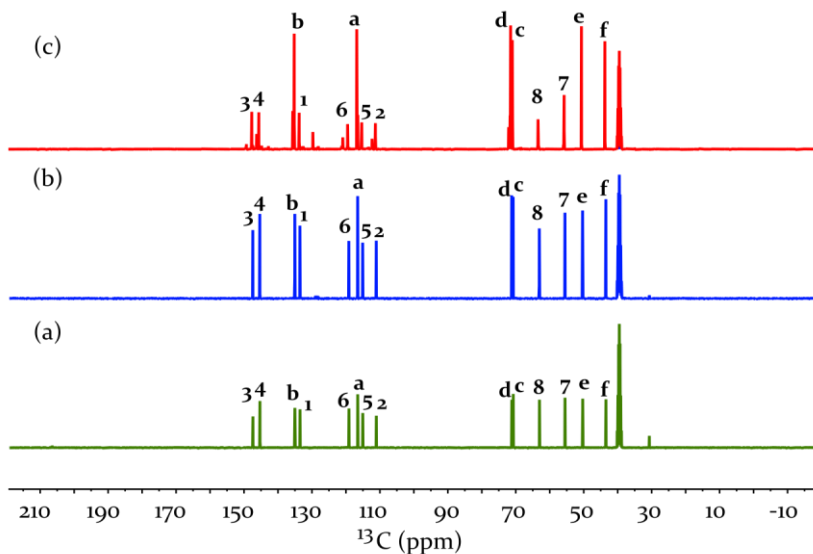

Figure S7.2 ^{13}C NMR spectra of vanillyl alcohol (VA) and allyl glycidyl ether (AGE) reacted for 1 h at different temperatures: (a) 40 °C; (b) 75 °C; and (c) 150 °C without 1-methylimidazole (1-MIM)
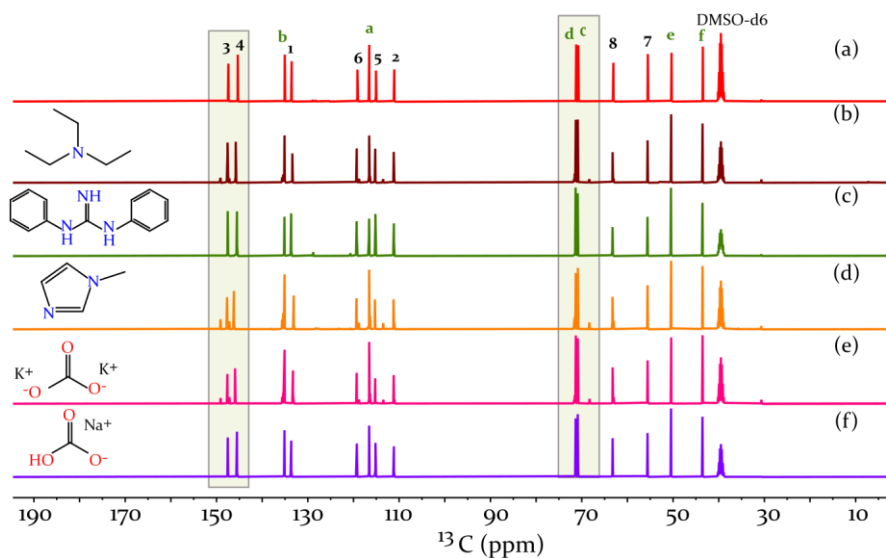
Figure S7.3 ^{13}C NMR spectra of vanillyl alcohol (VA) and allyl glycidyl ether (AGE): (a) without catalyst; and with catalysts (b) triethylamine (TEA); (c) diphenyl guanidine (DPG); (d) 1-methyl imidazole (1-MIM); (e) potassium carbonate (K$_2$CO$_3$); (f) sodium bicarbonate (NaHCO$_3$) reacted at 75 °C for 1 h

7

References

(1) Park, S.; Chung, M.; Lamprou, A.; Seidel, K.; Song, S.; Schade, C.; Lim, J.; Char, K. High Strength, Epoxy Cross-Linked High Sulfur Content Polymers from One-Step Reactive Compatibilization Inverse Vulcanization. Chem Sci 2021, 13 (2), 566–572.

(2) Cetin, N. S.; Hill, C. A. S. An Investigation of the Reaction of Epoxides with Wood. Journal of Wood Chemistry and Technology 1999, 19 (3), 247–264.

(3) Casarano, R.; Matos, J. R.; Fantini, M. C. A.; Petri, D. F. S. Composites of Allyl Glycidyl Ether Modified Polyethylene and Cellulose. Polymer 2005, 46 (10), 3289–3299.

(4) Alwadani, N. S.; Fatehi, P. Modification of Kraft Lignin with Dodecyl Glycidyl Ether. ChemistryOpen 2019, 8 (10), 1258–1266.

(5) Tänzer, W.; Reinhardt, S.; Fedtke, M. Reaction of Glycidyl Ethers with Aliphatic Alcohols in the Presence of Benzyl Dimethylamine. Polymer 1993, 34 (16), 3520–3525.

(6) Baidya, M.; Brotzel, F.; Mayr, H. Nucleophilicities and Lewis Basicities of Imidazoles, Benzimidazoles, and Benzotriazoles. Org. Biomol. Chem. 2010, 8 (8), 1929–1935.

(7) Fulmer, G. R.; Miller, A. J. M.; Sherden, N. H.; Gottlieb, H. E.; Nudelman, A.; Stoltz, B. M.; Bercaw, J. E.; Goldberg, K. I. NMR Chemical Shifts of Trace Impurities: Common Laboratory Solvents, Organics, and Gases in Deuterated Solvents Relevant to the Organometallic Chemist. Organometallics 2010, 29 (9), 2176–2179.

(8) Spectral Database for Organic Compounds. https://sdbs.db.aist.go.jp (National Institute of Advanced Industrial Science and Technology) (accessed 2022-09-01).

(9) Lee, B. F.; Kade, M. J.; Chute, J. A.; Gupta, N.; Campos, L. M.; Fredrickson, G. H.; Kramer, E. J.; Lynd, N. A.; Hawker, C. J. Poly(Allyl Glycidyl Ether)-A Versatile and Functional Polyether Platform. J. Polym. Sci. A Polym. Chem. 2011, 49 (20), 4498–4504.

(10) Obermeier, B.; Frey, H. Poly(Ethylene Glycol-Co-Allyl Glycidyl Ether)s: A PEG-Based Modular Synthetic Platform for Multiple Bioconjugation. Bioconjugate Chem. 2011, 22 (3), 436–444.

(11) Mitani, R.; Yamamoto, H.; Sumimoto, M. Theoretical Study on the Reaction Mechanism of Imidazole-Catalyzed Phenol-Epoxy Ring-Opening Reaction and the Evaluation of Catalyst Performance. Chemical Physics Letters 2020, 742, 137143.

(12) Pham-Ho, M.-P.; Pham, B.; Huynh, L.; Pham, H.; Marks, M.; Truong, T. Density Functional Theory Study on Mechanisms of Epoxy-Phenol Curing Reaction. Journal of computational chemistry 2014, 35.

(13) Amit, T. A.; Roy, R.; Raynie, D. E. Thermal and Structural Characterization of Two Commercially Available Technical Lignins for Potential Depolymerization via Hydrothermal Liquefaction. Current Research in Green and Sustainable Chemistry 2021, 4, 100106.

(14) Milotskyi, R.; Szabó, L.; Takahashi, K.; Bliard, C. Chemical Modification of Plasticized Lignins Using Reactive Extrusion. Frontiers in Chemistry 2019, 7, 633.

(15) Şolpan, D.; Güven, O. Thermal Stability of the Copolymers of Allyl Glycidyl Ether with Acrylonitrile and Methyl Methacrylate Obtained via Gamma Irradiation1. Radiation Physics and Chemistry 2000, 57, 173–177.

7

(16) Mallela, Y. L. N. K.; Kim, S.; Seo, G.; Kim, J. W.; Kumar, S.; Lee, J.; Lee, J.-S. Crosslinked Poly(Allyl Glycidyl Ether) with Pendant Nitrile Groups as Solid Polymer Electrolytes for Li–S Batteries. Electrochimica Acta 2020, 362, 137141.

(17) DeArmitt, C.; Rothon, R. Particulate Fillers, Selection, and Use in Polymer Composites. In Encyclopedia of Polymers and Composites; Palsule, S., Ed.; Springer: Berlin, Heidelberg, 2014; pp 1–19.

(18) Manakhov, A.; Fuková, Š.; Nečas, D.; Michlíček, M.; Ershov, S.; Eliaš, M.; Visotin, M.; Popov, Z.; Zajíčková, L. Analysis of Epoxy Functionalized Layers Synthesized by Plasma Polymerization of Allyl Glycidyl Ether. Physical Chemistry Chemical Physics 2018, 20 (30), 20070–20077.

(19) García Quintero, A.; Palencia, M. Theoretical and Experimental Study of the Functionalization Reaction of Allyl Glycidyl Ether with Sodium Hydrosulfide. Journal of Science with Technological Applications 2020, 9, 9–17.

(20) Viviani, M.; Laurens Meereboer, N.; Ananda Saraswati, N. L. P.; Loos, K.; Portale, G. Lithium and Magnesium Polymeric Electrolytes Prepared Using Poly(Glycidyl Ether)-Based Polymers with Short Grafted Chains. Polymer Chemistry 2020, 11 (12), 2070–2079.

(21) Boeriu, C. G.; Bravo, D.; Gosselink, R. J. A.; van Dam, J. E. G. Characterisation of Structure-Dependent Functional Properties of Lignin with Infrared Spectroscopy. Industrial Crops and Products 2004, 20 (2), 205–218.

(22) Momayez, F.; Hedenström, M.; Stagge, S.; Jönsson, L. J.; Martín, C. Valorization of Hydrolysis Lignin from a Spruce-Based Biorefinery by Applying γ-Valerolactone Treatment. Bioresource Technology 2022, 359, 127466.

(23) Md Salim, R.; Asik, J.; Sarjadi, M. S. Chemical Functional Groups of Extractives, Cellulose and Lignin Extracted from Native Leucaena Leucocephala Bark. Wood Sci Technol 2021, 55 (2), 295–313.

(24) Naserifar, S.; Kuijpers, P. F.; Wojno, S.; Kádár, R.; Bernin, D.; Hasani, M. In Situ Monitoring of Cellulose Etherification in Solution: Probing the Impact of Solvent Composition on the Synthesis of 3-Allyloxy-2-Hydroxypropyl-Cellulose in Aqueous Hydroxide Systems. Polym. Chem. 2022, 13 (28), 4111–4123.

(25) Ibrahim, M.; Iqbal, A.; Shen, C.; Bhawani, S.; Adam, F. Synthesis of Lignin Based Composites of TiO2 for Potential Application as Radical Scavengers in Sunscreen Formulation. BMC Chemistry 2019, 13.

(26) Jo, H.; Park, D.; Joo, M.; Choi, D.; Kang, J.; Ha, J.-M.; Kim, K. H.; Kim, K. H.; An, S. Performance-Enhanced Eco-Friendly Triboelectric Nanogenerator via Wettability Manipulation of Lignin. EcoMat 2023, 5 (11), 12413–12427.

(27) Limper, A. Mixing of Rubber Compounds; Hanser Publications: Cincinnati, Ohio, 2012.

7

8. Conclusions and Recommendations

The primary objective of this study was to examine the reinforcing potential of hydrothermally treated (HTT) lignin in a non-polar rubber. In pursuit of this objective, various surface modifiers, such as silane- and non-silane-based ones, were identified, and their impact on the reinforcing properties of the HTT lignin-filled rubber compound was evaluated. Furthermore, the study investigated the functional groups involved in the coupling reaction between HTT lignin and the different surface modifiers. This chapter summarizes the key findings of this research and underscores the need for further studies to optimize the coupling efficiency of surface modifiers, a crucial step in enhancing the reinforcing potential of HTT lignin. Suggestions for further research are also provided.

8.1 Conclusions

The primary investigation conducted in this research was the evaluation of the reinforcing capability of hydrothermally treated (HTT) Kraft lignin in comparison to the initial feedstock Kraft lignin, conventional reinforcing carbon black and silica filler. This comparative study was performed in solution styrene butadiene/butadiene rubber (SSBR/BR) using a conventional mixing technique, i.e., mixing rubber, filler, and all other ingredients in an internal mixer, and was discussed in **Chapter 3**. The study demonstrated that the hydrothermal process significantly impacts the filler characteristics of Kraft lignin. Consequently, the reinforcing properties of the HTT lignin-filled SSBR/BR compound were superior to that of the initial feedstock Kraft lignin-filled one. The high reinforcing effects of HTT lignin were attributed to the reduced oxygen-containing functional groups and smaller primary particles (or higher BET specific surface area) compared to Kraft lignin. This led to a better dispersion of HTT lignin in the rubber matrix, as evidenced by the atomic force microscopy (AFM) studies. However, compared to the conventional reinforcing carbon black and silica, the reinforcing power of HTT lignin in the investigated rubber system is relatively low. It was ascribed to its low BET specific surface area (SSA - 37 m²/g) and the presence of still a high content of polar functional groups, which led to poor compatibility with the polar rubber. Furthermore, the HTT lignin-filled compound exhibited an extended scorch time and a slower cure rate than silica- and carbon black-filled ones. This indicates that a considerable amount of accelerators and/or curatives could be absorbed at the HTT lignin surface. This study emphasizes that the currently available form of HTT lignin cannot directly replace the reinforcing fillers carbon black and silica in SSBR/BR for tire application. Therefore, further improvements in the properties of HTT lignin filler are necessary.

To enhance the reinforcing potential of HTT lignin in rubber compounds, further studies were conducted to investigate the effects of altering one of the filler characteristics – surface chemistry – via surface modification. Two different classes of modifiers, silane- and non-silane-based ones, were investigated for this purpose. In the case of silane-based modifiers, the modification reactions were performed in-situ during the mixing of rubber compounds. For non-silane-based modifiers, the modification of HTT lignin was carried out ex-situ before the rubber mixing procedure to avoid any side reactions of selected modifiers with other rubber ingredients. The reinforcing potential of the modified HTT lignin rubber compounds was evaluated in terms of cure, filler-filler interaction, and mechanical properties.

Chapter 4 examined different silane-based coupling (bifunctional-modifier containing filler and rubber reactive functionalities) and shielding (monofunctional-modifier having only a filler reactive group) agents as surface modifiers for HTT lignin. The study showed that the use of specific silane coupling agents, namely, unblocked or shielded thiol, (3- mercaptopropyl)monoethoxy polyether silane (Si363®/MPMEPS), and sulfur silane, bis(triethoxysilylpropyl)tetrasulfide (Si69®/TESPT), enhances the in-rubber properties of

HTT lignin-filled compound compared to the shielding ones. However, these types of silane (TESPT and MPMEPS) developed sponge-like HTT lignin clusters in the rubber matrix, which negatively affected the micro-dispersion of HTT lignin in the rubber matrix. Conversely, such clusters were not detected while using blocked thiol silane, octanoylthio-1 propyltriethoxysilane (NXT®/OTPTES) and showed filler dispersion similar to that of unmodified HTT lignin-filled vulcanizate. Surprisingly, the resulting mechanical properties of OTPTES containing HTT lignin-filled SSBR/BR were found to be comparatively inferior to those of the TESPT- and MPMEPS-containing HTT lignin-filled compounds. This study revealed that the effects of silane coupling agents in HTT lignin-filled rubber compounds vary depending on the type of silane used, and only those containing reactive sulfur moieties were observed to impact the performance of HTT lignin-filled compounds positively. This observation raised ambiguities in the mechanism of silane modification reactions.

In **Chapter 5**, model reactivity studies were conducted to elucidate the coupling mechanism of silane and HTT lignin. Lignin model substances (guaiacol and vanillyl alcohol) and different surface modifiers, such as trimethylethoxy silane, 1-hexane thiol, and mercaptopropyltriethoxysilane, were used for this investigation. A comprehensive NMR analysis carried out on the different modified lignin model substances revealed that the ethoxysilyl (or the generated silanol upon hydrolysis) functionality of the silane is almost unreactive towards HTT lignin, while the silane is coupled to the HTT lignin via the thiol group. Additionally, the silane-coupled HTT lignin via the thiol group is attached to another silane-modified HTT lignin by condensation of the available ethoxysilyl (or the silanol) functionality on the surface. This resulted in the formation of HTT lignin clusters. Thus, the results of the study indicate that the coupling mechanism of HTT lignin with silane is different from that of traditional silica-silane coupling. In other words, the reactivity of the functional groups of HTT lignin, i.e., the phenolic and aliphatic hydroxyl group (C-OH), towards the silane is different from that of silanol groups (Si-OH) of silica. Based on these findings, a new coupling mechanism was postulated for HTT lignin-silane through a thiol group. The study suggests that results discussed in the prior literature need to be re-evaluated using the latest knowledge on the coupling mechanism of HTT lignin-silane. The low performance of the OTPTES-modified HTT lignin-filled SSBR/BR compound discussed in **Chapter 4** can be attributed to the findings of this study. Specifically, the absence of free thiol in OTPTES (blocked thiol silane) hinders its coupling with HTT lignin. The deblocking reaction of octanoyl groups in OTPTES is expected to occur in the presence of rubber accelerators that are added to the rubber compound during the second mixing stage. It is also inferred that when a coupling reaction between a reactive sulfur or thiol silane and HTT lignin occurs in the rubber matrix, as in the case of TESPT- and MPMEPS-modified HTT lignin-filled SSBR/ BR compounds, it can trap some rubber chains within the filler cluster formed as a result of the condensation reaction taking place between the unreacted ethoxysilyl functionalities. This simultaneous coupling and condensation reaction forms sponge-like filler clusters in the rubber matrix.

8

Besides, there is also a possibility that the (un)hydrolyzed ethoxysilyl groups on the silane-modified HTT lignin surface can undergo condensation with the triethoxysilyl groups of end-chain functionalized SSBR rubber. Consequently, this increases the degree of chemical filler-polymer interactions in TESPT- and MPMEPS-modified HTT lignin-filled SSBR/BR and thus resulting in higher mechanical properties than the other silane-modified and unmodified HTT lignin-filled compounds.

With this newly gained knowledge of the HTT lignin/thiol interaction, **Chapter 6** investigated the thiol agent as a non-silane-based surface modifier for HTT lignin. Two different thiol-based coupling agents, 1,2-bis(2-mercaptoethoxy)ethane (MEE) and liquid polysulfide polymer with thiol end groups (LPST), were evaluated for the surface modification of HTT lignin. The impact of thiol modification on the chemical structure of HTT lignin and the reinforcement of HTT lignin-filled SSBR were investigated. The results show that approximately 69 % of the MEE and 41 % of the LPST used were grafted to the surface of HTT lignin under the modification conditions. The lower conversion yield of LPST is attributed to its oxidation during the modification. The ^{13}C NMR and DRIFT study confirmed that neither the MEE- nor LPST-grafted HTT lignin contained any free thiol that could be used for the coupling reaction with rubber. These results indicated that the used thiol modifiers modified the surface of HTT lignin. When incorporated into the rubber, thiol-modified HTT lignins improves cure properties and tensile modulus of HTT lignin-filled SSBR compared to the unmodified HTT lignin-filled compound. However, the tensile strength of thiol-modified HTT lignin-filled vulcanizates remains similar to the unmodified ones. This may be due to the absence of a rubber reactive group on the MEE-modified HTT lignin surface, which theoretically should couple the modified filler to the polymer chains chemically and increase filler-polymer interactions. This indicates that MEE acts more like a shielding agent. For LPST-modified HTT lignin, the observed effects indicates that coupling between rubber and HTT lignin occurs via the disulfide moieties. However, less grafting of LPST to HTT lignin led to a comparable tensile strength to that of the MEE-modified HTT lignin-filled compound. Thus, it was inferred from this study that using a thiol-based coupling agent for HTT lignin is critical, as the thiol moiety is highly reactive to HTT lignin.

Following the thiolation of HTT lignin, a screening of other modification reactions, such as esterification, etherification, and urethanization, was performed to identify suitable non-silane surface modifiers in **Chapter 7**. The outcome of this investigation suggested that all three reactions are feasible for the hydrophobation of HTT lignin. The etherification of HTT lignin was selected as the most promising one, and the modification was carried out using allyl glycidyl ether (AGE). Two different concentrations of AGE (low and high) were used for the surface modification of HTT lignin, and the impact of concentration on the reinforcing effect of HTT lignin was investigated in SSBR. It was demonstrated that the coupling of AGE to HTT lignin occurs via the epoxy ring opening and subsequent interaction with the phenolic hydroxy of HTT lignin. In the case of the

HTT lignin modified with high AGE content, the high degree of grafting of AGE and/or the oligomerized or homopolymerized AGE have a negative influence on the thermal stability and phase characteristics of the obtained HTT lignin. Furthermore, the vulcanizate properties of this modified HTT lignin are inferior to that of the unmodified HTT lignin filled compound. The observed adverse reinforcing effects were attributed to the reduction of filler-polymer interaction and polymer-polymer interaction as a result of a possible self-crosslinking of allyl groups via sulfur and/or due to the presence of oligomerized structure on the HTT lignin surface. Thus, this study indicated that using a high quantity of AGE may lead to the unavailability of sulfur for the crosslinking reaction of rubber since the allyl groups consume sulfur to crosslink or couple with each other. In contrast, HTT lignin modified using low AGE content enhanced the in-rubber properties of the SSBR vulcanizate compared to the unmodified one. This could be due to the lower amount of allyl groups grafted on the HTT lignin surface, which did not compete with the rubber vulcanization for sulfur and/or a negligible amount of homopolymerized or oligomerized AGE. As a result, chemical polymer-filler interactions via the allyl functionality and/or physical polymer-filler interactions due to surface hydrophobation are not negatively affected, unlike the vulcanizate containing high AGE content modified HTT lignin.

It can be concluded from the second part of the investigations (**Chapters 4, 6, 7**) of this thesis that the application of both types of surface modifiers (silane and non-silane) alters the surface chemistry of HTT lignin and, to a certain extent, reinforces the rubber. Model studies using a lignin model substance, vanillyl alcohol, identified the primary functional group of HTT lignin that participated in the coupling reaction with selected modifiers. For example, in the case of thiol modification, the 4-(hydroxymethyl)phenol structures of HTT lignin (i.e. a hydroxy group in the α-position on the aromatic ring in combination with the para-hydroxy group) have been identified as the reactive groups. Conversely, with epoxy modification, the phenolic hydroxy groups are the reactive ones Moreover, the model studies confirm that the coupling of the selected modifiers, such as silane, thiol, and epoxy, to HTT lignin occurs, and based on this, the mechanism of the coupling of HTT lignin with different surface modifiers was proposed. The performed in-rubber studies demonstrated that the reinforcing effects of the modified HTT lignin-filled compounds are better than unmodified lignin and are dependent on the concentration and type of modifier used. However, it is not superior to the highly reinforcing carbon black or silica. The surface modification makes HTT lignin a semi-reinforcing filler compared to carbon black N330. The results indicate that this effect is observed due to relatively larger particle size and a lack of strong interfacial interactions between HTT lignin and the rubber. In the case of the investigated accessible sulfur-silanes, unblocked thiol-silane and non-silane with a thiol-functionality can couple via the thiol functionality to the HTT lignin and the rubber chain. However, as evidenced by the studies, there is competition for the thiol moiety between the HTT lignin and the rubber at mixing temperatures. Thus, the formation of the HTT lignin→thiol→rubber network is critical

8

and challenging. In the case of allyl glycidyl ether, it was hypothesized that the incorporation of the allyl groups (an unsaturated site) leads to competing reactions between sulfur crosslinking of rubber and sulfur-initiated self-crosslinking of allyls. Thus, this negatively affects the expected improvement in HTT lignin-rubber interactions. For both lignin modifications, i.e., via thiol and epoxy functionality, the chemical filler-polymer interactions were only partially improved. Thus, a better understanding of the reaction that is taking place between the different modified HTT lignin and the rubber matrix can help to improve the reinforcing performance of HTT lignin in rubber.

Another reason for the semi-reinforcing effect of HTT lignin could be related to the quality of its dispersion in the rubber matrix in the presence of the modifiers. In the case of reactive silane-modified HTT lignin-filled rubber vulcanizates, clustering of filler negatively affects the micro-dispersion, and, thereby, the resulting mechanical properties are relatively lower than the conventional reinforcing fillers.

8.2 Recommendations

The work performed in this thesis is a first step towards understanding the reinforcing behavior of hydrothermally treated lignin as a filler in a (non-polar) rubber compound. Further work is necessary to exploit the full potential of this bio-based material by systematically studying how various mono- and bi-functional chemicals may affect the lignin-rubber compatibility. Having already discussed the specific recommendations at the end of each chapter, in the following the most decisive suggestions based on the investigations carried out in this thesis are summarized:

1. As a first step, modification of HTT lignin by (a) hydrophobation and (b) introduction of functional groups suitable for chemical coupling to rubber was identified to enhance the reinforcing effects of HTT lignin in an SSBR/BR or SSBR formulation. Furthermore, the modification of HTT lignin by the selected surface modifiers, i.e., coupling between the surface modifier and HTT lignin, was investigated in detail using model lignin substances. However, the coupling between this surface modifier and the rubber was not studied in detail. An assumption was made that some special functional groups, like thiol, vinyl, and allyl, should react with the rubber. But, as discussed in **Chapters 6 and 7**, it was found that these groups are also involved in the reaction with lignin (e.g., thiol) and may undergo self-crosslinking (e.g., allyl). Understanding the coupling efficiency of surface modifiers to polymer is highly beneficial in optimizing the final in-rubber properties. Besides, from the gained knowledge, it needs to be investigated whether such a coupling reaction between modified HTT lignin and rubber can occur during vulcanization, as observed in the silica/silane system. Thus, the reactivity of the selected surface modifier to the rubber needs to be studied explicitly.

2. Identifying the preferred way of modifying HTT lignin: ex-situ or in-situ. Both ways of modification were discussed in the thesis with a focus primarily on ex-situ modification, assuming that a higher coupling yield can be achieved between HTT lignin and surface modifier in this way.

3. Though the thesis primarily focused on the surface modification of HTT lignin with a given specific surface area (SSA) of 37 or 47 m²/g and aimed to investigate the impact of the modification on the reinforcing properties of HTT lignin-filled rubber, the effect of an even decreased particle size (or an increased SSA) on the rubber reinforcement was not investigated. It is expected that improved filler characteristics in terms of morphology can further enhance the reinforcing potential of HTT lignin.

4. The dispersion behavior of different silane-modified HTT lignins was studied using atomic force microscopy. However, the filler dispersion of thiol and epoxide-modified HTT lignin was not analyzed. Since improper filler dispersion can have a negative impact on the mechanical performance of HTT lignin-filled compounds, further study is required.

5. The quality of mixing is one of the crucial parameters for the final in-rubber properties of the compound. Therefore, the impact of other mixing strategies, like latex mixing and heat-treatment methods, on the dispersion of HTT lignin in the rubber matrix should be studied.

6. One of the effects observed with unmodified- and modified-HTT lignin-filled compounds was a lower apparent crosslink density compared to the conventional reinforcing fillers. The impact of HTT lignin and modified HTT lignin on rubber crosslinking was not investigated in detail. Therefore, it is recommended that the amount of curatives and the type of accelerators used for HTT lignin-filled rubber compounds be evaluated. From the knowledge gained from the thiol/HTT lignin coupling, there is a high chance that the sulfur can also interact with HTT lignin. Thus, sulfur, accelerator, and activator interaction with HTT lignin must be examined in detail.

8

Through the investigations carried out in this thesis, it is proven that a better understanding of the reactivity of the surface modifier with both filler and polymer can pave the way for further use of HTT lignin as a reinforcing filler. The study also shows that the surface of HTT lignin is reactive at least to a certain degree, and different modifications, such as thiol coupling to benzylic alcohol and the addition of catalyzed epoxy ring opening to phenolic OH, can occur. Overall, further progress in the filler characteristics of lignin, such as smaller particles and reduction in polar functional groups by the hydrothermal process, is expected to promote filler-polymer interactions and, thus, reinforce the rubber better.

8

Research deliverables

Journal publications

Sekar, P., Noordermeer, J. W., Anyszka, R., Gojzewski, H., Podschun, J., & Blume, A. (2023). *Hydrothermally treated lignin as a sustainable biobased filler for rubber compounds*. ACS Applied Polymer Materials, 5(4), 2501-2512.

Sekar, P., Martinho, R. P., Talma, A. G., Gojzewski, H., Stücker, A., Schwaiger, B., Podschun, J., & Blume, A. (2023). *Horizons in Coupling of Sulfur-Bearing Silanes to Hydrothermally Treated Lignin toward Sustainable Development.* ACS Sustainable Chemistry & Engineering, 11(48), 16882-16892.

Patents

Surface-modified Organic Fillers and Rubber Compositions containing same, EP4341342A1

Organic Fillers with Thioether Linkages, WO2024105237A1

Conference Proceedings

Sekar P, Anyszka R, Gojzewski H, Podschun J and Blume A. *Hydrothermally Treated Lignin – A Feasible Particulate Bio-Filler for High performance Rubber Applications*. in 202th Technical Meeting of ACS Rubber Division Conference 2022. 11-13 Oct., Knoxville, Tennessee, United States

Presentations

Sekar P, Martinho RP, Talma AG, Gojzewski H, Stücker A, Schwaiger B, Podschun J, and Blume A. *Understanding the Raspberry-like Filler Cluster Formation of Bis-(triethoxypropyl)tetrasulfide modified Hydrothermally treated lignin in an SSBR/BR rubber matrix*. Rubbercon 2023, 11-12 May, Edinburgh, UK

Sekar P, Gojzewski H, Talma AG, Stücker A, Schwaiger B, Podschun J, and Blume A. *Understanding the Reinforcement behavior of Silane-modified Hydrothermally treated Lignin*. Tire Technology Expo 2023, 21-23 Mar., Hannover, Germany

Sekar P, Talma AG, Stücker A, Podschun J, Schwaiger B, Noordermeer JWM and Blume A. *Hydrothermally Treated Lignin – A Feasible Particulate Bio-Filler for Rubber Applications*. in International Rubber Conference 2022. 24-26 Nov., Bangalore, India

Award

Best presentation IRC 2022, Bangalore, India.

Acknowledgments

Reflecting on this journey, I realize how profoundly it has shaped me. Not only has my knowledge expanded, but I've also developed a newfound sense of confidence in my abilities. Reaching this point wouldn't have been possible without the invaluable guidance, support, and encouragement of so many, to whom I express my heartfelt appreciation.

First and foremost, I am immensely grateful to my supervisors, Prof.dr. Anke Blume and dr. Auke Talma, for their constant support, invaluable guidance, and insightful feedback throughout my research journey. I am particularly thankful to my supervisor and promotor, Anke, for the freedom I was given to explore my research interests, which has been crucial in shaping my path forward. Dear Anke, I want to express my gratitude for your belief in my abilities and your guidance. Additionally, I am also incredibly grateful for the time (including, your leisure hours) and effort you have dedicated to supporting me on this journey. Our discussions always made me reflect on the research from different perspectives, and your feedback significantly improved the quality of the thesis. I extend my appreciation to my co-promotor, Auke, for his willingness to guide me and delve deep into the nuances of my work. This has been invaluable in refining my ideas and methodologies. Dear Auke, thank you for our regular discussions and your support in my research pursuits. Without you, this thesis would not throw light on the coupling mechanisms or other chemistry-related aspects. Besides that, I enjoyed working with you.

My special thanks to Prof. Jacques Noordermeer for his input and ideas. Dear Jac, thank you for your mentorship. Your contributions have significantly enhanced the quality of this work. Despite not being my supervisor and your retirement, you always took the time to review my articles, providing valuable suggestions for improvement. Your dedication to my research truly made a difference and has always motivated me to conduct good research practices. I can't thank you enough for all the hard work you put into finalizing my first manuscript for publication. I consider myself fortunate to work with you. I would also like to thank Betty for her hospitality and patience. I want to express my profound gratitude to dr. Wilma, one of the supporting pillars during my PhD track. Dear Wilma, no matter the situation, you were always there when I needed a shoulder to lean. For that, I owe you a great deal of gratitude. Not only that, it was also you who convinced me that I could do a thesis in rubber chemistry. And here we are with this dissertation of mine! Thank you for believing in me and for supporting me unconditionally throughout my PhD journey. I acknowledge your helping hand in preparing the Dutch summary. Special

I would like to acknowledge the members of the graduation committee: prof. Kirsti Mikkonen, dr. Essi Sarlin, prof.dr. Karin Schroën, prof.dr.ir. Inna Gitman, dr. Pilar Ramiro dr. Jacob Podschun, for the time and effort you have dedicated to reviewing my thesis.

To my paranymphs Rafal and Marcin, I want to thank you for taking a special place in my ceremony. Rafal, your warm and friendly personality made me always count on you for your support. Thank you for your acceptance of being one of my paranymphs! It has always been a pleasure to have you as both a colleague and friend. You taught me critical thinking and designing experiments in the chemical lab, which facilitated my professional growth. Your dedication to Science inspired me to continue my career as a researcher. I really missed working with you during my PhD. But I look forward to collaborating with you in the near future. Marcin, I am thankful for your willingness to help whenever I needed it. It has been greatly comforting. I cherish our discussions in the office and the fun talks we shared in the chemical lab. Also, thank you for the endless discussions we had with elemental calculations.

I would also like to extend my appreciation to all the members of the ETE group for their warmth and support throughout my time at UT, especially Dries and Chris, for helping with the experimental work at the ETE. Ceciel, thank you for consistently demonstrating patience with my inquiries and promptly addressing various concerns. Pilar, thank you for procuring the chemicals needed for my experiments. Wisut and Fabian, thank you for your support and discussion. Carmela, my office mate and protective friend, thank you for the time-to-time little chats and the fortune chillies. I'm shielded from all the evil eyes! Jan Willem, my Dutch (German?) friend, I enjoyed your company and touches of sarcasm. I'm impressed at your ability to bring different yet like-minded people together. I'm sure you can keep up the good vibes. I'm deeply grateful to Sun, who supported me with ChemDraw and NMR predictions. Thank you for everything. I would also like to thank Gina for encouraging me in this journey since we met each other. Karnda, a special mention to you for all the support with HPLC and GC measurement. Thank you for patiently teaching the chemical calculations. Zuzanna, I'm grateful to have you as my colleague and friend. You have so much to teach me! Thank you for your support in proofreading the thesis.

I extend my deepest gratitude to my beloved friends for their unwavering presence throughout this journey. To my friend, Ranjani, thank you for shining a light on my academic career. Without you, this journey would be unthinkable. Dear Iqbal, your friendship has been a constant source of joy and strength. I am grateful for your timely support and continuous encouragement. I will cherish the incredible moments we've shared, from our engaging conversations to our joyful meals, fun outings, exercises, cycling, endless coffee breaks, and laughter. Ayush and Marzieh, your advice and support have been invaluable during my challenging period. Ayush, thank you for always boosting my confidence in me and teaching me survival skills. I enjoyed all the fun activities we had together and your special momos. Marzieh, I enjoyed your companionship, and thank

you for always being there for me when I needed someone to lend an ear. Special thanks to Keerthi, Shakshi, Kannan, Bharath, Andjelka, and Ramona for our fun-filled lunch talks.

I would like to thank every friend and colleague of mine whose name was not mentioned in this Acknowledgement.

Last but not least, I want to thank the dearest and the closest people to me, who supported me every step of the way. To my mother, Shanthi, your unwavering belief in my aspirations has been a guiding light, providing me with strength and motivation at every phase of my life. Your resilience and strength have been a beacon of inspiration for me. I dedicate this thesis to you and all your hardships. To my dear brother, Sridhar, I extend heartfelt thanks for patiently listening to my sobers. To my aunt Amutha, thank you for being a supporting pillar for us, without your help, it wouldn't have been possible to live peacefully in a foreign country. To my beloved partner, Anand, your encouragement, positivity, and unconditional love have been my anchor through every challenge. Your unwavering support for my dreams has been the driving force behind my resilience during the most challenging moments. I'm immensely grateful to have you beside me through every high and low.

-PRIYANKA